THE UNIVERSITY
of EDINBURGH

Apical-Out Chicken Enteroids with Leukocyte Component as a Model to Study Host-Pathogen Interactions

Tessa Nash

A dissertation submitted for the degree of Doctor of Philosophy

The University of Edinburgh

2021

Declaration

I declare that this thesis has been composed solely by myself, the work presented is entirely my own except where stated otherwise by reference or acknowledgement, and that it has not been submitted, in whole or in part, in any previous application for a degree or other professional qualification

Signed……Tessa Nash…….

Date…… 16/12/2021 ……..

Abstract

Over the last 20 years global poultry production has tripled with approximately 107 million tonnes of chicken meat and 1.3 trillion eggs now produced every year (FAOSTAT, 2019). Of particular concern for all types of poultry production systems are zoonotic infections such as avian influenza virus and salmonellae, but also protozoal parasites like *Eimeria* which have a significant impact on animal welfare and the economy. Most of these infectious agents enter the chicken via the respiratory or intestinal epithelium, however a detailed understanding of how certain pathogens infect the gastrointestinal tract and airways in the chicken is lacking. *In vitro* avian gastrointestinal studies have long been hampered by a lack of representative cell culture tools. Mammalian 3D enteroids mirror *in vivo* intestinal organisation and are powerful models to investigate host-pathogen interactions, food science and improved targeting and efficacy of pharmaceuticals. The main aim of this study was to develop and characterise an *in vitro* 3D enteroid culture system from the intestine of chickens which would recapitulate the *in vivo* gut epithelial cell content, architecture and function. Once these cultures were established the aim was to determine whether the enteroids could be used to study the interaction of various pathogens with the enteroid epithelia, and to explore induced mucosal immune responses. Throughout these studies the characteristics and responses of the chicken enteroids were to be compared to those of the *in vivo* chicken intestine.

From this work, protocols to successfully isolate stem-cell containing villi or crypts from the embryonic and mature poultry intestine and culture multi-budding enteroids have been developed. These 3D intestinal models are shown to mature rapidly within 1-2 days and re-create the 3D villus-like architecture. Methods used to validate the enteroid cultures show they remained viable for over 7 days. Histological, transcriptional and functional analyses demonstrate the cellular diversity, barrier and digestive functions of the *in vivo* chicken intestinal epithelium in this chicken enteroid model.

Unusually, the poultry enteroids develop rapidly and optimally in suspension without the structural support required to produce typical mammalian enteroids, resulting in an apical-out conformation with media-facing microvilli. Another striking feature of this model is the innate presence of functional intraepithelial and lamina propria leukocytes in a lamina propria core. Specifically NK cells, mononuclear phagocytes, and T cells have been identified, and phagocytosis studies have evidenced their functionality. Other lamina propria cell types have also been identified, revealing further complexity to this comprehensive *in vitro* model. To expand the potential applications of these cultures, enteroids were developed from two species of poultry and from different regions of the small and large intestine, which reflect *in vivo* intestinal architectural characteristics.

In-depth RNA seq analysis has confirmed the reproducibility and consistency of these cultures as well as further exploring their digestive and immune functions, cell content and stage of development in culture. Analysis of stem cell growth factor transcripts indicate enteroid differentiation and homeostasis is predominantly maintained by cell populations within the enteroids. The transcriptome analysis also indicated the difficulties in passaging this culture system may be caused in part by a combination of epithelial-mesenchymal transition and deficiencies in a small number of downregulated growth factors. Methods to cryopreserve both villi and enteroids have therefore been developed to reduce the requirement for fresh tissues for every experiment and enable the sharing of material between labs.

The rapid maturation and advantageous polarisation of these 3D cultures enabled active infection of the epithelial apical surface with the bacterium *Salmonella* Typhimurium, influenza A virus as well as the avian-specific protozoan *Eimeria tenella* without the need for complicated manipulation. Multiplexed RT-qPCR Fluidigm Arrays supported analysis of the enteroid immune response to infection, demonstrating the differential regulation of an array of genes which mirror *in vivo* studies. In addition, permeability assays to analyse the enteroid epithelial barrier were developed

and revealed significant differences in intercellular junction disruption between invasive and T3SS1 mutant *S.* Typhimurium infections.

The paucity of representative poultry gut *in vitro* models has limited research in this essential field of gut health and led to an over reliance on the use of live birds for experiments. This study has developed protocols to successfully isolate villi and crypts from the avian small intestine and derive 3D enteroids with an accessible epithelial layer. These rapidly maturing, highly reproducible cultures have been demonstrated to contain a comprehensive array of functional small intestinal and lamina propria cell types. The unique conformation in combination with the lamina propria component of the enteroids means they can be readily applied to study complex epithelial and leukocyte responses to bacterial, viral and protozoal pathogen challenge. The ability to biobank stem cell containing tissue alongside the demonstrated physiological relevance of this model, means the floating chicken enteroids satisfy many of the guiding principles of the 3R's which are being increasingly implemented in new legislation. In summary, this work has created a valuable analytical tool which enables a detailed view of how the intestines of the post-hatch chick grow and respond to external challenge *in vitro*. This model has the potential for use in host-pathogen, pharmaceutical and food science research as well as commercial applications for e.g. probiotic and vaccine batch testing.

Lay Summary

The global movement to reduce animal trials has resulted in an urgent need to develop alternative comprehensive non-animal lab models whose results closely resemble that of a living animal. Intestinal models are of particular interest for livestock studies since the gut is the target for many important pathogens and therapeutics, as well as being essential for nutrition and immunity. However, models commonly used to study the livestock intestinal surface present major limitations. For example, intestinal cell lines do not reproduce the array different of cell types or tissue functions found in the gut, and for poultry they are not even available. Scientists have recently developed 3D cultures of miniature intestines, known as enteroids, to improve research in gut biology. Enteroids contain most of the cell types of the gut surface, have a similar surface 3D architecture and reproduce many of the same intestinal functions. The development of these 3D cultures requires the ideal growth environment which was initially identified for the mouse and has required minimal adaptations for use in other mammal species. This involves embedding stem cell containing tissue inside a gel dome surrounded by cell culture liquid supplemented with various growth factors. In these conditions the stem cells can follow their own genetic instructions to self-organise and form structures that resemble miniature intestines with an internal lumen, the space to which nutrients, toxins and microorganisms are confined, and a difficult to access gut surface.

The techniques developed to culture mammal enteroids only allow the growth of thin spheroid structures composed of few cell types when applied to the chicken. Therefore the first major aim of this study was to develop an enteroid culture system of the poultry digestive tract that would overcome current limitations. This was achieved by developing methods to isolate tiny fragments of stem cell containing tissue from late embryonic chicken intestines and then culturing them floating in liquid cell culture. These techniques allowed the fragments to rapidly and consistently form enteroids within 1 – 2 days. The chicken enteroids contain multiple different intestinal

cell-types and re-create the 3D architecture and physiology of the post-hatch chick gut in remarkable detail. A novel feature of this model which makes it different to classical mammalian enteroids, is the apical-out phenotype with the gut epithelial surface now easily accessible facing the liquid cell culture. In addition, these are the first enteroid models to naturally include cells from the immune system, enabling a more comprehensive understanding of the chicken's response to infection. To expand the potential applications, enteroids were also developed from two species of poultry and from different regions of the small and large intestine.

The second aim of this study was to investigate whether this complex tool could be applied to study the infection mechanisms of avian intestinal pathogens and the host immune responses they induce. The infection and replication of avian influenza virus and *Salmonella* Typhimurium, infectious diseases which can also spread to humans, was demonstrated without the need for complicated manipulation of the enteroids. In addition, replication of *Eimeria tenella*, a chicken-specific parasite that causes welfare issues in its hosts and impacts poultry production globally, was demonstrated in a host (chicken) and site (caecum) specific model. The presence of immune cells in this model enabled analysis of the enteroid immune response to infection with each pathogen. This data showed a dynamic response of the enteroids to infection which mirrored published data of similar experiments in chickens. An assay to investigate the effect of external challenges to the enteroid gut barrier function was also developed.

This research shows that our novel floating chicken enteroid model will give scientists a detailed view of how the intestines grow and respond to their environment. Previously there have been few poultry-specific lab models which has limited research in the essential field of gut health and led to an over reliance on the use of live birds for experiments. This exciting comprehensive model could be used in analytical application for the feed and pharmaceutical industry, as well as providing new research insights on gut development, infectious diseases and the genetic basis to improve gut health.

Contents

List of Figures

List of Tables

List of Additional Files

Additional file 1: Nash et al. (2021) DOI: 10.1038/s42003-021-01901-z

Additional file 2: Differential heat maps for specified contrasts

Additional file 3a: ED18 intestinal villi and enteroid genes found in the largest 50 co-expression clusters

Additional file 3b: Mean expression profiles of the ED18 intestinal villi and enteroid genes in each of the largest 50 co-expression clusters

Additional file 3c: GO term enrichment annotations for the ED18 intestinal villi and enteroid genes in the largest 50 co-expression clusters

Additional file 4: Differentially expressed gene summary

Acknowledgements

I would first and foremostly like to thank my supervisors Prof Lonneke Vervelde, Prof Neil Mabbott and Dr Ad de Groof for their support, enthusiasm and fruitful discussions throughout my PhD. I also owe an immeasurable thanks to many past and present members of the Vervelde, Mabbott and de Groof lab groups as well as Dr P. Vermeij (MSD Animal Health, The Netherlands) for their continued guidance and advice over the last 4 years.

I am grateful to Prof S. Meddle and Dr A. Johnston (University of Edinburgh) for providing the quail tissue, Dr P. Vohra and Prof M. Stevens (University of Edinburgh) for providing the *Salmonella* strains, Dr E. Gaunt and Prof P. Digard (University of Edinburgh) for providing the PR8 virus and NP antibody, Dr E. Wattrang (National Veterinary Institute, Sweden) for providing the *Eimeria* sporozoites, and R. Fleming and S. Mitchell (University of Edinburgh) for excellent bio-imaging support. Dr E. Gaunt also kindly performed three of the seven biological replicate plaque titrations and the tubulin staining for the western blot in Chapter 8.

A final thank you goes to my partner Martyn Lewis for being a constant source of encouragement, strength and support.

This research was supported by an iCase studentship from the Biotechnology and Biological Sciences Research Council (BBSRC) in collaboration with MSD Animal Health (BB/MO14819), and Institute Strategic Program Grant funding from the BBSRC (BBS/E/D/10002071 and BBS/E/D/20002173).

Abbreviations and Acronyms

°C	Degree Celsius
µM/mM/M	Micromolar/Millimolar/Molar
µL/mL	Microlitre/Millilitre
ng/µg/mg	Nanogram/Microgram/Milligram
α-SMA	α-smooth muscle actin
ACTB	actin beta
AIV	Avian influenza virus
AKT	AK strain transforming
ALPI	Alkaline phosphatase
ANOVA	Analysis of variance
ANPEP	Membrane alanyl aminopeptidase
ARG2	Arginase 2
ATOH	Atonal homolog 1
ATP	Adenosine triphosphate
ASS1	Argininosuccinate Synthase 1
AvBD	Avian β-defensins
AVD	Avidin
BLIMP1	B lymphocyte-induced maturation protein 1
BMI1	B cell-specific Mo-MLV integration site
BMP	Bone morphogenic protein
CCL	Chemokine (C-C motif) ligand
CD	Cluster of differentiation
CDCA7	Cell division cycle associated 7
CFU	Colony forming units
CHGA	Chromagranin A
CLEC	Chicken lung epithelial cell line
CPM	Counts per million
CSF1(R)	Colony-stimulating factor 1 (receptor)
Ct	Cycle threshold
CXCLi	Chemokine (C-X-C motif) ligand
CXORF	Chromosome X open reading frame

DAPI	4', 6-diamidino-2-phenylindole
DC	Dendritic cell
DEG	Differentially expressed genes
Dll	Delta-like ligands
DMEM	Dulbecco’s modified eagle’s medium
DMSO	Dimethyl sulphoxide
DNA	Deoxyribonucleic acid
dpi	days post infection
DTX2	Deltex E3 ubiquitin ligase 2
ECM	Extracellular matrix
EdU	5-ethynyl-2′-deoxyuridine
EPHB	Ephrin type B receptor
E. tenella	*EImeria tenella*
ED	Embryonic days
EDTA	Ethylebediaminetetraacetic acid
EGF	Epidermal growth factor
EGTA	Ethylene glycol-bis(β-aminoethyl ether)-N,N,N’,N’-tetraacetic acid
EMT	Epithelial mesenchymal transition
ERK	Extracellular signal-regulated kinase
FABP	Fatty acid binding protein
FBS	Fetal bovine serum
FC	Fold change
FCRN	neonatal Fc receptor
FDR	False discovery rate
FGF	Fibroblast growth factor
FITC	Fluorescein isothiocyanate
FOM	Floating organoid media
FOX	Forkhead box
FZD7	Frizzled class receptor 7
GALT	Gut-associated lymphoid tissue
GAPDH	glyceraldehyde 3-phosphate dehydrogenase

(e)GFP	(enhanced) Green-fluorescent protein
GFR	Growth factor reduced
GO term	Gene ontology term
GUSB	Glucuronidase beta
h/hpi	hour/hour post infection
HBSS	Hank’s Balanced Salt Solution
HES	Hairy and enhancer of split
HOPX	Homeodomain only protein X
HPAIV	High pathogenic avian influenza virus
HPS5	Hermansky-Pudlak syndrome 5
IAV	Influenza A virus
IEL	Intra-epithelial leukocytes
IFIT	Interferon induced protein with tetratricopepide repeats
IFITM	interferon-inducible transmembrane protein
IFN	Interferon
Ig	Immunoglobulin
IGF	Insulin-like growth factor
IL	Interleukin
IL13RA/IL10RA	Interleukin 13/10 receptor subunit alpha
IL1R2	Interleukin 1 receptor type 2
IL4I1	Interleukin 4 induced 1
IRF	Interferon regulatory factor
ISC	Intestinal stem cell
ISG	Interferon stimulated gene
ITS	Insulin, transferrin, sodium selenite
JAK-STAT	Janus kinase/signal transducers and activators of transcription
KRT20	Keratin 20
LCT	Lactase
LDH	Lactate dehydrogenase
LGR5	Leucine-rich repeat-containing G-protein coupled receptor 5

LPAIV	Low pathogenic avian influenza virus
LPS	Lipopolysaccharide
LRIG1	Leucine rich repeats and immunoglobulin like domains 1
LRP	Lipoprotein receptor-related protein
L-WRN	mouse fibroblast line secreting WNT3a, RSPO3, Noggin
LYG2	Lysozyme G2
LYZ	Lysozyme C
MKI67H	Marker of proliferation Ki67
MAPK	Mitogen-activated protein kinase
MHC	Major Histocompatibility complex
MIF	Macrophage inhibitory factor
min	minute
MUC	Mucin
MX1	Myxovirus (influenza virus) resistance 1
MYD88	Myeloid differentiation primary response 88
NFκB	Nuclear factor-kappa B
NK cell	Natural killer cell
NP	Nucleoprotein
NLR	Nucleotide binding oligomerisation domain-like receptor
NOS	Nitric oxide synthase
OASL	Oligoadenylate synthetase like
OCLN	Occludin
OLFM4	Olfactomedin 4
PBS	Phosphate-buffered saline
PCA	Principal component analysis
PCR	Polymerase chain reaction
PCNA	Proliferating cell nuclear antigen
PGE_2	Prostaglandin E2
prg	phoP-repressed gene
PROX1	Prospero homeobox 1
R28S	ribosomal 28S
RAS	Rat sarcoma virus protein

REG3G	Regenerating family member 3 gamma
RIN	RNA integrity number
(m/t)RNA	(Messenger/transfer) Ribonucleic acid
RNF	Ring finger protein
ROCK	p160 rho-associated protein kinase
RSPO	R-spondin
RT-qPCR	Reverse transcription-quantitative polymerase chain reaction
SLC9A3R1	Solute carrier family 9 subfamily A member 3 regulator 1
SOCS	Suppressor of cytokine signalling
SOX9	SRY-box transcription factor 9
SPI1	Salmonella pathogenicity island 1
S. Typhimurium	*Salmonella enterica* serovar Typhimurium
T3SS	Type 3 secretion system
TBP	TATA-binding protein
TCF	Transcription factor
TCR	T cell receptor
TEER	Trans-epithelial electrical resistance
TEM	Transmission electron microscopy
TFS	Thermo Fisher Scientific
TGF	Transforming growth factor
TGM4	Transglutaminase 4
Th	T helper
TIMD4	T cell immunoglobulin and mucin domain containing 4
TIRAP	Toll/IL-1R domain-containing adaptor protein
TJP1	Tight junction protein 1
TLR	Toll-like receptor
TNF(AIP3)	Tumour necrosis factor (alpha induced protein 3)
TOLLIP	Toll interaction protein
TRAF3IP2	TRAF3 interacting protein 2
Treg	Regulatory T cells
TREH	Trehalase

VIM	Vimentin
WNT	Wingless-related integration site
WT	Wildtype
YAP	Yes-associated protein
ZNRF	Zinc and ring finger
ZO1	Zonula occludens

Chapter 1 General Introduction

Chapter 1 General Introduction

This chapter provides a comprehensive overview of the *in vivo* intestinal mucosal and the *in vitro* tools which aim to model this environment. A description of the composition and function of the chicken small intestinal epithelial layer and the intestinal lamina propria compartment, with a particular focus on the nuances specific to the late embryonic and post-hatch period, is presented initially. This is followed by an argument for the requirement of novel intestinal *in vitro* models in poultry and an account of the currently available options for livestock species. Finally a review of the culture methods and applications of livestock species enteroids, with an emphasis on enteroid cultures previously attempted in the chicken is presented. This is not a comprehensive review of human and mouse enteroid literature as that body of work is far too expansive to cover in this introduction however relevant studies in these species are discussed throughout the thesis where appropriate.

1.1 Overview of the chicken intestinal epithelium

1.1.1 Epithelial composition

General overview of the intestine

The intestinal tract is anatomically divided into two segments; the small and large intestine. In birds this is divided into five functional domains along the proximal-to-distal intestinal axis; the duodenum, jejunum and ileum make up the small intestine, and paired caeca and a short colon that opens into the cloaca make up the large intestine. These domains have distinct macroscopic and microscopic appearances and specialised functions which make them distinct sites of colonisation and ports of entry for many clinically important site-specific pathogens such as *Eimeria* spp. and *Campylobacter* spp.[1,2,3](reviewed in[4]). The duodenum receives food chime, bile and pancreatic secretions to complete chemical digestion, the jejunum is the main site for nutrient absorption, the ileum absorbs residual nutrients, vitamins and

conjugated bile acids, and the large intestine mainly functions to absorb water, electrolytes and microbial fermentation products.

There are three concentric tissue layers which make up the wall of the intestinal tract; the outermost layer is composed of smooth muscle sheets that, in conjunction with the intramural enteric nervous system, allow the intestine to perform peristalsis. Connective tissue comprises the middle layer, containing blood vessels, lymph vessels, nerve fibres, and numerous immune cells. The innermost layer of the luminal surface is a single cell thick epithelial layer which architecturally organises into crypts and long finger-like projections that project into the lumen called villi. The villus epithelium of the mammalian small intestine is composed of absorptive enterocytes, mucin-secreting goblet cells, hormone-secreting enteroendocrine cells, chemosensory tuft cells, antigen-transporting M cells and intraepithelial leukocytes (IELs). In the mature chicken this epithelial sheet renews every 4 days through a careful balance of cell production in the crypts, continuous upward migration of cells, and anoikis (a form of programmed cell death) and exfoliation from the villus tips (reviewed in[5,6])

Differentiated epithelial cells

Enterocytes in chickens have been shown to increase in size, develop a columnar appearance and grow microvilli on the apical surface by 24 h post-hatch. Although enterocyte density rates change little with age, the epithelial transit time is reduced in the early days post-hatch compared to the adult chicken with migration to the villus tips taking only 50 h in 2 day old chicks[7,8]. Goblet cells store mucin in large membrane-bound granules and release it from their apical surface by baseline secretion or compound exocytosis (reviewed in[6]). This cell type has been identified in chicken embryos from 17 embryonic days (ED) with numbers increasing and mucin composition changing rapidly post-hatch, presumably in response to exposure to microbial flora and food[9]. Enteroendocrine cells act as chemoreceptors initiating digestive actions, detecting harmful substances and instigating protective responses and have been identified in chickens from ED12 - 14[10].

Detailed information on the presence and development of rarer epithelial cell populations e.g. tuft cells in the chicken intestine is currently sparse due in part to limitations in the identification of cell-specific markers (reviewed in[5]).

Stem and Paneth cells

The differentiated cells of the villus epithelium originate from the transit amplifying cell region located at the crypt-villus junction. The highly proliferative transit amplifying cells are daughter cells of long-lived leucine-rich repeat-containing G-protein coupled receptor 5 (LGR5)+ intestinal stem cells (ISCs) (reviewed in[11]). The *LGR5* ISC marker has been identified in chicken small intestinal crypts, however olfactomedin 4 (*OLFM4*) appears to be more strongly expressed in these chicken ISCs[12]. The homeostatic, Wingless-related integration site (WNT)-sensitive LGR5+ cells are one of two proposed types of ISC in the mammalian gut epithelium, the other being quiescent B cell-specific Mo-MLV integration site 1 (BMI1+) cells located at position +4 directly above the Paneth cells. In direct contrast to LGR5+ cells, BMI1+ cells are insensitive to WNT modulation, contribute poorly to homeostatic regeneration, and are resistant to irradiation. Although the location and identity of ISCs is still hotly debated, the main function of BMI1+ cells appears to lie in injury-induced regeneration[13]. Intestinal crypts in mammals are composed of the LGR5+ cells which are interspersed between and in direct contact with Paneth cells. These specialized enterocytes support the ISC niche and maintain an antibacterial crypt environment through production of secreted bactericidal peptides such as lysozyme[14](reviewed in[15]). The existence, location and function of Paneth cells in the chicken is still disputed[12,16,17]. A rod shaped epithelial cell containing prominent cytoplasmic lysozyme granules has been described in the chicken, dispersed throughout the intestinal villi[18]. Interestingly, ISC-like cells have also been identified in the villus lining of the chicken intestine[19]. This indicates that in the chicken, the capacity for cell proliferation and differentiation may exist along the intestinal villi as well as in the crypts.

Epithelial immune cells

M-cells are specialized epithelial cells which are generally concentrated in the follicle-associated epithelium of intestinal Peyer's patches of the gut-associated lymphoid tissues (GALT) in mammals, but can also be found occasionally dispersed throughout the intestinal epithelium in association with isolated lymphoid follicles (reviewed in[20]). Peyer's patches are locations where particulate antigen and microorganism recognition occurs and mucosal immune responses can be initiated. They are composed of 3 domains spanning the lamina propria and the epithelium. The follicular area mainly consists of a germinal centre containing proliferating and differentiating B cells, T cells, follicular dendritic cells and macrophages. This is superimposed by the parafollicular area which comprises a dome containing B and T cells, dendritic cells (DCs) and macrophages. The follicle-associated epithelium overlies the follicles and is composed of enterocytes and a population of highly endocytic M-cells. Although chickens lack the draining lymph nodes found in mammals, they do have solitary or aggregated lymphoid follicles and M cells present throughout their intestines which resemble smaller versions of mammalian Peyer's patches[20,21,22]. Rudimentary versions of these follicular structures have been reported in the chicken embryonic gut from ED13[23].

IELs are a highly specialized group of lymphocytes, distinct from their systemic counterparts, which populate the intestinal epithelial layers. During postnatal development in the chicken, 35% of IELs are T cells, 50% have B cell markers (BU-1) but lack surface immunoglobulins (Ig), and 15% are non-B non-T non-monocyte cells[1]. These cell populations are sparse at hatch but continue to increase in number until birds are 8 weeks old. In adult birds, IEL populations are almost entirely composed of subsets of natural killer (NK) cells and T cells (both T cell receptor (TCR)αβ and TCRγδ) with very few B-like lymphocytes[24,25]. Of the T lymphocyte populations TCR1+ (γδ) T cells, which have been demonstrated to produce cytokines and interferons and have cytotoxic activity, make up a higher proportion of IEL in chickens than

TCR2+ (αβ) T cells, and cluster of differentiation (CD)8α T cell expression increases with age[26,27].

Intestinal epithelial development around day of hatch

The last few days pre-hatch and the first few days post-hatch are the most critical period for intestinal development. As a precocial species, chicks begin to forage for feed immediately post-hatch so there is a requirement for a rapid increase in morphological and functional development of their gastrointestinal tract. The weight of the intestine, as a proportion of the embryo, increases from 1% at ED17 to 3.5% at hatch, with waves of villi rapidly developing from ED19[28]. In most mammals, cell proliferation is present over the villi surface until birth, at which point proliferation is restricted to the crypts[29]. At day of hatch in the chicken however, there is an absence of a defined zone of propagation with all villus small intestinal enterocytes still showing evidence of proliferation. Levels drop rapidly by 2 – 3 days post-hatch with 50% of proliferation becoming restricted to the crypts, but at 10 days post-hatch there are still ~10% villus enterocytes still proliferating[19]. Lengthening of the villi in the duodenum is complete by 7 days post-hatch but the jejunal and ileal villi will continue to increase in size beyond 14 days of age[8,30]. In mice at birth the base of the villi are surrounded by ISC-containing small intervillus pockets, and it takes till 2 weeks after birth for crypts to form and for Paneth cells to start to populate them[31,32]. In the markedly faster maturing chicken, crypts increase from 1 rudimentary crypt per villus at hatch to 3-4 much larger crypts per villus before 2 weeks of age[33].

The precise types, roles and locations of avian intestinal epithelial cells (IECs) have not yet been fully defined so further characterization of the chicken epithelium is indicated to explore current questions arising in the literature e.g. whether chickens possess Paneth cells and the location of proliferation sites along the villi. Accurate definitions of the distribution and functions of chicken epithelial cell populations by digestive segment and age

would also be useful to understand pathogen site specificities and age-dependent innate immune responses.

1.1.2 Molecular signals involved in epithelial self-renewal

WNT signalling

On a molecular level there is a complex interplay of growth factors and signalling pathways that positively regulate self-renewal in LGR5+ cells and aid in differentiation of cell lineages (Fig. 1.1). The WNT signalling pathway plays a central role in maintaining the ISC population and promotes proliferation of the TA cell population. Multiple secreted WNT factors are produced by epithelial cells at the crypt base in mammals, generating a WNT gradient along the crypt-villus axis which is essential for regulation of stem cell hierarchy and budding structures (Fig. 1.1, reviewed in[34]). WNT binds to the Frizzled-low density lipoprotein-related protein (LRP)5/6 co-receptors to induce stabilization of β-catenin which then engages the transcription factor (TCF)4, thus activating a genetic program that supports stemness (Fig. 1.1, reviewed in[35]). WNT signals and gradients are also important for terminal differentiation of Paneth cells, and to position cells along the crypt-villus axis by inducing expression of the cell-sorting receptors Ephrin type B receptor (EPHB)2 and EPHB3[36,37]. As previously mentioned, the positioning of Paneth and proliferating cells does not appear confined to the crypts in chickens potentially indicating differences in the roles of their cell-sorting receptors and/or WNT gradients.

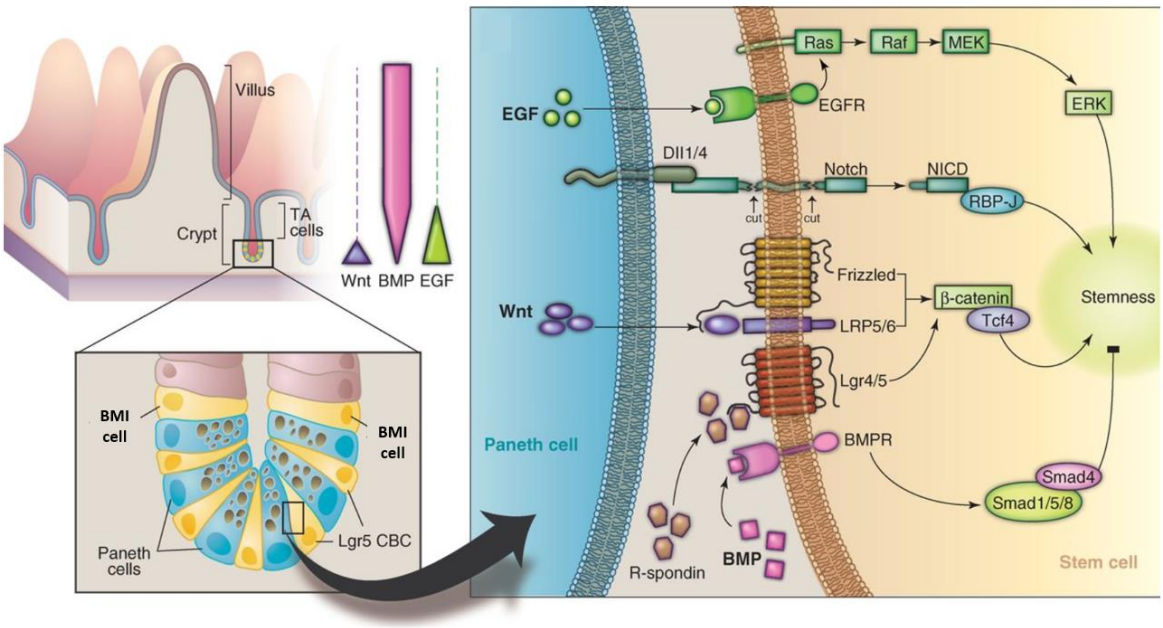

Figure 1.1: Molecular signals involved in intestinal stem cell homeostasis. A basic summary demonstrating how signals from Paneth cells (blue cells) e.g. EGF, Wnt and DII1/4 ligands, and sub-epithelial fibroblasts e.g. R-spondin and BMP, activate signalling cascades to either promote or inhibit ISC (yellow cells) homeostasis. Adapted from Sato & Clevers (2013) under the terms of the Creative Commons Attribution License (http://creativecommons.org/licenses/by/4.0/)[35].

R-spondin

The R-spondin (RSPO) family (1-4) are physiological ligands of LGR4 and LGR5, and are locally secreted in the crypts by sub-epithelial fibroblasts (Fig. 1.1)[38]. Upon binding to the LGR5 receptor, RSPO suppresses ring finger protein (RNF)43/zinc and ring finger (ZNRF)3-mediated degradation of WNT receptors and induces sustained WNT activation, which is essential for LGR5+ cell homeostasis[39]. Although ubiquitously present, RSPO amplifies the local response to short-range WNT produced by Paneth cells[40]. Higher levels of RSPO1 have been found in the chicken jejunum and ileum as compared to the duodenum but the cause and downstream effects of this still need to be investigated[41].

Bone morphogenic protein

Bone morphogenetic protein (BMP) is most concentrated in the villi where it inhibits the WNT pathway and negatively regulates mitogenic stem cell activity (Fig. 1.1). Engagement of BMP receptors by BMP leads to complexes between SMAD1/5/8 and SMAD4 which repress stemness genes in the nucleus (reviewed in[35]). Numerous BMPs including BMP4 are expressed by mesenchymal cells but requirement for BMP antagonism in mouse enteroid cultures (devoid of mesenchymal cells) indicates BMPs must also be produced by epithelial cells[42]. Noggin, a homodimeric glycoprotein secreted by subepithelial myofibroblasts, actively antagonises BMP in the crypts to create a crypt-permissive environment and allow proliferation of ISCs[43].

Notch ligands

ISCs are critically dependent on contact with Notch ligands at all times to maintain an undifferentiated state. This is achieved via physical contact with Paneth cells which express Notch ligands delta-like ligands (Dll)1 and DII4. Conditional knockout of Dll1 and Dll4 in the intestinal epithelium causes loss of transit amplifying cells and ISCs through their differentiation into goblet cells[40]. Notch also regulates differentiation of cells into the secretory (Paneth, goblet or enteroendocrine cells) or absorptive enterocyte lineage through its target genes hairy and enhancer of split (HES)1, HES3 and HES5 which negatively regulate atonal homolog 1 (ATOH1)[44].

Epidermal growth factor

Epidermal growth factor (EGF) is a common growth factor in epithelial tissues where its pathway activation is considered essential for induction of intestinal stem and TA cell proliferation. Upon binding to the EGF receptor, EGF initiates the rat sarcoma virus protein (RAS)/extracellular signal-regulated kinase (ERK), mitogen-activated protein kinase (MAPK) and P13 K/AK strain transforming (AKT) signalling pathways, inducing hyperplastic changes in the intestinal epithelium. Leucine rich repeats and immunoglobulin like domains (LRIG)1 is a negative regulator of EGF signalling which when deleted causes

an increase in proliferative zones in the intestine (reviewed in[35]). Paneth cells in mice express EGF alongside WNT3a, transforming growth factor α (TGF) (a mitogenic polypeptide and member of the EGF family) and the Notch ligands Dll4 and Dll1 (Fig. 1.1)[40].

Very little is currently known about the molecules that influence IEC differentiation and homeostasis in the chicken, especially in the late embryonic and post-hatch period. Transcriptome analyses of the chicken intestine during this timeframe may reveal the biochemical cues that are required to grow and maintain the intestinal mucosa in this species.

1.1.3 Epithelial functions

Protective gut barrier

The intestinal epithelial layer forms the first line of defence against invading microbes and its protective properties include the mucus layer, antimicrobial peptides and IgA (Fig. 1.2). The epithelium is covered by a thick mucus layer largely comprised of heavily glycosylated mucin proteins which are produced by goblet cells. This mucoid coating comprises a loose outer layer associated with the microbiome, where some microorganisms use mucin as a nutrient source, and a more hostile inner layer with high concentrations of secretory IgA and antimicrobial peptides (Fig. 1.2). The inner layer is important for the innate immune response and will increase in volume in response to inflammation and infection. Its aim is to aggregate invading microbes and prevent their attachment to the intestinal epithelium (reviewed in[45]). Secretory IgA is the predominant immunoglobulin isotype secreted across the intestinal epithelial surface and acts to neutralize toxins and viruses, block excessive bacterial binding, clear macromolecular structures and sample luminal antigen (reviewed in[46]). Although the lamina propria located plasma B cells produce secretory IgA, intestinal goblet cells have been shown to be important for its storage in adult chickens. Goblet cells have also been shown to store maternal IgA, obtained from the egg yolk, in newly hatched chicks[47,48]. Since chicks have a rudimentary immune system, maternally transferred antibodies are extremely important to confer passive immunity to

the late embryonic and post-hatch stages until they can mount an effective immune response of their own.

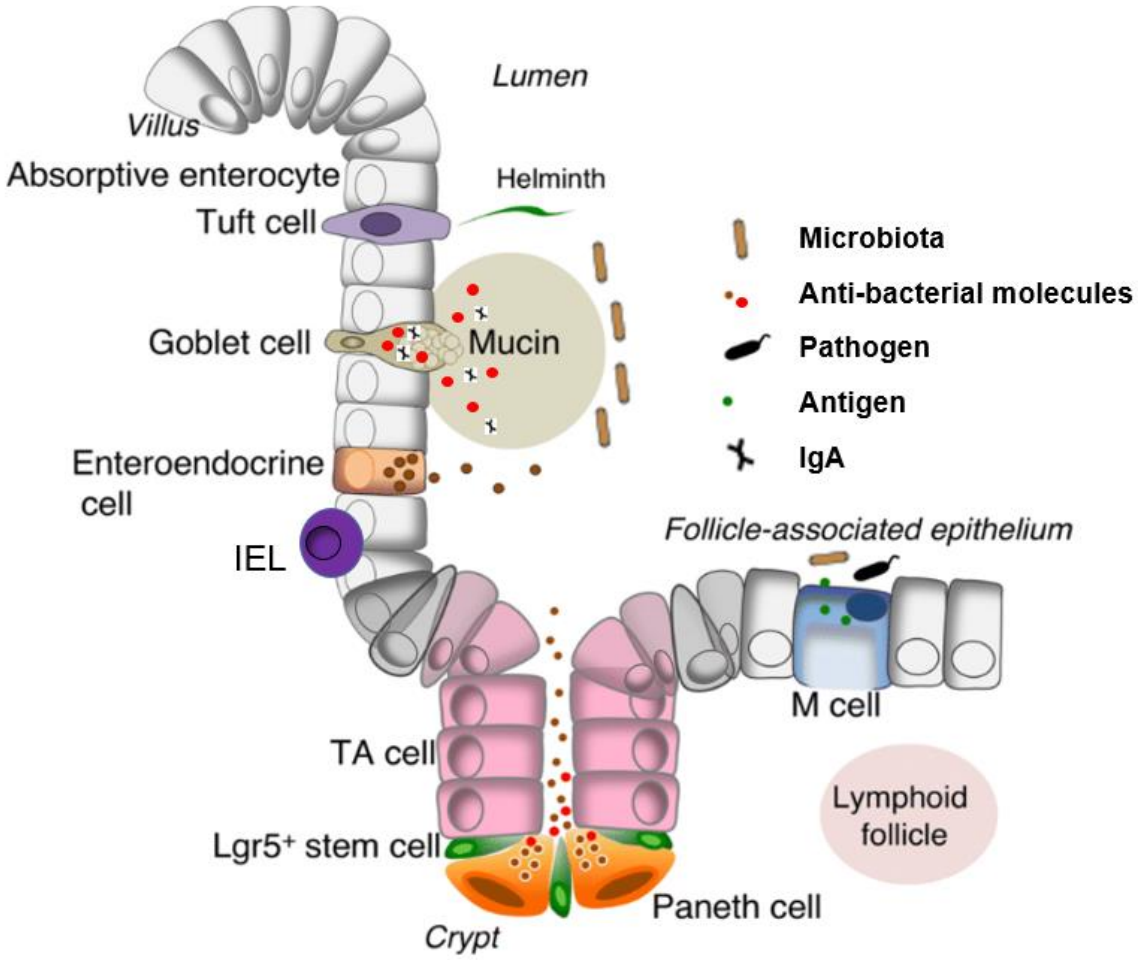

Figure 1.2: The intestinal epithelial barrier. A summary of many of the cellular and secretory components that make up the intestinal crypt and villus epithelial protective barriers. Adapted from Ohashi et al. (2019) under the terms of the Creative Commons Attribution License (http://creativecommons.org/licenses/by/4.0/) [49]

Avian IECs produce an array of antibacterial compounds at their surface including avidins, cathelicidins, lysozymes and β-defensins, all of which have demonstrated antimicrobial activity *in vitro* against bacteria, fungi and viruses (Fig. 1.2)[18,50,51]. Defensins interact directly with pathogen membranes, leading to the formation of pores that disrupt pathogen metabolism or structural integrity [52,53]. The chicken defensin repertoire is restricted to β-defensins of which fourteen β-defensin genes, called avian β-defensins

(AvBD), have been identified[54]. Chicken enteroendocrine cells been shown to produce AvBD9[55], and in mammals Paneth cells have been shown to secrete α- and β-defensins in addition to lysozyme and antimicrobial phospholipase A_2[15]. The AvBD are also produced by heterophils and macrophages and have been shown to be active against a wide range of avian pathogens [51,56,57,58,59,60]. In chicken primary IEC cultures, both avidin and lysozyme secreting cells were localized to the epithelial lining after stimulation with bacterial lipopolysaccharide (LPS) and lipoteichoic acid[18] . Lysozyme is a secreted protein with antibacterial and immunomodulatory properties including activation of pattern recognition receptors and leukocyte recruitment[61]. In the chicken three types of lysozyme have been identified in the small intestine; lysozyme *c* (LYZ) which is present in young birds but its protein levels are debatable in older birds, and lysozyme *g* (LYG) and *g2* (LYG2) which have been identified in chickens of all ages[16,17]. In the late-embryonic and post-hatch chick intestinal epithelium, lysozyme has been identified within three cell-types; goblet cells, cells within the crypts, and in rod-shaped enterocytes lining the villi[18]. Although the latter two cell types have not been functionally characterized they are predicted to be Paneth-like cells. In poultry, avidin has been demonstrated to be an acute phase protein produced by various cells and tissues in response to stress, thermal injury, and bacterial or viral challenge[62]. In chicken IEC cultures avidin staining has been primarily localized to goblet cells[18].

If the mucus layer is breached, microbes next encounter the IECs which form a mechanical barrier between food, toxins and bacteria in the lumen and the underlying tissues (reviewed in[63]). In order to perform this essential function, multiple junctional complexes such as adherens junctions, tight junctions, desmosomes and gap junctions, form tight seals between the IECs and help to control paracellular transport[64]. The molecular structure of the junctional complexes and structural proteins levels can be altered by diet derived compounds, dysbiosis and enteric pathogens[65,66,67]. A loss of intercellular junction integrity can result in decreased nutrient absorption, increased secretion of ions and water causing diarrhoea, and an influx of

macromolecules from the lumen which can induce intestinal inflammation (reviewed in [68]).

Digestion and absorption

The essential function of the intestine is digestion and absorption of food. In poultry, diets needs to be high quality and easily digestible due to the relative simplicity of their digestive system and to attain expected productive performance[69]. Enterocyte membrane-bound enzymes carry out the final stages of digestion at the brush border of the small intestine. Carbohydrates (maltose and small oligosaccharides) are quantitatively the most important fraction of pelleted chicken diets and are broken down to monosaccharides (of which ~80% are glucose) by maltase-glucoamylase and sucrase-isomaltase. Aminopeptidase-N hydrolyses peptides into amino acids. Fats, primarily triacylglycerols and phospholipids, are broken down by lipase to fatty acids which then reform into lipoproteins within the epithelial cells and are transported to the lymphatic system as chylomicrons.

The contents of the residual yolk are transferred to the hatchling via the blood and intestine for up to 72 h post-hatch[70]. The yolk primarily consists of lipids and proteins and is an important source of nutrients for intestinal development. There is a selective hierarchy at this age for fatty acid uptake over glucose or amino acids[71]. However, due to the nature of precocial species, the embryonic intestine has been shown to be capable of digesting and absorbing disaccharides and peptides from ED19. Indeed, RNA expression of brush border enzymes sucrase-isomaltase and peptidase, and the major transporters sodium-glucose transporter and ATPase, have been found in the avian intestine from ED15. Gene expression of these enzymes and transporters increases into the post-hatch period and their biochemical activities start to increase on day of hatch[8,28,72]. In contrast, mammals only develop the ability to digest food rich in complex carbohydrates at the suckling-to-weaning transition, which starts at 2 weeks postnatally in mice.

The embryonic gastrointestinal tract of precocial birds undergoes dramatic development within the first 24 h of hatch. During this time the epithelial layer

develops many of its adult functions including digestion and absorption of nutrients and protection against bacterial flora and food antigens in the lumen. Knowledge of epithelial functions at this fragile lifestage are relevant to enable adequate protection from infectious disease and optimise nutritional requirements.

1.1.4 Epithelial immune responses

Enterocytes

Enterocytes are multifunctional epithelial cells which actively regulate the induction and coordination of enteric immune responses to appropriate microorganisms. They enable the discrimination between pathogens and commensal microbiota through a set of pattern recognition receptors, including lectins, tag, Toll-like receptors (TLR) and nucleotide-binding oligomerization domain-like receptors (NLR), which recognize conserved bacterial and viral motifs[73]. In a homeostatic state the chicken intestinal microbiota is a diverse population of symbiotic bacteria, archaea and fungi which the epithelial cells can directly sense via micro-associated molecular patterns and metabolites (Fig. 1.2)[74]. The composition of the intestinal microbiome is multifactorial and can be influenced by diet, biological agents, host genetics, infection and host stress. Dysregulation of the microbiota is associated with a number of physiological diseases and the host immune response is important in maintaining the microbial balance. Unlike mice who are colonized after birth, both commensal and pathogenic bacteria are present in the avian intestine from ED17[75]. By binding to pattern recognition receptors on IEC these symbiotic microorganisms are believed to play important roles in gut development and differentiation, host metabolism and inducing local innate defences[76,77]. The microbiota is also important for shaping, educating and developing host whole body immunity which has been evidenced in chickens[78,79]. In addition, the microbiota directly act as a protective barrier separating the luminal side of the intestine from subepithelial tissues and restricting the outgrowth of opportunistic infections[80,81]. The aim of many poultry probiotic cultures is to manipulate this

gut barrier function by binding to the intestinal epithelial surface and inhibiting the attachment and colonization of pathogenic species. Addition of probiotic bacteria to the diet can also contribute to an increase in bioactive molecules beneficial for enterocyte growth and development, and improve intestinal barrier function[82].

The IECs of one day old chicks have been shown to express *TLR2* and *TLR4* and induce a myeloid differentiation primary response 88 (MYD88)-dependent signaling pathway after stimulation with LPS or LTA[18,83]. These inflammatory pathways will lead to a variety of functional outputs including activation of nuclear factor-kappa B (NFκB) and the production of cytokines. Pro-inflammatory cytokines and chemokines are important for maintaining homeostasis and defending the epithelial surface through recruitment of leukocytes and facilitating antigen presentation to immune cell populations (reviewed in[84]). Chicken IECs have been shown to express and secrete various cytokines and chemokines after exposure to pattern recognition receptor agonists. These include interferon (IFN)λ in response to avian influenza virus (AIV)[85]; Interleukin (IL)-1β, IL-6, chemokine (C-X-C motif) ligand 1 (CXCLi1) and IL-8 (CXCLi2) in response to *Campylobacter jejuni*[86]; and IL-10 in response to *Clostridium perfringens*[87]. Although yet to be confirmed in chickens, murine enterocytes also express major histocompatibility (MHC) class I molecules and under inflammatory conditions can be induced to express MHC class II molecules. This allows them to directly interact with both $CD8^+$ and $CD4^+$ $TCR\alpha\beta^+$ T cells in the lamina propria. Interactions with $TCR\gamma\delta^+$ T cells can also be mediated by non-classical MHC molecules on epithelial cells or, during epithelial damage, by expression of stress molecules. In mice these interactions are considered potentially important in regulating epithelial homeostasis and the response to enteric challenge [88 89,90].

Intraepithelial leukocytes and heterophils

IELs are a highly heterogeneous group of cells which form a component of the GALT (Fig. 1.2). Their position in the epithelial layer allows them direct

access to pathogens, food proteins and other foreign antigens, indicating they play a role in innate immunity. Their numbers increase during intestinal inflammation and infection, with studies in mice showing the importance of enterocyte-expressed chemokines in the recruitment and retention of IEL cell populations (reviewed in[6])[91,92]. Few heterophils are found within the intestinal epithelium of healthy chickens but these cells are important components of the innate immune system and will translocate across the epithelial barrier during infection [93,94]. Heterophils can detect (through a wide spectrum of TLRs) and kill invading pathogens as well as recruit other immune cell types to sites of inflammation[95]. In 1 day old chicks these cells show lower phagocytic and bactericidal capacities compared to those at 4 and 7 days old[96].

M cells

Immunogenic antigens can gain access to the GALT by passing through specialized epithelial cells called M cells (Fig. 1.2). The function of M cells is to phagocytose and transcytose lumen microorganisms, macromolecules and other particulate antigens, and pass them to antigen-presenting cells in intraepithelial pockets. M cells are critical for induction of specific mucosal immune responses and balance appropriate tolerogenic and/or inflammatory responses to food antigens, commensal bacteria and pathogens (reviewed in[20]). Avian M cells appear to resemble mammalian M cells in terms of antigen transcytosis and their ultra-structure but are limited in the size of microparticles they can uptake[21,97].

Goblet cells

Goblet cells are not only responsible for production of the protective mucus layer but in mice they have also been shown to sense and actively sample microbiota. The bacteria are transferred to nearby DCs which imprint gut homing on lymphocytes and induce regulatory T cell development and IgA production[98,99]. In addition, the enterocyte polymeric immunoglobulin receptor which mediates directional transport of IgA across the epithelium, has been shown to be stored in goblet cells in the chick[18]. This receptor shows

increased expression on the basolateral epithelial surface in response to bacterial stimulus in chickens, indicating a local inflammatory driven increase of IgA transport into the lumen[100].

The induction of intestinal inflammation in response to dysbiosis and pathogen challenge are particularly important issues for the poultry industry since a ban on antimicrobial growth promotors was introduced in the European Union in 2006 (Regulation (EC) No. 1831/2003). Much of what we currently know about IEC immunology stems from studies in mammal, therefore research to elucidate the similarities and differences in the chicken would be useful for the development of poultry-specific gut barrier interventions.

1.2 Overview of the chicken intestinal lamina propria

1.2.1 Lamina propria architecture

The intestinal mucosa is composed of the epithelial layer, a secreted layer of extracellular matrix (ECM) on which the epithelial cells sit called the basement membrane, and a thin layer of connective tissue located beneath these called the lamina propria. The loose structure of the lamina propria is made up of mesenchymal, neural, immune and vascular cells within a collagen framework, which cooperate to supply immune responses, nutrients, paracrine signalling and an ECM to the intestine[101,102,103,104]. In 1 day old chickens the lamina propria contains few lymphocytes, capillaries, lacteals, reticular and muscles fibres however this layer matures rapidly and by 17 days post-hatch all cell populations have significantly increased[105].

Myofibroblasts

Myofibroblasts have characteristics of both smooth muscle and fibroblasts and are typically identified by their intracellular cytoskeletal proteins e.g. α-smooth muscle actin (α-SMA), vimentin (VIM) and desmin, their structure, their sub-epithelial location and the absence of epithelial cytokeratins[106]. Other mesenchymal elements of the small intestinal lamina propria also have

α-SMA as a marker including mural cells, bone-marrow derived stromal stem cells and smooth muscle fascicles from the muscularis mucosa. Smooth muscle fibres are present within the villus core, surrounding the lacteal ducts which lie beneath the basement membrane and act to propel lymph away from the periphery (reviewed in[104]).

Blood and lymph vessels

Rich complex capillary networks populate the lamina propria of the intestinal villi, with patterns varying amongst species[107]. In general there is a single eccentrically placed arteriole which runs in parallel with the muscle fibres. This forms a capillary tuft-like network at the villus tip which anastomoses with the single eccentrically placed venule[108]. The arterioles originate from the arterial plexus in the submucosa, which branches from larger vessels which encircle the musculature of the small intestine. Small veins generally run parallel to the arterial circuitry and eventually drain venous effluent into the portal vein. The lymph vessels draining the gastrointestinal tract run close to the blood vessels with frequent anastomoses between the two[109].

The enteric nervous system

The enteric nervous system encompasses a vast network of interconnected ganglia found within the outer myenteric plexus and inner submucosal plexus. It is involved in numerous intestinal functions including controlling secretion of fluids and electrolytes, blood supply to the gut wall, and peristalsis. In the chicken, neuronal colonization of the gut and the formation of ganglia is completed by ED7 – 8[110]. Enteric neurons in both mammals and chickens are restricted to the ganglia but afferent and efferent nerve endings can reach into the lamina propria, all the way to the tips of the villi[111,112]. Enteric glial cells have been detected in the chick gut as early as ED4.5, and are present in the ganglia but also later colonise extraganglionic sites including the intestinal mucosa[113,114].

The gut-associated lymphoid tissues

The GALT of a chicken is composed of individual lymphoid cells in the epithelial lining and lamina propria as well as an organized series of solitary or aggregated lymphoid follicles (previously described in 1.1.1 and 1.1.3) located in the lamina propria, Meckel's diverticulum, Peyer's patches and caecal tonsils [115,116,117,118]. Since there is lack of draining lymph nodes in birds, the study of fundamental gut immunology in these species is severely limited[119]. Transgenic chickens, with colony-stimulating factor 1 receptor (*CSF1R*)-reporter genes that are specifically expressed at high levels in cells of the myeloid lineage, have been developed to permit visualisation of the Peyer's-like patches along the intestine and of more organised lymphoid tissues[21,120].

The gut lamina propria is highly concentrated with a diverse range of leukocyte populations, including heterophils, macrophages, DCs, NK cells and lymphocytes of the B and T cell lineages. The composition of the gut-associated immune cell populations varies dependent on intestinal locality, microbiota, diet, host genetics, age and exposure to pathogenic microorganisms. The most commonly found lymphocytes are B and T cells (~90%) with the remainder being NK cells. Most B cells in the lamina propria have undergone class switching to the secretory IgA isotype. In mature birds the T cell population has ~10% TCRγδ T cells and the larger TCRαβ T cell population is dominated by $CD4^+$ T cells, with a less prominent $CD8^+$ cell population.

At hatch the GALT is poorly developed but over the first 3 – 4 weeks of age there is a rapid increase in the size and cellular complexity of the lamina propria, IEL compartments and other defined intestinal lymphoid locations[1,121,122,123]. This proliferation of immune cells is predominantly directed by the enteric microflora population which colonise the gut. Indeed, germ-free chickens possess different T cell repertoires than chickens raised in conventional conditions[81,124]. The first wave of thymic TCRγδ T cells arrive at the periphery at ED15 - 17 closely followed by TCRαβ T cells at ED18 -

20. The second and third waves start around the time of hatch and 6-8 days post-hatch respectively, with TCRγδ subsets always preceding TCRαβ expressing T cells by ~2 days[125]. Bursal B cells begin to emigrate to the periphery around ED18[126]. The proportion of TCRαβ and CD4+ T cells increases with age until they predominate at 14 days post-hatch. CD8+ T cells are then elevated at 21 days, and B cells constitute the most abundant cell type in the lamina propria by 42 days post-hatch[27,122]. Both B and T lymphocytes are considered functionally immature at hatch with mature functions appearing in two phases around the second week post-hatch[123].

Innate immune cell populations develop in the chicken much earlier with macrophage phagocytic activity reported in the liver and spleen at ED12 and ED16 respectively, and large numbers of heterophils and monocytes present in the blood at hatch[127,128]. NK cells in poultry arrive in the periphery before T cells and a subset has been identified in the chicken lung and spleen at ED14[129]. They are considered to be an early line of immunological defence demonstrating non-MHC restricted spontaneous cytotoxicity during infections (reviewed in[130]). A rich source of NK cells in the chicken besides the embryonic spleen are the intestinal IELs which have been identified in ED19 embryos[131].

1.2.2 Lamina propria functions

Myofibroblasts

As mentioned in section 1.1.2, the mesenchymal cells play an important role supporting the ISC niche. They secrete non-canonical WNTs and WNT agonists to drive proliferation of the intestinal epithelium, WNT antagonists to control abnormal activity of this pathway, and BMP antagonists to stop epithelial differentiation in the crypts (reviewed in[132]). In mice, these cells also play important immunosuppressive and immunostimulatory roles in both the innate and adaptive immune response. They express TLRs which when engaged will induce expression of pro- or anti-inflammatory mediators, and aid in the recruitment of leukocytes to the site of inflammation. Expression of

MHC class I and II molecules also allows mesenchymal cells to specifically modulate the activity of lymphocytes (reviewed in[133]).

Blood and lymph vessels

Due to the high level of metabolic activity of the mucosal layer, this site receives 80% of the total intramural blood flow. The microcirculations of the lymphatic and vascular networks in the mucosal layer support important intestinal functions including secretion, the removal of absorbed water and chylomicrons, and engagement of adaptive immune responses through transport of immune cell populations.

Glial cells

Enteric glial cells play an array of critical roles including the support of neurons, regulating synaptic transmission, and mediating communication between neurons and the immune system. In the mouse intestinal mucosa this highly dynamic cell population is also thought to maintain the intestinal epithelial barrier and regulate mucosal immune responses[134]. Enteric glial cells can express TLRs and are a major target of the gut microbiota, who are thought to regulate the establishment, ongoing supply and turnover of glial networks within the gut wall[135].

1.2.3 Lamina propria immune response

Cells involved in the acute phase of infection

The intestinal immune system is complex, coordinating multiple cellular and non-cellular components of the innate and adaptive immune systems within the epithelial and lamina propria layers of the intestinal mucosa. The non-cellular innate immune elements include the previously described physical and chemical barriers e.g. tight junctions and mucin; antimicrobial proteins e.g. cryptidins and β-defensins; cytokines and chemokines; TLRs and NLRs; and enzymes e.g. peptidase and lipase (Fig. 1.2). In the lamina propria, the cellular components of innate immunity include cells of the mononuclear phagocyte system (Fig. 1.3). This is a network of macrophages, DCs and

monocytes which coordinate the innate and adaptive immune responses in order to maintain organ homeostasis. Tissue resident macrophages function to clear cell debris, engulf and eliminate harmful pathogens, resolve inflammation and modulate immune responses. DCs and macrophages can initiate the adaptive immune response through antigen presentation and prime the immune system to pathogen infection or toxin exposure. Monocytes circulate around the body where they can differentiate into macrophages in response to stimulatory signals or acquire antigen presenting abilities (reviewed in[136]). In the early phases of intestinal infection an infiltration of heterophils are also recruited to the lamina propria to aid in the elimination of harmful pathogens[137]. In mature chickens, NK cells and TCRγδ T cells are also considered important in the acute phases of gastrointestinal infection, helping to limit the establishment and spread of microorganisms (Fig. 1.3).

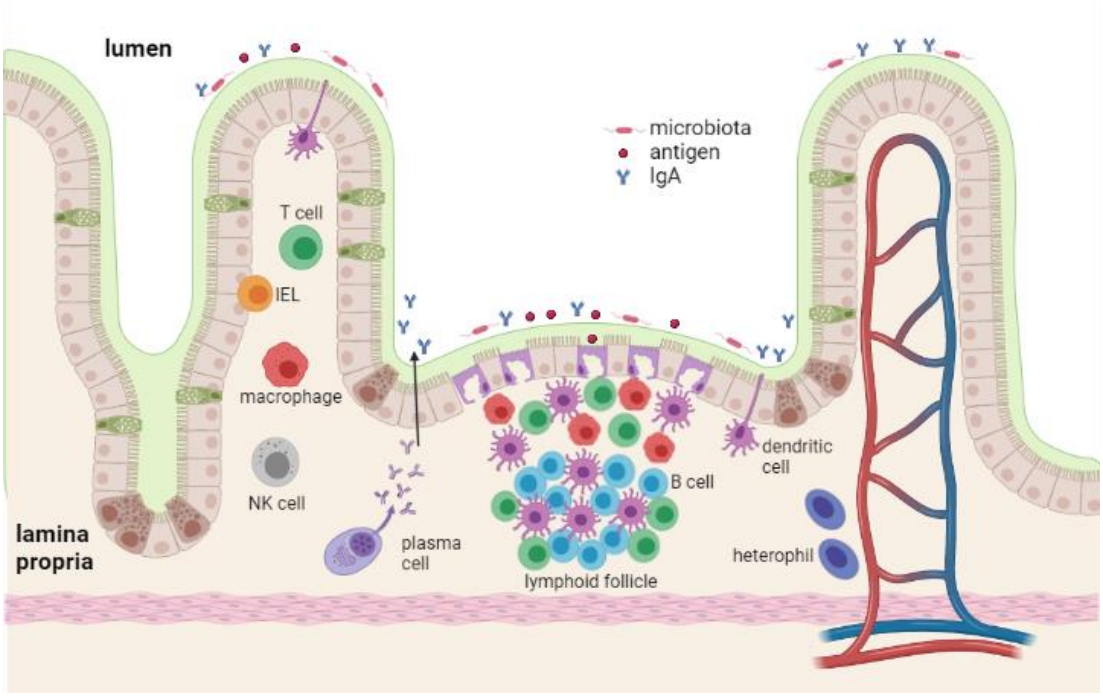

Figure 1.3: Immune cells of the lamina propria. Lamina propria leukocytes involved in early and late response to infection including tissue-resident macrophages and NK cells, antibody-producing plasma cells, T and B cells of the lymphoid follicles, and infiltrating heterophils. Created in Biorender.com by E. Nash.

Cells involved in later stages of infection

Activated TCRαβ (CD8+ and CD4+) T cells and B cells tend to infiltrate the lamina propria and IEL to help resolve infections at later stages (Fig. 1.3). Plasma B cells produce antibodies which agglutinate with and neutralize pathogens. CD8+ cytotoxic T cells primarily act to recognise and destroy pathogens through release of perforins and granzymes. In mice they also enhance the release of IFNγ, tumour necrosis factor (TNF)-α and TNF-β to promote macrophage activation, although in chickens TNF-α is in induced in CD4+ but not CD8+ T cells[138]. CD4+ helper T cells (Th) are responsible for the coordination of inflammatory immune responses through cytokine release (reviewed in[139]). The type of invading pathogen will activate different CD4+ subsets so, for example, Th1 responses defend against intracellular pathogens including viruses and bacteria, whereas Th2 cells are mostly associated with extracellular pathogens such as parasites[140]. The CD4+ Th cell subset repertoire in mammals has been expanded to include regulatory T cells (Treg), Th17, Th9 and follicular T helper cells[141]. Whilst chicken Th1, Th2 and Treg immune responses have been described, little is known about the other Th cell subsets in birds[142,143].

Nuances in the post-hatch chick

Chicks have immature immune systems in the neonatal period which makes them highly susceptible to infectious diseases. For example, *Salmonella enterica* serovar Enteritidis and *S.* Typhimurium cause severe systemic symptoms and high mortality in chicks less than 3 days old. In contrast these pathogens are restricted to the gut and cause relatively little clinical disease when chickens are over 2 weeks old[144,145]. Embryonic and neonatal chicks can mount their own humoral responses to antigen however these are generally at very low ineffective levels. They instead rely on protection offered by maternal antibodies from the yolk. High titers of maternal specific IgY, either from natural infection in hens (likely only those present at time of lay) or immunization, has been shown to protect chicks from *Eimeria, Salmonella* and *Camplyobacter* infection[146,147,148]. These maternal antibodies

will offer some cover for up to 3 weeks post-hatch although most are depleted by 10 days of age. Fortunately the reducing maternal antibody levels coincide with a marked development of the chicks own IgA secreting plasma B cells. These cells continue to increase in number until 4-6 weeks post-hatch and result in a large pool of IgA antibodies for the growing birds. The dramatic differences in infection biology post-hatch are demonstrated in challenge experiments using immunized or recently infected hens whose progeny display lower levels of infection when compared to progeny from control birds[146,147,148].

To study post-hatch immunity and gut maturation *in vitro,* detailed knowledge of the architecture and function of the intestinal lamina propria cell populations in the peri-hatch chick is required. The development of *CSF1R*-reporter transgenic birds and an increasing array of poultry-specific leukocyte antibodies are slowly improving our understanding of the intricacies of the chicken GALT. However much more research is required to describe the array of intestinal responses in the chicken in health and disease.

1.3 *In vitro* livestock species intestinal models

1.3.1 Importance of intestinal *in vitro* models in poultry

Emerging infectious diseases

Research in avian species is a global economic imperative and directly addresses the UN Sustainable Development Goals of no poverty, zero hunger and good health and well-being. Poultry constitute a major human food source and over the last 20 years global poultry production has tripled with approximately 107 million tonnes of chicken meat and 1.3 trillion eggs now produced every year[149]. Expansion of the industry is predicted to continue for at least 30 years, with most growth in Africa and Asia[150]. With intensification in both the informal and organised poultry sectors, pathogen variants with increased virulence, vaccine and/or antimicrobial resistance and broadened host ranges are becoming major issues. High stocking densities, fast turnover, genetic homogeneity, complex transport and trading networks,

live bird markets, poor biosecurity and inappropriate use of antimicrobials and vaccines all play roles in host-pathogen evolution. Of particular concern are zoonoses such as AIV and food-borne *Campylobacter* and *Salmonella* for their effects on public health[151]. The development of comprehensive species-specific intestinal cultures would improve the research community's ability to study species jumps of zoonotic enteric pathogens, as recently demonstrated with the modelling of SARS-Cov-2 in human and bat 3D gut models[152].

Antibiotic-free poultry production

Sustainable production of poultry meat and eggs requires the protection of chickens against a wide range of pathogens. This is becoming more challenging for the poultry industry with the increasing implementation of antibiotic-free poultry production. These antibiotic-free programs are essential to combat antimicrobial resistance in humans, however to be successful and sustainable for the poultry sector they require the development of a much better understanding of concepts related to poultry intestinal health. This includes not only feed and housing issues but also the non-antibiotic based control of enteric pathogens. Consequently one of the main methods of disease control and prevention in poultry are mucosally administered vaccines. In order to formulate effective vaccines a detailed understanding of how antigens are first acquired across the chicken's epithelium and how certain chicken-specific pathogens infect the gastrointestinal tract is required. Such species-specific pathogens include the protozoan *Eimeria* which infects the poultry intestine causing significant impacts on animal health, welfare and the economy. This organism only infects specific locations in the poultry intestine therefore invasion mechanisms are difficult to comprehensively study *in vitro* without species- and intestinal site-specific models.

Commercial tools

High-throughput intestinal *in vitro* tools are of particular interest for poultry pharmaceutical companies since the gut is the target for many important

pathogens and therapeutics. The current paucity of appropriate models for poultry means much industry research and product development is conducted in live birds, and large flocks of chickens are required for screening and production of *Eimeria* spp. vaccines. The intestinal epithelium is also important for nutrient absorption, formation of a protective barrier and active regulation of host-microbiota interactions which all contribute to maintain flock health and productivity. Therefore, the production of high-throughput intestinal screening tools to analyse the effects of bioactive compounds and microbiomes on the chicken intestinal barrier integrity and digestion are highly sought after by industry.

The 3Rs

Almost 200 million animals are estimated to be used in research and development experiments globally each year and birds make up a small but not insignificant 6% of total animal use. Chickens are predominantly used when birds are needed for a physiological study as they are easy to keep, and have been bred domestically for many years so a lot is known about their physiology. Research on most poultry pathogens is still performed using small groups of live birds, and chicken embryos and monocultures of their cells e.g. fibroblasts and stem cells, are well-defined models for cell biology studies (reviewed in[153,154]). As model animals, chickens are easy to access throughout the year and around the world and, as embryonic development occurs outside the body of the mother, they can be used to study all stages of development e.g. limb and nervous system. Embryonated eggs are also used in the production of vaccines by injecting virus into the allantoic fluid, allowing the virus to replicate and harvesting the fluid. This method has been used over the years to develop vaccines for chickenpox, smallpox and yellow fever and current manufacturing processes to produce influenza vaccines require millions of eggs[155]. Despite the obvious advantages to using live animal models, ethical concerns on the use of animals in research are rising. The global trend to reduce animal trials has resulted in an urgent need to develop comprehensive lab models whose results can be easily extrapolated to a living animal. *In vitro* models allow the provision of data to better define

hypotheses and optimise experimental plans, leading to replacement, reduction and/or refinement of animal numbers required *in vivo* (the 3Rs principles). In addition, they will allow more rapid, better controlled and more easily upscaled testing and/or production of therapeutics.

1.3.2 Intestinal *in vitro* models in livestock species

Cell lines

In vitro gastrointestinal studies in livestock species have long been hampered by a lack of representative *in vitro* cell culture tools. Intestinal *in vitro* studies have historically used cancer-derived or immortalized mammalian cell lines such as human Caco-2 and human HT29 colorectal adenocarcinoma cells. These cell lines have been in use for a long time and are cheap, easy to access and grow, and can be analysed using currently available technologies. However immortalised IEC lines lack cellular heterogeneity, do not reproduce full tissue functionality, and typically evolve chromosomal aberrations and mutations during continuous passage which can affect growth, metabolism, physiology and reproducibility[156]. In addition, since they are not species-specific for livestock species studies, they are not suitable for the study of species physiology or the interaction of species-specific intestinal pathogens with the intestinal epithelium.

Several non-transformed continuous porcine small intestinal cell lines have been established including IPEC-J1 from the ileum and jejunum, IPEC-J2 from the jejunum and PSI from the small intestine[157]. However these porcine lines exhibit extraordinarily high trans-epithelial electrical resistance (TEER) values (a measure of tight junction dynamics in cell culture) and low epithelial transport rates, unless cultured under defined species-specific conditions, making them less suitable for virus, nutrition and toxicology research[158,159]. Immortalized bovine small intestinal enterocyte cell lines have also been developed from fetal tissue although when characterised they were shown to have a low density of microvilli compared to the adult intestine[160,161]. The only established epithelial cell line in the chicken is the lung epithelial cell line (CLEC)-213[162].

Primary intestinal epithelial cell cultures

Ex vivo cultures of intestinal tissue explants and primary isolated IECs are closer in phenotype and function of *in vivo* tissues than immortalized cell lines and are therefore more capable of recapitulating key features of animal physiology and host-pathogen interactions. However, they are difficult and expensive to prepare and maintain and undergo senescence, cell death and necrosis over relatively short timespans (some after only 24 – 48 h) introducing concerns over the accuracy and reproducibility of biological experiments. A standard optimised isolation protocol for chicken primary small intestinal cultures does not exist but several groups have published methods. This includes an ED18 chicken IEC culture developed in 2004 which was used to investigate *E. tenella* infections and contained cells positive for epithelial-marker cytokeratin and epithelial adhesion marker cadherin1[163]. Monolayers with improved morphology have since been obtained from embryonic and adult intestines however these degenerate after 7 - 10 days in culture[164,165]. Adult IEC chicken cultures were maintained for 6 - 7 passages by Rath et al. (2018) however these were shown to have an atypical intercellular junction morphology[166]. A more recent primary IEC culture showed survivability for 12 days when growing the monolayers on a Matrigel-coated surface and using medium supplemented with sodium butyrate (which promotes the absorptive lineage), RSPO1, Noggin and CHIR99021(all canonical β-catenin/WNT pathway inducers), and EGF (to maintain proliferation). The epithelial nature of the cells was confirmed by staining for villin and cytokeratin, and intercellular tight junctions were identified using zonula occludens 1 (ZO1) and occludin (OCLN) markers. These cultures maintained appropriate TEER measurements indicating their application for cell barrier studies[167]. IEC cultures derived from ED17 chickens have been also been used in innate immunity studies to investigate inflammatory responses to bacterial products[18]. Primary cultures of jejunal intestinal cells expressing brush border and cytokeratin markers have also been described for the bovine[168].

Tissue explants

Although epithelial cell culture models are useful to measure barrier function and epithelial immune responses, they are limited in their ability to study leukocyte and other lamina propria cell interactions. Intestinal tissue explant models allow the investigation of short term inflammatory and secretory responses of the entire gut mucosa to external challenge. These tissue culture systems have been described for the pig[169,170] and bovine[171] small intestine mainly for studies on enteropathogens. However few groups have published explants of gastrointestinal tissue for the chicken. Chicken ileal explant models have been used to measure nitric oxide (NO) production, epithelial inflammatory markers (*TLR4, IL-1β, IL-8*) and epithelial secretory responses (mucin (MUC)2, IgA and polymeric immunoglobulin receptor) after stimulation with LPS[172,173]. However these cultures were not viable for long enough to evaluate tight junction responsiveness[173].

Ligated intestinal loop models

Ligated intestinal loop models are *in vivo* tools yet they markedly reduce the number of animals required for experiments so are briefly discussed. Gut loop segments in a single anaesthetised animal are ligated to form independent and hermetic compartments whilst the animal is under general anaesthesia. Experiments are performed within each loop e.g. injection of pathogens into the lumen, and samples for further analysis are collected a few hours of continuous general anaesthesia later. These models allow the use of multiple treatment and control groups in the same animal thereby reducing the number of hosts required to obtain significant results. In addition, any pain is controlled by general anaesthesia thus reducing ethical concerns when conducting pathogenesis experiments on live animals. These techniques are not commonly employed but they have been described in both calves and chickens[174,175].

Intestinal organoids and enteroids

Three-dimensional organoids are long-term self-renewing culture systems with the ability to simulate *in vivo* organ morphology and physiology, and hence are replacing traditional *in vitro* models in many areas. Organoids are multicellular clusters that contain a subset of self-renewing stem cells. The stem cells grow and self-organize into miniature spheres that undergo cell differentiation, eventually recreating 3D tissue-like structures with biological functions similar to the living organ. Over the past decade methods for generating organoid culture systems have been published for most human and mouse organs including intestine, lung, liver, kidney, and brain (reviewed in[176]).

Intestinal organoids and enteroids replicate much of the complexity of the gut epithelium. Enteroids are typically epithelial only and are developed from intestinal tissue containing adult ISC. These adult ISCs can originate from the tissue of juveniles and late stage embryos and are intrinsically programmed with their location specific functions[177,178](reviewed in[179]). Intestinal organoids often contain epithelial and mesenchymal cells and are typically developed from induced pluripotent or early embryonic stem cells. Embryonic stem cells are obtained from the inner mass of pre-implantation embryos whereas induced pluripotent stem cells are generated by reprogramming differentiated somatic cells e.g. skin fibroblasts, to regain pluripotency[180]. The induction cues needed to differentiate intestinal organoids from pluripotent stem cells have not yet been determined for livestock species so currently their 3D cultures are all derived from adult ISC.

Propagation of primary adult intestinal crypt cultures was initially achieved in 1992 when Evans et al. (1992) cultivated murine crypt epithelial cells on collagen in the presence of contaminating mesenchymal fibroblasts[181]. The expertise to grow self-organizing continuously expanding enteroids in a mesenchymal-free environment was first developed in the mouse in 2009[43]. Since then intestinal organoids and enteroids have been developed in various mammalian species using the same concepts as the murine culture

system[182,183,184](reviewed in[185]). These 3D models already facilitate research into basic biology, disease modelling, precision medicine and therapeutic development, proving to be more physiologically relevant than traditional monolayer culture techniques (reviewed in[35]). Indeed, transcriptome analysis of porcine jejunal enteroids showed their cellular diversity was more representative of the pig intestinal epithelium than that of the pig IPEC-J2 cell line which does not express enterohormone or mucin markers[186]. In addition, bovine enteroid cultures have been compared back to bovine small intestinal crypts and have shown high similarity with the tissue of origin[183].

Most current *in vitro* models for gastrointestinal studies are limited by their lack of species-specificity, cellular heterogeneity, intestinal architecture and/or long-term viability. Enteroid models appear to address many of these issues therefore development of such a physiologically relevant model for the chicken would be useful for both the poultry research community and poultry industry.

1.4 Development of livestock enteroid models

1.4.1 Culturing livestock enteroid models

Crypt isolation and embedding in Matrigel

Organoid models are a developing field, therefore a diverse array of enteroid culture methods for livestock species are in use across laboratories with no widely accepted standardized protocols. The isolation of intestinal crypts containing adult ISCs is achieved in most species using dissociation buffers containing various concentrations of ethylenediaminetetraacetic acid (EDTA) and dithiothreitol with a range of species- and digestive-segment specific incubation times and temperatures (reviewed in[185]). Once isolated the crypts are then typically embedded in a decellularised ECM called Matrigel which is set in the form of a small hemispherical gel dome attached to the base of a tissue culture well (Fig. 1.4). Matrigel is a complex mouse Engelbreth-Holm-Swarm sarcoma extract whose exact composition is unknown but variably contains ~60% laminin, ~30% collagen type IV, 8% entactin/nidogen, heparin

sulfate proteoglycans and growth factors such as TGF-β, insulin-like growth factor (IGF) and fibroblast growth factor (FGF) (reviewed in[187]). Matrigel is limited in its reproducibility and therefore applicability for high-throughput analysis due to inter-batch and between-batch mechanical and biochemical variability. It is also not amenable to manipulation to explore physical (density, stiffness and viscoelasticity) and biochemical ECM factors that govern stem cell expansion and organoid formation[188]. Therefore, although Matrigel is still used in most research laboratories, synthetic ECM alternatives have been developed which are xenogenic-free, chemically defined, highly tuneable and reproducible (reviewed in[189]).

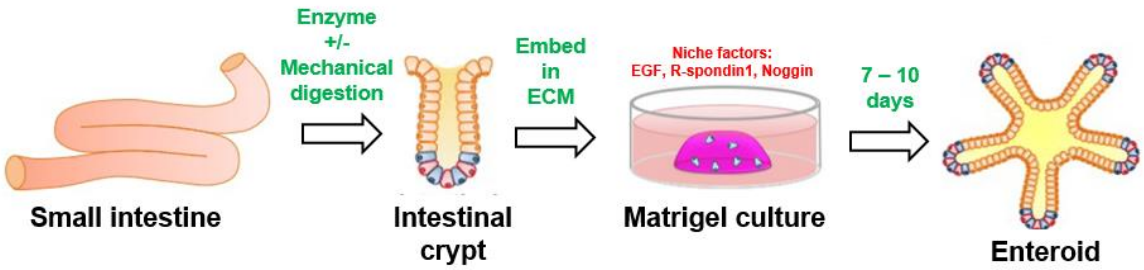

Figure 1.4: Method for culturing enteroids in Matrigel. Intestinal crypts are isolated from the small intestine using a combination of enzymatic and mechanical digestion. The crypts are embedded in a dome of Matrigel and surrounded by a media containing essential growth factors, enabling them to develop into enteroids over 7 - 10 days. Adapted from Chusilp et al. (2020) under the terms of the Creative Commons Attribution License (http://creativecommons.org/licenses/by/4.0/)[190].

Growth factors

The embedded crypts are surrounded by media usually containing defined external growth factors which most commonly include EGF to enhance intestinal epithelial proliferation, Noggin to antagonise BMP and induce crypt expansion, and WNT agonist RSPO1 which increases crypt proliferation (Fig. 1.4)[42,43]. Additional niche factors are often needed to recapitulate the ISC self-renewal and differentiation hierarchy dependent on the species. In man these include WNT3a, nicotinamide, a TGF-β inhibitor (typically anaplastic lymphoma kinase 4/5/7 inhibitors LY2157299, A8301 or SB43542 which promote WNT-driven cell proliferation) and a p38 MAPK inhibitor (SB202190

which suppresses secretory lineage differentiation so as not to deplete the ISCs)[42]. Long-term porcine and bovine cultures also require p38 MAPK inhibitors and TGF-β receptor inhibitors in part to limit epithelial mesenchymal transition (EMT)[191]. p160 rho-associated protein kinase (ROCK) inhibitor e.g. Y-27632 is commonly used for the first 2 - 3 days of culture and during crypt isolation to reduce dissociation-induced apoptosis in stem and epithelial cells[183,184,192]. Fetal bovine serum (FBS) has been used as an undefined but potent source of growth factors, and CHIR99021, a glycogen synthase kinase 3 inhibitor, is often used to activate the WNT pathway[193,194,195].

Mouse colonic organoids and human enteroids require exogenous WNT for successful cultivation, however addition of WNT to murine enteroid cultures results in down-regulation of ISC markers and formation of spherical structures that lack differentiated cell types and homogenously proliferate[40,42]. The mechanism of enteroid bud formation is initiated when *EPHB*+ (a WNT target gene) Paneth cells and LGR5+ cells are expelled from the initial cyst structure by cells expressing EphrinB, the EPHB counterstructure. Since EphrinB+ cells do not get exposed to WNT signals but Paneth and LGR5+ cells do, a WNT gradient is created. Transit amplifying cells are produced and are progressively pushed down the bud (and therefore down the WNT gradient) by newer transit amplifying cells. This migration drives terminal differentiation into their villus epithelial cell type (reviewed in[35]). WNT and/or WNT-agonists therefore often need to be reduced in concentration or omitted from cultures so a gradient can be introduced, allowing enteroid differentiation[196,197].

Growth factor containing enteroid media, optimized for mouse and human enteroids, is available commercially as Intesticult (Stemcell Technologies). The mouse media is also required for bovine enteroid cultures with added growth factors[183,198]. Recombinant growth factors are generally not commercially available for livestock species so human and mouse proteins are typically used. Conditioned medias are now available from engineered cell lines such as L-WRN (a mouse fibroblast cell line secreting WNT3a,

RSPO3 and Noggin cloned from murine transcripts)[195,199]. Other basic constituents of enteroid media often include HEPES (a buffer maintaining physiological pH), antibiotics and antifungals, and a stable glutamine (an energy source). Where serum-free conditions are required, N2 and B27 supplements can provide a multitude of vitamins and hormones, and N-acetylcysteine is commonly added for its antioxidant properties.

Proliferation and differentiation of enteroids

Enteroids for livestock species are cultured at 37°C with media changes every 2 - 3 days. Interestingly although the body temperature of pigs is 39°C, porcine enteroids express higher levels of *LGR5* when cultured at 37°C[193]. This has been proposed to be due to the increased stability of the human and mouse recombinant growth factors at the lower temperature. Using these methods, 3D epithelial enteroids are cultivated over 7 – 10 days before being enzymatically or mechanically dissociated and passaged (Fig. 1.4). Effective cultures should develop enteroids with organized crypt and villus domains, a polarised epithelium, a functional lumen and comprising most differentiated cell types at normal ratios[43]. In porcine and bovine enteroids, markers for most cell types have been identified including stem and proliferation cell markers LGR5, SRY-box transcription factor 9 (SOX9), Ki67, proliferating cell nuclear antigen (PCNA); intercellular junction markers tight junction protein 1 (TJP1), OCLN, cadherin1; enterocyte markers alkaline phosphatase (ALPI) and keratin 20 (KRT20); goblet cell marker MUC2; enteroendocrine cell markers peptide PYY and chromagranin A (CHGA); and Paneth cell markers regenerating family member 3 gamma (REG3G) and lysozyme amongst others[183,186,192,193,195,196,200].

Mouse enteroids cultured in this serum- and mesenchymal-free environment can remain genetically stable and expand for years[43]. Although enteroid cultures in other species have not yet attained the passage longevity of mouse cultures, transcriptomic profiling of 12 week pig enteroid cultures[186] and bovine enteroid cultures passaged 5 times[183] has shown their mean gene expression profiles remain similar over time. A stable enteroid

transcriptome over long-term culture should ensure reproducibility of results[183].

Digestive-site and developmental-age specific enteroids

Protocols to grow digestive-segment specific murine organoids from the small intestine, caecum and colon have been developed, with alternative combinations of growth factors/morphogens required for development and differentiation of each site[177]. For example, murine caecal enteroids require 50% WNT3A-conditioned medium for development and 10% WNT3A plus FGF-10 supplementation for organoid differentiation, whereas small intestinal enteroids do not require either of these growth factors[43,201,202]. These segment specific enteroids have been shown to commit to the *in vitro* phenotype of their tissue of origin. This has been demonstrated in pigs where jejunal enteroids reflect *in vivo* characteristics, showing higher levels of digestion and nutrient transport-related genes compared to ileal enteroids[186]. In addition, due to differences in expression of viral entry receptors porcine small intestinal enteroids demonstrate a greater susceptibility to porcine epidemic diarrhoea virus and porcine deltacoronavirus infection than porcine colon organoids which is reflected *in vivo*[192,203].

Fetal human and murine enteroid cultures, derived from embryonic week 10 - 22.5 and ED14 - 16.5 respectively, propagate indefinitely as fetal spheroids[204,205,206]. However murine enteroids derived from later stages of fetal development i.e. ED19 (of a 3 week pregnancy), will seamlessly and rapidly undergo maturation to adult function. This has been assessed by simultaneous downregulation of neonatal markers e.g. Argininosuccinate Synthase 1 (*ASS1),* B lymphocyte-induced maturation protein 1 (*BLIMP1)* and neonatal Fc receptor *(FCRN)*, upregulation of adult markers e.g. *SIS,* Trehalase (*TREH)* and Arginase 2 *(ARG2),* and increased activity levels of brush border enzymes e.g. lactase, sucrase and arginase[207]. In addition, assessment of age-dependent intestinal markers show porcine enteroids obtained from different ages of piglets do not retain their stage of development, all attaining the same level of intestinal maturity in culture[208].

Thus, past a certain stage of fetal development, epithelial maturation appears to be intrinsically programmed and is not dependent on stimulation by microenvironment, diet or hormonal signals.

Reverse-orientated enteroids

Typically, mammalian enteroid crypts feed into a central functional lumen and are lined by a single layer of highly polarized epithelial cells. The apical brush borders of these epithelial cells face the lumen and the basolateral surfaces lie in contact with the ECM scaffold[209]. This means the luminal surface, which typically interacts with nutrients, toxins and microorganisms, is not directly accessible. A common method to access the enteroid apical epithelium includes microinjection into the lumen but this technique is labour intensive, variable volumes are injected, and it requires a sizeable hollow lumen which is often reduced in differentiated organoids[210]. Co et al. (2020) demonstrated that by removing the ECM they could reverse the epithelial polarity of enteroids, allowing easy access to the apical surface[211]. Their method involved an initial embedding step where the human and murine enteroids were established within Matrigel for 7 to 20 days before moving them into a suspension. The first step appears necessary so the mammalian enteroids can successfully retain their structural integrity in suspension. The mammalian apical-out enteroids were not described as surviving past 5 days in suspension culture and the ability to passage enteroids in this orientation does not appear possible. This technique has also been repeated in porcine enteroids where, similar to the human and mouse cultures, ~20% enteroids did not reverse their polarisation[212]. This raises concerns with reproducibility and, alongside the loss of enteroid viability after a few days in suspension culture, restricts longer term use of this technique (reviewed in[185]). Reverse polarity has also been achieved in human intestinal organoids using pro-inflammatory TNF-α, IL-1 and IL-6[213].

2D enteroids

Development of 2D enteroid epithelial monolayers is another method used to enable access to the apical epithelial surface. These polarised monolayers

are more amenable than 3D organoids to studies where the effects of epithelial barrier stimulants, such as feed additives, need to be measured in a standardised way. Typically, dissociated IECs are seeded in transwell inserts coated with collagen or Matrigel and these are cultivated to form a robust 2D layer with an intact epithelial barrier and differentiated epithelial cell types. Paracellular epithelial permeability and barrier function can then be measured using TEER. This culture technique has now been achieved in many species including pigs, cattle and chickens and has the potential to be used in high-throughput systems[18,164,192,196,200]. The main limitations of these monolayer cultures are the limited number of propagations, difficulty in forming confluent monolayers, occasional loss of some epithelial cell types, and absence of the crypt-villus architecture of their 3D counterparts (reviewed in[214]).

Cryopreservation

The cryopreservation of isolated epithelial crypts, intestinal tissue fragments and enteroids would allow sampling of a large numbers of animals at one time without the immediate need to conduct time-consuming crypt isolations, reduce the requirement for repeated fresh tissue collection, and create shared biobanks of material available for use by the research community. Cryopreservation methods have been developed in various species using a freezing media containing FBS, dimethyl sulfoxide ± a ROCK inhibitor. This has enabled the recovery of frozen enteroid stocks and generation of enteroids from frozen isolated crypts, after thawing from long-term liquid nitrogen storage[193,195,198]. The resuscitated cultures retain functionality similar to that of the tissue of origin.

1.4.2 Culturing chicken enteroid models

Tissue isolation

Although most advances in 3D enteroids are limited to mammalian species, the development of chicken enteroid models has been ongoing for almost 10 years. However attempting to grow chicken enteroids in the

microenvironments successful for most mammals has so far yielded limited results. As with other livestock species, a lack of pluripotent stem cells means with all cultures are created from adult ISCs. Various ages of chickens have been used ranging from ED18 to mature birds (Table 1.1)[215,216]. Although the majority of cultures are small intestinal in origin, Powell & Behnke (2017) created cultures from caecal tissue (Table 1.1)[195]. There is so far no uniform crypt dissociation method, with collagenase, EDTA or ethylene glycol-bis(β-aminoethyl ether)-N,N,N',N'-tetraacetic acid (EGTA) used for enzymatic digestion and one group utilising only mechanical digestion[217]. The enzyme digest incubation temperatures range from 4 to 37°C, and incubation timings vary between 3 x 30 min, interspersed with shaking and/or filtering steps, to a consistent 1.5 h (Table 1.1)[195,215,216]. Ultimately these techniques all result in isolated tissue fragments for further culture which are identified as 'fragments of epithelium'[215,218], 'crypts' from adult birds[195,216] or 'mucosal villus' from 1 day old chicks[217].

Matrigel-based cultures

Most enteroid cultures are modified from the classical murine method where the ISC containing tissues are embedded in Matrigel domes and surrounded by growth factor containing media[43]. Pierzchalska et al. (2012) first published evidence of chicken enteroids grown using these methods from ED18 – 20 small intestine (Table 1.1)[215]. They were cultured in Matrigel domes with comparable morphology found when using prostaglandin E_2 (PGE_2) as a cost-effective alternative to RSPO1 and Noggin. The isolated epithelial fragments were observed to close into spheres with an expanding lumen enclosed by a thin intact layer of cells (Table 1.2). These structures remained viable for several weeks but did not form crypt-like buds. In current organoid nomenclature these non-budding thin-walled spherical structures are closest in description to enterospheres so shall be described as such from now on[219]. Using these methods, 4 chicken embryos were required to produce material sufficient to start one 12 well plate[218]. This group has subsequently published variations on this model including a hanging drop culture system where enterospheres were suspended in media containing 5% Matrigel[220]. The

basic media is composed of Dulbecco's modified eagle's medium (DMEM)/F12, antibiotics/antimycotics, ITS (insulin, transferrin and sodium selenite), PGE_2 and EGF. Later versions of the culture media include the addition of RSPO1, Noggin and 0.25% chicken serum or WNT3a to increase the speed of enterosphere growth (Table 1.1 and 1.2)[218,220,221]. Enteroid cultures attempted from adult bird intestine include a study by Powell and Behnke (2017) who demonstrated the ability to passage Matrigel-embedded caecal enterospheres over 30 times when cultivated in a DMEM, FBS and L-WRN based media supplemented with ROCK inhibitor and TGF-β inhibitor (Table 1.1 and 1.2)[195]. In addition, Li (2018) showed the culture of adult chicken jejunal enterospheres in Matrigel and investigated the effects of various concentrations of EGF, Noggin, RSPO1 and CHIR99021 on their growth (Table 1.1 and 1.2)[216]. Similar to pigs, despite the chicken's body temperature being 41°C, all cultures appear to be incubated at 37 – 38°C.

Table 1.1: Details of chicken enteroid culture materials and methods.

Publication	Gut section	Bird age	Crypt/villi isolation	ECM	Culture media
[215]	small intestine	ED18 - 20	EGTA. 0.5% glucose, 4°C, 15 min then 45 min x 2	Matrigel	DMEM/F12, antibiotic & antimycotic, ITS, EGF, (RSPO1 and Noggin, or PGE_2)
[221,222]	ED19 small intestine or hens duodenum	ED19 (and 20 wk hens[222])	EGTA. 0.5% glucose, 4°C, 15 min then 45 min x 2	Matrigel	DMEM/F12, antibiotic & antimycotic, ITS, chicken serum, RSPO1, Noggin, EGF, PGE_2 , (WNT3a ± ROCKi[221])
[195]	caecum	mature birds	collagenase, 37°C, 1 - 1.5 h	Matrigel	50% (DMEM + 10% FBS), 50% L-WRN media, ROCKi, TGF-βi
[220]	small intestine	ED18	EGTA. 0.5% glucose, 4°C, 15 min then 45 min x 2	hanging drop (5% Matrigel)	DMEM/F12, antibiotic & antimycotic, ITS, EGF, PGE_2, WNT3a
[216]	jejunum	2 - 3 wk old hens	EDTA, 4°C, 30 min x 3	Matrigel	DMEM/F12, HEPES, GlutaMAX, antibiotic & antimycotic, EGF, Noggin, RSPO1, CHIR99021
[217]	small intestine	1 day old chicks	Mechanical; trituration x 2, overnight culture, then triturate	none	DMEM/F12, Glutamine, HEPES, sodium bicarbonate, sodium pyruvate, antibiotic & antimycotic, 10% FBS, ITS, polyamine, bovine pituitary extract

Table 1.2: Chicken enteroid culture morphology. Brightfield images of enteroids or enterospheres developed from chicken intestinal tissue. Images adapted from publications under the terms of the Creative Commons Attribution Licenses (http://creativecommons.org/licenses/by/3.0), (http://creativecommons.org/licenses/by/4.0/).

Publi-cation	Culture Images
215	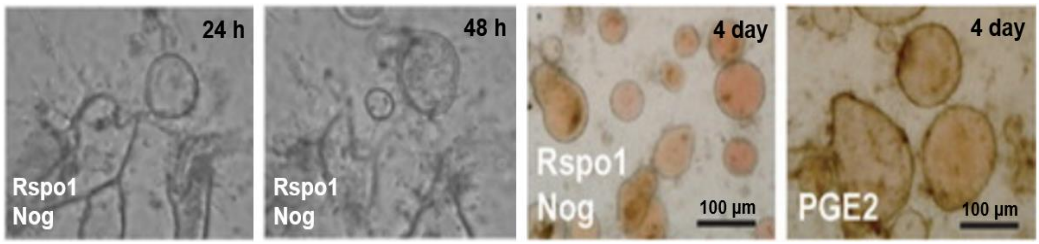
222	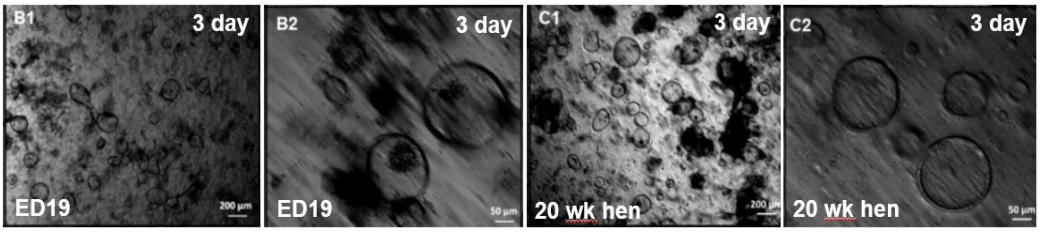
195	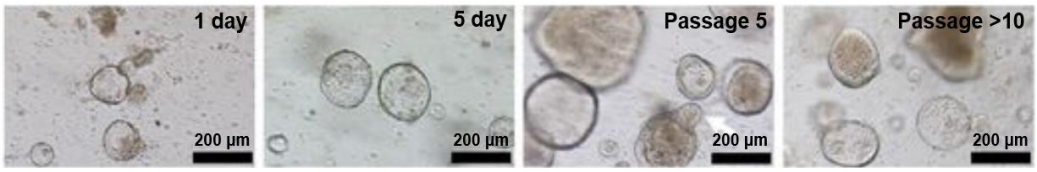
220	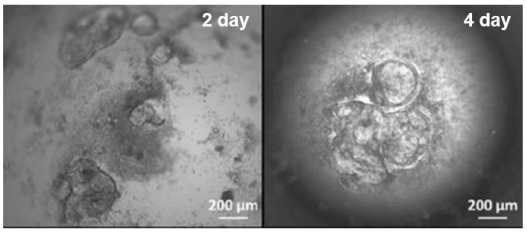
216	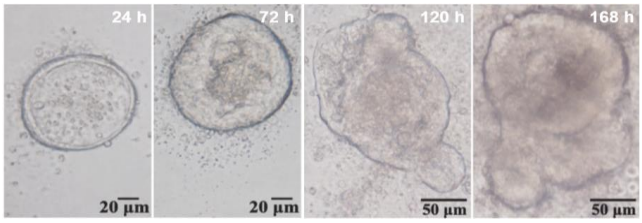
217	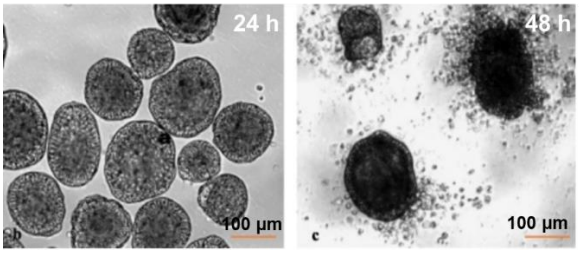

All Matrigel-based culture methods have so far resulted in thin-walled cystic structures with few if any defined crypt- and villus-like domains. These therefore do not resemble the *in vivo* intestine nor the classical enteroid morphology of other species. Indeed, these enterospheres have only been evidenced to contain enterocytes (by identifying villin and sucrase isomaltase markers, and microvilli on transmission electron microscopy (TEM)) and proliferating/stem cells (by identifying *OLFM4, LGR5*, homeodomain only protein X (*HOPX*), *ZNRF3,* SOX9 and/or PCNA markers)[195,215,216,220]. Pierzchalska et al. (2012) also identified myofibroblasts strongly attached to the enterosphere surfaces when they were seeded in Matrigel domes[215]. These were assumed to originate from epithelial-mesenchymal transition however low expression of both the myofibroblast marker *α-SMA* in the hanging drop cultures, and mesenchymal marker vimentin in Matrigel dome cultures from other groups indicates the presence of this cell type is variable and could be caused by isolation or culture factors[195].

A floating culture method

In 2020, Acharya et al. demonstrated the growth of compact spheroids from isolated day old chick villi when they were floated in suspension. The basic media contained numerous additional culture supplements to those previously described for the chicken including sodium bicarbonate, sodium pyruvate, polyamine and bovine pituitary extract but no growth factors e.g. EGF, PGE_2 (Table 1.1). The resultant floating structures displayed an external epithelial layer and a solid core of tissue. They shed large numbers of cells from the surface, as would be expected along the villus in intestinal homeostasis, but did not exhibit budding themselves (Table 1.2)[223]. The epithelial layer was identified through staining for keratin I and II and ion channel protein Na-K-ATPase. In addition, strong staining for the enterocyte enzyme alkaline phosphatase was present. This is ubiquitously expressed in the intestine to aid in the absorption of fatty acids and protection against inflammation, however its activity did not change in these cultures after application of inflammatory factors[224]. Although staining for lysozyme (indicative of Paneth-like cells), mucin (indicative of goblet cells), and

serotonin, chromogranin A and tryptophan hydroxylase (indicative of enterochromaffin cells) was performed it was difficult to convincingly identify cell-specific staining in the epithelial layer. In addition, cadherin staining was not restricted to the expected interepithelial locations[217]. The effects of various growth factors, hormones, micronutrients, toxins and drugs on enteroid morphology were assessed under brightfield microscopy. Enterotropic effects, displayed by limited budding from the main spheroid structure, were only noted after stimulation with EGF and human IGF-1. BMP2, dexamethasone, thyroxine and other growth supplements either had no or detrimental effects. Monensin, an ionophore, antibiotic and anticoccidial drug commonly used as an oral supplement in poultry production, caused degeneration of the enteroids which correlates with toxic effects on the intestine seen in some *in vivo* studies[225].

Lancaster and Knoblich (2014) stated organoids by definition should resemble their native counterparts in cellular content, multicellular architecture and functional features[178]. Therefore despite continued improvements, these 3D chicken cultures still do not meet the conditions required to qualify as an organoid and consequently have limited applications. Culture components and techniques to develop and maintain enteroids of different mammalian species are diverse and are continually being optimised. Fortunately, cells *in vitro* tend to follow a semi-autonomous differentiation trajectory so precise knowledge of the timing, locations and/or concentrations of growth factors are generally not required. However, to generate effective enteroid models an understanding of the molecular mechanisms required to drive cell differentiation and organ assembly from ISCs is required. Comparison of the transcriptome in the avian intestine with an avian enteroid model could indicate which of the vast array of culture constituents are required to create physiologically relevant chicken enteroids with budding architecture and differentiated cell types, and that consequently demonstrate organ-like functions.

1.5 Current applications of livestock enteroids

1.5.1 Host-pathogen studies with enteroids

Most research studies using livestock enteroids have predominantly focused on the study of host-microbe interactions including mechanisms of entry, intracellular replication and propagation, and exit of pathogens from the intestinal epithelium. These *in vitro* models have also introduced the ability to study the roles of specific cell types during infection and the impact of pathogens on cell development and function (Table 1.3). As previously discussed, a practical limitation of the enclosed internal lumen of classical 3D enteroids is that they prevent easy access to the apical epithelial surface. Since most intestinal pathogens bind to cell receptors expressed on the apical surface this particular issue limits the models applications. To enable interactions with the natural site of infection, pathogens have been added to disassociated enteroids[226,227], microinjected into the enteroid lumen[228,229] or applied to 2D enteroid cultures[192,203,230,231]. Porcine apical out enteroids have been also developed and employed for infection studies[212].

Table 1.3: Pathogen infections in livestock species 3D enteroids.

Species	Pathogen	Publication
Porcine	Porcine epidemic diarrhoea virus	192
	Salmonella Typhimurium *Toxoplasma gondii*	198
	Swine enteric virus	212
	Lawsonia intracellularis	232
	Porcine deltacoronavirus	233
Bovine	*Salmonella* Typhimurium *Toxoplasma gondii*	198
	Escherichia coli	234,235
	Rotavirus	197

Viral pathogens

The gastrointestinal tract is a common route for viral invasion where these pathogens can cause cell death, disrupt tight junctions and ion transport, and/or induce pro-inflammatory cytokine and chemokine responses. The first successful culture of pathogens with organoids was achieved by Finkbeiner et al. (2012) who propagated rotavirus within human intestinal organoids[226]. Enteroids from pigs have since modelled infections with swine enteric viruses, many of which have been previously difficult to culture in cell lines. These studies have identified pathogen-targeted cell types, IFN defence mechanisms and tropism of the viruses to specific intestinal segments[192,203,212]. Bovine enteroids have been modelled with group A rotaviruses[197].

Bacterial pathogens

Various bacterial pathogens have been used to infect human and mouse enteroids including *Salmonella* Typhi [236] and *Escherichia coli*[237]. Two-dimensional pig enteroids were employed to study changes in intestinal cell gene expression in response to *Lawsonia intracellularis* infection[232], and the generalist *S.* Typhimurium has been studied in both bovine and porcine 3D enteroids[198]. In terms of modelling stimulation with bacterial toxins, *Escherichia coli* Shiga-toxin resulted in reduction in growth of bovine ileal organoids, and *Staphylococcus aureus* and *Clostridium perfringens* enterotoxins caused the disintegration of floating chicken enteroids[217,234]. *Salmonella* Typhimurium LPS induced inflammation in porcine intestinal enteroids however it caused no discernible changes to the morphology of floating chicken enteroids after 48 h of stimulation[217,238].

Protozoal pathogens

Enteroids are an attractive target for protozoal studies since these particular microorganisms are notoriously difficult to culture for their entire life-cycle *in vitro. Toxoplasma gondii* has been cultured in both pig and cow enteroids however the mechanical disruption technique employed means both apical

and basolateral epithelial surfaces were exposed to the pathogen which is not reflective of natural *in vivo* infection[198].

Enteroids provide an *in vitro* system in which to study how pathogens bind to host cell receptors, modulate host tissue intracellular signalling and functions, and respond to antimicrobial compound testing. In addition they have helped to rapidly unravel insights into the pathology of novel viruses as evidenced for SARS-Cov-2[152]. The use of enteroids to study host-pathogen interactions has led to striking findings in the human field but studies are currently limited in livestock species. Despite the promise of this system, as yet no pathogen infections have been demonstrated using chicken enteroid models.

1.5.2 Enteroid and innate immunity studies

Gaps in our knowledge regarding the chicken GALT can now be explored *in vivo* with novel tools such as *CSF1R*-reporter transgenic birds. Enteroids have been successfully used as *in vitro* tools to study epithelial innate immune responses, most commonly in relation to pathogen challenge. For example swine coronaviruses have been shown to regulate the gene expression of type-I IFNs and inflammatory cytokines in porcine enteroids[192,203]. A study using murine and porcine enteroids also showed species differences in the effect of interleukins in the regulation of mucin production[239].

Enteroid co-cultures

Of more interest to the research field is the reciprocal crosstalk between pro-inflammatory and epithelial cells and the roles these play in the development of innate and adaptive immunity. However, investigating intestinal immunity *in vitro* remains challenging since most currently available intestinal cultures are strongly reduced epithelial-only models. To better study the intestinal microenvironment, methods to integrate lamina propria cell populations into epithelial enteroid cultures are under development (reviewed in[240]). The co-development of enteroids with immune, endothelial and neural cells is not widely reported due to difficulties in maintaining an accurate representation of

the native organ. Instead, co-culture strategies that allow for the controlled development of the epithelial layer have been trialled. These include 1) mixing dissociated enteroids with cells of interest in Matrigel, where they can stay in the surrounding matrix or incorporate into epithelial layer; 2) microinjection of cells of interest into the lumen; 3) growing 2D organoid monolayers in Transwell inserts and adding cells of interest to the underside of the upper chamber; and 4) air liquid interfaces in which adult ISC containing tissue fragments are seeded in an acellular layer which is in contact with medium containing the cells of interest. These methods are complicated to develop and are not always representative of the array of cell sub-populations *in vivo*[231,237,241].

The incorporation of lamina propria cell types, which are all variably involved in intestinal immune defences, into livestock species enteroid cultures has not yet been investigated. However co-cultures of murine enteroids with IELs, and human enteroids with macrophages or T lymphocytes have been demonstrated[231,242,243,244]. These co-cultures have confirmed that the immune system supports the ISC niche, regulates intestinal regeneration and maturation, and enhances the barrier function of the intestinal epithelium. Human and mice enteroids have also been co-cultured with subepithelial myofibroblasts, creating larger more complex enteroid cultures which require less growth factor supplementation[245,246]. In addition, co-cultures of human intestinal organoids with enteric neural crest cells, from which the enteric nervous system is mainly derived, have been shown to develop functional neurons and glia[247]. The advent of 3D bioprinting, which has been demonstrated for the bovine, may eventually enable co-culturing of large animal enteroids with defined spatial positioning of different cell populations[196].

M cell induction in enteroids

Receptor activator of nuclear factor-κB ligand (RANKL) is expressed by subepithelial stromal cells beneath the FAE and is critical to controlling M-cell differentiation from LGR5+ stem cells. Following from *in vivo* studies where

systemically treating mice with RANKL induced ectopic M cells from villous enterocytes, Lau et al. (2012) have induced the M cell phenotype in mouse intestinal organoids through addition of RANKL[248,249]. Chicken RANKL has been produced but its ability to induce M cells in chicken enteroids is currently unknown[250].

1.5.3 Additional applications for livestock enteroids

Digestion studies

Differentiated cell types with prominent roles in digestion e.g. absorptive enterocytes and digestive hormone secreting enteroendocrine cells, have been identified in enteroids from many species. In addition, the identification of surface microvilli, digestive enzymes (sucrase-isomaltase) and ion/nutrient transporters (monocarboxylate transporter 1, sodium/glucose cotransporter 1, sodium-hydrogen exchanger 3) indicates enteroids in livestock species could be used to measure effects on food digestion, nutrient absorption and gut hormone regulation[192,198,200,251]. Studies in pig enteroids have already demonstrated functional apical to basolateral transport of nutrients and increased epithelial proliferation after supplementation with dietary glutamine[186,252]. In addition these models have been used to show the impact of feed-associated vitamin A, L-glutamine and mycotoxins on ISC homeostasis, as well as insights into host-pathogen interactions in relation to feed efficiency in pigs[192,252,253].

Epithelial barrier studies

The strength and function of the intestinal barrier is another important parameter to assess for feed efficiency. Increased intestinal permeability is a sign of perturbed intestinal barrier function and can be measured by recording the passage of permeability solutes over the epithelial layer via paracellular routes (reviewed in[254]). Porcine 3D enteroid studies have been used to shown changes in gut barrier integrity on exposure to heat-stress[194]. However it is difficult to perform large-scale epithelial barrier experiments on gel-embedded intestinal organoids as, in order for feed substances or

pathogens to contact the luminal surface, microinjection is required[255,256,257]. To address this limitation, 2D porcine enteroids have been developed and used to study pathogen effects on the intestinal barrier[194,258,259,260]. Since feed costs make up to 70% of the costs of broiler production, and feed efficiency is a major variable to determine the cost of meat, the availability of enteroid-based tools to study and screen food compounds would prove useful for the poultry industry. In particular, development of methods to allow high-throughput epithelial barrier assessment of 3D enteroids would be of interest as these models are more reflective of the *in vivo* intestine than their 2D counterparts.

1.6 Aims and Hypotheses

The overarching aim of this study is to develop an innovative complex 3D enteroid culture system of the chicken digestive tract whose results can be easily extrapolated to the live bird. Current *in vitro* models used to study the poultry gut present major limitations. For example, immortalised IEC lines lack cellular heterogeneity and for poultry they are not even available, and primary IEC cultures lack the 3D architecture of the *in vivo* intestine. These restricted tools make it difficult to reliably extrapolate *in vitro* results from e.g. host-pathogen studies to the *in vivo* environment.

Aim 1: Create a physiologically relevant chicken enteroid model

The initial aim of this study is to create and validate a comprehensive physiologically relevant model for the poultry intestine that could overcome such limitations. Enteroid models have been successfully developed in many species but the chicken cultures published so far are lacking in the 3D architecture and cell content of the *in vivo* intestine. The first hypothesis is that protocols for chicken intestinal crypt isolation and enteroid culture could be developed to create a more representative and applicable model of the chicken intestine. To test this hypothesis various methods for adult ISC isolation will be trialed, the effects of different ECM scaffolds, growth factors and other culture supplements will be investigated, and RNA-seq analysis

from the enteroid cultures will be analysed to identify key regulatory molecules that might maintain the chicken ISCs in culture (Chapters 3 and 5). The resultant model would need to demonstrate that it recapitulates the *in vivo* intestinal architecture, differentiated epithelial cells and various organ functions such as epithelial barrier integrity and digestion. To perform this enteroid characterisation TEM, immunocytochemistry, RNA-seq and functional studies will be used to compare the enteroid model back to the chicken intestine, as well as to confirm the reproducibility and stability of the model (Chapters 4 and 5).

Aim 2: Demonstrate that the chicken enteroids can be used to model host-pathogen interactions

Enteroids have been employed in other species to study aspects of attachment, invasion and replication of enteric pathogens, including those previously difficult to grow *in vitro*. This work therefore further aimed to characterise the chicken enteroid cultures as a model for host-pathogen interactions using species-specific protozoan and zoonotic viral and bacterial pathogens. The second hypothesis is that, once a chicken enteroid culture system has been established, it can be used as a novel growth system for species-specific and zoonotic pathogens of importance to human and animal health. To test this hypothesis I planned to infect the enteroids with an influenza A virus (IAV) or the bacterium *S.* Typhimurium and use immunohistochemistry and replication studies to characterize their attachment, invasion and replication rates (Chapters 6 and 8). For *Salmonella* infections I will also use functional studies to assess their effect on the enteroid epithelial barrier. In addition, the chicken protozoal parasite *Eimeria* has not yet been cultured for its entire lifecycle *in vitro* in a chicken IEC model. I hypothesized that a species- and digestive site-specific enteroid culture would allow both asexual and sexual replication of the parasite. To test this hypothesis I will develop and characterize digestive site-specific chicken enteroid models, infect them with a site-specific *Eimeria* spp., and identify life-cycle stages at various timings post enteroid infection (Chapter 7).

Aim 3: Demonstrate that the chicken enteroid model can be used to study innate immune responses

The post-hatch chick with its immature immune system is at particular risk of infection by enteric pathogens. Therefore the development *in vitro* models to study the gastrointestinal innate immune responses of this particular lifestage in poultry are necessary. Enteroids have been shown to be capable of mounting epithelial responses to pathogen challenge and, in co-culture with immune cells, can be used to study more complex immune responses. The hypothesis was that late embryonic chicken enteroid/immune cell co-cultures could be induced to elicit appropriate early immune responses after viral, bacterial and protozoal pathogen infection. To test this hypothesis late embryonic chicken enteroid/immune cell co-cultures will be developed and characterised using immunocytochemistry, RNA-seq and functional studies. Their immune responses to challenge with *Eimeria* spp., IAV and *S.* Typhimurium infection will then be analysed using a multiplexed reverse transcription-quantitative PCR (RT-qPCR) 96.96 Fluidigm Dynamic Array containing chicken innate immune response genes. The results will be compared back to *in vivo* infection literature to confirm that enteroid/immune cell co-cultures induce appropriate immune responses.

Overall this thesis describes the development and morphological and functional characterisation of a novel comprehensive chicken enteroid model. It also details the enteroids application in host-pathogen modelling and innate immunity studies with the use of important bacterial, viral and protozoal pathogens.

Chapter 2 Methods

Chapter 2 Methods

Chapter partially adapted from Nash et al. DOI: 10.1038/s42003-021-01901-z (Additional file 1)

2.1 Animals

Experiments were performed using ED18 to 9 week old Hy-Line Brown chickens (*Gallus gallus*), ED17 *CSF1R*-eGFP transgenic chickens[120] and 2 day old quail (*Coturnix coturnix*) obtained from the National Avian Research Facility, Edinburgh, UK. Five month old C57BL/6 mice were provided by the Biological Research Facility, University of Edinburgh, UK.

Ethical approvals were obtained from The Roslin Institute's and University of Edinburgh's Animal Welfare Ethics Review Board. The experiments were also performed under the authority of UK Home Office Project Licences (PA75389E7, PE263A4FA) in accordance within the guidelines and regulations of the UK Home Office 'Animals (scientific procedures) Act 1986.

2.2 Enteroid culturing

2.2.1 Isolation of avian intestinal tissue containing stem cells

The embryonic small intestine was removed post-mortem, cut open longitudinally then into 5 mm sections and collected into Ca^{2+}- and Mg^{2+}-free Phosphate-buffered saline (PBS) and washed. The tissue was digested in DMEM (Thermo Fisher Scientific (TFS)) with 0.2 mg/mL Collagenase from *Clostridium histolyticum* Type IA (Merck) at 37°C for 50 min. The tube was shaken vigorously, tissue allowed to settle then supernatant collected. These steps were repeated to generate 4 fractions. Fractions were centrifuged at 100 x *g* for 4 min and tissue integrity assessed. The crypts or villi were counted and resuspended in floating organoid media (FOM) at ~200/mL and plated out (day 0 of culture); Advanced DMEM/F12 (TFS) supplemented with 10 mM HEPES (TFS), 2 mM L-Glutamine (TFS), 50 U/mL Penicillin/Streptomycin (Merck) and 2% B27 supplement (50X; TFS). Where

indicated the FOM was supplemented with 10 - 100 ng/mL EGF (Prepotech), 25 ng/mL Noggin (Enzo Life Sciences or Prepotech), 250 - 500 ng/mL RSPO1 (R&D Systems), 100 mM Y-27632 (Cambridge Bioscience), 100 - 1000 mM SB202190 (Enzo Life Sciences), 5 mM LY2157299 (Cambridge Bioscience), 0.2 – 5 µM CHIR99021 (Stratech Scientific), 10 - 100 µl/mL chick embryo extract (prepared in house), 5 µg/mL PGE_2 (Cambridge Biosciences), 2% B27 supplement -vitamin A/- antioxidants/PLUS (50X; TFS), 1 µl/mL MITO+ serum extender (Corning) and/or 0.5 – 1 mM sodium butyrate (Sigma-Aldrich); the DMEM/F12 was substituted for DMEM; and/or the plates were coated with 0.1 – 0.4 mg/mL collagen (Sigma-Aldrich), or growth factor reduced (GFR) or non-GFR Matrigel (Corning). Differentiation of avian enteroids occurred at 37°C, 5% CO_2. After 24 h (day 1 of culture) the floating enteroids were transferred to wells containing fresh media. Since the enteroids gravitated to the centre of the well, half the media could be replaced every 2 days by tilting the plates and, using a 200 µL pipette, gently removing media surrounding the centrally clustered enteroids.

For duodenal, jejunal, caecal enteroids the isolation and culture protocols were kept the same.

For post-hatch birds (quail and chicken) the protocols were similar except the luminal contents were flushed out and the initial washing of the separated intestinal tissue fragments was more vigorous and repeated to remove the mucus. For the post-hatch chickens the intestinal surface was scraped with a glass slide to separate the superficial luminal layers (including the epithelium) from the deeper mucosa and the digestion incubation continued for 60 min.

To seed chicken intestinal crypts or villi in GFR or non-GFR Matrigel, they were resuspended in equal volumes of FOM and ice-cold GFR Matrigel to allow for 50 crypt or villi per 50 µL and cultured as described below for mouse intestinal crypts, using FOM instead of Intesticult medium (Stemcell Technologies)[209].

2.2.2 Isolation of mouse intestinal crypts

Isolated mouse small intestines were opened longitudinally, chopped into ~2 mm fragments and washed with cold PBS. Intestinal crypts were dissociated from the tissue fragments using Gentle Cell Dissociation Reagent (GCDR, Stemcell Technologies) for 15 min at room temperature. After removal of the GCDR, the tissue fragments were vigorously suspended in cold PBS containing 0.1% bovine serum albumin. The supernatant was filtered through a 70 µm filter (BD Bioscience) and the filtrate was labelled 'Fraction 1'. These steps were repeated to generate 4 fractions which were then centrifuged at 290 x *g* for 5 min. Resultant pellets, containing crypts, were resuspended in cold PBS containing 0.1% bovine serum albumin then centrifuged at 200 x *g* for 3 min. Crypts were resuspended in equal volumes of Intesticult medium and ice-cold GFR Matrigel to allow for 50 crypts per 50 µL. A 50 µL aliquot was used to form a dome in the centre of a well of a 24-well plate and surrounded with 750 µL Intesticult medium. Differentiation of mouse enteroids occurred at 37°C, 5% CO_2 with the media was replaced every 2 days[209]. Crypts to be cultivated without GFR Matrigel were seeded floating in Intesticult medium at ~200 crypts/mL and fresh medium was replaced every 2 days by tilting the plates as described for the chicken enteroids.

2.3 Enteroid viability assessments

2.3.1 Morphological assessment of enteroid cultures

Enteroids were divided into 4 groups based on morphological appearance; villi, enteroids with >1 bud, enteroids with ≤1 bud, and disintegrating enteroids. Manual counts of these enteroids, within a well of a 24-well plate, were then made every 2 days of culture using a bright-field microscope (Axiovert 25, Zeiss, Germany). Qualification as a non-viable enteroid was based on loss of total epithelial integrity, termed 'disintegrating'. This disrupted epithelial structure on bright-field microscopy has been used to constitute major cell death in murine enteroids[261].

2.3.2 Enteroid viability detection assay

A 24-well tissue culture plate containing enteroids was centrifuged at 170 *x g* for 1 minute then 100 µl supernatant was collected and added to wells a 96-well plate. 3 wells were prepared for each condition; media only (background control), supernatant of 0.05 mM TritonX100 (TFS) treated enteroids (positive control), supernatant of non-treated enteroids (negative control). The enteroids were lysed for the positive control by adding 0.05 mM TritonX100 to the contents of 3 wells then incubated for 30 min at 37°C. 100 µl reaction mixture (Cytotoxicity Detection Kit, TFS) was added to each prepared well and the plate was incubated for 20 min protected from light at room temp. Absorbance of samples was measured by an ELISA reader at 492 nm. Supernatant from the same culture wells were sampled every 2 days for this assay, and 50% of the total media in the wells was changed for fresh FOM after sampling. Therefore this assay does not fully represent cumulative cell/enteroid death over 17 days. Positive controls were optimised by incubating TritonX100 concentrations ranging from 0.005 mM to 0.05 mM with the enteroids.

2.4 Enteroid propagation

2.4.1 Passaging

Enteroids were chemically disrupted using 0.2 mg/mL Collagenase from *Clostridium histolyticum* Type IA, 250 µl/mL 1X trypLE (Gibco) or GCDR. In half the treated wells, enteroids were also mechanically disrupted by vigorous pipetting using a 200 µl pipette and tip, or with a 5 mL syringe and 25g x 1” needle. The dissociated enteroid fragments were centrifuged at 100 *x g* for 1 min, supernatant removed and fragments re-suspended and cultured as described for chicken enteroids in 2.2.1, with and without the listed growth factors. Additional growth factors trialled post-passage included 0.5 – 1 mM valproic acid (Sigma-Aldrich), 10 ng/mL human WNT3a (R&D systems), 20 µl/mL chicken serum (Gibco), 10 µl/mL N-2 supplement (100X Gibco), 10

µl/mL ITS premix (100X Gibco), 0.1 M nicotinamide (Sigma-Aldrich) and/or plates were coated with chick embryonic fibroblasts (prepared in house).

2.4.2 Villi and enteroid cryopreservation

Villi, immediately post-isolation, and enteroids, after 2 days of culture, were pelleted at 290 × *g* for 4 min at room temperature then resuspended in 4°C Cryostor CS10 cryopreservation medium (Stemcell Technologies) at ~1000 crypts or villi/mL. An alternative method involved resuspending the crypt pellet in 900 µl foetal bovine serum (FBS, Gibco), placing this on ice for 15 min, then adding an equal volume of 4°C freezing medium (80% FOM mixed with 20% dimethyl sulfoxide (DMSO, Sigma-Aldrich)). Cryovials (Greiner) were stored overnight at −80°C, and then transferred to −155°C.

To resuscitate the villi and enteroids, cryovials were thawed and mixed with 10 mL prewarmed DMEM then centrifuged at 290 × *g* for 5 min at room temperature. The crypt or villi or enteroids were re-suspended and cultured as described for avian enteroids in 2.2.1.

2.5 Imaging

2.5.1 Transmission electron microscopy

Enteroids and villi were fixed in 3% glutaraldehyde in 0.1 M sodium cacodylate buffer, pH 7.3, for 2 h and processed as described previously[183]. Ultrathin sections (60 nanometre) were stained in uranyl acetate and lead citrate and imaged using a JEOL JEM-1400 Plus TEM and analysed using ImageJ (v1.52e, Fiji).

2.5.2 Whole mount and immunohistochemical staining

Enteroids were fixed with 4% paraformaldehyde then blocked with 5% v/v goat serum in permeabilisation solution (0.5% v/v bovine serum albumin and 0.1% v/v Saponin in PBS) and stained with primary and secondary antibodies (Table 2.1) at 4°C. DNA was stained with 4', 6-diamidino-2-phenylindole (DAPI; TFS) or Hoechst (TFS) and, where indicated, F-actin was visualised

with Alexa Fluor conjugated Phalloidin (TFS). Enteroids were then mounted in ProLong® Diamond Antifade Mountant (TFS). Isotype and negative controls were prepared for each staining. Samples were visualised using a LSM710 or LSM880 Confocal Microscope (Zeiss) and processed using ImageJ v1.52e.

Proliferation was assessed in a 5-ethynyl-2′-deoxyuridine (EdU) incorporation assay, by using a Click-iT EdU Alexa Fluor 488 cell proliferation assay kit (Invitrogen). Enteroids were incubated with 10 μM EdU for 1 h and nuclei stained (Hoechst; TFS).

Intestinal tissue was snap frozen in liquid nitrogen, 10 μm sections were prepared on a Leica Cryostat CM1900 and mounted on Superfrost Plus slides (TFS). Tissues were fixed in 50% methanol then blocked and stained as described for staining of whole mount enteroids.

Table 2.1 Primary antibodies used for immunohistochemistry

Target	Antibody details	Clone	Catalog number	Dilution
Mucin 5AC	Mouse anti-MUC 5AC[a]	45M1	Ab212636	20 µg/mL
Lysozyme C	Rabbit anti-LYZ[a]	polyclonal	Ab391	20 µg/mL
Chromogranin A [SP1]	Rabbit anti-Chromogranin A[b]	polyclonal	20085	1.3 µg/mL
Sox9 [phospho S181]	Rabbit anti-SOX9 [a]	polyclonal	Ab59252	2 µg/mL
Villin	Mouse anti-villin [c]	1D2C3	Sc-58897	4 µg/mL
E-Cadherin	Mouse anti-E-Cadherin [d]	36/E-Cadherin	610181	5 µg/mL
Tight junction protein	Rabbit anti-ZO1 [a]	polyclonal	Ab216880	10 µg/mL
Virus nucleoprotein	Mouse anti-NP[a]	AA5H	Ab20343	1/500
CD45	Mouse anti-CD45[f]	AV53	n/a	1/100
ChB6	Mouse anti-Bu-1[g]	AV20	839502	2 µg/mL
CD3	Mouse anti-CD3[h]	CT-3	820009	2 µg/mL
βIII-tubulin	Mouse anti-βIII tubulin[i]	2G10	T8578	10 µg/mL
HuC/HuD	Mouse anti-HuC/HuD[j]	16A11	A21272	10 µg/mL
NeuN	Mouse anti-NeuN[k]	A60	MAB377	4 µg/mL
PSD95	Mouse anti-PSD95[l]	K28/43	810401	2 µg/mL
Vimentin	Mouse anti-VIM[a]	V9	ab8069	20 µg/mL

[a] Abcam
[b] Immunostar
[c] Santa Cruz Biotechnology
[d] BD Biosciences
[e] provided by Prof P. Digard; Noton et al. 2007 http://doi.org/10.1099/vir.0.82809-0
[f] Institute for Animal Health; Garceau et al. 2015 http://doi.org/10.1186/s12915-015-0121-9
[g] Southern Biotech; Rothwell et al. 1996 http://doi.org/10.1016/S0165-2427(96)05635-8
[h] Southern Biotech; Göbel et al. 1994 http://doi.org/10.1002/eji.1830240734
[i] Sigma-Aldrich; Lee et al. 1990 https://doi.org/10.1002/cm.970170207
[j] Invitrogen; Ratie et al. 2014 https://doi.org/10.3389/fnana.2014.00158
[k] Chemicon; Garcia-Moreno & Molnar 2015 https://doi.org/10.1073/pnas.1506377112
[l] Biolegend

2.6 Functionality assays

2.6.1 Phagocytosis assay

Enteroids (100/well) were grown to 3 and 7 days of culture and then seeded into 48 well plates (Corning) containing 125 µg/mL pHrodo red *zymosan* bioparticles (Molecular Probes) in FOM. Controls had 20 µM Cytochalasin D (Cayman Chemical) added to the media to inhibit zymosan uptake. Enteroids were incubated at 37°C, 5% CO_2 and samples were taken at 8 h and 48 h post-incubation. Samples were fixed, stained and imaged as described in 2.5.2.

2.6.2 Epithelial barrier Integrity

For the epithelial barrier characterisation assay enteroids were washed and resuspended in fluorescein isothiocyanate (FITC)-Dextran (4 kDa, 2 mg/mL in PBS, Sigma-Aldrich). FITC-dextran is a well-documented paracellular probe used to study intestinal permeability *in vitro*[262]. Positive controls were treated with 2 mM EDTA in Hank's Balanced Salt Solution (HBSS, Gibco) for 15 min, then washed and resuspended in FITC-Dextran solution. Enteroids were immediately imaged using a LSM880 Confocal Microscope and processed using ImageJ.

2.7 RNA sequencing

2.7.1 Experimental design

The small intestine (duodenum and jejunum) from 3 x ED18 Hy-Line chickens were pooled to form 1 biological replicate. This was to allow enough ED18 intestinal villi and enteroids to be available for sampling for each technical replicate at each time point. This biological replicate tissue was processed as described in 2.2.1 to isolate the villi. The villi from each biological replicate were seeded (at 100 villi/well) in two identical 24-well tissue culture plates which were cultured in identical conditions. Each culture plate was treated as a technical replicate, therefore there were 2 technical

replicates for each biological replicate. For sample collection, 8 wells per plate were collected at each of the defined time points (0 h, 1 day, 3 day, 4 day and 7 days of culture) and pooled to form one sample for transcriptomic analysis. A total of 3 biological replicates (each culture composed of 3 x ED18 chicks) were used for the RNA-seq analysis.

2.7.2 RNA extraction

Enteroids were collected using a Pasteur pipette and lysed in RLT buffer (Qiagen) containing 10 µg/mL 2-mercaptoethanol (Sigma-Aldrich). Samples were stored for at least 24 h at 4°C then homogenised using Qiashredder columns (Qiagen). RNA was extracted using the RNeasy mini kit (Qiagen) according to the manufacturer's protocol, including DNase I (Ambion) treatment, then stored at -80°C until required.

2.7.3 Sequencing

Libraries were prepared and sequenced on an Illumina Novaseq 6000 using 150-bp paired-end sequencing. Obtained reads were trimmed for quality and to remove adaptor sequences using Cutadapt [263]. Reads were trimmed at the 3' end using a quality threshold of 30 and for adapter sequences using the TruSeq stranded mRNA kit (AGATCGGAAGAGC). Reads after trimming were required to have a minimum length of 50 bases.

2.7.4 Functional annotation of transcriptome

Paired-end reads from Illumina sequencing were aligned to the *Gallus gallus* genome (Gallus_gallus-5.0) from Ensembl. The annotation used for counting was the standard GTF-format annotation for that reference (annotation version 91). Reads were aligned to the reference genome using STAR[264] specifying paired-end reads and the option --outSAMtype BAM Unsorted. All other parameters were left at default. Raw counts for each annotated gene were obtained using the featureCounts software (version 1.5.2[265]).

2.7.5 Technical validation

1. **RNA integrity.** The transcriptomes of 29 enteroid samples from three individual cultures at 4 time points were sequenced. Before constructing RNA-Seq libraries, the concentration and quality of total RNA were evaluated using the D1000 Screentape Agilent System (Agilent). The total amount of RNA and RNA integrity were used to estimate the quality, content and degradation level of RNA samples. In the present study, RNA samples that qualified to construct the sequencing library had a mean total RNA concentration of 255 ng/μL (SD of 96 ng/μL), and a mean RNA integrity number (RIN) of 8.26 (SD of 1). The COB_2_168hr sample was excluded due to a RIN value of <6.
2. **Quality filtering of Illumina sequencing raw reads.** The raw counts were filtered to remove genes consisting predominantly of near-zero counts, filtering on counts per million (CPM) to avoid artefacts due to library depth. Reads were then normalised using the weighted trimmed mean of M-values method. For unmerged replicates, of the 24881 genes before filtering 17778 remained after filtering. Where indicated the transcriptome data analysis was performed on merged data, for which the sumTechReps function in edgeR was used to merge the technical replicate raw data.

2.7.6 Exploratory analysis

A principal component analysis (PCA) was undertaken on the filtered normalised expression data from the unmerged technical replicates, to explore observed patterns with respect to experimental factors; time, technical replicate, biological replicate and technical replicate per time point. Principal components (PC) 1 and 2 were both associated with 2 factors: Technical replicate per time point (P =1.7e-13 and P = 1.15e-07 respectively) and time (P =1.7e-13 and P =1.15e-07 respectively). PC3 was associated with Time (P =0.0027) and biological replicate (P =0.00511). These P-values were obtained from an analysis of variance (ANOVA) test which assessed

the associations between continuous value ranges in principal components and categorical experimental variables.

2.7.7 Differential analysis

A differential gene expression analysis was performed on both merged and unmerged technical replicates within the Bioconductor edgeR package (version 3.16.5[266]). The most differentially expressed genes (DEGs) in this analysis were defined as those with maximum false discovery rate (FDR) <0.05 and minimum log fold change (FC) >1. Differential analysis was carried out with the contrasts between groups 0 h and 1 day, 1 day and 3 day, 3 day and 4 day, 4 day and 7 day. Statistical assessment of DEGs within these groups was carried out with the quasi-likelihood F test. Heatmaps illustrating the top 50 DEGs in the 0 h to 1 day and 4 day to 7 day contrasts were composed.

The RNA sequencing, quality filtering, PCA, ANOVA test and differential analysis were performed by Edinburgh Genomics.

2.7.8 Network analysis

The annotated villus and enteroid RNA seq normalised data sets were imported into the bioinformatics tool Graphia to create and visualise a network graph (Kajeka, Edinburgh, UK). Graphia allows the identification of the patterns and trends between multiple data sets and the sets of genes that are robustly co-expressed across them[267,268,269]. The dataset consists of unique identifiers for each probe (gene name and gene id) on the array and the non-log transformed data values (transcripts/million reads (TPM)) for each villi or enteroid sample.

A pairwise gene-to-gene Pearson correlation matrix was calculated based on each probe set's profile across each of the samples. The technical replicates were merged (average rather than sum due to the absence of the COB_2_168hr sample) for this part of the analysis to give more reproducible results. To assemble an undirected network graph of the transcriptome data, the Pearson correlation coefficient/initial threshold value was selected from

the region of a plot of node (gene/transcripts) versus edge (relationship between genes) counts, where the number of nodes begins to decrease more rapidly, in this case ≥0.95. Therefore any relationship <0.95 correlation was not connected by an edge. The nodes of the graph were then divided into clusters (groups of genes) that shared similar expression profiles by using the Markov clustering algorithm, adjusting the granularity of clustering to 2.2. The first 50 clusters were manually grouped into similar gene expression profiles in relation to time points of culture, and each cluster location was identified on the network graph.

To enable functional annotation and interpretation of the clusters, the top 20 significantly overrepresented gene ontologies (GO) within each expression profile group were identified using the Molecular Signatures Database[270] (MSigDB molecular signatures database. http://software.broadinstitute.org/gsea/msigdb/. Accessed 24 April 2020). To be accepted as significant, an over-represented GO terms needed a hypergeometric P <0.05, and FDR <0.05. Where the same genes within clusters represented several GO terms, only the most significant or informative GO terms were selected for further consideration.

Individual genes associated within the RNA-seq normalised dataset were also assessed for cellular functions and activities using a combination of literature review, KEGG Pathway database (https://www.genome.jp/kegg/pathway.html . Accessed 12th May 2020) and GeneCards database (https://www.genecards.org/. Accessed 4 May 2020). Heatmaps were constructed in R using the pheatmap package (v. 1.0.10[271]).

2.8 Infection of enteroids

2.8.1 *Salmonella* infections and LPS challenge

Salmonella enterica subspecies enterica serovar Typhimurium wildtype (WT) strain 4/74, carrying a chromosomal pFVP25.1::gfp fusion linked to the naladixic acid resistance gene or defined mutant, ST4/74 *nal*^{R} *ΔprgH::kan* were utilised for infections of the chicken enteroids (both strains kindly

provided by Prof M. Stevens and Dr P. Vohra). The phoP-repressed gene (*prgH)* mutant was confirmed to have a reduced *Salmonella* pathogenicity island 1 (SPI1), Type 3 secretion system 1 (T3SS1) by analysing secretion of SipC, a *Salmonella* T3SS1 effector protein. It was also transformed with the plasmid pFVP25.1 which constitutively expresses GFP[21,272]. Strains were cultured overnight in Luria-Bertani broth with 50 µg/mL kanamycin (not used for WT ST4/74 *nal*^{R}), 50 µg/mL ampicillin and 20 µg/mL naladixic acid at 37°C. Wells were inoculated with 10^3 bacteria/enteroid in antibiotic-free FOM and incubated statically at 37°C, 5% CO_2. Alternatively enteroids were incubated with *S.* Typhimurium LPS (Sigma-Aldrich) in antibiotic-free FOM at 1 µg/mL. Samples were collected after 30 min, 4 h or 6 h post challenge for imaging analysis. Total RNA was isolated at 4 h and 8 h post challenge as described in 2.7.2.

2.8.2 Gentamicin protection assay

Bacterial replication was measured by incubating enteroids in antibiotic-free FOM with the *Salmonella* strains at 37°C, 5% CO_2 for 1 h. High-dose gentamicin (50 µg/mL) was added to the wells for 30 min, then enteroids were washed and seeded in FOM containing low-dose gentamicin (10 µg/mL). Enteroids were collected at 0, 3 and 8 h post high-dose gentamicin treatment and disrupted using steel beads in a Tissue-Lyser. Serial dilutions were plated on naladixic acid containing Luria-Bertani agar in duplicate and incubated at 37°C overnight. The compared results were expressed as mean ± SD.

2.8.3 Epithelial barrier challenge assay

For the epithelial barrier challenge assay the experiment was performed as in 2.6.2 except enteroids were treated with 1, 4 and 8 mM EDTA in HBSS for 30 min, or incubated with 1 µg/mL *S.* Typhimurium LPS (Sigma-Aldrich) for 6 h, or infected with the WT or T3SS1 mutant *S.* Typhimurium strains (described in 2.8.1) at 10^2, 10^3 or 10^4 colony forming units (CFU) per enteroid for 6 h. To quantify the epithelial barrier disruption, confocal images (100 x magnification

with uniform enteroid distribution per field) were opened in ImageJ and the area of enteroid in each image was calculated by counting number of pixels with minimum mean gray value of 49 (value visually estimated to differentiate pixel containing enteroid from pixel containing FITC-dextran). In order to visualise the data as relative enteroid permeability (FITC-dextran fluorescence within enteroid), for each image the gray area (number of pixels containing enteroid) was subtracted from 1,300,000 (figure chosen as it was the closest whole number to the highest gray area recorded in the dataset = 1,290,156 pixels).

2.8.4 Influenza infections

Fifty enteroids were incubated with $2x10^7$ plaque forming units (PFU) H1N1 virus (A/Puerto Rica/8/34 (PR8), kindly provided by Prof P. Digard) in DMEM supplemented with 50 U/mL Penicillin/Streptomycin and 50X v/v B27 at 37ºC, 5% CO_2 for 1 h. Control cultures were either treated with PBS or a paired mock (construct engineered in parallel with PR8 virus but missing segment 1, encoding polymerase (basic) protein 2). After the incubation step (0 hours post infection (hpi)), the enteroids were washed and reseeded in DMEM media supplemented with 2 μg/mL L-(tosylamido-2-phenyl) ethyl chloromethyl ketone treated trypsin. Samples were collected at 0 and 48 hpi for imaging analysis, protein and/or total RNA isolation. Supernatants were harvested at 0 and 48 hpi and titrated by plaque assay on Madin-Darby Canine Kidney cells as previously described[273]. The compared results were expressed as mean ± SD.

2.8.5 *Eimeria* infections

Frozen purified *Eimeria tenella* sporozoites (kindly provided by Dr E. Wattrang, SLU Sweden) were washed in warm DMEM and labelled with PKH67 Green Fluorescent Cell Linker kit (Sigma-Aldrich) according to manufacturer's protocol. ~5 x 10^4 sporozoites in PBS were added to each well containing fifty 2 day old chicken enteroids and incubated at 37ºC, 5% CO_2. Controls were treated with PBS. Fresh caecal enteroids, cultured for 2

days, were added to the cultures at 4 and 6 days post infection (dpi) to provide fresh epithelial cells for the merozoite stages. Enteroids were collected for imaging analysis and RNA isolation at 1, 2, 4, 7 and 9 dpi. This sporozoite stock was used to compile the data in Chapter 7, Fig. 7.1.

Due to a limited availability of frozen purified sporozoites, *E. tenella* infected enteroid RNA samples to be run on the 96.96 Dynamic Array were collected from experiments using sporozoites freshly isolated from sporulated oocysts (a vaccine strain kindly provided by MSD-AH and used ~5 months after sporulation). The method for sporozoite isolation was provided by MSD-AH and is confidential. For the these experiments, fresh enteroids were not added to the cultures at 4 and 6 dpi, and RNA samples were collected at 2, 4, 6, and 8 dpi.

2.9 Quantification of mRNA and protein expression

2.9.1 RNA preparation

RNA was isolated as described for 2.7.2. Isolated RNA concentration was assessed using the Spectrophotometer ND-100 (NanoDrop) and samples stored at -20 or -80°C depending on how rapidly they were used.

2.9.2 PCR

Reverse transcription of RNA samples was performed according to manufacturer's instructions using the Superscript III First Strand Synthesis System (Invitrogen). Random primers, oligo (dT)20, 10mM dNTP mix and RNaseOUT recombinant RNase inhibitor (Invitrogen) and 1 µg of total RNA were used alongside the PTC-225 Peltier thermal cycler (MJ Research). The cDNA samples were stored at -20°C until required.

A polymerase chain reaction (PCR) was performed on the cDNA using the Taq DNA Polymerase kit (Invitrogen) according to manufacturer's instructions, the PTC-225 Peltier thermal cycler, and using previously described *EtGAM56* PCR primers[274]. PCR products were run in a 3% agarose gel and bands at the appropriate size had their DNA extracted using

the QIAquick Gel Extraction Kit (Qiagen) according to manufacturer's instructions. The purified DNA fragments were sent for Sanger sequencing at Edinburgh Genomics with the *EtGAM56* primers.

2.9.3 High-throughput qPCR using the 96.96 dynamic array

Reverse transcription was performed on RNA samples using a High Capacity Reverse Transcription Kit (Applied Biosystems) according to manufacturer's instructions. Random primers, oligo (dT) and 100 ng total RNA were added to a final volume of 10 µl and processed in a PTC-225 Peltier thermal cycler. The cDNA samples were stored at -20°C until further use.

Preamplification of the cDNA, exonuclease treatment step, and qPCR were performed as previously described[275]. The primers described in Borowska et al. (2019) were used in the array for the *Salmonella*/LPS and *Eimeria* infected enteroid samples[275]. For the Influenza virus infected enteroids, 53 genes from the published array were used and 37 different genes were selected from published transcriptome data.

2.9.4 Western blot

Samples were harvested in Laemmli buffer and stored at 4°C until required. Samples were heated at 100°C for 10 min to denature proteins then processed as previously described[276]. Primary antibodies used for western blot were mouse anti-NP AA5H monoclonal antibody (Abcam. 1/1000 dilution) and rat anti-β tubulin monoclonal antibody (Abd-Serotech, 1/5000 dilution). Blots were probed with primary antibody diluted in 5% dehydrated milk in Tris-Buffered Saline (TBS) overnight, followed by the Alexa Fluor secondary antibodies (TFS, 1/5000) for 1 h. Bands were visualised in a G:Box Gel Scanner (Syngene).

2.10 Statistics and reproducibility

The legend of each figure provide most details of sample sizes, numbers of replicates, number of repeats and statistics used. Unless otherwise stated, experiments are representative of data from at least 3 independent cultures

each containing 2 - 3 embryos. RNA sequencing data is representative of 3 independent experiments, each comprising of 2 technical replicates, each containing 3 embryos. In each avian culture of 48 wells or murine culture of 12 wells, 4 pooled wells with ~100 enteroids/well were used for each histology sample. Each RNA sample was comprised of 8 pooled wells containing ~100 enteroids/well. Protein samples were comprised of 2 wells containing ~50 enteroids/well. All measurements were recorded from distinct samples except for Fig. 3.3 and Fig. 3.5 where repeated measurements were made against the same enteroids over time i.e. dependent. Data presented in bar graphs are mean ± SD or SEM. Values of T >2 or <-2 and P ≤0.05 were accepted as significant (*), P ≤0.001 as very significant (**), and P ≤0.0001 as extremely significant (***).

Anderson-Darling normality tests were used to assess the normal distribution. For normally distributed data, significant differences between samples at different time points were determined by Student's *t*-test. Where results were not normally distributed and there were more than 2 groups, a Kruskal-Wallis test was used to confirm whole dataset significance. Where variance was not equal between two groups a Mann-Whitney U test was used. A linear regression test was employed to model the relationship between time (h) and *Salmonella* replication (CFU, Fig. 6.1). A linear mixed effects model with post hoc pairwise *t*-tests were used to model the relationship between time (day) and enteroid morphology (Fig. 3.3a). The R^2 coefficient of determination was used to measure the correlation between visually dying (disintegrating) enteroids and LDH (lactate dehydrogenase) release (Fig. 3.3c).

In the RNA-seq data an ANOVA test was performed to compare the associations between continuous value ranges in principal components and categorical experimental factors (Table 5.2). Statistical assessment of the RNA-seq differential expression data was carried out using a quasi-likelihood F-test on the contrasts 0 to 1 day, 1 to 3 day, 3 to 4 day, and 4 to 7 day (Fig. 5.3). A Pearson's correlation coefficient was used to measure the strength

and direction of the linear relationship between genes/transcripts in the RNA-seq network analysis (Fig. 5.5).

The qPCR data pre-processing, normalisation, relative quantification and statistics were performed in GenEx5 and GenEx Enterprise (MultiD Analyses AB). The data was corrected for 0.9 reaction efficiency. The most stably expressed reference genes for each dataset were actin beta (*ACTB),* glyceraldehyde 3-phosphate dehydrogenase *(GAPDH),* glucuronidase beta *(GUSB),* ribosomal *(r)28S* and TATA-binding protein (*TBP)* for the *Salmonella* and influenza datasets, and *ACTB* and *TBP* for the *Eimeria* dataset. These were identified from a panel of 6 reference genes using geNorm and NormFinder, as previously described[277] and the geometric means of the most stably expressed reference genes were used to normalise all samples in GenEx5. The normalised dataset technical replicates were averaged and unpaired 2-tail Student's t-test comparisons using delta cycle threshold (ΔCt) values were performed (GenEx5). Further normalisation to the highest ΔCt value for a given gene was performed and relative quantities were transformed to logarithmic scale (log2) before performing the PCA.

2.11 Data availability

The enteroid mRNA expression datasets for 0 h, 3 day and 7 days of culture have been deposited in the European Nucleotide Archive at EMBL-EBI under accession number PRJEB37491 (https://www.ebi.ac.uk/ena/data/view/PRJEB37491).

Chapter 3 Development of the chicken enteroid model

Chapter 3 Development of the chicken enteroid model

Chapter partially adapted from Nash et al. DOI: 10.1038/s42003-021-01901-z (Additional file 1)

In vitro avian gastrointestinal studies have long been hampered by the lack of representative intestinal cell culture models. Mammalian 3D enteroids mirror *in vivo* intestinal organisation and are powerful tools to investigate intestinal cell biology and host-pathogen interactions. As yet, chicken enteroids grown in microenvironments successful for other species fail to recapitulate the morphology of their organ of origin and as such are limited *in vitro* models. This chapter describes the development of protocols to culture complex multilobulated chicken enteroids from intestinal embryonic villi and adult crypts. The floating growth conditions are distinct from traditional enteroid cultures and enable the rapid development of 3D models which resemble the *in vivo* intestinal architecture. Although floating enteroid passage techniques have not been established, the cultures maintain viability for over a week and can be successfully cryopreserved.

3.1 Introduction

Prior to the development of 3D enteroids, the fundamental analysis of gut biology and applied research of intestinal tract physiology had been hampered by the lack of appropriate *in vitro* model systems[278]. This is particularly apparent for avian species for which there are no IEC lines available. The expertise to grow self-organising enteroids from adult ISC has now been developed in numerous mammalian species[42,183,193,209]. By isolating intestinal crypts or single multipotent adult ISC, embedding the cells in a gel matrix and adding external growth factors, 3D epithelial enteroids can be generated with organized crypt and villus domains, a polarised epithelium, a functional lumen and comprising most differentiated cell types at normal ratios[43].

However, attempting to grow chicken enteroids in the microenvironments successful for other species has so far yielded limited results, revealing structures more akin to enterospheres with few if any defined crypt- and villus-like domains[195,215,216]. While most published chicken protocols gel embed the adult ISCs in a Matrigel scaffold, a 5% Matrigel hanging drop culture and a floating culture have also been demonstrated[217,220]. Various growth factors that support mammalian enteroid proliferation have also been trialled including EGF, RSPO1, Noggin, PGE_2 and WNT3a[195,215,216,220]. However, although some of these supplements positively influence the chicken cultures[215,216,217], the resultant 3D structures have not been shown to resemble the array of differentiated cells found in the avian *in vivo* intestine[164,279]. Organoids by definition should resemble their native counterparts in cellular content, multicellular architecture and functional features[219]. Therefore despite continued improvements in the chicken enteroid field, the cultures do not meet the organoid criteria and consequently have limited functional applications.

The aim of this chapter is to develop a novel *in vitro* long-term self-renewing culture system to grow chicken enteroids which recapitulate *in vivo* intestinal epithelial structures. The main objectives include developing protocols to cleanly isolate crypts/villi whilst maintaining the integrity of the resident ISC population from both the embryonic and mature chicken small intestine. Followed by extensive optimisation of 3D enteroid culture and passaging techniques involving the testing of various scaffolds and growth factors to identify the most effective combination. In order to validate the resultant enteroid model and investigate the effect of growth or inhibitory factors on the cultures, complimentary methods to quantitatively and qualitatively measure enteroid growth and viability will also be investigated.

3.2 Results

3.2.1 Optimising the chicken crypt or villi isolation protocol

An extensive variety of parameters were tested in an attempt to optimise clean crypt or villi isolation from the chicken intestine, as well as the differentiation and maintenance in culture of chicken enteroids. In general, a single independent variable was tested against a control (variable unchanged) then the digestion fractions and cultures were compared using brightfield microscopy for amount of debris and enteroid budding respectively. Direct comparisons of the individual components of the crypt isolation protocol were not always possible as, initially, the increased time required to complete more than two isolations from the same intestinal samples in parallel was in itself causing poor enteroid budding and reduced culture longevity.

The crypt or villi isolation variables included age of chicken or embryo, enzyme digestion steps, filtering of digested fractions to remove cell debris, and temperature and media composition (Fig. 3.1, Table 3.1). Variables that were obviously detrimental to the isolation protocols, and therefore enteroid cultures, included using cold media and cold plastics, taking a prolonged time to isolate the crypts or villi, not cleaning the tissue effectively pre-digestion, digesting for an inappropriate time at an inappropriate shaking-incubator speed, and not filtering the digested fractions (Table 3.1). Embryonic intestines were identified as having the cleanest crypt or villus isolation and forming the healthiest looking chicken enteroid cultures, based on budding kinetics and bud length.

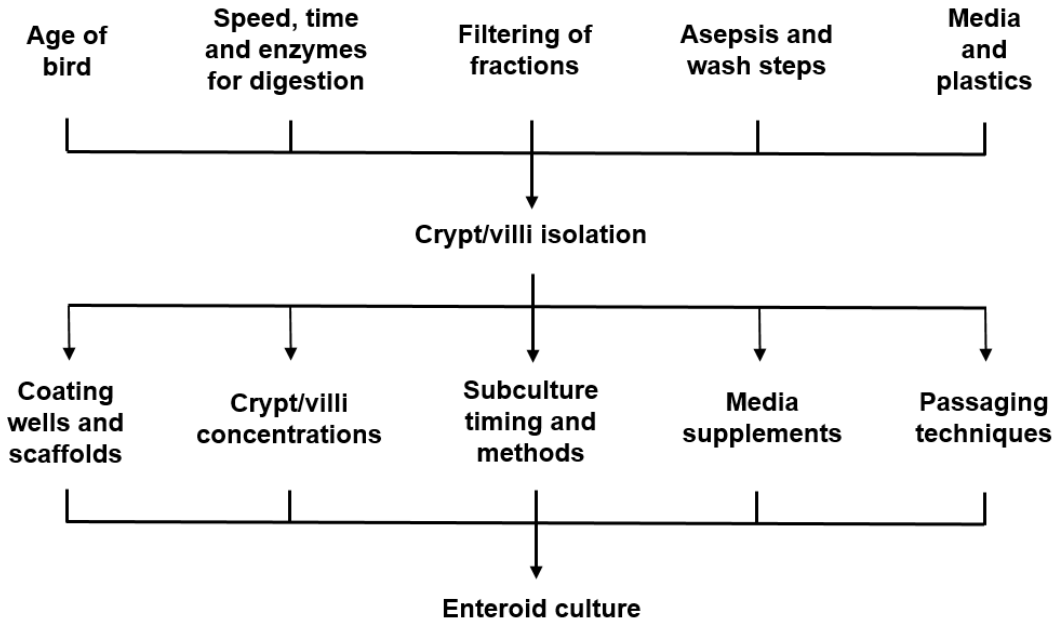

Figure 3.1: General variable categories tested for development of the crypt or villi isolation and enteroid culture protocols. Schematic diagram summarising the general variables tested when developing and optimising the chicken intestinal crypt or villi isolation and chicken enteroid culture protocols.

Table 3.1: Protocol variables causing poorly budding cultures. Chicken crypt or villi isolation and enteroid culture protocol variables which were identified as resulting in poorly budding enteroid cultures. Variables which caused no effect on cultures are not included. Each variable trial was representative of at least 3 independent cultures.

Variable	Cause of poorly budding cultures
Age of bird	>ED20 and post-hatch birds
Practical skills	prepping >7 embryos at a time not shaking vigorously post-digestion
Media and plastics	cold plastics and cold media
Speed, time, temp for digestion	> or < 200 rpm, > or < 50 min, > or < 37°C digestion
Asepsis and wash steps	gentamicin addition to media penicillin/streptomycin omission from media <3 wash steps pre-digestion Isolation outside TC hood
Crypt/villi concentrations	Seeding >200 crypts or villi per well
Coating wells	growth factor reduced (GFR) Matrigel
Subculture timing and methods	subculture >24 h after crypts or villi initially seeded too much time out of incubator repeated centrifuging
Filtering of fractions	no filter step for fractions (results in excess single cells)
Scaffold	Matrigel embedding (GFR + non-GFR) suspension in 5% GFR Matrigel

In brief, the final optimised protocol involved removal of the embryonic small intestine immediately post-mortem which was cut open longitudinally then into 5 mm sections. The tissue fragments were collected into warmed Ca^{2+}- and Mg^{2+}-free PBS and washed at least 3 times. Tissue fragments were then digested in DMEM with 0.2 mg/mL Collagenase from *Clostridium histolyticum* Type IA at 37°C for 50 min in a shaking incubator at 200 rpm. After digestion, the tube was vigorously shaken, tissue allowed to settle then the supernatant was collected and filtered. These steps were repeated to generate 4 fractions. Fractions were centrifuged at 100 x *g* for 4 min and resuspended pellets of crypts or villi were assessed. Fractions were selected based on

good crypt or villi integrity and minimal debris, then crypts or villi were counted. These experiments resulted in the optimisation of a protocol ensuring the clean and efficient isolation of crypts or villi from the small intestine of chicken embryos in a way that maintained their integrity and organisation. This optimised protocol proved an essential contribution to the subsequent extensive budding and longevity of cultured enteroids.

3.2.2 Differentiation of multilobulated 3D chicken enteroids.

Using the protocol from 3.2.1 for isolating crypts or villi, the next aim was to develop enteroids which had an architecture, cellular diversity and function comparable to the *in vivo* intestine. This required the testing of a large array of culture variables including the number of crypt or villi seeded per well, type and concentration of gel ECM, methods of subculturing and addition of exogenous growth factors (Fig. 3.1, Table 3.1). Culture techniques that were obviously detrimental included seeding the crypts or villi at high concentrations, not subculturing the enteroids 24 h after initial seeding, and the addition of gentamicin and 5% Matrigel (Table 3.1). As seen in previous publications, embryonic crypts or villi seeded in Matrigel gel domes formed empty spheroid structures that increased in size over 7 days of culture, however the architecture remained basic with no obviously defined crypt-villus development (Fig. 3.2a, b)[195,215].

By omitting the gel ECM and simply floating the chicken crypts or villi in media alone, enteroid morphology dramatically improved, indicating that the presence of a scaffold or another component of Matrigel was responsible for inhibiting enteroid bud formation (Fig. 3.2c, d). The floating enteroid protocol involved resuspending the crypts or villi of selected fractions from 3.2.1.in a floating organoid media (FOM) at ~200/mL and plating them out. The FOM contained advanced DMEM/F12 supplemented with 10 mM HEPES, 2 mM L-Glutamine, 50 U/mL Penicillin/Streptomycin and 2% B27 supplement (50X). Differentiation of avian enteroids occurred at 37°C, 5% CO_2. After 24 h the floating enteroids were transferred to wells containing fresh media and half the media was replaced every 2 days by tilting the plates.

Live cell imaging using the optimised isolation and culture protocols showed crypts or villi rapidly and consistently formed compact spheroid structures by 4 h of culture, and by 24 h multiple budding domains began to establish (Fig. 3.2e, supplementary Video 1 from Nash et al.. 2021 PMID: 33742093). By day 2 - 3, chicken enteroids appeared fully mature with multiple elongated buds (Fig. 3.2c) which continued to lengthen over the following 1 - 2 weeks in culture (Fig. 3.2d).

Supplementation of FOM with human growth factors Noggin, RSPO1 and EGF, conferred no obvious advantage in development or resultant architecture of embryonic floating enteroids during the first 9 days of culture (Fig. 3.2f - i). These small molecules did initially support large numbers of empty enterosphere-like structures with budding events (Fig. 3.2f) which persisted for a couple of days. However, subsequently the cultures began to resemble those without growth factor supplementation where the enteroids have solid spheroid cores (Fig. 3.2g, i).

These results demonstrated that multiple budding chicken enteroids developed rapidly when floating in culture media. In contrast, attempting to seed these cultures in Matrigel or supplement them with typical mammalian growth factors failed to result in obvious benefits for the chicken enteroid development.

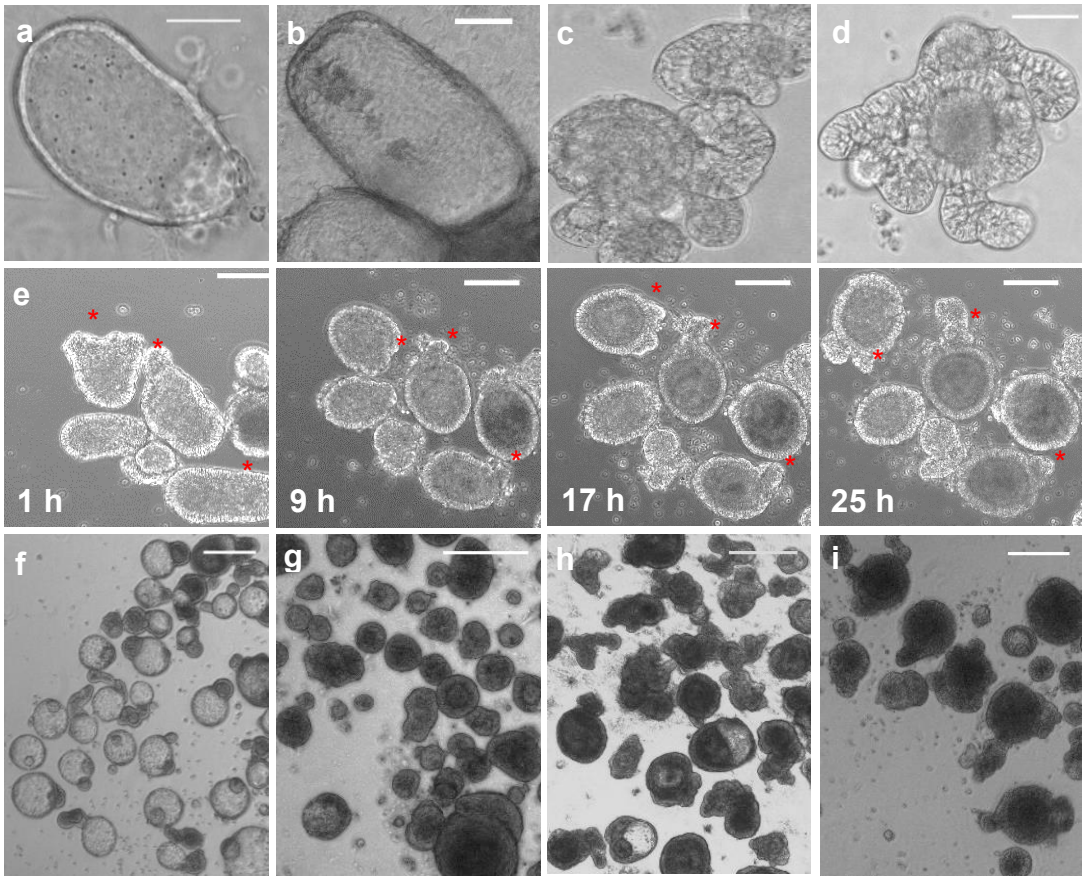

Figure 3.2: Optimising the chicken enteroid protocol. a Matrigel-embedded embryonic chicken spheroids increase in size but lack budding at day 1 and (**b**) day 7 of culture. **c** Floating large multilobulated chicken enteroid structures develop over 3 days and (**d**) are maintained at day 9 of culture. Scale bar: 50 µm. **e** Time-lapse images (from Supplementary video 1 Nash *et al.* 2021 PMID: 33742093) showing the formation of budding crypt-like structures (marked by red star *) in floating embryonic enteroids. Images are representative of data from at least 20 independent cultures each containing 2-3 embryos. Scale bar: 100 µm. **f** Brightfield images of representative enteroid cultures supplemented with EGF, RSPO1 and Noggin at day 1 and (**g**) day 9 compared to FOM-only at (**h**) day 1 and (**i**) day 9 of culture. Images are representative of 3 independent cultures. Scale bar: 200 µm.

3.2.3 Changes in chicken enteroid culture viability over time

Complimentary techniques to quantitatively measure the floating chicken enteroid culture viability over time were investigated. The aim of establishing

these standard baselines was to assist in measuring the effect of external stimuli on the enteroids in ongoing studies and to assess replication of the culture protocol when performed by different individuals and laboratories.

The first technique employed brightfield microscopy to simply classify and count enteroid morphologies in a culture dish. Multiple budding enteroid numbers were seen to increase significantly in the first day of culture then decreased between 5 - 7 days (Fig. 3.3a). Over the following 1 - 2 weeks some enteroids remained active with continued lengthening of the buds whereas others lost their buds but continued in the cultures in a spheroid form. There was a slow but steady disintegration and loss of enteroids from the cultures 3 days after villus isolation (Fig. 3.3a).

A colorimetric assay for quantitating enteroid culture viability by measuring LDH activity released from damaged cells was used for the second technique. This method is more objective and indicated a steady increase in enteroid cell death from 1 - 13 days of culture (Fig. 3.3b). The cytotoxicity percentage didn't rise above 50% from 7 - 17 days post isolation but since fresh FOM needed to be added during the LDH analysis, this dilution may have affected cumulative enteroid cytotoxicity calculations. However a significant correlation between numbers of disintegrating enteroids and LDH release was demonstrated (Fig. 3.3c), indicating these quantitative methods are complimentary to each other.

In summary, both chicken enteroid morphology counts by brightfield microscopy and quantitation of LDH activity in the cultures proved effective methods to measure changes in the enteroid cultures over time.

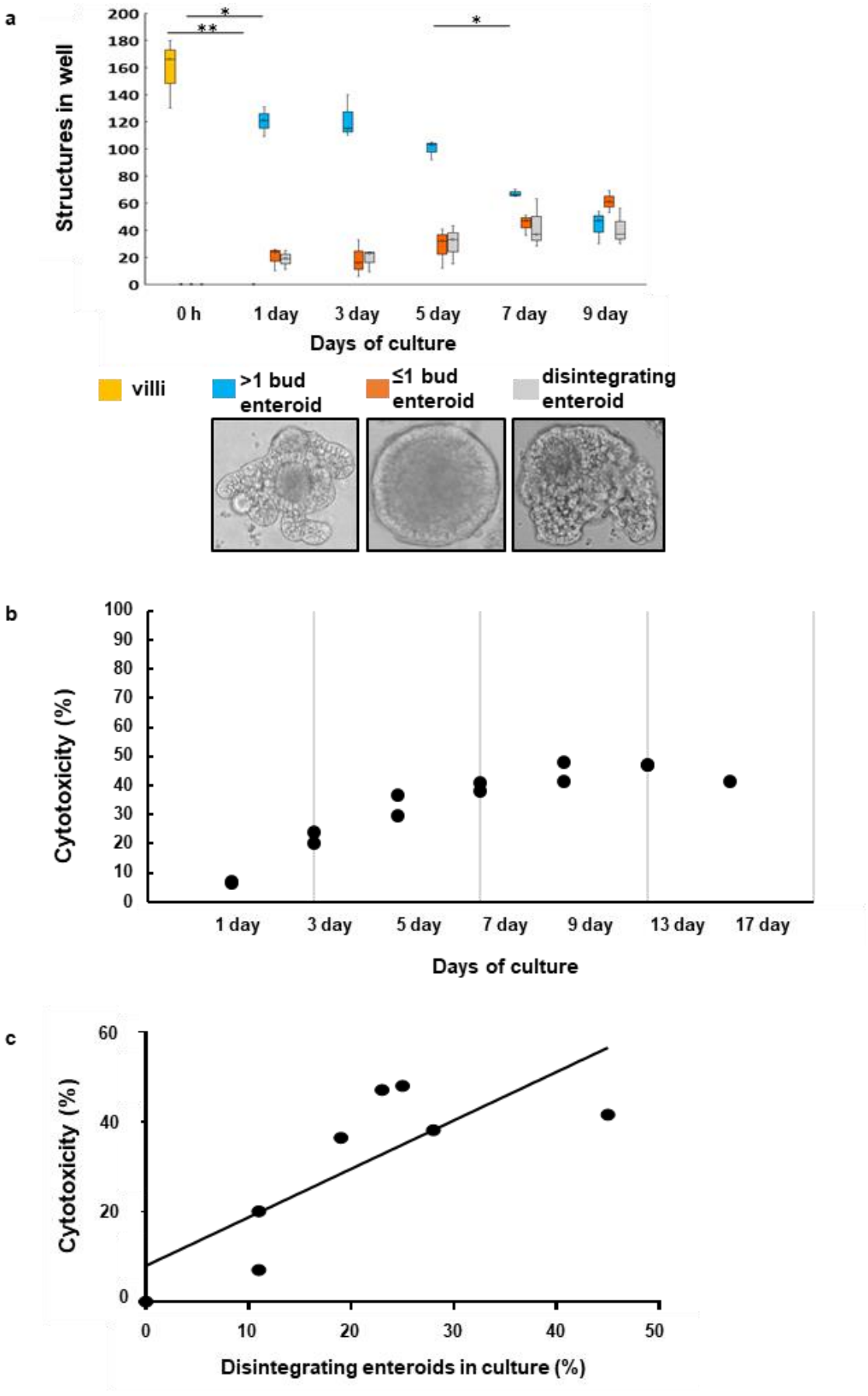
a
Structures in well
200
180
160
140
120
100
80
60
40
20
0
*
**
*
0 h
1 day
3 day
5 day
7 day
9 day
Days of culture
villi
>1 bud enteroid
≤1 bud enteroid
disintegrating enteroid
b
Cytotoxicity (%)
100
90
80
70
60
50
40
30
20
10
0
1 day
3 day
5 day
7 day
9 day
13 day
17 day
Days of culture
c
Cytotoxicity (%)
60
40
20
0
0
10
20
30
40
50
Disintegrating enteroids in culture (%)

Figure 3.3: Viability assessments of floating chicken enteroids. a Quantification of floating embryonic enteroid numbers and morphology. Data averaged for 3 cultures containing 2-3 embryos, 3 wells/culture, ~180 villi seeded per well at day 0. Error bars = ± CI. Villi/crypts: *t = 3.58, F = 8.07, df =1; >1 bud enteroid: *t = 4.26, F = 0.03, df =1 using a linear mixed effects model. Villi 0 h – 1 day: *P = 0.009, t = 10.65; >1 bud enteroid 0 h – 1 day: **P = 0.003, t = -18.92; >1 bud enteroid 5 – 7 day: *P = 0.008, t = 10.8 using post hoc pairwise *t*-tests. **b** Viability detection assay: colorimetric assay which quantitates enteroid viability by measuring cytotoxicity (LDH activity released from damaged cells). **c** Correlation between visually dying (disintegrating) enteroids and LDH release *P = 0.019, R^2 = 0.792.

3.2.4 Proliferation, apoptosis and stress in the chicken enteroid model

To demonstrate that the enteroids were budding as a result of cell division rather than reorganisation, EdU staining was performed. EdU is a thymidine analogue that is incorporated into newly synthesised DNA by cells and was incubated with enteroid cultures for 1 h. The growing enteroid buds contained numerous proliferating (EdU+) cells at 14 h of culture (Fig. 3.4a, e) and cell proliferation continued to occur in the core and buds at 3 and 7 days of culture (Fig. 3.4b - e). The percentage of proliferating cells in the enteroids dropped from almost 10% at 14 h to 5% after 7 days of culture.

In order to characterise the floating chicken enteroid model at the level of the transcriptome, and here to specifically to assess the level of apoptosis and stress in the cultures over the first week of culture, RNA-seq was performed on 0 h (freshly isolated ED18 intestinal villi) and 1, 3, 4 and 7 day chicken enteroids (Chapter 2, 2.7). The RNA-seq experimental design involved three biological replicates, where isolated villi of three embryos were pooled to make one biological replicate, and each culture was split into two technical replicates after villus isolation (Chapter 5, Fig. 5.1).

The subsequent transcriptome analysis showed a relatively stable expression of apoptotic markers over the culture period (Fig. 3.4f). This static apoptotic gene signature and continued evidence of EdU+ cells may represent the

natural process of proliferation and apoptosis in *in vivo* intestinal cell turnover. In addition, although a range of cell stress associated genes (derived from murine studies[43]) were expressed in the enteroids, there was no significant evidence of modulation of their expression across the time points (Fig. 3.4g). Steady expression of both the apoptotic and stress gene sets throughout the time points, alongside ongoing evidence of proliferation, indicates the enteroid cultures remain stable over at least 7 days.

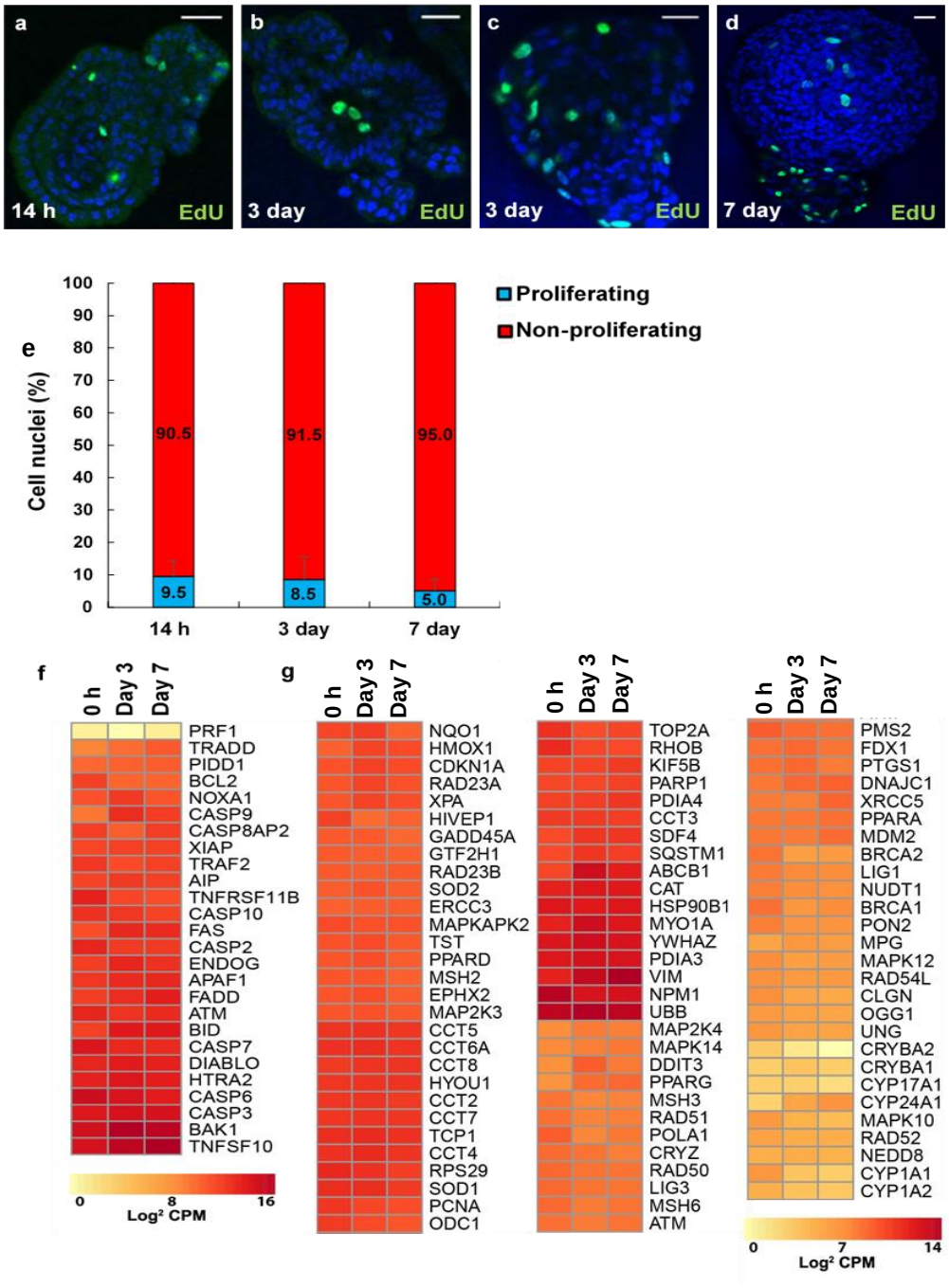

Figure 3.4: Proliferation, apoptosis and stress in the chicken enteroid cultures. Confocal images of floating embryonic enteroids showing proliferating cells (green, EdU) in both buds and core at (**a**) 14 h, (**b, c**) 3 days and (**d**) 7 days of culture. Images are representative of 3 independent cultures. Scale bar: 200 µm. (**e**) Graph demonstrating the percentage of proliferating (EdU+) cells within enteroids over 7 days of culture. Gene expression in freshly isolated villi or crypts (0 h), 3 and 7 day chicken enteroids was compared by RNA sequencing analysis. Heat maps show the expression levels (log2 CPM reads) of a range of (**f**) apoptosis-related and (**g**) stress-related genes over 7 days of culture. RNA sequencing data is representative of 3 independent experiments each comprising of 2 technical replicates each containing 3 embryos**.**

3.2.5 Isolating crypts and deriving enteroids from mature chicken intestine

To investigate whether crypts or villi isolated from mature birds would form enteroids in floating culture, protocols for intestinal crypt or villi isolation from 6 and 9 week old birds and subsequent enteroid culture were established. The basic embryonic gut protocol was followed with alternative steps to flush and scrape the mucosa and wash the tissue fragments (Chapter 2, 2.2.1). The resultant protocol efficiently isolated mature chicken crypts or villi (Fig. 3.5a, a1), which then successfully formed floating enteroids (Fig. 3.5b - d). However fractions also contained small amounts of mucus and debris (Fig. 3.5a) which may partly explain why mature chicken enteroids developed fewer buds and the longer-term viability of the cultures was lower compared to enteroids prepared from embryonic tissue (Fig. 3.5e).

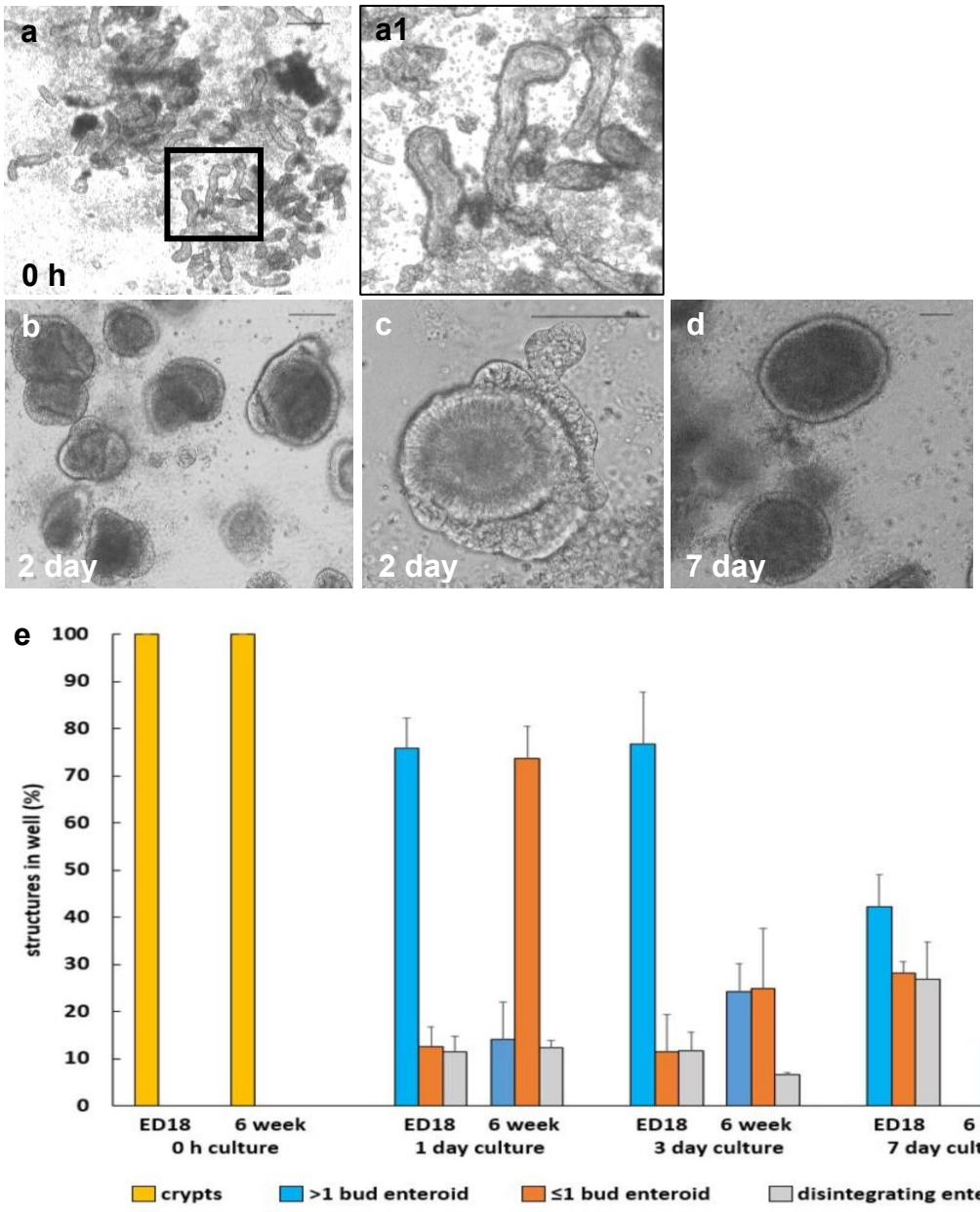

Figure 3.5: Enteroids derived from mature chicken gut. **a – e** Brightfield images of **(a, a1** magnified image of a**)** chicken crypts/villi isolated from 9 week old chickens developed into enteroids at **(b, c)** 2 days and **(d)** 7 days of culture. Images are representative of 3 independent cultures. Scale bar: a1 20 µm, a, b – d 100 µm**. e** Budding and viability of enteroids derived from 6 week old chicken gut compared to enteroids derived from embryonic tissue. Bars represent mean ± SD derived from 3 independent experiments each containing 2 - 3 embryos or one 6 week old chicken, 3 wells/culture.

3.2.6 Challenges in chicken enteroid passaging

A consistent yield of embryonic chicken enteroids suitable for further analysis had been routinely achieved with the developed protocols. However, as demonstrated in the viability assessments (Fig. 3.3a - c), the cultures started to deteriorate within the first week. They therefore did not have the prolonged passage-dependent lifespan described for enteroids from other species[43,183]. To attempt to passage 7 day old enteroids (Fig. 3.6a) we initially used mechanical disruption to remove the crypt-domain buds (Fig. 3.6b). Despite the addition of supplements reported to improve passage in other species e.g. ROCK inhibitor Y-27632, TGF-β inhibitor LY2157632, MAPK inhibitor SB202190, EGF, RSPO1 and Noggin[42,183,184] there was no post-passage growth or budding of the enteroids after 3 days in either un-supplemented (Fig. 3.6c) or supplemented FOM (Fig. 3.6d). Various other combinations of mechanical and chemical passaging techniques were trialled (Chapter 2, 2.4.1, Fig. 3.6e - h) and numerous other growth and inhibitory supplement combinations were added to the passaged cultures (data not shown) including valproic acid and sodium butyrate (HDAC inhibitors which promote proliferation and self-renewal of stem cells). However despite the assessment of a range of techniques, supplements and variables the floating enteroids failed to display proliferation post-passage.

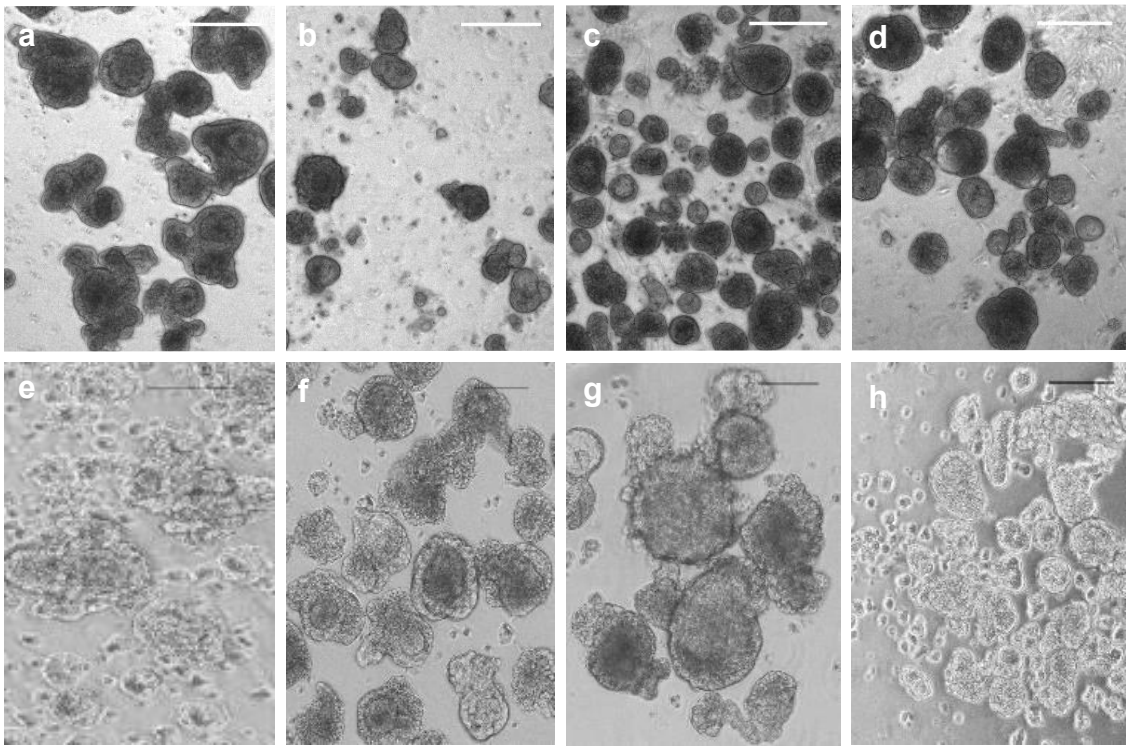

Figure 3.6: Chicken enteroid passage trials. Chicken enteroids at (**a**) day 4 culture, (**b**) immediately post-passage (repeated pipetting through a 200 µl tip) and (**c**) day 3 post-passage in plain and (**d**) growth factor supplemented media (ROCK inhibitor Y-27632, TGF-β inhibitor LY2157632, MAP kinase inhibitor SB202190, EGF, RSPO1 and Noggin). Additional passage techniques included (**e**) 0.2 mg/mL collagenase from *Clostridium histolyticum* Type 1A digest, (**f**) trypLE digest, (**g**) trypLE digest followed by repeated pipetting through a 200 µl tip, and (**h**) repeated 25G needle passage without enzyme digest.

3.2.7 Cryopreservation of the chicken enteroids

In the absence of the ability to passage the enteroids, an alternative method to enable rapid and universal access to the chicken enteroid cultures and ensure utilisation of the maximum numbers of crypts or villi from every embryo was required. A protocol was therefore developed to cryopreserve the crypts or villi at the point of isolation from intestinal tissue, as well as chicken enteroids during early culture. Successful recovery of embryonic small intestinal crypts or villi from cryopreserved stocks (Fig. 3.7a) was

demonstrated by their subsequent resuscitation and growth into extensively budding enteroids (Fig. 3.7b) at similar rates to freshly isolated crypts or villi (Fig. 3.7c, d). Two day old enteroids were also successfully recovered from liquid nitrogen storage (Fig. 3.7e) and after 2 days (Fig. 3.7f) the gross morphology resembled 4 day enteroid cultures from freshly isolated crypts or villi (Fig. 3.7g, h).

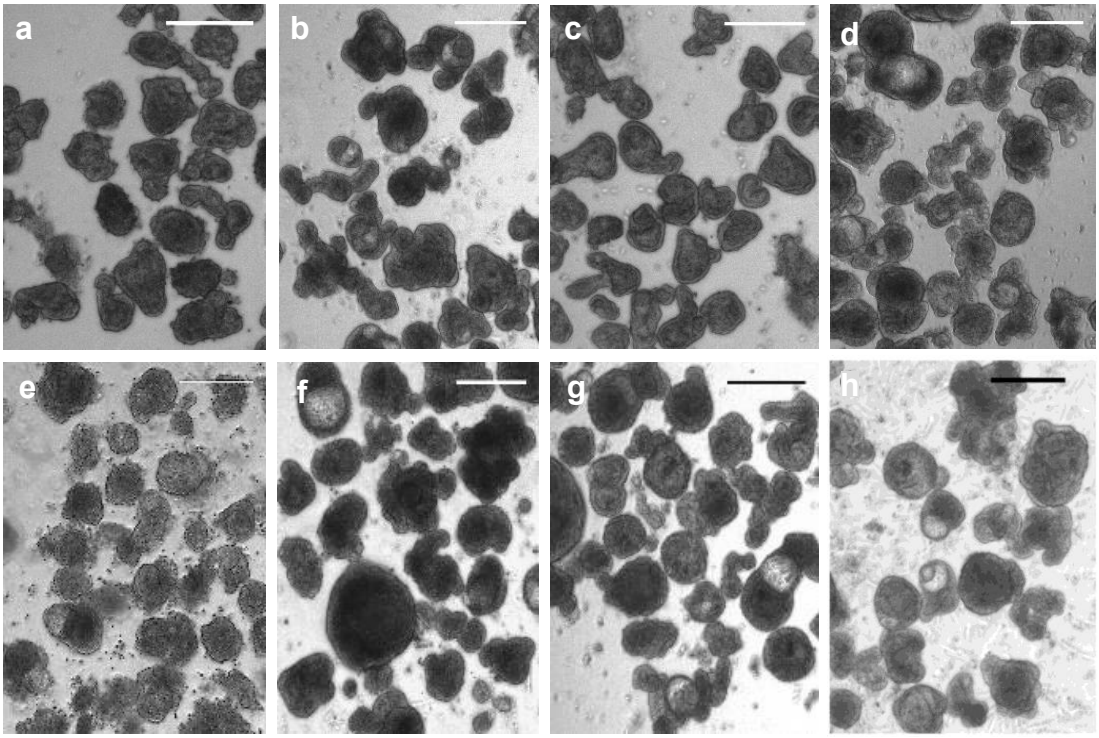

Figure 3.7: Cryopreservation of chicken crypts or villi and enteroids. Cryopreserved crypts or villi at (**a**) point of thaw and (**b**) after 4 days of culture compared to (**c**) freshly isolated crypts or villi then (**d**) cultured for 4 days. **e** Cryopreserved 2 day enteroids at point of thaw and (**f**) after 3 days of culture post-thaw, compared to (**g**) freshly cultured 2 day enteroids and (**h**) 5 day enteroids. Images **a - h** are representative of at least 3 independent cultures each containing 2 - 3 embryos. Scale bar: 200 µm.

In summary, a protocol to successfully cryopreserve both embryonic crypts or villi and floating chicken enteroids has been established.

3.3 Discussion

Mammalian 3D enteroids already facilitate research into multicellular biological mechanisms, proving to be more physiologically relevant than traditional monolayer cultures of cell-lines and reducing the number of *in vivo* studies. The use of established protocols originally devised for the culture of murine crypts has so far failed to generate avian enteroids that are representative of the intestine[195,215,216]. Here we describe a method to successfully differentiate self-organising, extensively budding avian enteroids from both embryonic and mature chicken gut that mimic the *in vivo* architecture of the avian small intestine.

Floating chicken crypts or villi in media, in the absence of a gel scaffold, results in the rapid development of enteroids with multiple villus-like buds proliferating from the central core. This is in stark contrast to the thin-walled non-budding empty enterospheres produced when chicken crypts or villi are cultured in Matrigel. Mammalian enteroids have also been shown to survive floating in media, when first developed and differentiated in Matrigel, but they do not appear to last longer than 3 – 5 days in this culture environment[211,212]. Many complex 2-way interactions between ISC and ECM molecules have been shown to influence intracellular signalling and govern differentiation in enteroids. For example the physical properties (elasticity or stiffness) of the matrix may play a role in the observed differences between the species[188]. Yes-associated protein (YAP), an effector in the Hippo signalling pathway, is crucial for ISC self-renewal and is also implicated in cellular mechanosensing and mechanotransduction, displaying enhanced activation in response to mechanical tension[280,281,282]. Stiff matrices have been shown to initially enhance YAP activity and nuclear translocation within mammalian ISC and encourage enteroid expansion, but continued growth within a stiff environment leads to YAP inactivation, retarding ISC differentiation and inhibiting *in vitro* organogenesis[188]. In the chicken enteroids *YAP1* is downregulated at 24 h then steadily upregulated over the remainder of the culture (Additional file 4) however post-transcriptional modifications and

nuclear translocation levels are unknown. Comparing the YAP activation status and cellular location in chicken and mouse enteroids in the floating and matrix-embedded state may indicate whether this pathway is responsible for the proliferation and differentiation dissimilarities.

Mouse ISCs embedded in ECMs which mimic the basic physical properties of Matrigel but do not contribute any biochemical signals, fail to form lumen-containing colonies. By enriching 3D ECMs with fibronectin, laminin-111, collagen IV, hyaluronic acid and perlecan, ISC survival is increased and proliferation becomes evident[188]. This demonstrates that basolateral cell receptors need to interact with specific combinations of ECM proteins for the development of enteroids from isolated crypts[188,283]. Ongoing investigations of chicken enteroid growth within different ECM analogues with variable mechanical and chemical compositions are required to determine the physical niche that is beneficial for chicken enteroid ISC survival and differentiation within a gel scaffold.

Floating chicken enteroids produce multiple buds and survive for a period of time without the addition of growth factors essential for mammalian cultures. Addition of common murine and human small molecules to the basic media of our floating embryonic cultures did not obviously positively affect the enteroid survival, size or budding capacity. This is in contrast to mammalian enteroid cultures where supplemented growth factors are essential. For example, in the absence of RSPO1 gel-embedded crypts isolated from mature mice close to form enteroids but then cease growth and die after 24 hours[261]; without Noggin these same murine enteroids lose *Lgr5* expression and cease proliferation[43]; and gel-embedded mature-human enteroids lacking EGF supplementation show reduced growth within a week[284]. Non-budding chicken enteroids/enterospheres have previously been shown to display positive responses to growth factors. Li et al. (2018) demonstrated Matrigel-embedded spheroid diameter is dependent on the concentration of supplemented EGF, Noggin and RSPO1[216], and Acharya et al. (2020) showed floating chicken spheroid cultures had an enterotropic response to IGF-1 and EGF[217]. Addition of recombinant chicken Noggin and RSPO to

chicken enteroid media has also not shown any significant beneficial effect on cultures (P. de Graaf, unpublished data), although the biological activity of these recombinant proteins was not assessed. Maturation of these floating chicken enteroid cultures in the absence of small molecule supplementation indicates that the cells within the enteroids are supplying the required factors for efficient ISC proliferation and differentiation. However to achieve longer-term cultures, trialling a greater variety of small molecules at various concentrations and/or producing an array of chicken-specific growth factors could be beneficial.

Crypts or villi from mature chickens, cultured in a manner similar to embryos, also formed multilobulated enteroids providing evidence that enteroid culture techniques can be successfully applied to other ages of bird. However, enteroids prepared from older birds have poorer budding and longevity as compared to those derived from embryonic individuals which, in part, is likely due to a decrease in the proportion of proliferative cells/ISC, lining the intestinal villi with age[7]. Differences in ISC abundance may also explain why the chicken enteroids mature markedly faster than their mammalian counterparts, although these growth rates may also be due to fundamental differences in their ISCs, and/or a limiting effect of growing the enteroids in an ECM versus floating.

The counts of buds per enteroid and numbers of enteroids showed a marked increase in multiple budding enteroids up to 3 days of culture followed by a steady decline in both after 5 days. However, a significant issue with morphological and phenotypical screening analyses is subjectivity. The LDH assay was therefore adopted as a more objective way to measure enteroid survival. The results correlated well with the microscopy counts, indicating viable enteroids were still present at 17 days. Other published methods used for large-scale monitoring of enteroid integrity and viability include the acid phosphatase assay and the AlamarBlue assay, in combination with various culturing platforms[285,286]. Although the viability assessments in this chapter have not yet been utilised in chicken enteroid challenge conditions, these results prove they will be useful analytical tools for enteroid modelling in

infectious disease, nutritional, pharmaceutical, and breeding company research.

Passaging results in the generation of a large number of organoids from a small piece of tissue. Mouse enteroids can be passaged weekly at a 1:5 ratio for over 1.5 years with a phenotype and karyotype that remains unchanged[35]. Without the ability to passage the floating chicken enteroid cultures, they do not have the longevity of those grown in more conventional culture systems[42,43]. This is likely due in part to the relative absence of exogenous growth and/or inhibitory factors. However, floating mammalian enteroids with an inside out polarity have only been shown to survive for up to 5 days in growth factor supplemented-culture and evidence for long-term propagation was not reported[211,212]. Therefore, the influence of the mechanical environment may also play a role in ISC survival and cell differentiation. Since the avian enteroids mature more quickly than their mammalian counterparts and can be used after 24 - 48 h for further experimentation, the lack of long-term culture longevity is not a substantially prohibitive factor. In addition, successful cryopreservation of enteroid-forming embryonic crypts or villi and 2 day old enteroids enables use of the same culture material for multiple studies. This biobanking technique also adheres to the 3Rs guidelines which are becoming increasingly implemented in new legislation, and allows transport of culture-forming material from different breeds and locations.

In summary, protocols to successfully isolate ISC containing crypts or villi from the embryonic and mature chicken intestine and derive multiple budding enteroids using a floating culture technique have been developed. These enteroids mature rapidly within 1 - 2 days and re-create 3D villus-like gross architecture thereby providing a more physiologically accurate chicken intestinal model than 2D cell cultures.

Chapter 4 Characterisation of the chicken enteroid model

Chapter 4 Characterisation of the chicken enteroid model

Chapter adapted from Nash et al. DOI: 10.1038/s42003-021-01901-z (Additional file 1)

Protocols to develop complex multilobulated floating chicken enteroid cultures from intestinal embryonic villi and adult crypts have been described in Chapter 3. These avian enteroids develop optimally in suspension without the structural support required to produce mammalian enteroids, although they cannot be passaged. In order to demonstrate this 3D culture is a good working model of the small intestine, evidence of differentiated epithelial cell types and intact cell-cell junctions is required. This chapter uses several histological, transcriptional and functional analyses to map the unusual epithelial polarisation, complex cellular architecture and functional cell junctions of the floating chicken enteroid model. In addition, the innate presence of functional intraepithelial and lamina propria leukocytes, a novel and striking feature of this enteroid model, is described. To expand the potential applications of the model, enteroids from two species of poultry and from different regions of the small and large intestine were also developed.

4.1 Introduction

Attempting to grow chicken enteroids in the microenvironments successful for other species has previously yielded limited results, revealing thin-walled structures with few if any defined crypt- and villus-like domains or the array differentiated cells found *in vivo*[195,215,216,279]. Chapter 3 describes the development of protocols to isolate intestinal embryonic and adult villi or crypts and to cultivate rapidly budding chicken enteroids in floating culture. A scaffold-free culture for poultry enteroids has previously been investigated by Acharya et al. (2020) but, in contrast to the cultures developed in Chapter 3, their non-growth factor supplemented media only produced solid spheroid structures with no budding[217]. Our floating growth conditions allow the

enteroids to grow and differentiate multiple elongated villus-like structures which more closely resemble the architecture of the *in vivo* intestine.

The intestinal epithelial layer has many essential functions in protection and digestion therefore a representative *in vitro* model of the gut surface must also be demonstrated to maintain the cellular repertoire, polarity and barrier functions present *in vivo* (reviewed in[63]). Typically, enteroid crypts feed into a central functional lumen and are lined by highly polarized epithelial cells whose apical brush borders face internally and basolateral surfaces lie in contact with the ECM scaffold[209]. A practical limitation of the 3D geometry and internal lumen of classical enteroids is that they prevent easy access to the apical epithelium. It was recently discovered that mammalian enteroids cultivated floating in media displayed a reverse polarisation of their epithelial layer[211,212]. Although the culture techniques are not identical, with mammalian enteroids established as mature cultures before floating, the chicken enteroid epithelial orientation may be similarly affected. In addition, mammalian enteroids are epithelial in nature with an empty central lumen however the floating chicken enteroids have an atypical cell dense core. It would be interesting to investigate the origin and cellular make-up of this component and therefore what it contributes to the models functional attributes.

The aims of this chapter are therefore to characterise the epithelium and central core of our floating enteroid model. This will involve using immunohistochemistry, TEM, RNA-seq and functional assays to describe the array of differentiated cell types and their function. I also intend to establish the epithelial polarity across different culture systems and species, in addition to creating site- and species-specific enteroid models of the chicken small and large intestine. This in-depth characterisation will indicate whether the floating avian enteroid model is capable of recapitulating the different functions of the intestinal surface, and therefore what future applications this 3D culture system could be used for.

4.2 Results

4.2.1 Floating poultry enteroids demonstrate an apical-out phenotype

Phalloidin staining to detect F-actin in the floating enteroids, showed that the epithelial cells of self-organising embryonic floating chicken enteroids at 2 and 7 days of culture had an atypical reversed polarity (Fig. 4.1a, b). The F-actin positive apical brush border could be visualised on the external surface of the epithelial cells, facing the media (Fig. 4.1a closed arrow). Whereas the basal epithelial cell surface abutted a dense central cellular core (Fig. 4.1a open arrow).

To confirm the apical-out phenomenon was unique to floating enteroids, isolated embryonic chicken crypts or villi were embedded in Matrigel and imaged at 2 and 7 days of culture (Fig. 4.1c, d). The orientation of the epithelial layer in chicken enterospheres at both time points reflected their mammalian Matrigel-embedded enteroid counterparts (Fig. 4.1k), with the basal cell surface polarised towards the outside, touching the Matrigel, and enterocyte brush borders creating a central luminal surface. The epithelial apical-basolateral polarity of Matrigel-embedded enteroids was uniformly opposite to that of the floating enteroids (Fig. 4.1a, b).

To investigate if the reverse polarity was related to the age and type of progenitor enteroid tissue, the same staining was performed on 2 and 7 day enteroids derived from 6 - 9 week old chicken crypts or villi (Fig. 4.1e-h). These enteroids/enterospheres displayed identical epithelial polarisation to enteroids developed from embryos, both when grown in Matrigel (internal brush border) or floating (external brush border). Unlike the embryonic enteroids however, some adult gel-embedded structures displayed evidence of budding on the internal surface (Fig. 4.1g)

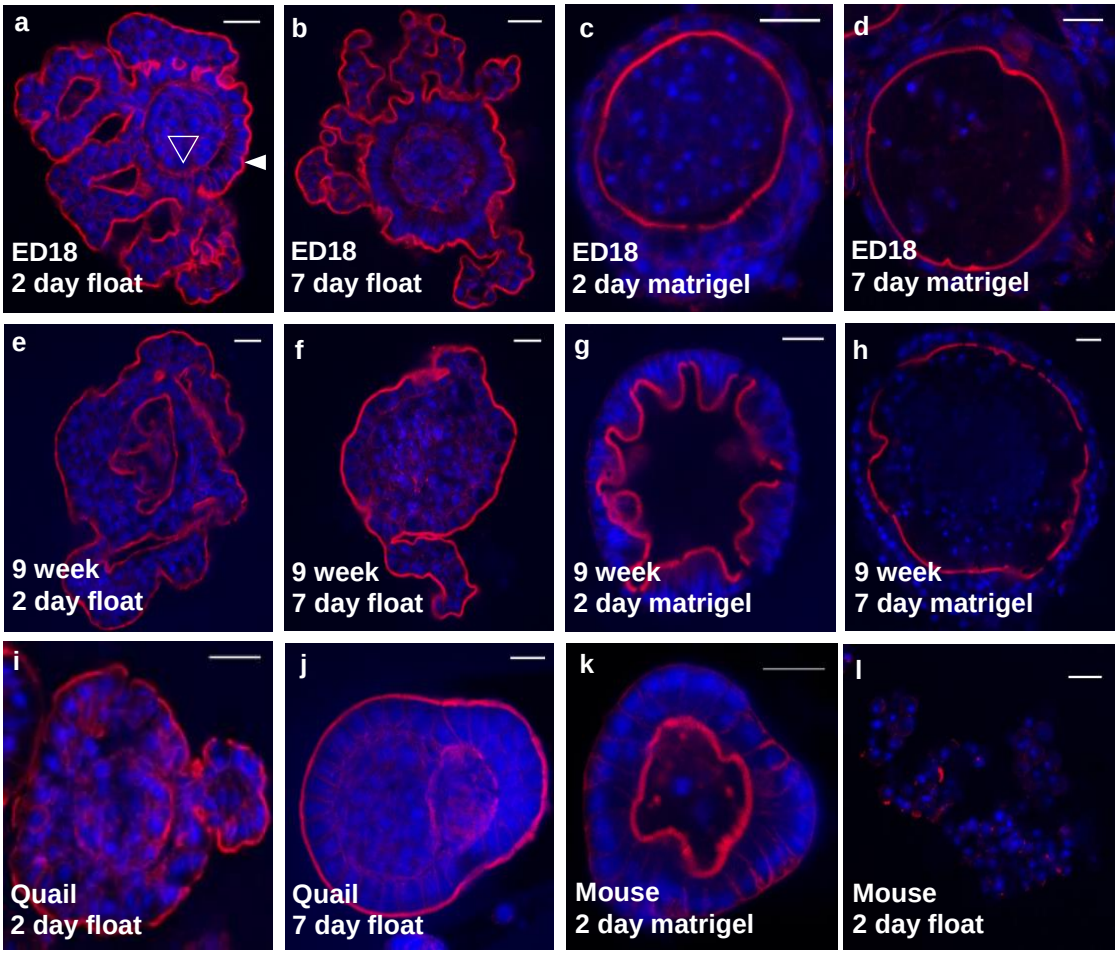

Figure 4.1: Reverse polarisation of avian floating enteroids. Confocal images of whole-mount enteroids stained to detect F-actin-expressing brush borders (red) and DAPI to visualise cell nuclei (blue). **a** Floating embryonic chicken enteroids at 2 days of culture showing epithelial cells polarised with the apical brush border (closed arrow) facing the media and basal lamina (open arrow) sits on a central core of cells. **b** Embryonic chicken enteroids at 7 days of culture showing apical-out polarisation. **c** Embryonic enteroids cultured in Matrigel for 2 days with epithelial cells polarised so the apical brush border is facing a central lumen. **d** Embryonic enteroids cultured in Matrigel for 7 days. **e** Enteroids from 9 week old chickens at 2 days and (**f**) 7 days in floating culture. **g** Matrigel-embedded enteroids from 9 week old chickens at 2 days and (**h**) 7 days. **i** Enteroids derived from 1 week old quail also show apical-out polarisation at 2 days and (**j**) 7 days of culture. **k** Matrigel-embedded mouse enteroid, from adult mouse, with internal lumen at 2 days in culture. **l** Floating mouse enteroid at 2 days in culture showing dissociated crypt cells. Scale bar: 20 µm. Images **a - j**, and **k - l** are representative of 3 cultures composed of 3 birds and 1 mouse per culture respectively.

F-actin staining of floating enteroids from 2 day old quail was performed at 2 and 7 days of culture, to explore whether the development of apical-out enteroids from floating crypts or villi was species-specific (Fig. 4.1i, j). Quail enteroids mirrored the data obtained from chickens demonstrating that isolated crypts or villi of at least two avian species will create apical-out enteroids when floating in culture.

To expand the range of species analysed, we explored the phenotypic plasticity of isolated mouse intestinal crypts in a liquid environment. When seeded in Matrigel, mouse crypts predictably formed structures with an internal lumen, developing into spheroids by 2 days (Fig. 4.1k) and multi-budding enteroids by 7 days of culture. In contrast, when these isolated crypts were floated in Mouse IntestiCult medium without a gel scaffold, they did not maintain structural integrity and by 2 days of culture there were no enteroids visible (Fig. 4.1l).

In summary, floating cultures of isolated chicken villi or crypts result in reverse orientated enteroids with an externally facing apical epithelial surface. This is in contrast with gel-embedded chicken and mammalian enteroids whose epithelial apical brush borders face inwards to a central lumen. Freshly isolated floating murine crypts cannot maintain structural integrity in a similar floating environment.

4.2.2 Floating chicken enteroids reproduce the cellular diversity of the intestinal epithelium

To investigate whether the array of cell types characteristically present in the gut epithelium *in vivo* were displayed in the floating chicken enteroids, TEM and immunofluorescent staining were performed. Late embryonic and 6 – 9 week chicken jejunal tissue sections were compared with ED18 enteroids from 2 to 7 days of culture. Lysozyme C (LYZ) is synthesized and secreted by crypt dwelling Paneth cells in the mouse and human small intestine. In the floating chicken enteroids and embryonic chicken small intestine, LYZ-expressing cells were instead observed scattered throughout the epithelium

(Fig. 4.2a, i; TEM Fig. 4.2m). This distribution may reflect the multiple sites of proliferation expected along late stage embryo and newly hatched chick villi, assuming chicken Paneth-like cells play a similar ISC homeostatic role as their human/mouse counterparts[7,40]. In the mature chicken gut sections, LYZ was not detected by immunohistochemical staining (Fig. 4.2e) which could reflect a reduction in gene expression with age[17]. However, as a more recent publication demonstrated *LYZ* mRNA expression in chickens up to 8 weeks post-hatch, the lack of staining could be due to reduced protein levels through complex gene regulatory mechanisms[16]. SOX9 is expressed in ISCs, transit amplifying cells and terminally differentiated Paneth cells, and was particularly evident in epithelial cells lining mature chicken crypts and the embryonic villi (Fig. 4.2c, g). Localisation of both EdU+ (Chapter 3, Fig. 3.4) and SOX9+ cells to the embryonic enteroid bud epithelium (Fig. 4.2k) strongly indicated proliferation and differentiation of ISC and progenitor cells was occurring in these villus-like structures.

Enteroendocrine cells ($CHGA^+$ cells, Fig. 4.2d, h, l) and goblet cells ($MUC\ 5AC^+$ cells, Fig. 4.2b, f, j; TEM Fig. 4.2n) were found scattered through the villus epithelium of the embryonic and mature chicken gut sections as well as the enteroid epithelium. Uniformly polarized enterocytes with apical villin-expressing brush borders (Fig. 4.2o), internal basal lamina (Fig. 4.2p closed arrow) and external microvilli (Fig. 4.2p open arrow) lined the enteroid epithelium. Globally the enteroid cell type distribution appeared to be similar to the patterns observed in the *in vivo* embryonic intestine.

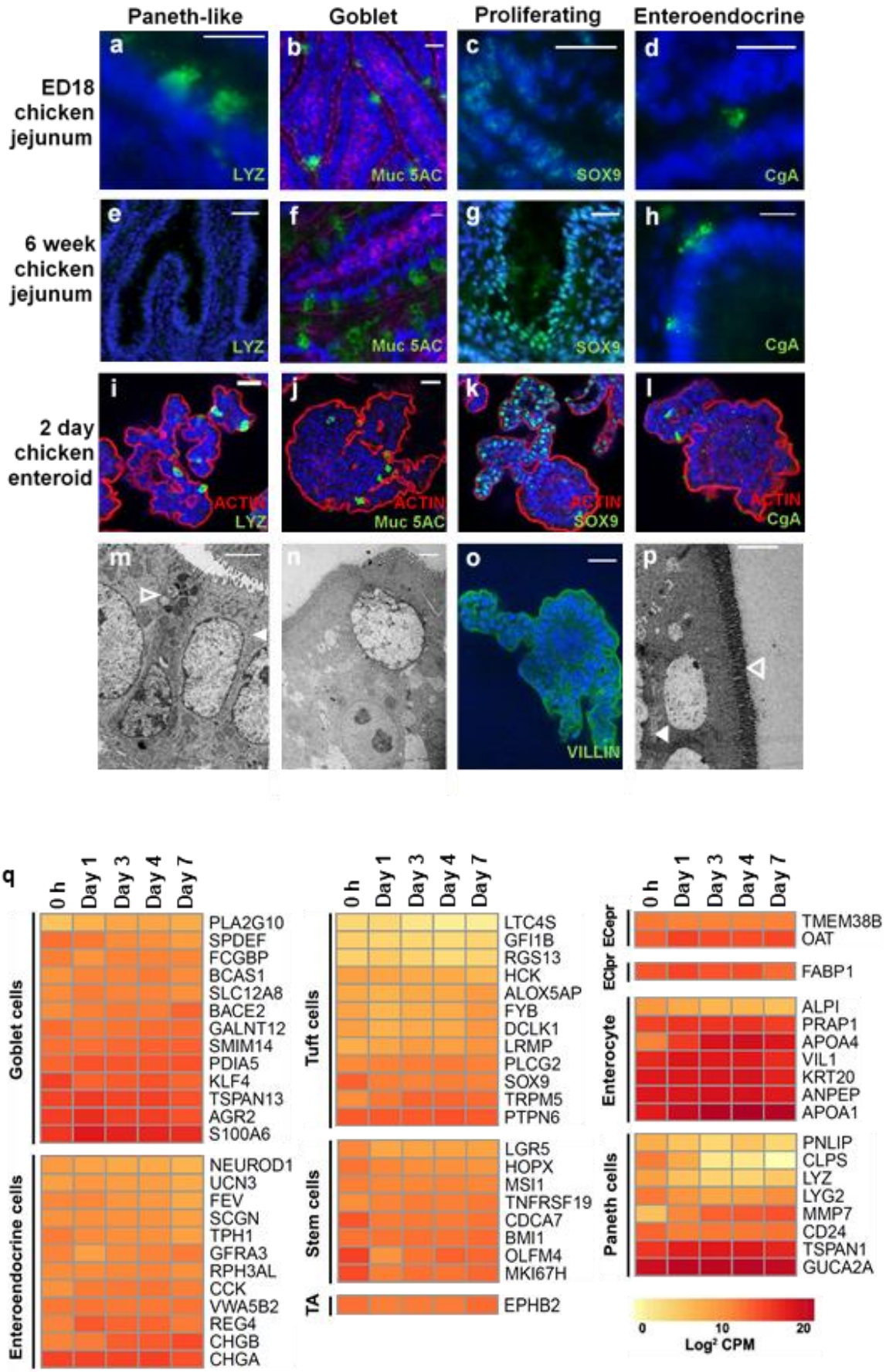
Paneth-like
Goblet
Proliferating
Enteroendocrine
ED18 chicken jejunum
6 week chicken jejunum
2 day chicken enteroid
LYZ
Muc 5AC
SOX9
CgA
ACTIN
VILLIN
q
0 h
Day 1
Day 3
Day 4
Day 7
Goblet cells
PLA2G10
SPDEF
FCGBP
BCAS1
SLC12A8
BACE2
GALNT12
SMIM14
PDIA5
KLF4
TSPAN13
AGR2
S100A6
Enteroendocrine cells
NEUROD1
UCN3
FEV
SCGN
TPH1
GFRA3
RPH3AL
CCK
VWA5B2
REG4
CHGB
CHGA
Tuft cells
LTC4S
GFI1B
RGS13
HCK
ALOX5AP
FYB
DCLK1
LRMP
PLCG2
SOX9
TRPM5
PTPN6
Stem cells
LGR5
HOPX
MSI1
TNFRSF19
CDCA7
BMI1
OLFM4
MKI67H
TA
EPHB2
ECepr
TMEM38B
OAT
EClpr
FABP1
Enterocyte
ALPI
PRAP1
APOA4
VIL1
KRT20
ANPEP
APOA1
Paneth cells
PNLIP
CLPS
LYZ
LYG2
MMP7
CD24
TSPAN1
GUCA2A
0
10
20
Log² CPM

Figure 4.2: Multicellular composition of chicken enteroids. Confocal images of (**a – d**) embryonic jejunum, (**e – h**) 6 week old chicken jejunum, and (**i - l, o**) embryonic chicken enteroids at 2 days of culture. All cells are counterstained with DAPI (blue). The cells are stained for (**a, e, i**) LYZ (green, Paneth cells), (**b, f, j**) MUC5AC (green, goblet cells), (**c, g, k**) SOX9 (green, proliferating cells) and (**d, h, l**) CGCA (green, enteroendocrine cells). **i - l** Chicken enteroids stained to detect F-actin-expressing brush border (red). **m** Transmission electron microscopy of chicken enteroids (4 h in culture) demonstrates an enterocyte (closed arrow) and Paneth cell (open arrow). **n** TEM of chicken enteroids (7 days in culture) demonstrates a goblet cell. **o** Confocal image of chicken enteroid stained for villin (green, epithelial microvilli). **p** TEM of chicken enteroid 7 days in culture, enterocyte basal lamina (closed arrow) and microvilli (open arrow). Scale bar: **a - l, o** 20 µm. **m, n, p** 2 µm. Images **a - p** are representative of data from at least 3 independent cultures each containing 2 - 3 embryos. **q** Expression of IEC lineage-specific genes in freshly isolated villi (0 h) and enteroids at 1, 3, 4 and 7 days of culture compared by RNA sequencing analysis. Heat maps show the relative expression levels (log2 CPM reads) of a range of mammalian IEC lineage-related genes. TA: transit amplifying cells, ECepr: early enterocyte precursor cells, EClpr: late enterocyte precursor cells. RNA sequencing data is representative of 3 independent experiments, each comprising of 2 technical replicates, each containing 3 embryos.

Chicken enteroid samples for transcriptome analysis were collected at 0 h (freshly isolated ED18 intestinal villi) then at 1, 3, 4, 7 days of culture. Expression of gene sets characteristically associated with mammalian Paneth cells, goblet cells, enterocytes and enteroendocrine cells were identified in the embryonic enteroid transcriptional profile at 0, 1, 3, 4 and 7 days post cultivation (Fig. 4.2q)[279]. In addition, for cell subpopulations that could not be detected by microscopy such as transit amplifying cells, ISCs and tuft cells, expression of their classical markers was demonstrated (Fig. 4.2q)[183,279,287]. During the cultivation period the transcriptome for most cell-types was relatively stable, suggesting that the cellular diversity of the *in vivo* epithelium doesn't noticeably fluctuate in the enteroids for at least 7 days.

There were some gene markers with striking transcript changes particularly within the Paneth cell and enterocyte gene sets. *MMP7,* a Paneth cell-

associated gene which activates antimicrobial peptides, was significantly upregulated (FDR <0.05, logFC >2 for DEGs between adjacent time points) between 0 – 72 h (Chapter 5, Additional file 4) but another marker *CLPS*, a co-enzyme involved in fat digestion, was downregulated. Other lipid digestion-related genes were significantly upregulated across the 0 - 72 h cultures including those mapping to the peroxisome proliferator-activated receptor signalling pathway e.g. *APOA5 (*a key intestinal metabolism regulator)*, ME1* and *APOA1,* as well as *APOA4,* an enterocyte-related marker involved in lipoprotein metabolism*.* In addition *SLC13A1,* which is the main apical sodium-dependent enterocyte transporter, and brush border enzyme *ARG2* were significantly upregulated. Since the chicken enteroids develop strong expression of digestion-related genes and associated pathways this indicates that the *in vitro* culture conditions contain the cues for maturation to a post-hatch gut model. A more in-depth analysis of enteroid digestive function is described in Chapter 5 (5.2.5) but ideally digestion assays would be carried out to confirm that the described transcript changes in the chicken enteroids are functionally significant.

4.2.3 Digestive site specific enteroids resemble *in vivo* architecture

Differentiated chicken duodenal, jejunal and caecal enteroids were individually prepared to provide digestive site-specific models for *in vitro* infection studies (Fig. 4.3a - l). The small intestinal enteroids utilised the same growth requirements as the caecal (large intestinal) enteroids. Enteroids from all digestive-sites displayed an apical-out conformation and contained a similar abundance of cell types. After 2 days of culture statistically significant differences in bud numbers between the different regions of the small intestine were identified (Fig. 4.3m). The caecal enteroids more often lacked buds (0) or had only 1 bud compared to duodenal and jejunal enteroids. The jejunal enteroids had more buds (3+) in comparison to duodenal and caecal enteroids. In addition, the length of the buds resembled the *in vivo* architecture, since the buds differentiated from

jejunal and duodenal tissue were significantly longer than those from caecal enteroids (Fig. 4.3n).

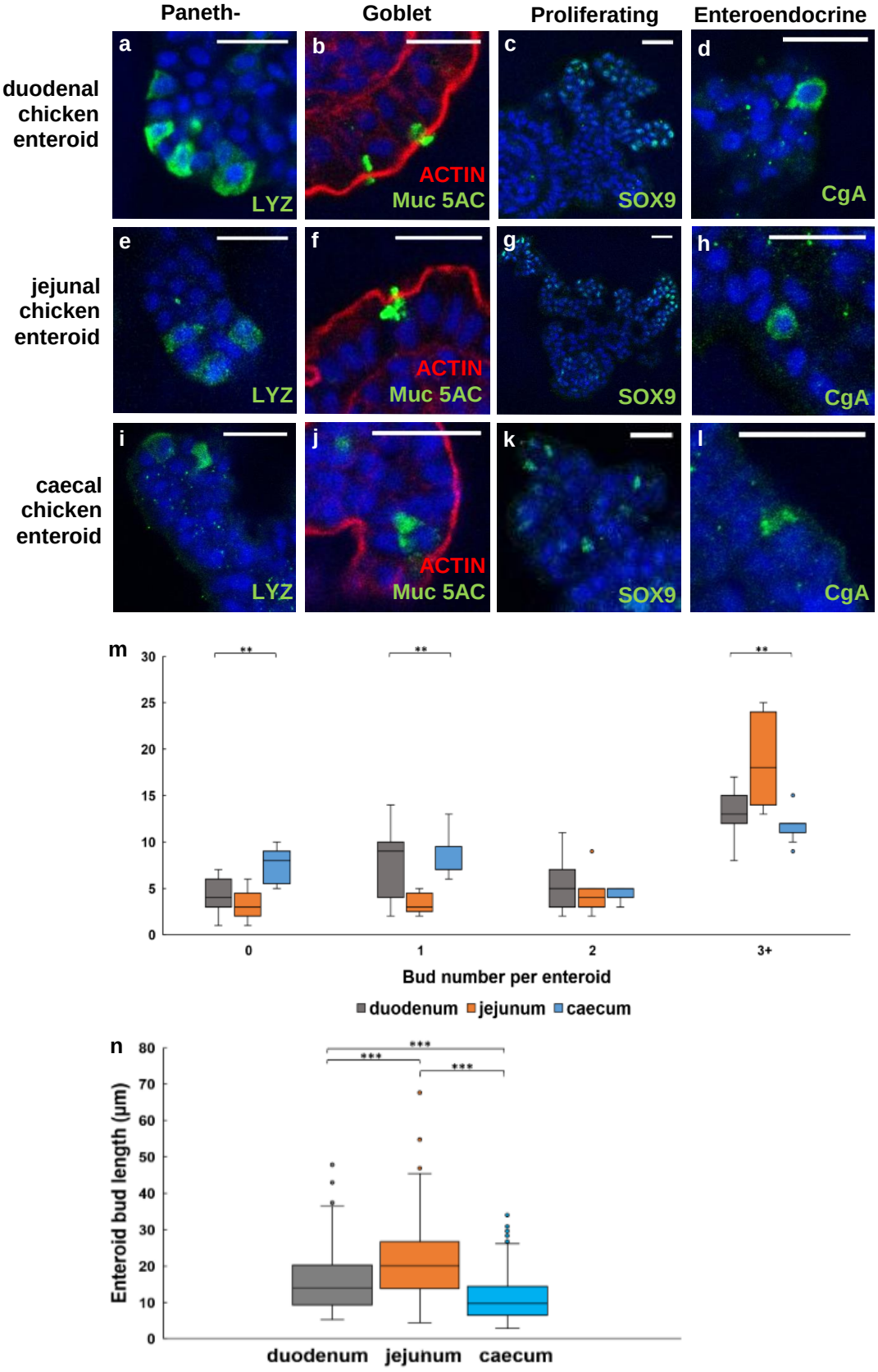

Figure 4.3: Site-specific chicken enteroids demonstrate *in vivo* multicellular composition and architecture. a - l Confocal images of ED18 chicken enteroids at 2 days of culture grown from the duodenum, jejunum and caeca. Stained for (**a, e, i**) LYZ (green, Paneth cells), (**b, f, j**) MUC5AC (green, goblet cells), (**c, g, k**) SOX9 (green, proliferating cells), and (**d, h, l**) CGCA (green, enteroendocrine cells). All counterstained with DAPI (blue). **b, f, j** Stained to detect F-actin-expressing brush border (red). Scale bar: 20 µm. Images are representative of data from at least 3 independent cultures, each containing 2 - 3 embryos. **m** Enteroids were cultured for 2 days and the number of buds (0, 1, 2, 3 or more per enteroid) were counted. **n** The length of the buds from jejunal, duodenal and caecal enteroids were measured. Box and whisker plot data derived from 3 independent experiments each containing 2-3 embryos, at least 260 enteroids and 150 buds measured per location for (m) and (n) respectively. Statistics performed using a Kruskal-Wallis test; (**m**) 0 budding, **P ≤0.001, H = 14.06, df = 2; 1 budding, **P ≤0.001, H = 13.42, df = 2; and more than 3 budding, **P ≤0.001, H = 13.62, df = 2, enteroids between the duodenal, jejunal and caecal cultures. (**n**) ***P ≤0.0001, H = 110.08, df = 2, with *post hoc* Mann-Whitney U tests (two-sided); duodenum – jejunum, ***P ≤0.0001, W = 23230, 95% CI for difference (-6.820, -3.266); duodenum – caecum, ***P ≤0.0001, W = 29697.5, 95% CI for difference (13.914, 9.780); jejunum – caecum, ***P ≤0.0001, W = 46327.5, 95% CI for difference (7.249, 10.707).

4.2.4 Isolated crypts and villi can both build enteroids

The epithelial brush borders in the digested tissue fragments (the seeded starting material in the enteroid cultures) were visualised using TEM and phalloidin staining. This identified that the isolation procedure from late embryonic chicken intestine resulted in collection of villus structures rather than crypts. This was evident from the distinct staining of the external brush border and cell-dense internal structure (Fig. 4.4a, d). In contrast, imaging of digested and fractionated mouse and mature avian small intestine showed isolated crypts with an internal dense F-actin positive brush border (Fig. 4.4b, c, e).

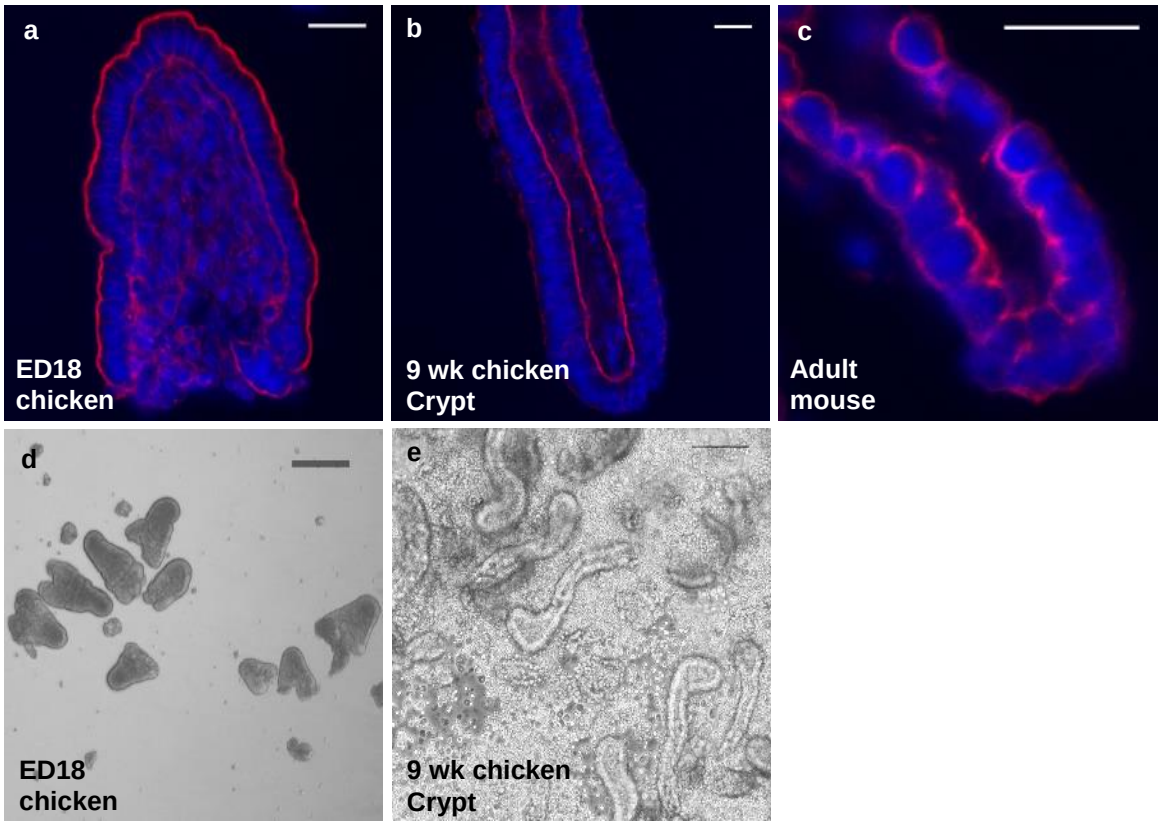

Figure 4.4: Identification of crypts and villi as starting culture material. **a - c** Confocal images of villi and crypts stained to detect F-actin-expressing brush border (red), counterstained with DAPI (blue). **a**, **d** Tissue isolated from late embryonic chicken intestine to form enteroids are villi. **b**, **e** Isolated crypts from 9 week old chicken intestine. **c** Isolated crypts from adult mouse intestine. Scale bar **a** - **c**: 20 µm, **d** – **e**: 100 µm. Images **a** and **d**, **b** and **e,** and **c** are representative of 3 cultures composed of 3 chicken embryos, 1 chicken and 1 mouse per culture respectively.

4.2.5 Leukocytes identified in the enteroid lamina propria and epithelium

Since embryonic enteroids develop from intestinal villi I hypothesised that the inner core represented cell populations of the intestinal lamina propria. To explore this I initially determined whether they contained intestinal lamina propria immune cells. Immunohistochemistry identified $CD45^{+}$ leukocytes predominantly scattered throughout the central cell-dense enteroid core (Fig.

4.5a - c) but also occasionally present within the epithelial layer (Fig. 4.5b) at 2 days (Fig. 4.5a, b) and 7 days (Fig. 4.5c) of culture. Subsequent immunostaining demonstrated cytoplasmic $CD3^+$ cells, typical of NK cells which are detected in embryos from $ED14^{288}$ (Fig. 4.5d). $CD4^+$ cells and $CD8\beta^+$ cells were also present which can represent both NK and T cell populations (Fig. 4.5e, f). $ChB6^+$ cells which are indicative of both B cells and NK cells were also identified (Fig. 4.5g)[1]. Occasional chicken $TCR\alpha\beta_1$+ (TCR2) and chicken $TCR\alpha\beta_2$+ (TCR3) cells were found in the lamina propria core of the enteroids (Fig. 4.5h - i). These latter two cell types are only expected to start to arrive at the periphery at ED18 – 20 which explains the low numbers in the late embryonic enteroids[125]. Enteroids cultured from *CSF1R*-reporter transgenic chicken embryos, which express eGFP in myeloid lineage cells, were employed to visualise tissue mononuclear phagocytes[120]. The presence of multiple *CSF1R* transgene$^+$ cells were imaged in the *CSF1R*-eGFP transgenic chicken enteroids, demonstrating the presence of macrophages and dendritic cells within the enteroid core at 2 days (Fig. 4.5j) and 7 days (Fig. 4.5k, k1) of culture.

Expression of gene sets encoding various leukocytes of the mammalian enteric immune system were shown on transcriptional analysis of mRNA from the floating enteroid cultures (Fig. 4.5l). These genes had relatively stable expression across the 7 days of culture with particularly strong expression of macrophage-related genes *CSF1R, LRP1, UQCRC1, CTSB, PHB2, CKB* and *HADHB*. Gene sets associated with T cells, B cells, dendritic cells, and NK cells were also represented, but their expression profiles suggest they are present in lower numbers than macrophages.

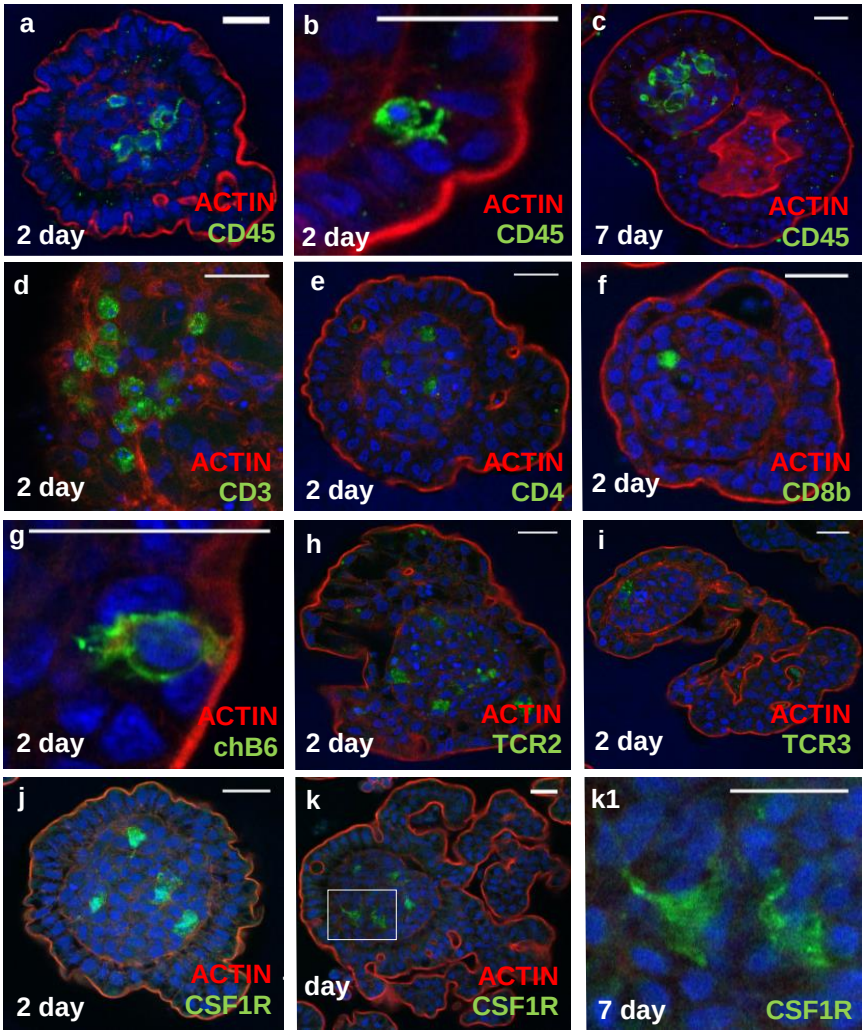
a
2 day
ACTIN
CD45
b
2 day
ACTIN
CD45
c
7 day
ACTIN
CD45
d
2 day
ACTIN
CD3
e
2 day
ACTIN
CD4
f
2 day
ACTIN
CD8b
g
2 day
ACTIN
chB6
h
2 day
ACTIN
TCR2
i
2 day
ACTIN
TCR3
j
2 day
ACTIN
CSF1R
k
day
ACTIN
CSF1R
k1
7 day
CSF1R

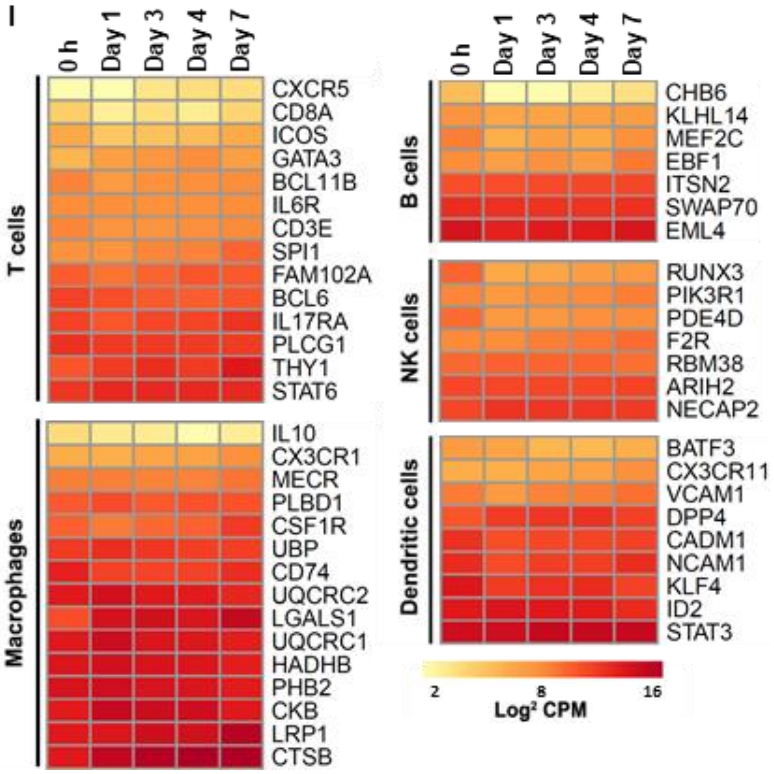
0 h
Day 1
Day 3
Day 4
Day 7
T cells
CXCR5
CD8A
ICOS
GATA3
BCL11B
IL6R
CD3E
SPI1
FAM102A
BCL6
IL17RA
PLCG1
THY1
STAT6
Macrophages
IL10
CX3CR1
MECR
PLBD1
CSF1R
UBP
CD74
UQCRC2
LGALS1
UQCRC1
HADHB
PHB2
CKB
LRP1
CTSB
B cells
CHB6
KLHL14
MEF2C
EBF1
ITSN2
SWAP70
EML4
NK cells
RUNX3
PIK3R1
PDE4D
F2R
RBM38
ARIH2
NECAP2
Dendritic cells
BATF3
CX3CR11
VCAM1
DPP4
CADM1
NCAM1
KLF4
ID2
STAT3
2
8
16
Log² CPM

Figure 4.5: Composition of immune cells within chicken enteroids. **a - i** Confocal images of chicken enteroids stained for leukocyte markers (green) at 2 or 7 days of culture. All enteroids are counterstained with DAPI (blue) and stained to detect F-actin-expressing brush border (red). **a - c** Enteroids stained for CD45 (green) showing leukocytes in the (**a, c**) lamina propria and (**b)** epithelium. Enteroids at 2 days of culture stained for (**d**) CD3, (**e**) CD4, (**f**) CD8β, (**g**) chB6, (**h)** TCR2 (chicken TCRαβ$_1$), (**i**) and TCR3 (chicken TCRαβ$_2$). **j – k** Enteroids cultured from *CSF1R*-eGFP transgenic embryos at (**j**) day 2 and (**k1** magnification of **k**) day 7 of culture. Scale bar: 20 µm. (**l**) Expression of immune cell-related genes in freshly isolated villi (0 h), 1, 3, 4 and 7 day chicken enteroids was compared by RNA sequencing analysis. Heat maps show the expression levels (log2 CPM reads) of a range of immune cell-related genes. RNA sequencing data is representative of 3 independent experiments, each comprising of 2 technical replicates, each containing 3 embryos. Scale bar: 20 µm. Images are representative of data from at least 3 independent cultures each containing 2 - 3 embryos.

4.2.6 Enteroid leukocyte viability and functionality

To investigate if the chicken enteroid immune cell populations had the functional ability to phagocytose particles from the surrounding medium, we added pHrodo zymosan bioparticles to 3 and 7 day enteroid cultures. These cultures were then imaged 8 h and 48 h after the zymosan addition. The zymosan bioparticles are pH-sensitive so fluoresce red in acidic pH (phagosomes). After 8 h their presence was detected within the enteroid epithelial cells (Fig. 4.6a), and after 48 h they were evident within CD45+ leukocytes in the enteroid core (Fig. 4.6b - c1). The lamina propria leukocytes in 7 day enteroid cultures also demonstrated zymosan phagocytosis 48 h after adding the bioparticles to the media. This indicates that the leukocytes were still functionally active in 7 day enteroid cultures. The uptake of the pHrodo zymosan bioparticles was blocked when the enteroids were treated with cytochalasin D, demonstrating this was active phagocytic activity (Fig. 4.6d).

To confirm the viability of the enteroid leukocytes the enteroids were double-stained with the cell proliferation marker EdU for 1 h followed by the CD45

leukocyte marker (Fig. 4.6e, f). EdU is incorporated into newly synthesized DNA so the double-stained cells, predominantly in the enteroid lamina propria core, represented proliferating leukocytes.

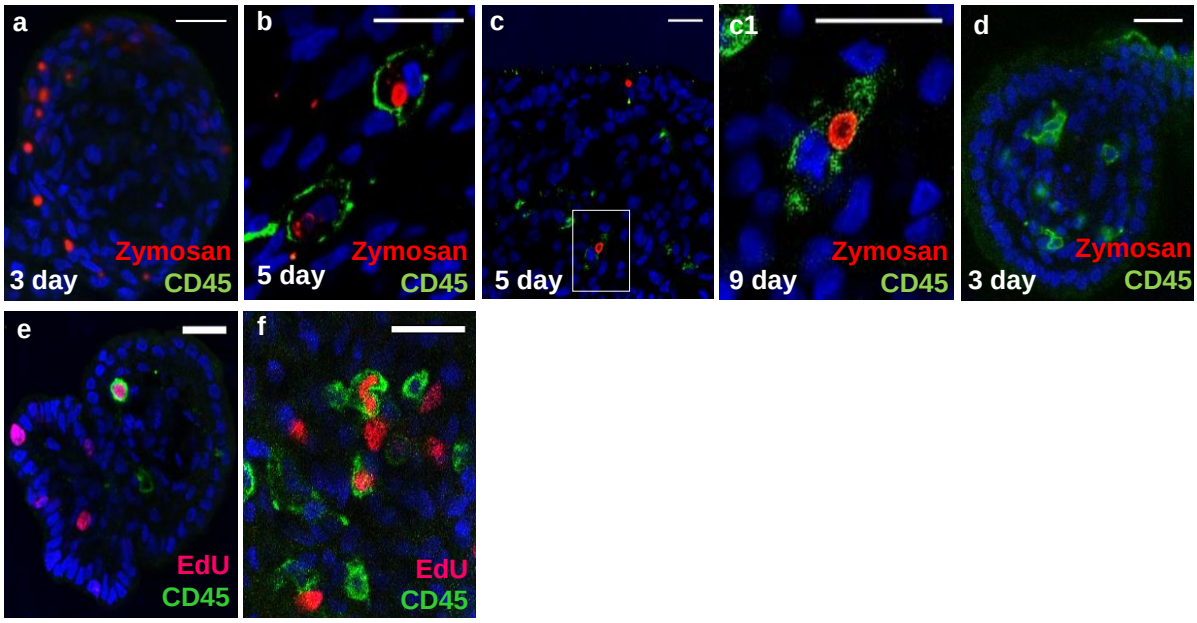

Figure 4.6: Viability and functionality of immune cells within chicken enteroids. **a – d** pHrodo zymosan bioparticles (red) were added to 3 day enteroid cultures and visualised (**a**) in the epithelium after 8 h and (**b**) in CD45^{+} leukocytes (green) after 48 h. (**c1** magnification of **c**) Zymosan was also added to 7 day enteroid cultures and phagocytosis of zymosan by leukocytes in the lamina propria core was visualised after 48 h. (**d**) Zymosan uptake was blocked in 3 day enteroid cultures treated with Cytochalasin D which inhibits actin polymerization. (**e, f**) Chicken enteroids stained for CD45 (green) and cell proliferation marker EdU (red) at 2 days of culture. Scale bar: 20 µm. Images are representative of data from at least 3 independent cultures each containing 2 - 3 embryos.

4.2.7 Other cell types within the lamina propria component

To investigate whether the enteroids contained additional populations of intestinal lamina propria cells, immunohistochemical staining for neural and fibroblast populations was performed. HuC/HuD is a pan-neuronal marker which labels neurons and glial cells[289]. Multiple HuC/HuD+ cells were identified scattered individually or in clusters throughout the central core of

the 2 day enteroids (Fig. 4.7a, b). Since the presence of neuronal cell bodies would not be expected in the lamina propria, these are likely glial populations, reflecting characteristic cellular and tissue spatial distribution patterns[290]. Double immunolabeling studies using glial markers such as glial fibrillary acidic protein[114], would be indicated to confirm their identity. NeuN is a postmitotic neuron-specific nuclear protein but has more recently been identified as RNA binding protein Fox3[291,292]. This multifunctional protein is expressed by a wide variety of cells and has been shown to be involved in the maintenance of stem cell compartments[293]. This may explain why nuclear NeuN was identified in the differentiating bud regions of the enteroids (Fig. 4.7c).

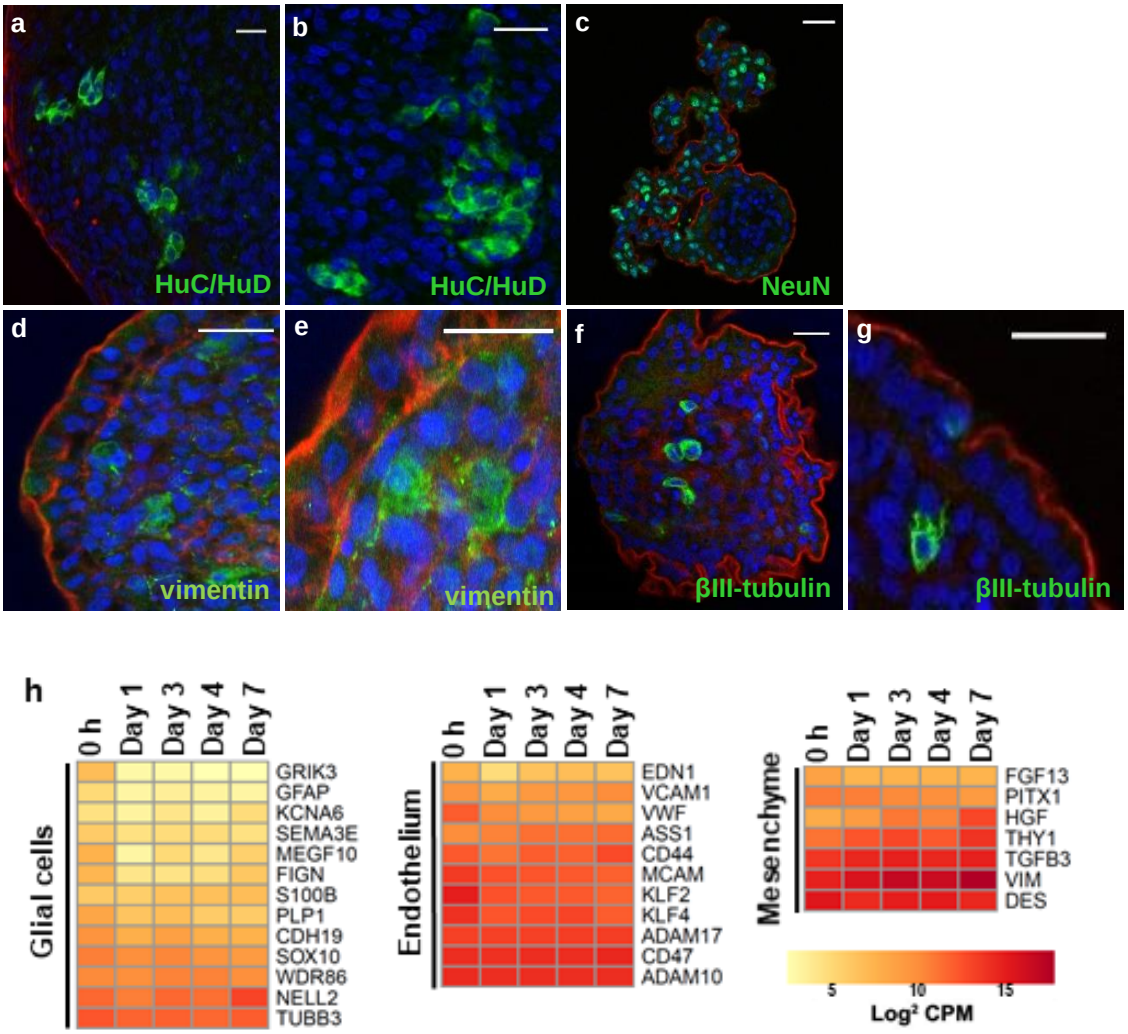

Figure 4.7: Other cell types identified in the chicken enteroid lamina propria. a - g Confocal images of chicken enteroids stained for lamina propria cell population markers (green) at 2 days of culture. All enteroids are counterstained with DAPI (blue) and Phalloidin (red). Enteroids at 2 days of culture stained for **(a – b)** HuC/HuD (green), **(c)** NeuN (green), **(d-e)** vimentin (green), **(f – g)** βIII-tubulin (green). Scale bar: 20 μm. Images are representative of data from at least 3 independent cultures each containing 2 - 3 embryos. (**h**) Expression of lamina propria cell population gene sets in freshly isolated villi (0 h), 1, 3, 4 and 7 day chicken enteroids was compared by RNA sequencing analysis. Heat maps show the expression levels (log2 CPM reads) of a range of mesechymal cell-, endothelial cell- and glial-cell related genes. RNA sequencing data is representative of 3 independent experiments, each comprising of 2 technical replicates, each containing 3 embryos.

Vimentin is the major cytoskeletal component of mesenchymal cells, and accordingly VIM+ cells were restricted to the enteroid lamina propria core (Fig. 4.7d, e). βIII-tubulin is generally used as a neuronal differentiation marker but it has also been shown to be expressed by other cell types including mesenchymal stem cells and perivascular cells, both of which are present in the intestinal lamina propria[104,294]. As previously mentioned neuronal bodies are known to be located in the submucosal ganglia, therefore the scattered βIII-tubulin+ cells in the enteroid core (Fig. 4.7e, f) are most likely representative of mesenchymal stem cells with typical perinuclear staining[295]. Staining of freshly isolated villi or embryonic intestinal samples would be a useful comparison for all markers.

The enteroid transcriptome was also analysed to assess gene sets encoding lamina propria cell populations (Fig. 4.7i). Glial cell markers displayed steady expression in the enteroid except for *NELL2*, a gene involved in cell growth and differentiation, which was significantly upregulated in 7 day cultures. Transcripts for the mesenchymal cells generally increased in expression over the enteroid cultures. The endothelial cell markers were relatively steadily expressed except for *vWF* which was significantly downregulated in enteroids compared to ED18 villi. *vWF* is an important haemostatic factor so its expression could be increased in the villi samples as a result of the recent

isolation trauma. Immunohistochemical staining of 2 day enteroids with a vWF antibody did not detect any positive cells although the staining protocol may need further optimisation.

4.2.8 Epithelial barrier integrity is present in the enteroids

The innermost layer of the intestinal luminal surface consists of a single cell thick epithelial lining which acts as a barrier, preventing the entry of harmful molecules and microbes while still allowing the selective passage of dietary nutrients, ions, and water[296]. Tight junction proteins together with adherens junctions and desmosomes are essential gut epithelia barrier components which maintain physiological homeostasis[297]. By using TEM and immunostaining for two major cell-adhesion molecules, the presence of these junctions in chicken enteroids was demonstrated. Tight junctions and desmosomes were visualised using TEM (Fig. 4.8a), intercellular E-cadherin identified adherens junctions (Fig. 4.8b) and ZO1, the tight junction-associated protein, was also identified in the epithelial layer (Fig. 4.8c).

The enteroids were then immersed in 4 kDa FITC-dextran to determine whether the cell-cell junctions were functional. The positive controls consisted of enteroids treated with 5mM EDTA to disrupt the tight junctions. Untreated enteroids demonstrated mechanical integrity through intact intercellular junctions by excluding the FITC-dextran probe (Fig. 4.8d). In stark contrast, EDTA-treated enteroids displayed breakdown of the epithelial barrier by allowing permeation of FITC-dextran through the intercellular spaces (Fig. 4.8e).

A large range of genes encoding components of mammalian focal adhesions, tight junctions, gap junctions, adherens junctions and desmosomes were found to be expressed on transcriptional analysis (Fig. 4.8f). A generally stable expression pattern throughout the culture period was also found with the cell stress-related genes (Chapter 3, Fig. 3.4g) which is supportive of stable enteroid cultures.

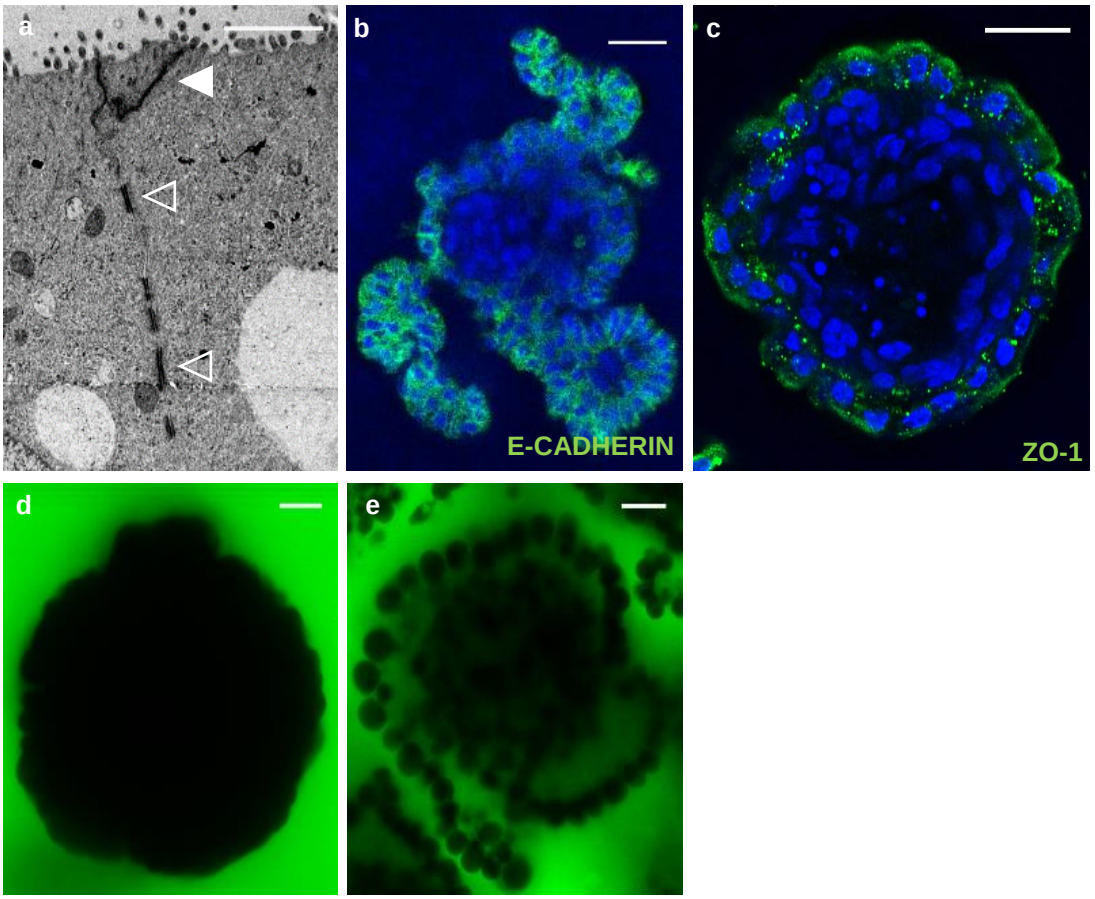
a
b
E-CADHERIN
c
ZO-1
d
e

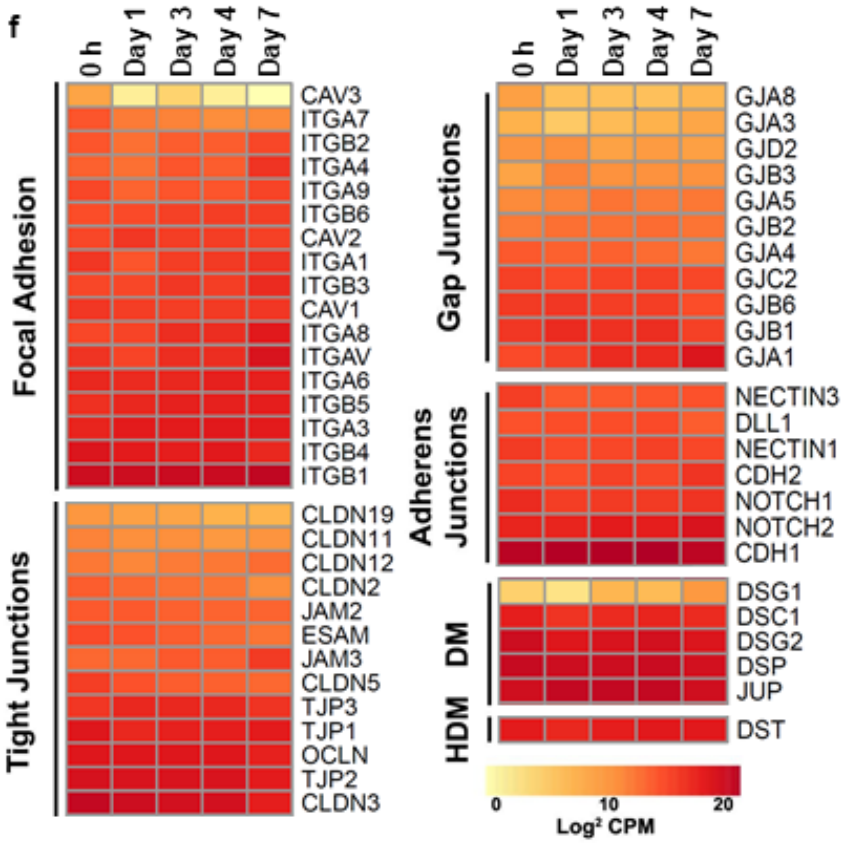
f
0 h
Day 1
Day 3
Day 4
Day 7
Focal Adhesion
CAV3
ITGA7
ITGB2
ITGA4
ITGA9
ITGB6
CAV2
ITGA1
ITGB3
CAV1
ITGA8
ITGAV
ITGA6
ITGB5
ITGA3
ITGB4
ITGB1
Tight Junctions
CLDN19
CLDN11
CLDN12
CLDN2
JAM2
ESAM
JAM3
CLDN5
TJP3
TJP1
OCLN
TJP2
CLDN3
Gap Junctions
GJA8
GJA3
GJD2
GJB3
GJA5
GJB2
GJA4
GJC2
GJB6
GJB1
GJA1
Adherens Junctions
NECTIN3
DLL1
NECTIN1
CDH2
NOTCH1
NOTCH2
CDH1
DM
DSG1
DSC1
DSG2
DSP
JUP
HDM
DST
0
10
20
Log² CPM

Fig. 4.8: Chicken enteroids display epithelial barrier integrity, express cell-junction related genes. a TEM of chicken enteroids (7 days of culture) demonstrate tight junctions (closed arrow) and desmosomes (open arrows). Confocal images of chicken enteroids (2 days of culture) stained for (**b**) E-cadherin (green, adherens junctions) and (**c**) ZO1 (green, tight junctions) and counterstained with DAPI (blue). **d - e** Confocal images of chicken enteroids (2 days of culture) immersed in FITC-dextran 4 kDa showing epithelial barrier integrity in (**d**) untreated and (**e**) loss of barrier integrity after EDTA-treatment. Scale bar: **a** 2 µm, **b - e** 20 µm. Images are representative of data from at least 3 independent cultures each containing 2 - 3 embryos. **f - g** Expression of (**f**) epithelial cell junction-related genes and (**g**) cell stress-related genes in freshly isolated villi (0 h) and chicken enteroids at 3 and 7 days of culture was compared by RNA sequencing analysis. **f** Heat maps show the expression levels (log2 CPM reads) of a range of epithelial cell junction-related genes. DM: desmosomes HD: hemi-desmosomes. **g** Heat map shows minimal change in expression levels of a range of mammalian cell stress-related genes over 7 days of culture. RNA sequencing data is representative of 3 independent experiments, comprising 2 technical replicates, each containing 3 embryos.

4.3 Discussion

This chapter reports the characterisation of the floating avian enteroid model described in Chapter 3, showing they maintain the cellular diversity, polarity and barrier function present within the chicken intestinal epithelium *in vivo,* without the use of a gel scaffold. Transcriptional and histological analyses show these enteroids contain ISCs, Paneth cells, enteroendocrine cells, goblet cells and enterocytes. In addition, the natural presence of IEL and lamina propria leukocytes, glial cells and mesenchymal cells are indicated making this a distinctive model from their mammalian counterparts. The floating growth conditions allow the enteroids to display a reverse architecture where a continuous epithelial layer is polarised so the abundant apical microvilli face the media. To expand the potential applications of this avian culture system in basic and translational research, enteroids were developed from different regions of the small and large intestine and from several poultry species.

The classical matrix-embedded enteroid possesses an internal lumen which proves limiting for host-pathogen studies where enteroid fragmentation cannot guarantee the pathogen entry route, and monolayers and microinjections add increasing layers of cost and complexity to the infection process. Seeding chicken villi or crypts in Matrigel, a biologically active basement membrane matrix, resulted in enterosphere structures with internally polarised microvilli akin to their mammalian gel-embedded counterparts. These empty structures closely resemble human and murine early fetal spheroids, which exhibit WNT-dependent unlimited self-renewing properties but have a poorly differentiated phenotype[204,206]. This is in marked contrast to the prolifically budding, differentiated, apical-out enteroids produced when chicken villi are floated in media. In 1990 Madin-Darby canine kidney epithelial spheroids were observed to have their basal cell surface polarised out when in collagen gel, and their apical cell surface facing out when in suspension[298]. Co et al. (2019)[211] recently replicated this phenomenon with human and mouse enteroids[211]. These mammalian cultures were initially matured for 7 – 20 days embedded in a gel ECM, before being transferred to suspension where the epithelial cell polarity of ~80% of the enteroids reversed over a period of 3 days. ECM proteins were identified as key regulators of the observed epithelial polarity changes, specifically β1 integrin signalling[211,299,300]. A gel-free system for chicken enteroids was recently published by Acharya et al. (2020)[217]. However the cultures only consisted of solid spheroid structures, with exogenous growth factor supplementation required to produce small budding domains[217]. Other mechanisms that may be contributing to the differences in polarity, cell differentiation and budding in chicken enteroids grown in different environments include ligand-receptor interactions with soluble growth factors[283], the mechanical properties of Matrigel[280,301,302] and the crypt or villi isolation techniques.

The rapid dissociation of floating murine crypts into disorganised clumps of cells is likely caused by the loss of integrin signalling through basal membrane attachments. Previous studies have shown that the absence of

these attachments, normally provided by the gel scaffold in enteroid cultures, induces rapid anoikis in IECs[303]. However, several mammalian epithelial cell types have overcome cell-matrix-anchorage associated anoikis when cell-cell contact is preserved, likely through compensatory mechanisms provided by E-cadherin[304]. Differences between the species in cell adhesion protein dynamics may reveal why loss of cell-matrix anchorage doesn't negatively affect mature avian crypts. Other contributing factors may include differences in crypt isolation protocols, polarity-reversal rates, soluble growth factors and structural integrity of isolated crypts or villi.

By demonstrating the floating enteroids contain the array of epithelial cell types present *in vivo*, it may be assumed they will recapitulate the different digestive and absorptive functions determined by the proximal-distal intestinal axis. Indeed, maturation to a post-hatch digestive phenotype was indicated by the transcriptome analysis. Proliferation of cells in the enteroid epithelium and lamina propria core, increase in expression of digestion-related genes, and phagocytosis of zymosan bioparticles by lamina propria leukocytes indicates this complex intestinal model sustains *in vivo* functions for more than 7 days.

The isolation of villi instead of crypts from late embryonic birds is because crypt structures are still only at a rudimentary stage of development. It takes till 2 days post-hatch for chicks to develop intestinal epithelial invaginations with crypt fission and enlargement continuing until 9 days post-hatch[7,33]. Budding enteroids can be developed from these villus tips because almost all villus cells are known to be proliferative at hatch, with cell mitosis playing a key role in post-hatch hyperplasia[7].

Species-specific intestinal epithelial-immune cell models are a necessary advancement to studying coordinated enteric immune responses in health and disease. Identification of both sub- and intraepithelial leukocytes, alongside other lamina propria cell populations which also contribute to the intestinal immune defences (reviewed in[133,305]), in these floating enteroids show such a model has now been cultivated for the chicken. This has been

achieved by a much simpler means than the staged murine and human co-culture protocols currently published[244,306,307]. Evidencing enteroid lamina propria leukocyte functionality using phagocytosis studies and mapping the dynamic behaviour of CSF1R$^+$ cells using enteroids derived from *CSF1R*-eGFP transgenic chickens demonstrates the versatility of this *in vitro* epithelial-immune cell tool. Gut macrophages have been shown to improve IEC maturation and barrier stability, therefore their presence in the enteroids is likely contributing to the maintenance of their intact epithelial barrier in the absence of external growth factors[306]. The application of single cell sequencing would be beneficial to further explore the maturation and function of the individual cell populations in the enteroids over time, and to characterise any changes that occur in the face of exogenous stimulation.

In vivo, ISC are supported for maintenance, self-renewal and differentiation by a surrounding cellular niche which includes Paneth cells, stromal cells, neural cells and the ECM (reviewed in[308]). In Chapter 3 we demonstrated that the floating chicken enteroids produce elongated buds and survive for a period of time without external supplementation from major growth or inhibitory factors required for enteroid cultures in other species e.g. EGF, RSPO, WNT, Noggin [42,43,183,195]. Identification of many of the ISC niche populations within the floating chicken enteroids indicates that the required biochemical factors and gradients for ISC proliferation and propagation are likely being generated endogenously[308]. In addition, the orientation of the floating enteroids, where the ISC basolateral receptors are not accessible, may explain why growth factors supplemented into the media have so far been ineffective.

These floating enteroids reflect the 3D architecture, barrier function and polarity of the *in vivo* intestinal epithelium. In addition, both epithelial and lamina propria cell diversity and function has been demonstrated, qualifying them as an effective *in vitro* model of the post-hatch and mature chicken intestine. The apical-out phenotype and leukocyte component of these enteroids could provide an inexpensive and uncomplicated model in which to research host-pathogen interactions, and their scope could easily be

extended for pharmaceutical, nutritional and developmental studies. A more in-depth description of the enteroids transcriptional signature would be beneficial to further explore and define this new model in terms of culture stability and their relatedness to the *in vivo* intestine.

Chapter 5 Temporal transcriptome profiling of floating chicken enteroids

Chapter 5 Temporal transcriptome profiling of floating chicken enteroids

The previous results chapters describe the development and characterisation of an apical-out leukocyte-containing chicken enteroid model. However the replicate consistency, culture stability, *in vivo* comparability, and cause of our inability to passage these enteroid cultures has not yet been fully explored on a transcript level. In this chapter, the transcriptional profiling of chicken embryonic intestinal villi and enteroid cultures using bulk RNA-seq is reported. Culture consistency and stability is demonstrated through comparison of replicates and culture time points, confirming the reproducibility of our enteroid-based experiments. The temporal expression of numerous cell subpopulation and function markers indicates that these *in vitro* intestinal models differentiate from embryonic intestinal villi to recapitulate many of the digestive, immune and gut-barrier functions seen *in vivo* post-hatch. Transcriptional changes especially notable in later cultures have provided ideas of interventions that may contribute to longer term cultures but further work on this problem is still required. These results represent a comprehensive characterization of the expression profiles of chicken enteroids at different stages of development in comparison to the *in vivo* chicken gut and lay the ground work for future studies.

5.1 Introduction

Sequencing technologies now offer the opportunity to obtain the transcriptome from organoids enabling a better understanding of the maturation stage, functions and responses of these *in vitro* culture models. Several RNA-seq datasets describing mammalian enteroids have already been published[42,43,183] and our lab recently published the 3 and 7 day floating chicken enteroid RNA-seq dataset as the first such avian resource[309]. This dataset also included the transcriptome of ED18 villi which is the only transcriptome-wide analysis available of the late embryonic chicken intestine. Most RNA-seq studies for the chicken intestine focus on functionality-related

genes involved in digestion and absorption of energy and nutrients[310,311,312], and host-pathogen responses[313,314] in mature birds. The late-embryonic to post-hatch gut undergoes immense changes in growth, metabolism and development so having also access to the gene sets involved in these critical lifestage processes would be useful for e.g. improved nutrition of the post-hatch chick[7,28,33].

Chapters 3 & 4 describe a protocol to culture floating avian enteroids from embryonic intestinal villi and, using a more comprehensive dataset than previously published, showed they reflect the cellular diversity and barrier function of the chicken intestinal epithelium and lamina propria[309]. However, to demonstrate the chicken enteroids are a robust cell culture model it is necessary to provide evidence of gene expression homogeneity within the cultures and between biological replicates. In order to reduce biological variation of the cultures, embryos from the same breed and age are used and they are incubated in the same conditions. However it is not known if inherent (epi)genetic and environmental variation among individual embryos will make the biological replicates highly heterogeneous. In addition, with the advanced complexity of the floating chicken enteroids and their potential diverse array of uses in nutritional, pharmaceutical and host-pathogen research it is important to expand on the current enteroid analysis and demonstrate the relatedness of this model to the function of the *in vivo* intestine. Transcriptional analysis could also help to address propagation issues with the model since, despite many passage technique and supplementary growth factor trials, for reasons currently unknown the floating chicken enteroids cannot be sustained long-term in culture.

In this chapter the time course transcriptome profiling of floating reverse orientated avian enteroids and ED18 chicken intestinal villi are reported. The initial aims were to assess for homogeneity between replicates in order to demonstrate the consistency of this culture method, and to assess for stable gene expression in the cultures to indicate optimal time points to conduct experiments. The second aim was to describe the functional maturation of the enteroids compared to the *in vivo* intestine by tracking gene expression

patterns across the chicken enteroid developmental continuum and comparing them back to the villi samples and published data. The final aim was to assess why the floating enteroids cannot be indefinitely propagated and ascertain what interventions may address this culture longevity issue.

5.2 Results

This study proposed an exploratory functional analysis, differential gene analysis and network analysis on the ED18 small intestinal villi and chicken enteroids. The experimental design involved three biological replicates, where isolated villi of three embryos were pooled to make one biological replicate, and each culture was split into two technical replicates after villus isolation (Fig. 5.1). Samples for transcriptome analysis were collected at 0 h (freshly isolated ED18 intestinal villi) then at 1, 3, 4, 7 days of culture. The 1 - 4 day time points were selected as they represent a time of rapid and major morphological changes in the enteroids, whereas 7 day enteroids were of interest as they appear to have reached an arrested stage of development. The embryonic intestinal villi samples were used to represent both the ED18 intestinal villi and the 0 h time point for the ED18 cultures. Technical validation of the samples by tapestation confirmed they had good RNA integrity (RIN 6.1 – 9.6) and concentration (104 – 427 ng/µl) (Table 5.1).

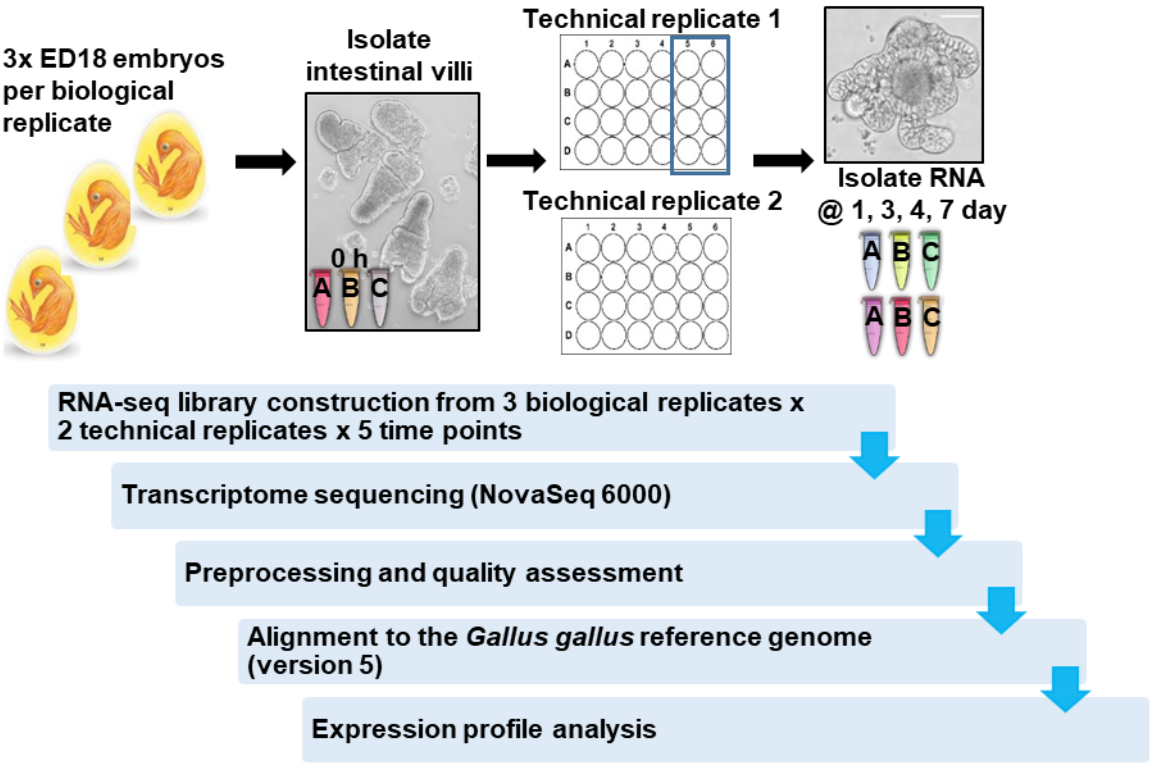

Figure 5.1: Overview of experimental design and RNA-seq data analysis pipeline. RNA was isolated from enteroids at 1, 3, 4 and 7 days and the freshly isolated ED18 intestinal villi (0 h). The validated RNA was sequenced on an Illumina NovaSeq 6000 system. All RNA-seq reads were preprocessed for a quality assessment. The filtered transcriptome reads were aligned to the genome and the expression profile was analysed.

Table 5.1: Samples collected for the transcriptome sequencing. Description of the ED18 intestinal villi and chicken enteroid RNA samples submitted for RNA sequencing with details of quality (RIN), concentration (both obtained by tapestation) and raw reads (obtained by NovaSeq S2 100PE)**.** *(*Gallus gallus*)

Samples	Sample description	Biological replicate	Technical replicate	RIN	Concentration (ng/µl)	Raw reads ($x10^8$)
COA_1_0hr	Chicken* villi 0hr	1	1	9.1	345.8	1.83
COA_2_0hr	Chicken* villi 0hr	1	2	9.2	327.6	1.62
COA_1_24hr	Chicken* enteroids 1 day culture	1	1	6.1	153.4	1.42
COA_2_24hr	Chicken* enteroids 1 day culture	1	2	6.1	212.55	1.68
COA_1_72hr	Chicken* enteroids 3 day culture	1	1	7.7	107.25	1.68
COA_1_72hr	Chicken* enteroids 3 day culture	1	2	8.1	198.25	1.47
COA_1_96hr	Chicken* enteroids 4 day culture	1	1	8.6	135.85	1.65
COA_2_96hr	Chicken* enteroids 4 day culture	1	2	7.3	291.85	1.51
COA_1_168hr	Chicken* enteroids 7 day culture	1	1	9.5	260.65	1.59
COA_2_168hr	Chicken* enteroids 7 day culture	1	2	9.3	375.05	1.79

Samples	Sample description	Biological replicate	Technical replicate	RIN	Concentration (ng/µl)	Raw reads ($x10^8$)
COB_1_0hr	Chicken* villi 0hr	2	1	9	421.2	1.54
COB_2_0hr	Chicken* villi 0hr	2	2	8.8	427.05	1.56
COB_1_24hr	Chicken* enteroids 1 day culture	2	1	6.7	378.3	1.58
COB_2_24hr	Chicken* enteroids 1 day culture	2	2	6.4	208	1.47
COB_1_72hr	Chicken* enteroids 3 day culture	2	1	7.9	107.25	1.45
COB_1_72hr	Chicken* enteroids 3 day culture	2	2	7.2	343.2	1.5
COB_1_96hr	Chicken* enteroids 4 day culture	2	1	7.7	260.65	1.62
COB_2_96hr	Chicken* enteroids 4 day culture	2	2	8.1	234.59	1.5
COB_1_168hr	Chicken* enteroids 7 day culture	2	1	9.6	274.3	1.65

Samples	Sample description	Biological replicate	Technical replicate	RIN	Concentration (ng/µl)	Raw reads ($x10^8$)
COC_1_0hr	Chicken* villi 0hr	3	1	9.2	298.35	1.6
COC_2_0hr	Chicken* villi 0hr	3	2	9.1	283.64	2.15
COC_1_24hr	Chicken* enteroids 1 day culture	3	1	7.5	156.65	1.33
COC_2_24hr	Chicken* enteroids 1 day culture	3	2	7.6	244.4	1.67
COC_1_72hr	Chicken* enteroids 3 day culture	3	1	7.9	178.1	1.47
COC_1_72hr	Chicken* enteroids 3 day culture	3	2	8.6	269.75	1.95
COC_1_96hr	Chicken* enteroids 4 day culture	3	1	8.9	104.65	1.55
COC_2_96hr	Chicken* enteroids 4 day culture	3	2	8.9	148.2	1.81
COC_1_168hr	Chicken* enteroids 7 day culture	3	1	9.8	257.4	1.82
COC_2_168hr	Chicken* enteroids 7 day culture	3	2	9.5	396.5	1.46

5.2.1 Enteroid cultures are highly reproducible

To assess the reproducibility of the cultures, the degree of heterogeneity in the biological and technical replicate global transcriptional profiles was compared. In the PC1 and 2 plot technical replicate per time point and time were the main drivers for the differences seen among the samples (Fig. 5.2, Table 5.2). The biological and technical replicates tightly clustered by time point with overlapping of the 3 and 4 day groups (Fig. 5.2). In the PC2 and 3 plot, biological replicate and time drove the variation in PC3 (Table 5.2). Samples within time point groups were more widely distributed along the PC3 axis confirming that biological replicates did account for a small variability in the data (Fig. 5.2). In contrast, the technical replicates stayed closely paired and this variable was not found to be significantly associated with changes in the structure of the data in the first 10 PCs (Table 5.2). The majority of DEGs were shared between the technical replicates confirming a high degree of similarity within cultures (Fig. 5.3). The technical replicates were therefore merged for further analysis to limit the impact of measurement error, unless otherwise indicated. In summary, the PCA and differential analysis confirm there is good reproducibility between both biological and technical replicates.

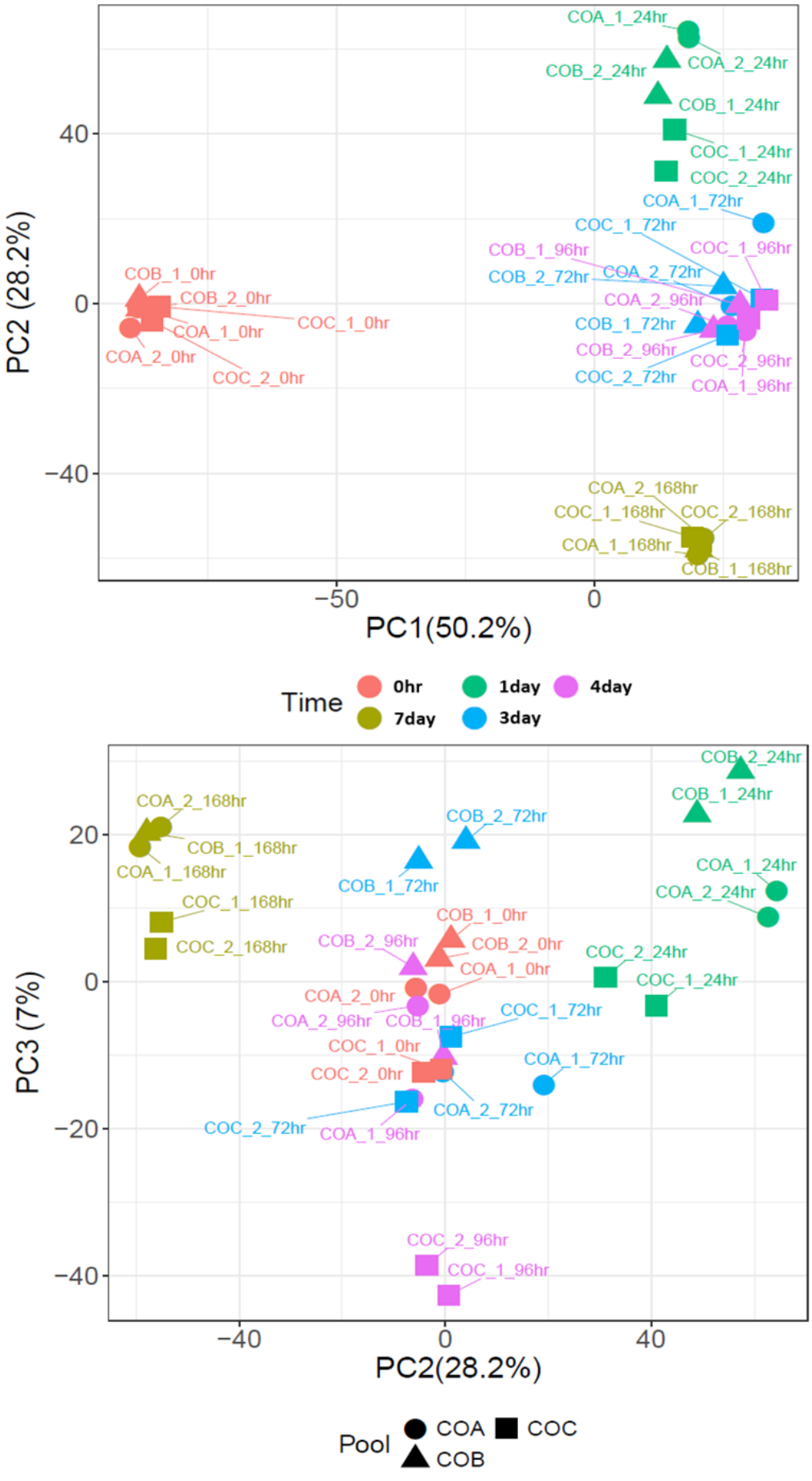
COA_1_24hr
COA_2_24hr
COB_2_24hr
COB_1_24hr
COC_1_24hr
COC_2_24hr
COA_1_72hr
COC_1_72hr
COB_1_96hr
COC_1_96hr
COB_2_72hr
COA_2_72hr
COA_2_96hr
COB_1_72hr
COB_2_96hr
COC_2_96hr
COC_2_72hr
COA_1_96hr
COB_1_0hr
COB_2_0hr
COC_1_0hr
COA_1_0hr
COA_2_0hr
COC_2_0hr
COA_2_168hr
COC_1_168hr
COC_2_168hr
COA_1_168hr
COB_1_168hr
40
0
−40
−50
0
PC2 (28.2%)
PC1(50.2%)
Time
0hr
1day
4day
7day
3day
COB_2_24hr
COB_1_24hr
COA_2_168hr
COB_2_72hr
COB_1_168hr
COA_1_168hr
COB_1_72hr
COA_1_24hr
COA_2_24hr
COC_1_168hr
COB_1_0hr
COC_2_168hr
COB_2_96hr
COB_2_0hr
COC_2_24hr
COA_1_0hr
COC_1_24hr
COA_2_0hr
COA_2_96hr
COB_1_96hr
COC_1_72hr
COC_1_0hr
COA_1_72hr
COC_2_0hr
COA_2_72hr
COC_2_72hr
COA_1_96hr
COC_2_96hr
COC_1_96hr
20
0
−20
−40
−40
0
40
PC3 (7%)
PC2(28.2%)
Pool
COA
COC
COB

Figure 5.2: Principle Component Analysis of RNA-seq expression data. Plots of the first, second and third PCs from PCA using all samples. In PC1 and PC2, technical replicate per time point and time were the significant drivers for differences. In PC3, biological replicate and time drove the variation. Sample 'COA_1_0hr' describes '**C**hicken **O**rganoid, biological replicate **A**, technical replicate **1**, **0 hr** time point' etc.

Table 5.2: ANOVA P-values of PCA. Table of statistics showing ANOVA P-values for the association between PCs and categorical experimental variables. Where different values of experimental variables are associated with large changes in the data, these P-values are expected to be significant (P ≤0.05) for early components responsible for large proportions of variance. The % values after the PCs indicate their contribution to the variability in the data.

Principal components	Technical replicate per time point	Biological replicate	Time	Technical replicate
PC1 (50.2%)	1.28e-21	0.96	1.87e-28	0.874
PC2 (28.2%)	1.71e-11	0.826	3.68e-16	0.92
PC3 (7%)	0.0832	0.00511	0.0027	0.935
PC4 (3.7%)	0.381	1.31e-06	0.0302	0.996
PC5 (2.6%)	0.908	6.09e-10	0.393	0.989
PC6 (1.3%)	0.453	0.165	0.163	0.629
PC7 (0.9%)	0.999	0.996	0.959	0.575
PC8 (0.8%)	0.994	0.864	0.833	0.975
PC9 (0.7%)	0.75	0.854	0.323	0.407
PC10 (0.7%)	0.321	0.899	0.0412	0.538

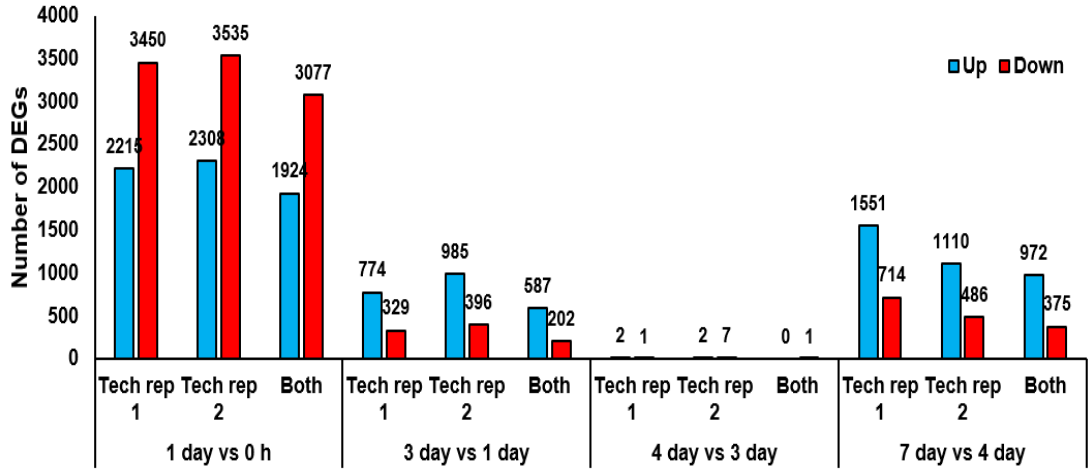

Figure 5.3: Differential analysis of adjacent culture time points. Numbers of DEGs in individual technical replicate 1 and technical replicate 2, and number of DEGs shared between both technical replicates, according to the threshold on minimum FC (2) and maximum FDR (0.05). Bars represent mean of 3 biological replicates.

5.2.2 Enteroid cultures have stable expression of stem cell homeostasis pathways

Morphologically 1 - 5 day enteroids appeared healthy with plentiful budding activity and little enteroid disintegration indicating they represented a good timeframe for experimentation (Chapter 3, Fig. 3.3). Using the enteroid transcriptome analysis I aimed to address this hypothesis by exploring whether this was a period of stable gene expression. Defined clustering of ED18 intestinal villi (0 h) on the left side and the enteroids (1 - 7 day) on the right side of the PC1 axis indicated gene expression of the *in vitro* cultures was consistently different from the freshly isolated tissue (Fig. 5.2). This was reflected in the differential analysis with just over 5000 DEGs, shared between both technical replicates, evident when comparing the 1 day enteroids and 0 h villi (Fig. 5.3). In contrast, the remaining enteroid culture time point comparisons showed relatively few DEGs; 789 in the 3 versus 1 day analysis, 1 DEG in the 4 versus 3 day analysis, and 1347 DEGs in the 7 versus 4 day analysis (Fig. 5.3). The similar gene expression profiles of the 3

and 4 day cultures indicated by the differential analysis was also evident on the PCA 1 and 2 plot with combined clustering of these groups (Fig. 5.2).

Stem cell maintenance is essential for stable enteroid cultures and is dependent on the WNT signalling pathway. Of the top 50 DEGs (by FDR) identified in the 1 day enteroid versus 0 h (villi) comparison, several genes associated with the WNT signalling pathway were downregulated such as *CSRNP1,* which is induced in response to a negative regulator of WNT signalling, and *TCIM,* a positive regulator of the WNT/β-catenin pathway (Additional file 2). On further analysis, a number of stem cell markers and *WNT6*, typically produced by Paneth cells in murine crypts[315], were also downregulated in the enteroids compared to the freshly isolated villi (Fig. 5.4a, b). However, there were also many stem cell and WNT signalling pathway genes that were steadily expressed in the enteroids. This included *WNT4* and *WNT5a* which are both expressed by mesenchymal cells in mice[316]. There was also a marked down-regulation of negative WNT regulators e.g. *ZNRF3H1, ZNRF3H2, RNF43* in the enteroids compared to the villi (Fig. 5.4b).

An analysis of gene sets associated with IEC differentiation showed a generally stable picture of expression across the culture time points, although there was a reduction in gene expression associated with differentiation to enteroendocrine cells including *NEUROG3, PDX1* and *FOXA2* (Fig. 5.4c). Transcript expression of enteroendocrine cell markers was stable across the cultures (Chapter 4, Fig. 4.2) therefore this reduction in differentiation expression may just be reflective of the low abundance (~1%) of this cell population in the gut.

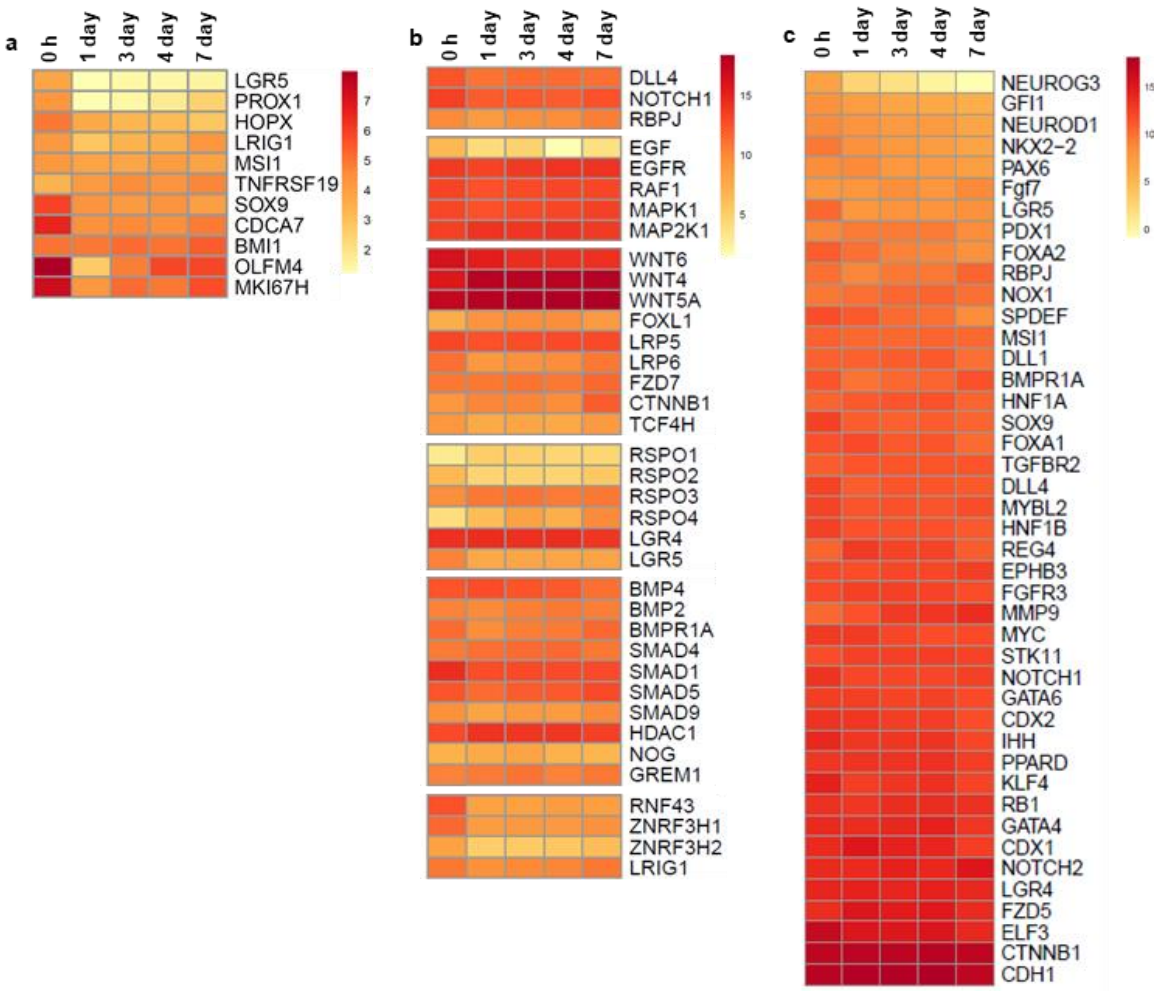

Figure 5.4: Single gene analyses related to culture homeostasis. Expression of **(a)** stem cell markers, **(b)** Wnt signalling pathway genes, and **(c)** intestinal epithelial cell differentiation related genes in ED18 intestinal villi (0 h) and enteroids at 1, 3, 4 and 7 days of culture were analysed by RNA sequencing. Heat maps show the relative expression levels (log2 CPM reads) of a range of mammalian gene sets. RNA sequencing data is representative of 3 independent experiments, each comprising of 2 technical replicates, each containing 3 embryos**.**

In summary, a large amount of transcriptional differences are evident between the villi and 1 day enteroids whereas the 3 – 4 day time points have extremely stable gene expression. Although there is an initial downregulation of some ISC markers, the enteroids display stable expression of many stem cell niche and epithelial cell differentiation genes across the time points. This supports the morphological findings that 1 – 5 day cultures are a suitable stable timeframe for experimentation.

5.2.3 Early enteroid cultures undergo rapid development

In order to explore the functional enteroid maturation and issues with propagation, the villi and enteroid transcriptomes were analysed using a gene-to-gene correlation network graph (Fig. 5.5). This was created using a Pearson correlation threshold of r ≥0.95 of which the top 50 clusters (groups of genes with expression profiles correlated ≥0.95) contained ≥17 genes (Additional file 3a). Clusters with similar mean expression profiles typically occupied similar regions of the network graph. The clusters typically spanned circularly in a chronological fashion progressing clockwise from those predominantly expressed in embryonic intestinal villi (Fig. 5.5a), to those predominantly expressed at higher levels in all enteroids (Fig. 5.5b), through the culture time points (Fig. 5.5c - e), ending with to those predominantly expressed in 7 day enteroids (Fig. 5.5f).

The mean gene expression profiles and representative human GO term enrichment annotations, from the functional categories biological process, cellular component and molecular function, for the largest 50 clusters from the network graph were analysed in further detail (Additional files 3b and 3c). A summary of GO term enrichment annotations from select clusters was created for ease of reference which highlighted processes and functions for cell cycle, tissue development and cell functions concentrated within different villi and enteroid culture time points (Table 5.3a, b).

The ED18 intestinal villi denote a stage of rapid development in the late embryonic intestine and accordingly GO terms associated with tissue development were predominant in the villus clusters including regulation of cell differentiation, organ growth and cell cycle (Table 5.3a). Analysing cell cycle related cluster 1 in more detail, multiple individual genes displaying the villi-associated expression profile were identified in the KEGG *Gallus gallus* cell cycle pathway map e.g. *CDK1, WEE1, CDC25A, ERF1* (Fig. 5.6, Additional file 3a). GO terms associated with cell cycle were also found in 1 – 4 day enteroid clusters and many of the genes enriched in ED18 intestinal villi and 1 day enteroids were involved in transcription and translational

regulation GO terms including translational initiation, peptide biosynthetic process and RNA processing (Table 5.3a, b). Cluster 3, which is characterised by high gene expression in 1 day enteroids, revealed proliferation-related GO terms associated with cell energy production such as generation of precursor metabolites and energy and adenosine triphosphate (ATP) metabolic process (Table 5.3b). This transcriptional analysis confirmed data from Chapter 3, Fig. 3.4 which indicated that cell proliferation is especially prevalent in the first couple of days of the developing enteroid cultures, a timeframe reflective of the rapid development of the post-hatch chick intestine *in vivo*.

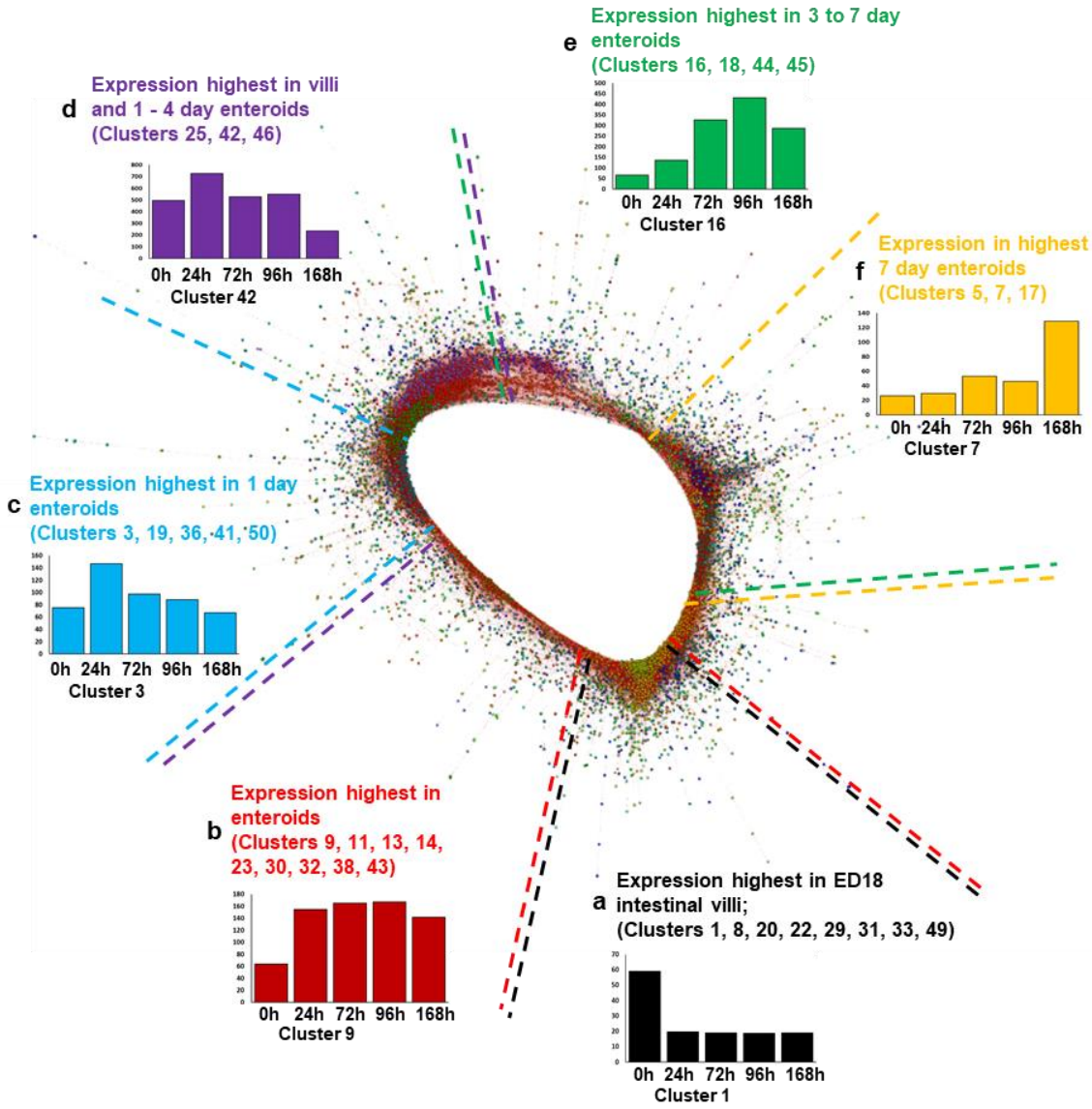

Figure 5.5: Network analysis of ED18 intestinal villi-enteroid RNA-seq expression data. Main component of the network graph derived from all five data sets samples. Here, the nodes represent transcripts (genes) and the edges represent correlations between individual expression profiles above r ≥ 0.95. Coloured broken lines delineate regions of network graph containing clusters of genes with mean expression profiles similar to the adjacent graph (**a – f**). The graph *x* axis shows the samples ordered from time of cultures with 0 h representing isolated ED18 intestinal villi. The *y* axis shows the mean expression intensity (TPM) for the cluster. Coloured broken lines delineate regions of network graph containing clusters of genes predominantly expressed at higher levels in matching coloured and located time-points**.**

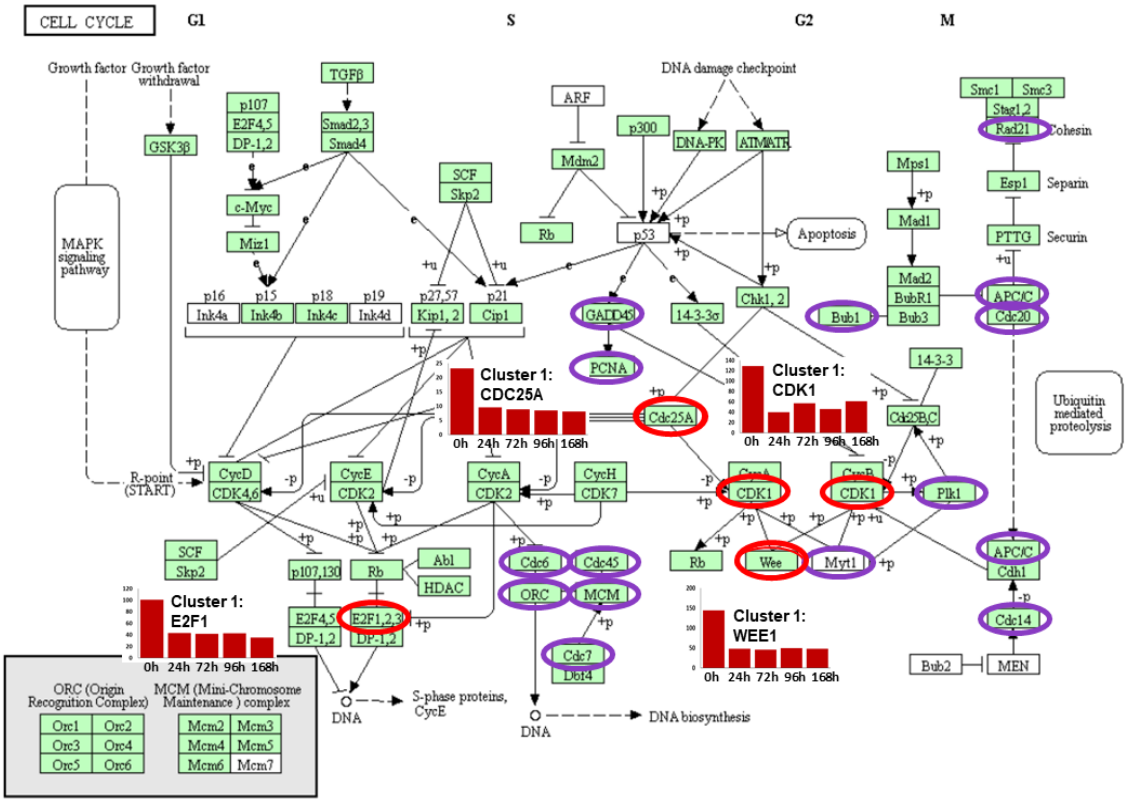

Figure 5.6: Cell cycle related genes highlighted in the ED18 intestinal villi. KEGG pathway: Cell cycle *Gallus gallus* (chicken). Purple and red circled genes were contained in embryonic tissue analysis Cluster 1 whose mean gene expression profile was high in ED18 intestinal villi compared to enteroids. Associated GO terms in Cluster 1 were predominantly expressed in the cell cycle. Red circled genes have their mean expression profiles demonstrated in adjacent graphs. The graph *x* axis shows the samples ordered from time of cultures with 0h representing isolated ED18 intestinal villi. The *y* axis shows the mean expression intensity for the cluster (TPM).

Table 5.3a: GO term enrichment annotations for ED18 intestinal villi-enteroid network clusters grouped into similar time-point expression profiles. GO terms of interest were chosen to highlight the various biological processes occurring at each time-point.

High villi (0 day)							
cluster	**GO term no.**	**Significantly-enriched GO term (p <0.05)**	**p value**	**Genes in gene set**	**Genes in cluster**	**Genes in overlap**	**% overlap**
1	7049	CELL CYCLE	4.30E-63	1864	1190	175	9.39
1	51301	CELL DIVISION	8.78E-36	598	1190	76	12.71
1	9893	POSITIVE REGULATION OF MULTICELLULAR_ORGANISMAL_PROCESS	1.71E-29	1825	1190	123	6.74
1	15630	MICROTUBULE CYTOSKELETON	6.93E-32	1220	1190	102	8.36
1	22008	NEUROGENESIS	2.92E-34	1625	1190	123	7.57
1	51276	CHROMOSOME ORGANIZATION	3.53E-35	1223	1190	107	8.75
1	45595	REGULATION_OF_CELL_DIFFERENTIATION	1.52E-30	1881	1190	127	6.75
8	35295	TUBE_DEVELOPMENT	9.42E-10	1122	194	18	1.60
8	2520	IMMUNE SYSTEM DEVELOPMENT	1.05E-09	990	194	17	1.72
8	7517	MUSCLE_ORGAN_DEVELOPMENT	1.43E-07	407	194	10	2.46
20	43005	NEURON_PROJECTION	6.85E-08	1317	64	11	0.84
20	45202	SYNAPSE	5.74E-15	1332	64	17	1.28
20	7269	NEUROTRANSMITTER SECRETION	2.17E-08	168	64	6	3.57
31	33002	MUSCLE_CELL_PROLIFERATION	1.01E-07	241	28	5	2.07
31	35265	ORGAN GROWTH	2.76E-06	203	28	4	1.97
High 0h and 1day							
cluster	**GO term no.**	**Significantly-enriched GO term (p <0.05)**	**p value**	**Genes in gene set**	**Genes in cluster**	**Genes in overlap**	**% overlap**
10	43043	PEPTIDE_BIOSYNTHETIC_PROCESS	2.94E-91	736	159	73	9.92
10	6413	TRANSLATIONAL_INITIATION	6.11E-111	192	159	62	32.29
12	6396	RNA_PROCESSING	1.66E-10	917	131	16	1.74
High 0h and 3-7 day							
cluster	**GO term no.**	**Significantly-enriched GO term (p <0.05)**	**p value**	**Genes in gene set**	**Genes in cluster**	**Genes in overlap**	**% overlap**
15	5768	ENDOSOME	1.10E-06	918	92	11	1.20
21	70160	TIGHT JUNCTION	0.0000079	126	47	4	3.17
21	5912	ADHERENS_JUNCTION	0.0000238	169	47	4	2.37
21	43297	APICAL_JUNCTION_ASSEMBLY	3.57E-05	64	47	3	4.69
21	2520	IMMUNE SYSTEM DEVELOPMENT	4.65E-05	990	47	7	0.71
26	42582	AZUROPHIL_GRANULE	3.56E-06	155	36	4	2.58
26	46903	SECRETION	1.02E-05	1680	36	8	0.48
26	33043	REGULATION OF ORGANELLE ORGANIZATION	1.59E-05	1267	36	7	0.55
21	7010	CYTOSKELETON_ORGANIZATION	4.03E-05	1335	47	8	0.60
28	44257	CELLULAR_PROTEIN_CATABOLIC_PROCESS	1.49E-06	782	34	7	0.90
High 0h and 7 day							
cluster	**GO term no.**	**Significantly-enriched GO term (p <0.05)**	**p value**	**Genes in gene set**	**Genes in cluster**	**Genes in overlap**	**% overlap**
2	7049	CELL_CYCLE	2.09E-32	1864	824	110	5.90
2	51254	POSITIVE_REGULATION_OF_RNA_METABOLIC_PROCESS	9.94E-36	1710	824	110	6.43
2	51276	CHROMOSOME_ORGANIZATION	9.45E-33	1223	824	89	7.28
2	15630	MICROTUBULE_CYTOSKELETON	1.76E-22	1220	824	74	6.07
24	2521	LEUKOCYTE_DIFFERENTIATION	7.01E-14	520	44	11	2.12
24	2682	REGULATION_OF_IMMUNE_SYSTEM_PROCESS	3.44E-12	1670	44	14	0.84
24	46649	LYMPHOCYTE_ACTIVATION	8.65E-14	736	44	12	1.63

Table 5.3b: GO term enrichment annotations for ED18 intestinal enteroid network clusters grouped into similar time-point expression profiles. GO terms of interest were chosen to highlight the various biological processes occurring at each time-point.

High 1 day							
cluster	**GO term no.**	**Significantly-enriched GO term (p <0.05)**	**p value**	**Genes in gene set**	**Genes in cluster**	**Genes in overlap**	**% overlap**
3	6091	GENERATION_OF_PRECURSOR_METABOLITES_&_ENERGY	9.68E-59	532	704	81	15.23
3	46034	ATP_METABOLIC_PROCESS	9.19E-56	303	704	64	21.12
3	7005	MITOCHONDRIAL_ORGANIZATION	4.17E-71	528	704	91	17.23
19	98798	MITOCHONDRIAL_PROTEIN_COMPLEX	2.19E-08	260	69	7	2.69
19	16071	MRNA_METABOLIC_PROCESS	2.65E-09	840	69	11	1.31
High 1 to 7 day							
cluster	**GO term no.**	**Significantly-enriched GO term (p <0.05)**	**p value**	**Genes in gene set**	**Genes in cluster**	**Genes in overlap**	**% overlap**
9	46903	SECRETION	1.32E-08	1680	179	24	1.43
9	5773	VACUOLE	7.76E-10	781	179	18	2.30
9	44257	CELLULAR_PROTEIN_CATABOLIC_PROCESS	5.64E-09	782	179	17	2.17
11	70727	CELLULAR_MACROMOLECULE_LOCALIZATION	2.49E-07	1930	143	20	1.04
11	6508	PROTEOLYSIS	6.74E-08	1779	143	20	1.12
13	44255	CELLULAR_LIPID_METABOLIC_PROCESS	2.80E-07	1064	109	14	1.32
13	16050	VESICLE_ORGANIZATION	2.97E-11	330	109	12	3.64
14	30199	COLLAGEN_FIBRIL_ORGANIZATION	4.24E-06	55	100	4	7.27
14	43062	EXTRACELLULAR_STRUCTURE_ORGANIZATION	4.99E-08	373	100	9	2.41
High 1 to 4 day							
cluster	**GO term no.**	**Significantly-enriched GO term (p <0.05)**	**p value**	**Genes in gene set**	**Genes in cluster**	**Genes in overlap**	**% overlap**
4	44281	SMALL_MOLECULE_METABOLIC_PROCESS	1.06E-22	1962	658	83	4.23
4	44257	CELLULAR_PROTEIN_CATABOLIC_PROCESS	9.84E-23	782	658	52	6.65
4	6886	INTRACELLULAR_PROTEIN_TRANSPORT	7.04E-29	1151	658	71	6.17
6	6629	LIPID_METABOLIC_PROCESS	4.53E-13	1405	355	38	2.70
6	7049	CELL_CYCLE	3.37E-11	1864	355	41	2.20
High 3 to 7 day							
cluster	**GO term no.**	**Significantly-enriched GO term (p <0.05)**	**p value**	**Genes in gene set**	**Genes in cluster**	**Genes in overlap**	**% overlap**
16	34378	CHYLOMICRON_ASSEMBLY	4.54E-07	10	88	3	30
16	42304	REGULATION_OF_FATTY_ACID_BIOSYNTHETIC_PROCESS	1.99E-06	56	88	4	7.14
16	46486	GLYCEROLIPID_METABOLIC_PROCESS	4.25E-06	414	88	7	1.69
18	6887	EXOCYTOSIS	2.29E-06	900	69	10	1.11
18	8047	ENZYME_ACTIVATOR_ACTIVITY	2.56E-05	520	69	7	1.35
18	46903	SECRETION	1.87E-05	1680	69	12	0.71
High 7 day							
cluster	**GO term no.**	**Significantly-enriched GO term (p <0.05)**	**p value**	**Genes in gene set**	**Genes in cluster**	**Genes in overlap**	**% overlap**
5	30030	CELL_PROJECTION_ORGANIZATION	3.09E-29	1545	491	72	4.66
5	45595	REGULATION_OF_CELL_DIFFERENTIATION	2.03E-23	1881	491	71	3.77
5	35295	TUBE_DEVELOPMENT	4.70E-18	1122	491	48	4.28
5	22008	NEUROGENESIS	1.95E-29	1625	491	74	4.55
7	31012	EXTRACELLULAR_MATRIX	1.55E-17	531	320	28	5.27
7	48870	CELL_MOTILITY	1.75E-13	1758	320	42	2.39
7	48514	BLOOD_VESSEL_MORPHOGENESIS	5.18E-13	686	320	26	3.79
7	46695	REGULATION_OF_CELL_DIFFERENTIATION	5.59E-14	1163	320	38	3.27
7	30030	CELL_PROJECTION_ORGANIZATION	5.59E-14	1545	320	40	2.59
7	22008	NEUROGENESIS	5.12E-16	1625	320	44	2.71
7	22610	BIOLOGICAL_ADHESION	7.11E-19	1425	320	45	3.16
7	1816	CYTOKINE_PRODUCTION	3.72E-12	808	76	12	1.49
7	2521	LEUKOCYTE_DIFFERENTIATION	1.83E-08	520	76	8	1.54

5.2.4 Development of a comprehensive lamina propria component

As previously described in Chapter 4, the ED18 villi isolation and floating culture conditions resulted in an apical-out enteroid phenotype with a lamina propria core, which has not previously seen in mammalian enteroid cultures. *In vivo* the lamina propria is composed of multiple elements including many immunologically competent cells, components of the enteric nervous system, blood and lymphatic vessels, and myofibroblasts. The chicken enteroid inner core was indicated to contain many of these elements in Chapter 4 (Fig. 4.5 - 4.7), although immunostaining did not detect endothelial cell markers. An aim of this more detailed transcriptome analysis was to explore the development and functionality of the enteroid lamina propria component.

As expected for this late stage of embryonic maturation, development of both the enteric nervous system and the muscularis mucosa was indicated in the ED18 villus transcriptomes with associated GO terms of neuron projection, synapse and muscle cell proliferation (Table 5.3a). Further analysis of genes within villi-associated cluster 20 confirmed most encode proteins associated with synaptic signalling e.g. *AMPH, KIF1A;* neurotransmission e.g. *CHAT, PHOX2B;* neuron growth e.g. *CSPG5, SLITRK1;* as well as ligand- or voltage-gated ion channels e.g. *CHRNA3, CHRNB4, GRIN3A, IL1RAPL1, P2RX3* (Additional file 3a). The 7 day clusters harbour GO terms not only associated with neurogenesis but also blood vessel morphogenesis and epithelial or endothelial tube development (Table 5.3b). A major contributor to angiogenesis, vasculogenesis and endothelial cell growth is *VEGFA*, which is produced by many cell types including macrophages, and its transcript levels are steadily expressed over the enteroid cultures (Fig. 5.7a). Indeed analysis of genes specifically related to intestinal development showed many have steady or increasing transcript levels through the enteroid cultures (Fig. 5.7a)[317].

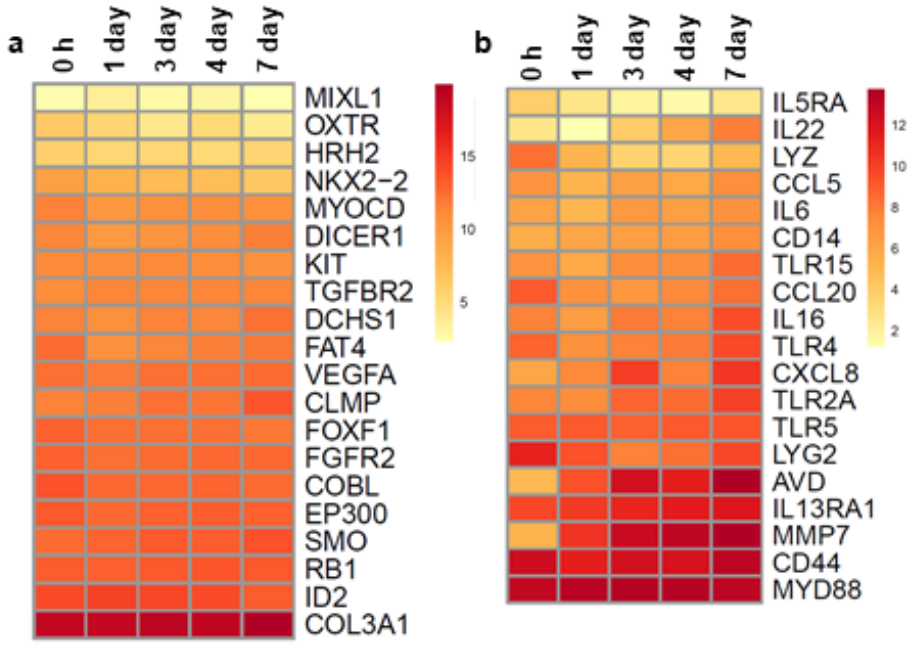

Figure 5.7. Single gene analyses of the enteroid lamina propria. Expression of **(a)** intestinal development-associated genes and **(b)** gut barrier related genes in ED18 intestinal villi (0 h) and enteroids at 1, 3, 4 and 7 days of culture were analysed by RNA sequencing. Heat maps show the relative expression levels (log2 CPM reads) of a range of mammalian gene sets. RNA sequencing data is representative of 3 independent experiments, each comprising of 2 technical replicates, each containing 3 embryos**.**

Immune system development and function related GO terms were prevalent in both ED18 intestinal villi and enteroid clusters and included functions such as regulation of immune system development, leukocyte differentiation, lymphocyte activation and cytokine production (Table 5.3a, b). Further scrutiny of these immune system associated clusters show they contain genes representative of several populations of lymphocytes e.g. *LY96, IKZF1, BTK, BANK1, BLK, SPI1, HCLS1, FYB1, CD274, LCP2, IL18R1*, and cells of the myeloid lineage e.g. *CD200R1A, TREM2, ITGB2, CSF1R, MARCO, LAMP3, WDFY4*, in agreement with the immunocytological analyses performed on the enteroids in Chapter 4, Fig. 4.5 (Additional file 3a). The clusters also contain genes associated with pattern recognition e.g. *TLR4, TLR2A, TLR15* and cytokine and chemokine signalling e.g. *CCL5, IL16*. There were also gene sets associated with GO term functions of

secretory cells i.e. goblet cells, Paneth cells, enteroendocrine cells, in 3 – 7 day clusters including exocytosis and enzyme activator activity. Many of these immune functions play a role in maintaining the intestinal barrier, and genes specifically associated with this essential role of the gut showed an increasing trend in expression over the culture time points (Fig. 5.7b).

This transcriptome analysis, alongside previous cell-type identification from Chapter 4, demonstrates the presence, development and functions of lamina propria components within the chicken enteroid model.

5.2.5 Digestive function gene expression develops in the enteroid cultures

In order to confirm if this *in vitro* intestinal model accurately represented the typical array of *in vivo* functions, the transcriptome was also investigated for evidence of absorption and digestion. Clusters where gene expression was enriched in enteroids compared to ED18 intestinal villi were indeed predominantly associated with digestion-related GO terms e.g. cellular lipid metabolic process, chylomicron assembly, cellular protein catabolic process and glycerolipid metabolic process (Table 5.3b). Looking at small intestinal digestion related genes in the enteroids in further detail, there was a general trend of increased expression for many genes over the sample time points including brush border enzymes e.g. *LCT* and *SLC13A1*, and those involved in fat metabolism e.g. *APOA1 and APOA4* (lipid transport), *FABP2* (fatty acid transport), and *SCP2* (cholesterol uptake and transport) (Fig. 5.8a)[317,318].

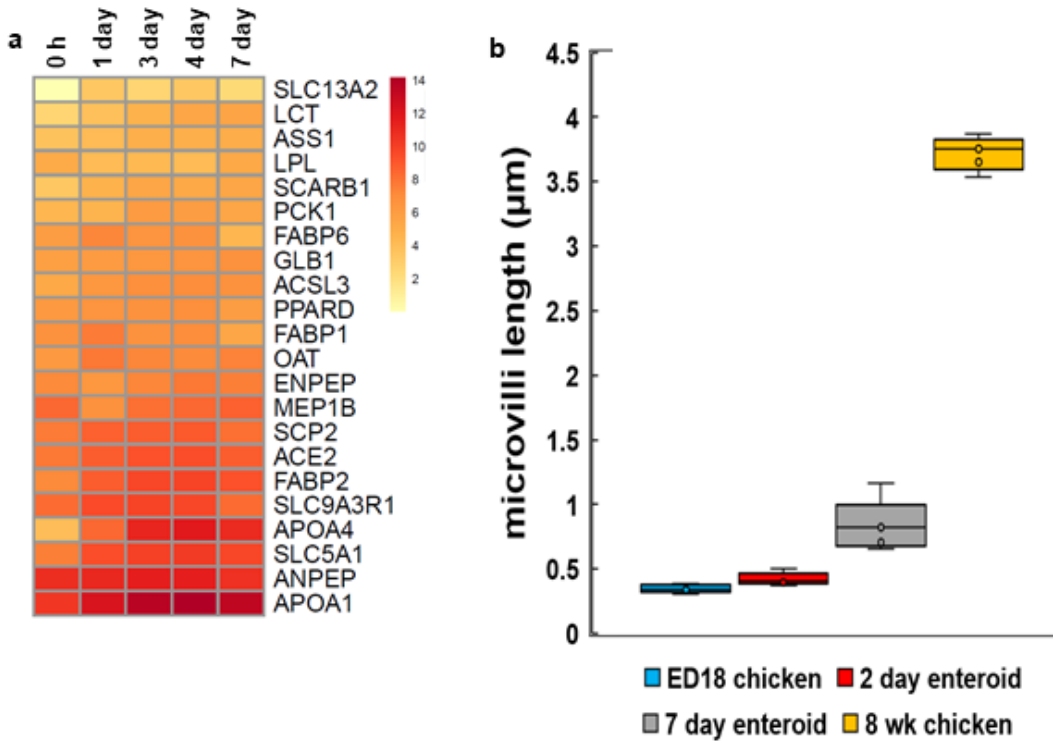

Figure 5.8. Morphological and transcriptional evidence for digestive function in the enteroid cultures. Expression of **(a)** digestion related genes in ED18 intestinal villi (0 h) and enteroids at 1, 3, 4 and 7 days of culture were analysed by RNA sequencing. Heat maps show the relative expression levels (log2 CPM reads) of a range of mammalian gene sets. RNA sequencing data is representative of 3 independent experiments, each comprising of 2 technical replicates, each containing 3 embryos**. (b)** Quantification of microvilli length in ED18 intestine, 3 and 7 day enteroids measured from TEM images; averaged for 3 cultures containing 2-3 embryos.

The GO term cell projection organization in the 7 day enteroids may describe microvilli development, essential structures which increase intestinal epithelial surface area for both secretion and absorption. To confirm whether the microvilli of apical-out enteroids continue to develop *in vitro*, their length was measured from TEM images (Fig. 5.8b) and indeed the microvilli length of 7 day enteroids was found to be markedly longer than that of ED18 intestine. This morphological analysis alongside the transcriptome data indicates the enteroids develop post-hatch digestive functions over the

course of the cultures, although functional studies should also be performed to confirm this.

5.2.6 Ongoing developmental activity in 7 day enteroids

Although the floating chicken cultures develop profuse villus-like structures without external supplementation, they are not viable long-term. In Chapter 3, Fig. 3.4 the enteroid cultures displayed no general increase in cell stress-related genes indicating culture conditions are not causing excessive necrosis. Therefore one of the possible causes of reduced enteroid longevity could be due to changes in cell type and function. During EMT, epithelial cells acquire mesenchymal fibroblast-like properties, losing apical-basal polarity, weakening cell-cell junctions, rearranging the cytoskeleton and acquiring increased motility (reviewed in[319]). EMT will occur in enteroids of certain mammalian species unless there is inhibition of certain pathways by externally supplemented p38MAPK- and TGFβ-inhibitors. In the 7 day versus 4 day DEG comparison a number of genes associated with epithelial migration were upregulated at 7 days e.g. *FAP, CCDC88A, AFAP1, HGF, ITGA4* (Additional file 2) and an analysis of genes generally upregulated during EMT showed a trend of increased expression of across the enteroid time points (Fig. 5.9a). However EMT associated transcription factors show a trend of decreased expression, and ongoing epithelial development and digestive function is indicated at 7 days of culture (Fig. 5.4 and 5.8).

To ascertain if deficiencies in supplemented growth factors and/or inhibited molecules, typically targeted in mammalian cultures, may be the cause of reduced culture longevity, their gene expression was analysed in ED18 intestinal villi and chicken enteroids (Fig. 5.9b). Most genes had consistent to increasing expression across the cultures except for *EGF*, *WNT6*, *RSPO2* which were downregulated in the enteroids compared to ED18 villi. Of note, *MAPK14* and *MAPK11* which are targeted by p38MAPK-inhibitors, and *TGFB1* and *ROCK1* which are targeted by TGFβ-inhibitors were also steadily expressed.

In summary, both EMT and growth factor deficiencies may contribute to the inability to passage the enteroids however further studies are required to ascertain both the cause and potential solutions to this longevity problem.

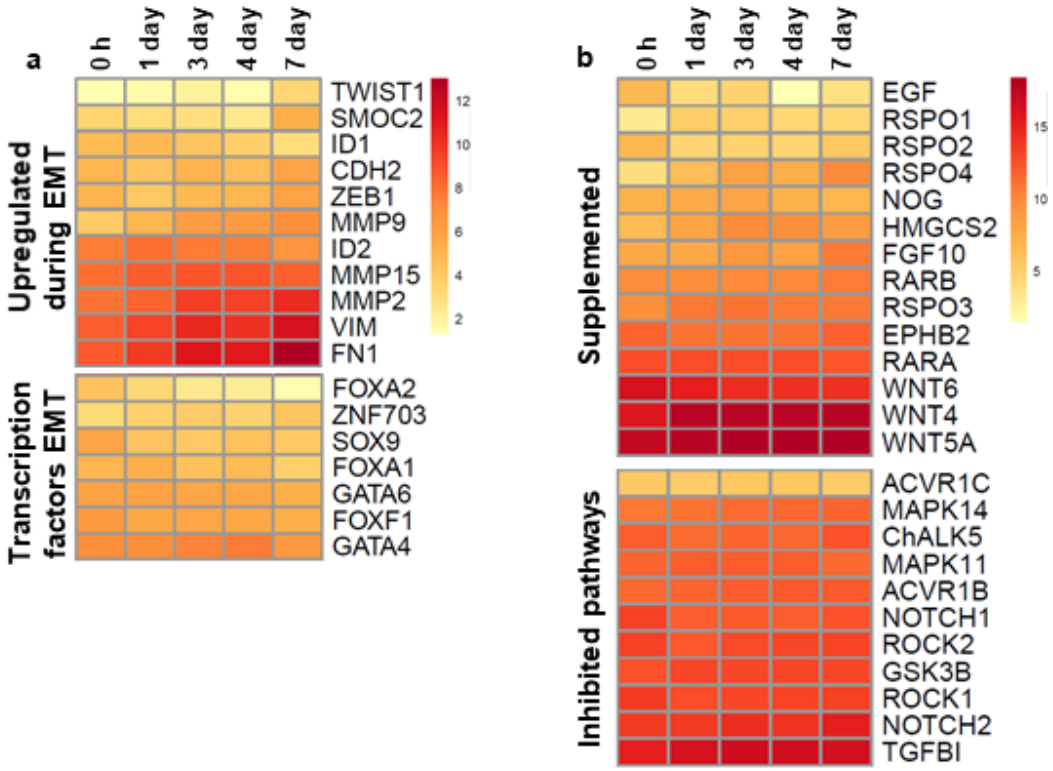

Figure 5.9. EMT and growth factor single gene analysis of villi and enteroid cultures. Expression of **(a)** EMT and **(b)** growth factor associated genes in ED18 intestinal villi (0 h) and enteroids analysed by RNA sequencing. Heat maps show the relative expression levels (log2 CPM reads) of a range of mammalian described gene sets. RNA sequencing data is representative of 3 independent experiments, each comprising of 2 technical replicates, each containing 3 embryos.

5.3 Discussion

Chapters 3 and 4 utilised chicken enteroid transcriptome data to describe the presence of epithelial and lamina propria differentiated cell populations, epithelial intercellular junctions, and stable apoptotic and stress signatures of the cultures. In this chapter a more rigorous transcriptome profiling of the chicken embryonic intestinal villi and chicken enteroid cultures using bulk

RNA-seq is reported. Part of this analysis involved assessing the reproducibility and stability of gene expression within and between cultures. Culture consistency was demonstrated through comparison of biological as well as technical replicates, confirming the reproducibility of floating chicken enteroid-based experiments. The stability of *in vitro* models is important for a robust analysis and the enteroids display steady transcriptional profiles for cell differentiation and homeostasis gene sets across 1 – 7 days of culture, although 3 – 4 days is highlighted as a particularly stable timeframe.

The divergence of ED18 intestinal villi and enteroid samples to opposite sides of the PC1 axis highlights a marked difference in their global gene expression profiles. This disparity is likely due to the dramatic and rapid development of budding enteroids from embryonic villi, in addition to adaptions to the *in vitro* culture environment. In the chicken during the first 24 h post-hatch there are striking changes in the mucosal morphology of the small intestine, including intensive cryptogenesis and a dramatic increase in villus length[7,8]. Similar morphological changes are demonstrated by the growing chicken enteroids where there is rapid closure of the villi fragments within hours of plating out and development of multiple buds by 1 day which continue to lengthen over the following days (Chapter 3, Fig. 3.2). In conjunction with this behaviour, the 1 day enteroid transcriptome denotes upregulation of many genes involved in development, proliferation and differentiation. This amazingly rapid enteroid growth in chicken cultures is in stark contrast to the slower developing mammalian enteroids[43,183].

In Chapter 4, the natural presence of innate intestinal immune components were demonstrated in the floating avian enteroid model including differentiated epithelial cells, an intact epithelial barrier, and intraepithelial and lamina propria leukocytes. Evidence of mucosal immunity is also seen in the transcriptome with many significantly enriched immune-related GO terms associated with both the ED18 intestinal villi and enteroids. In terms of epithelial defences, although the classical Paneth cell secretion genes *LYG2* and *LYZ* are gradually downregulated in the enteroids, their expression does increase in 7 day cultures. The general increase in many gut barrier-related

genes e.g. interleukin 13 receptor subunit alpha (*IL13RA)1, IL6 and IL22* which are involved in induction of immune response, may reflect natural development in the mucosal immune system post-hatch[1,123,320]. Indeed, GO terms associated with immune system development and leukocyte differentiation appear at most cultures time points. The goblet cell secretion avidin (*AVD*), which has previously been shown to increase in expression with age alongside increasing goblet cell numbers[321], and *CD44,* which is specifically involved in establishment of intestinal epithelial pathogen resistance during development, are also increased across the cultures (reviewed in[322]). *In vivo*, complete maturation of the intestinal immune system seems to occur only after the intestine is challenged post-hatch with both microbial and nutritional antigens[123,320]. It would therefore be interesting to analyse the differences in immune response of the enteroids with the presence of a microbiome, although due to the lower oxygen requirements of microbiota this is currently technologically challenging.

In parallel with the morphological changes, the ability of the chick intestine to digest and absorb nutrients has been shown to increase steadily during the first week post-hatch[8,28,323]. For example, *in vivo* brush border enzyme activities have been shown to increase rapidly in the post-hatch chicken and the enteroids mirror this with an increase in expression of selected brush border enzyme genes (Fig. 5.8a)[8]. Although the transcript differences may not be functionally significant, that the chicken enteroids develop strong expression of digestion-related genes and associated pathways strongly indicates that the *in vitro* conditions contain the important cues for post-hatch maturation. This hardwiring of the developmental program into the gut epithelium has previously been noted in murine enteroids developed from later stages of fetal development[207]. As the fetal mouse enteroids mature they show a downregulation of *ASS1* and a switch to *ARG2* expression to allow catabolism of arginine which is abundant in solid food. These gene expression patterns are mirrored in the chicken enteroids over the first few days of culture. In addition, fatty acid binding protein (*FABP)2,* a critical

function enzyme required for digestion in the adult intestine, has enhanced expression over the course of the cultures (Fig. 5.8a)[317].

Currently there is no evidence for the ability to passage floating enteroid cultures[211,212,309]. Despite various trials in the floating chicken enteroids, continued bud growth after passage has not been recognised (Chapter 3, Fig. 3.6). Analysis of the chicken enteroid transcriptome for potential underlying causes indicated that EMT could be occurring in the enteroids. Blockade of p38MAPK and TGF-β pathways in human, bovine and porcine enteroid cultures is required, in part, to help to protect the cells within them against EMT[42,324,325,326]. However trials of p38MAPK and TGF-β molecular inhibitors in floating chicken enteroid media showed no improvement in post-passage growth or budding (Chapter 3, 3.2.6). Murine enteroid cultures require active supplementation with TGF-β in order to induce an EMT model indicating species-specific differences in these pathways which may also be present in the chicken[327].

Analysis of genes associated with typical enteroid culture supplements identified reduced expression of *WNT6, RSPO2* and *EGF* in the enteroids as compared to the villi. Previous *in vivo* studies have shown that blocking all epithelial WNT sources, or even genetically removing Paneth cells, doesn't negatively affect the stem cell niche if alternative sources of WNT ligands are available from stromal cells[328]. Therefore the upregulation of stromal-expressed *WNT4*, *WNT5A* and forkhead box (*FOX)L1,* a marker for a mesenchymal cell population which express specific *WNT* mRNAs, indicates the enteroid lamina propria may be providing alternative WNT ligands in place of WNT6 (Fig. 5.9b)[329]. RSPO functions have not been shown to completely overlap therefore, despite upregulation of *RSPO1* and *RSPO4* across the cultures, the decreased expression of *RSPO2* may be specifically detrimental for chicken ISC homeostasis (reviewed in[330]). This diversity in function could also explain why external supplementation of RSPO1 had no positive effects on the cultures (Chapter 3, 3.2.6). Culture supplementation with EGF also saw no benefits, which could be due to the enteroids reverse polarisation prohibiting contact of these ligands with their basolateral

epithelial receptors[331]. However, Acharya et al. (2020) demonstrated enterotrophic effects of EGF supplementation in floating chicken enteroid cultures therefore further trials with different EGF concentrations and RSPO2 in the enteroids may show benefit[217].

Using RNA-seq and transcriptome-wide comparisons of chicken enteroids and chicken embryonic intestinal villi I have demonstrated the consistency of this culture model and identified hallmarks of multiple key intestinal functional attributes. The enteroids have been demonstrated to have a transcriptomically stable timeframes where they are morphologically mature, indicating useful culture stages to conduct experimental work. These results indicate that this unique model is an adequate *in vitro* tool for post-hatch chicken intestinal studies. In addition, introduction of the floating chicken enteroid and ED18 chicken intestinal villi transcriptome to the wider scientific community will provide a valuable resource for future avian intestinal research.

Additional file 2: Differential heat maps for specified contrasts. Top most 50 differential rows selected by false discovery rate, for contrast 0 h vs 24 h and 96 h vs 168 h.

Additional file 3a: ED18 intestinal villi and enteroid genes found in the largest 50 co-expression cluster derived from the RNA-seq analysis data. Table providing list of genes found in each co-expression cluster in the network graph derived from the RNA-seq analysis data.

Additional file 3b: Mean expression profiles of the ED18 intestinal villi and enteroid genes in each of the largest 50 co-expression clusters. Individual mean expression profiles of the genes in each of the largest 50 co-expression clusters derived from the network graph. The *x* axis shows the samples ordered by time of cultures with 0 h representing isolated ED18 intestine. The *y* axis shows the mean expression intensity (TPM) for the cluster.

Additional file 3c: GO term enrichment annotations for the ED18 intestinal villi and enteroid genes in the largest 50 co-expression clusters. Table listing the representative GO term enrichment annotations for the genes in the largest 50 co-expression clusters derived from the network graph.

Additional file 4: Differentially expressed gene summary. Table of normalised genes from the RNA-seq analysis with statistics (P-value, log2 fold change (FC) and false discovery rate (FDR)) observed from a differential analysis of each time contrast (adjacent time points).

Chapter 6 The mucosal response to *Salmonella* Typhimurim in the chicken enteroid model

Chapter 6 The mucosal response to *Salmonella* Typhimurium in the chicken enteroid model

Salmonellosis remains a major public health concern globally with human infections frequently associated with consumption of contaminated poultry meat and eggs. Non-typhoidal *Salmonella* strains also cause severe disease and high mortality in young chickens. Current *in vitro* models of the poultry intestine are limited in cellular complexity and gut architecture. By improving these tools we can hope to better understand the molecular mechanisms of early *Salmonella* infection and the innate immune responses to different strains in poultry, whilst adhering to the 3Rs. Previous chapters described the development of an apical-out leukocyte-containing chicken enteroid model. In this chapter the enteroids were explored as a host-bacterial infection model by analysing their response to wildtype (WT) or type 3 secretion system 1 (T3SS1) mutant *Salmonella enterica* serovar Typhimurium infection (*S.* Typhimurium) and LPS challenge. A combination of fluorescence imaging, bacterial replication, epithelial barrier integrity assays and transcriptomics analysis show that the T3SS1 mutants display reduced invasion and replication compared to the WT strain, but induce a similar but delayed immune response. This data demonstrates the enteroids can be utilised as a comprehensive *in vitro* tool for the exploration of avian gut epithelial and leukocyte responses in *Salmonella* research.

6.1 Introduction

Salmonella enterica are Gram-negative rod-shaped facultative anaerobic bacteria that are comprised of over 2,000 serovars[332]. Non-typhoid *Salmonella* strain *S. enterica* serovar Typhimurium (*S.* Typhimurium) has a broad host range and transmits, via contaminated food or water, from avian to human hosts in both developing and developed countries. It is an intracellular bacterium which uses virulence factors encoded in *Salmonella* pathogenicity island 1 (SPI1) to penetrate host M cells[333] and enterocytes[334] in the small intestine. One of these virulence factors is the T3SS1 which

becomes active on contact with IECs and translocates effectors across the plasma membrane which then induce membrane ruffling, bacterial invasion and acute intestinal inflammation[335]. These membrane 'ruffles' are a well-characterised feature of *Salmonella* virulence, promoting internalization of the pathogen by non-phagocytic cells (reviewed[336]). This food-borne pathogen, alongside another common non-typhoid strain *S.* Enteriditis, predominantly causes gastroenteritis in hosts[332]. In 2018, approximately 92,000 human cases of Salmonellosis were identified in the European Union with 119 reports deaths[337]. In mature chickens *S.* Typhimurium only results in a mild self-limiting enteritis however in young chicks it causes severe intestinal pathology and spreads systemically via infected macrophages causing high levels of mortality[338].

In vivo studies have provided considerable knowledge about the virulence and mucosal immune response to *S.* Typhimurium in the mature chicken and post-hatch chicken gut[137,339,340,341,342]. However experiments in live birds contain many variables and cannot accurately capture the early infection time points so complementary *in vitro* studies are also desirable. Current 2D models of the chicken intestine have limited cell-types and/or intestinal architecture so cannot reproduce certain hallmarks of natural infections. Since 3D enteroids more closely mimic the morphology and physiology of the intestine they are emerging as infection models to study host-pathogen interactions. Zhang et al. (2014) were the first to demonstrate *S.* Typhimurium infection in enteroids showing that *Salmonella* invaded the mouse epithelial cells, disrupted the tight junctions and displayed inflammatory responses through activation of the NFkB pathway[343]. Human, bovine and porcine enteroids have since displayed similar results to *Salmonella* infection[198,344]. However, the fully enclosed lumen of the typical mammalian enteroid poses a challenge to deliver the bacteria to the epithelial surface. Recently, apical-out human enteroids were developed and were shown to recapitulate specific morphological hallmarks of *S.* Typhimurium infection in man including epithelial barrier disruption and cytoskeletal reorganisation[211]. The floating avian enteroids described in Chapters 3 - 5

have the same advantageous apical-out phenotype with easily accessible microvilli facing the media, and they also contain a unique lamina propria core containing functional leukocytes.

The initial aim of this study was to see whether the floating apical-out leukocyte-containing chicken enteroid model could facilitate natural infection with *S.* Typhimurium by simply adding the microorganisms to the media. The subsequent aims were to evaluate differences in epithelial barrier disruption and enteroid immune response to LPS, WT and T3SS1 *S.* Typhimurium strains. By describing the complex interplay between the avian enteroid cells and *S.* Typhimurium I hope to demonstrate this intestinal model has the potential to improve our understanding of bacterial invasion events and innate inflammatory responses in young birds.

6.2 Results

6.2.1 Chicken enteroids are susceptible to infection by *Salmonella*

To investigate whether floating chicken enteroids could be infected with a bacterial pathogen, WT *S*. Typhimurium or a *prgH* T3SS1 mutant strain, defective in the SPI1-encoded T3SS1, were added to the media. The T3SS1 mutant exhibits WT growth characteristics in bacterial culture but cannot translocate *e*ffector proteins through the T3SS1 to induce host-cell actin remodelling on the apical surface of polarized epithelial cells. At 4 hpi dense actin rings surrounded individual WT bacteria (Fig. 6a, a1, c) and large numbers of WT bacteria were disseminated intracellularly throughout the enteroids (Fig. 6b, b1). In contrast, few non-invasive T3SS1 mutant *S.* Typhimurium were found in contact with the microvilli and no dense cytoskeletal modifications were visualised (Fig. 6d, d1, f, f1). The only T3SS1 mutant bacteria identified on the surface appear to have been trapped in the enteroid surface folds and so avoided being washed off during staining (Fig. 6d1, f1). Only very occasional intracellular T3SS1 mutant bacteria were identified by 4 hpi (Fig. 6e, g, h). Gentamicin protection assays confirmed

significantly increased numbers of WT *Salmonella* in enteroids at 0 h post high-dose gentamicin treatment, versus those incubated with the T3SS1 mutant strain, and only the WT strain demonstrated significant net replication over the following 8 h (Fig. 6i).

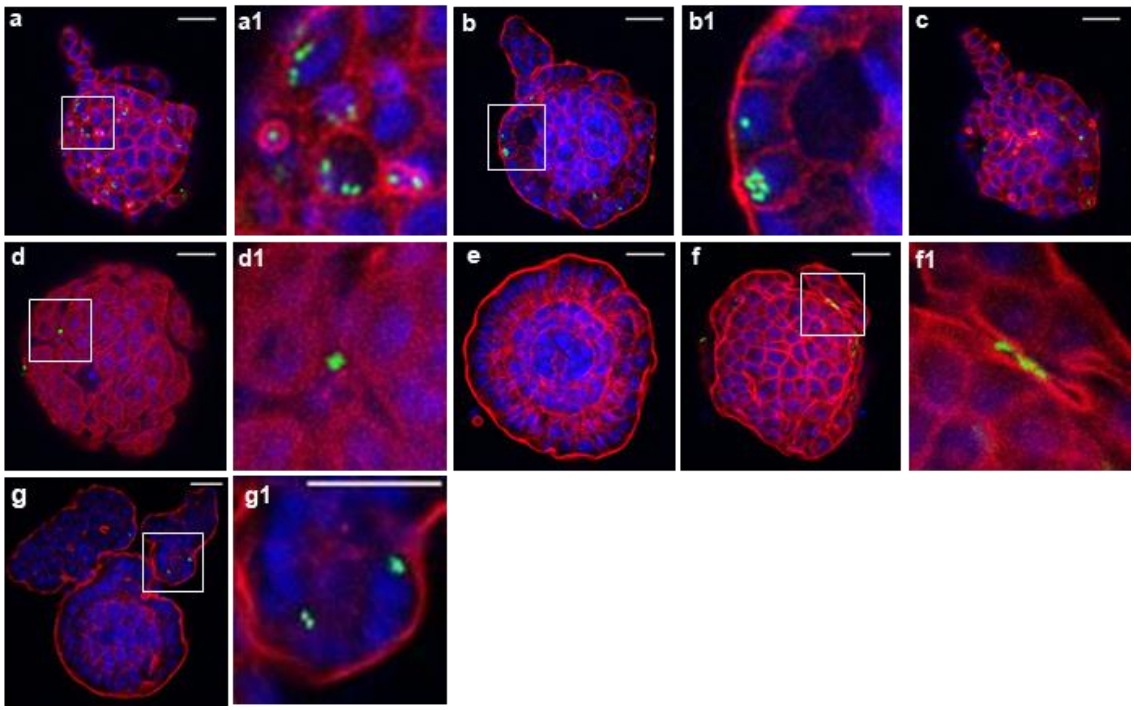

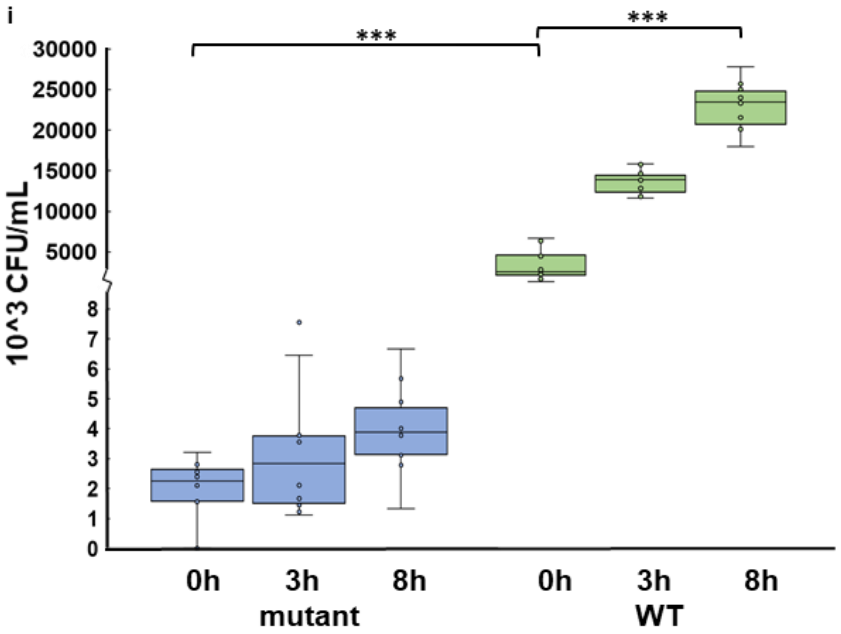

Figure 6.1: Infection and replication of *S.* Typhimurium in enteroids. a - h Representative z-axis projections of 2 day chicken enteroids whole-mount stained to detect cell nuclei (DAPI, blue) and F-actin-expressing brush border (red). Enteroids infected with **a - c** WT *S.* Typhimurium-GFP (green) at 4 hpi, with magnified images of (**a1)** actin remodelling, (**b1)** intracellular bacteria. **d - h** T3SS1 mutant *S.*Typimurium-GFP (green) infected enteroids at 4 hpi with (**d1, f1)** magnifications demonstrating lack of actin remodelling, but **(g, g1**) showing occasional intracellular bacteria. Images are representative of data from at least 3 independent cultures each containing 2 - 3 embryos. Scale bar: 20 µm. **i** Gentamicin protection assay showing *Salmonella* counts for 2 day old enteroids infected with WT or T3SS1 mutant *Salmonella* strains for 0, 3 or 8 hours. Box and whisker plots represent bacterial count from ~800 infected enteroids post high-dose gentamicin treatment. Data derived from 5 independent experiments with 2 - 3 embryos per culture. ***P ≤0.0002, W = 55, 95.5% CI for n1 – n2 is (-419850, -189760) using a Mann-Whitney U test (two-sided). The assay also showed WT *Salmonella* replicated in the enteroids over 0 – 8 hpi. ***P ≤0.0001, R^2 = 0.73, df = 29 using a linear regression test.

In summary, this data showed the apical-out polarity of the avian enteroids allows for the imitation of the natural infection process with WT *S.* Typhimurium by simply adding the bacteria to the same media as the enteroids. In addition, the T3SS1 mutants failed to induce epithelial cell actin remodelling and had reduced invasion and replication rates as compared to WT infected enteroids.

6.2.2 The enteroid epithelial barrier integrity is disrupted by *Salmonella* in a concentration dependent manner

Chapter 4 demonstrated the presence of functional enteroid cell-cell junctions by measuring the paracellular flux of FITC-dextran (Chapter 4, Fig. 4.8). To determine whether it was possible to measure varying levels of enteroid epithelial barrier disruption, the enteroids were treated with increasing concentrations of EDTA for 30 min. The images showed marked differences in FITC-dextran permeation through the intercellular spaces in EDTA-treated enteroids compared to PBS-treated controls (Fig. 6.2a). In order to quantify

the enteroid permeability, confluent culture images had their grey value (amount of enteroid) measured and this was used to calculate the relative enteroid permeability (permeation of FITC-dextran through the intercellular spaces) for each treatment group (Fig. 6.2b, c). This analysis showed that exposing the enteroids to increasing EDTA concentrations caused significantly increasing levels of epithelial barrier disruption. This demonstrated that the enteroid model can reflect a varied and quantifiable epithelial barrier response to external challenge.

The ability of *S.* Typhimurium to cause gastroenteritis with diarrhoea has been indicated to correlate with its ability to disrupt the epithelial barrier[345,346]. To determine whether this hallmark of *Salmonella* invasion was present in the chicken enteroids, cultures challenged with *S.* Typhimurium LPS (1 µg/ml) or infected with increasing CFU concentrations of either WT or T3SS1 mutant *S.* Typhimurium were analysed using the FITC-dextran-diffusion assay. The FITC-dextran images showed a marked disruption of the enteroid epithelial surface in the WT infected samples compared to PBS-treated controls (Fig. 6.2a). Quantitative analysis using ImageJ showed that LPS challenged enteroids and enteroids infected with 10^2 CFU/enteroid T3SS1 mutant *S.* Typhimurium showed no significant difference in their ability to exclude FITC-dextran compared to controls (Fig. 6.2c). This indicated that these challenge conditions do not affect enteroid intercellular junctions. In contrast the WT *S.* Typhimurium samples were all significantly different from the controls (WT vs control at 10^2 CFU P =0.004, 10^3 CFU P =0.003, 10^4 CFU P =0.001) with enteroid permeability significantly increased with increasing CFU concentrations (Fig. 6.2c). At higher CFU concentrations, the T3SS1 mutant *S.* Typhimurium also caused a significant increase in enteroid permeability (mutant vs control at 10^3 and 10^4 CFU P =0.003). However the relative enteroid permeability for T3SS1 mutant infections was significantly lower than its equivalent WT CFU group (WT vs mutant at 10^3 CFU P =0.003, 10^4 CFU P =0.005) (Fig. 6.2c). These findings indicated that WT *S.* Typhimurium bacteria are more effective at disrupting enteroid intercellular junctions than T3SS1 mutant bacteria.

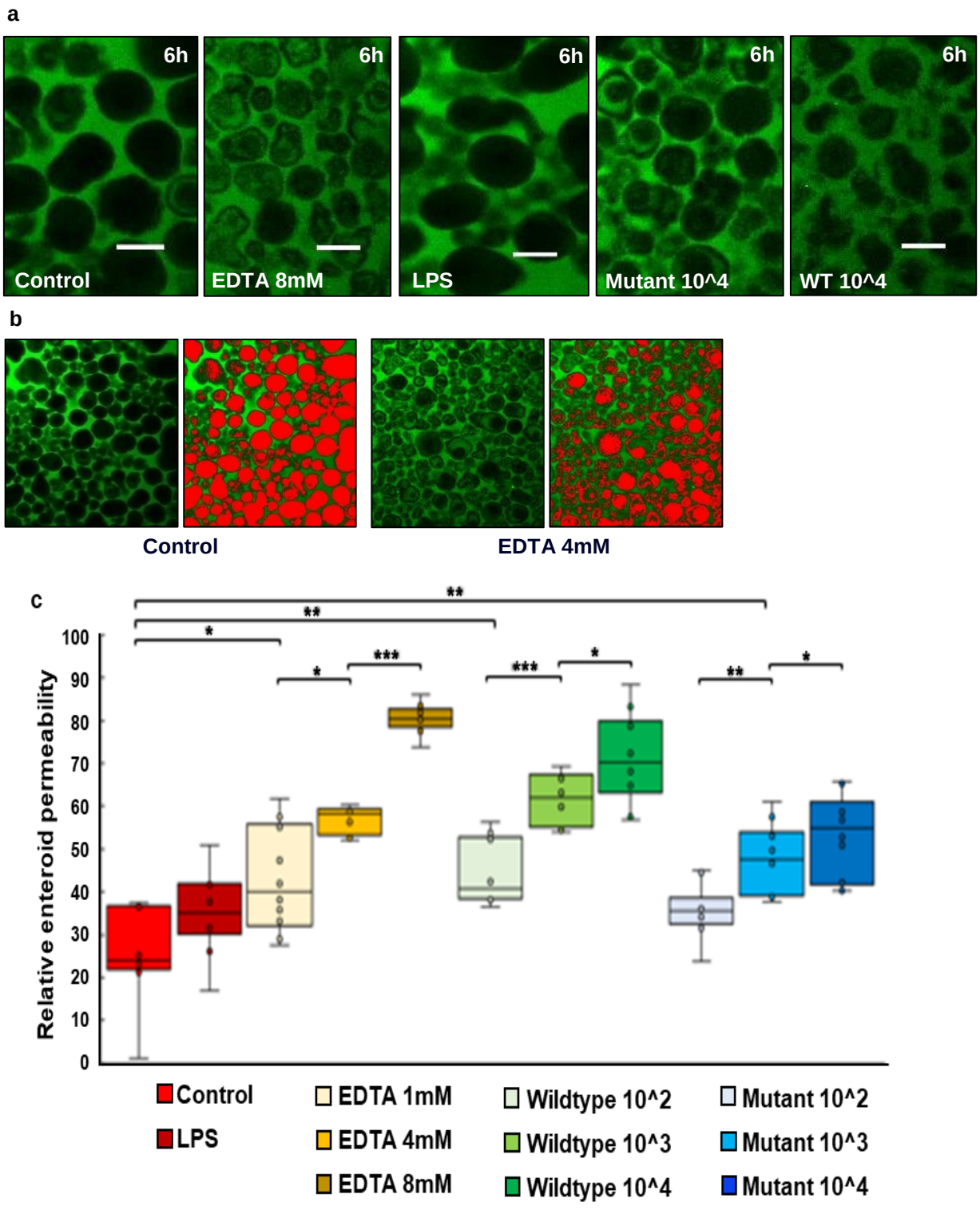

Figure 6.2: Effect of *S.* Typhimurium on epithelial barrier integrity. a Confocal images of unstained 2 day old enteroids immersed in FITC-dextran 4 kDa; control enteroids and enteroids challenged with EDTA 8 mM for 30 min or 1 µg/ml LPS for 6 h, or infected with T3SS1 mutant *S.* Typhimurium or WT *S.* Typhimurium at 10^4 CFU

per enteroid for 6 h. Scale bar = 100 µm. **b** Image J analysis of number of gray pixels (gray area) in control 2 day enteroids and 2 day enteroids challenged with 4 mM EDTA for 30 min immersed in FITC-dextran. **c** Relative enteroid permeability (1.3×10^6 – image gray area) under control and challenge conditions; LPS (6 h), EDTA (30 min), WT (6 hpi) and T3SS1 mutant (6 hpi) *S.* Typhimurium. Data derived from 4 independent experiments with 2 - 3 embryos per culture and 3 low powered fields (40 x magnification) measured per replicate. ***P ≤0.0005, **P ≤0.005, *P ≤ 0.05 using post-hoc Mann-Whitney U tests (two sided). Kruskal-Wallis test confirmed whole dataset significance. ***P ≤0.0005, H = 79.99.

6.2.3 Enteroids show a global differential gene expression after *Salmonella* infection and LPS challenge

To investigate whether the floating chicken enteroids could raise an immune response to bacterial infection, a multiplexed RT-qPCR 96.96 Fluidigm Dynamic Array was employed. This contained a panel of 89 genes selected from an RNA-seq analysis of the transcriptional response of chicken macrophages, DCs and heterophils to agonists of innate immunity and from published transcriptome data[275]. Of these, almost all of the genes from the qPCR array were found in common with the list of transcribed enteroid culture RNA-seq genes. Two genes were not found in the RNA-seq data; *R28S* which is in the enteroid transcriptome but is unannotated, and *ENSGALG00000053880* for which the same is likely true in the genome assembly used (Table 6.1).

Table 6.1: Genes on the 'bacterial' qPCR array. List of the 96 genes on the RT-qPCR 96.96 Fluidigm Dynamic Array. Genes highlighted in yellow are unannotated in the RNA-dataset from 0 h (ED18 villi), 1, 3, 4, and 7 day non-challenged/infected enteroid cultures. Genes in blue are reference genes.

ABCG2	***EGR1***	***IRF1***	***RASD1***
ACOD1	***ENSGALG00000037166***	***IRF9/10***	***SAAL1***
ACTB	***ENSGALG00000045596***	***IRF7***	***SDC4***
ADAMTSL2	***ENSGALG00000053860***	***JUN***	***SELE***
ATF3	***ETS2***	***LYG2***	***SERPINE2***
B2M	***G0S2***	***LYZ***	***SLCO4C1***
BATF3	***GAPDH***	***MADPRT1***	***SNX10***
BCL2A1	***GCH1***	***MAFA***	***SOCS1***
C3orf52	***GLUL***	***MAFF***	***SOCS3***
CCL19	***GUSB***	***MYD88***	***STEAP1***
CCL20	***HPS5***	***MYO10L***	***STEAP4***
CCLi3	***IFIT5***	***NDNF***	***TBP***
CCL5	***IL10RA***	***NFKB2***	***TGM4***
CD200L	***IL12B***	***NFKBIZ***	***TIMD4***
CD40	***IL13RA2***	***NLRC5***	***TIRAP***
CD72	***IL17REL***	***NOS2***	***TLR15***
CD80	***IL18***	***NR4A3***	***TLR4***
CD83	***IL1B***	***PFKFB3***	***TNFAIP3***
CSF1	***IL1R2***	***PKD2L1***	***TNIP2***
CXCL13L2	***IL4I1***	***PLK3***	***TOLLIP***
CXORF21	***IL6***	***PPARG***	***TRAF3IP2***
DTX2	***IL8***	***PRSS23H***	***TUBA8B***
EAF2	***IL8L1***	***PTGS2***	***UPP1***
EDN1	***IRAK2***	***R28S***	***WDR24***

RNA samples from enteroids challenged with *S.* Typhimurium LPS (1 µg/ml), or infected with WT *S.* Typhimurium or T3SS1 mutant *S.* Typhimurium (10^4 CFU/enteroid) for 4 and 8 h were run on the qPCR array. If fluorescence was not detected in a chamber it was represented by a black filled square on the heatmap (Fig. 6.3a). There was a distinct difference visible between control and infected groups on the heatmap, but much more subtle differences between the control and LPS treatment groups. The Ct values were normalised in GenEx software to the most stable reference genes of which 5 (out of 6) were identified for this dataset; *ACTB, GAPDH, GUSB, R28S* and *TBP*. Technical replicates were averaged and ΔCt or log2 relative quantity

(relative to the sample with the lowest expression for each gene) values were used for further analysis.

When comparing the whole dataset by PCA, general clustering of biological replicates for each treatment group was apparent with separation of clusters based on treatment and time (Fig. 6.3b). The LPS expression profile was very loosely clustered closest to the controls whereas the WT *Salmonella* samples were more tightly clustered furthest away from controls along the PC1 axis. The 4 and 8 hpi samples from each Salmonella strain were separately clustered, indicating a difference in gene expression with increased infection time. The 8 hpi T3SS1 mutant and 4 hpi WT samples had a marked overlap on the PCA indicating similar gene expression profiles (Fig. 6.3b). These results indicate bacterial infection of the enteroids induces a marked innate immune response as compared to controls but LPS challenge has a more limited effect.

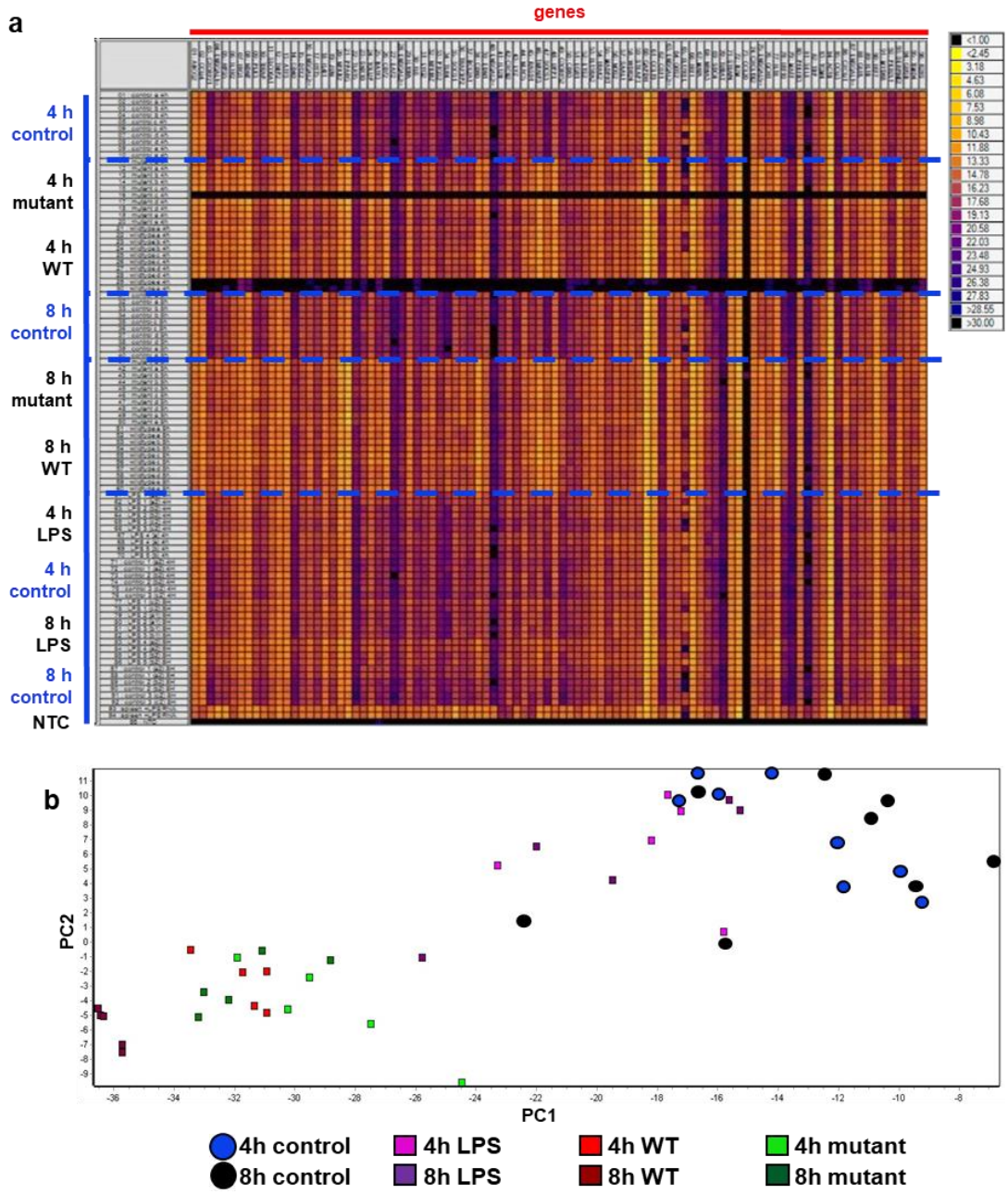

Figure 6.3: Whole dataset immunogenicity patterns in *S.* Typhimurium infected enteroids over time. a Heatmap view of the qPCR array run with individual genes on the x axis and individual samples on y axis. The RNA was extracted from 2 day old enteroid samples infected with WT or T3SS1 mutant *S.* Typhimurium at 10^4 CFU per enteroid, challenged with 1 µg/ml LPS, or controls at 4 and 8 hpi; 5 biological replicates were collected per treatment group and were run in duplicate. Black filled squares represent chambers where no gene expression was detected. NTC = non-template control. **b** PCA for qPCR array dataset showing

immune-related genes expressed in enteroid samples infected with WT or T3SS1 mutant *S.* Typhimurium, challenged with LPS, or control at 4 and 8 hpi.

6.2.4 LPS challenged enteroids induce more innate immune DEGs at 4 h than at 8 h post challenge

In order to explore the differential kinetic immune response elicited by LPS challenged chicken enteroids in more detail, unpaired 2-tail Student's t-tests were performed on the gene expression data between LPS challenged enteroids and their respective controls at 4 and 8 h post challenge.

The number of significant DEGs ($P \leq 0.05$) induced in LPS enteroids, as compared to controls, was markedly lower than those expressed in the bacterial infected enteroids which mirrors the heatmap and PCA findings (Fig. 6.4). There were markedly more DEGs at 4 h compared to 8 h post challenge, with most showing upregulation (Fig. 6.4). The most inducible genes (ΔΔCt (infected – control) of >1) at 4 h post challenge included co-stimulatory type 1 membrane molecule *CD80*, pro-inflammatory chemokine *CCL4*, interferon stimulated genes *CXORF21* and *CXORF52*, apoptosis inducer *EAF2* and anti-inflammatory *SOCS3* (Fig. 6.5a). *CCL4, CXORF21* and *TIRAP,* an adaptor protein in the TLR signalling pathway, were the only 3 genes significantly upregulated at 4 and 8 h post challenge, with expression falling over time for the latter 2 genes (Fig. 6.5b).

This data shows, relative to bacterial infection, LPS challenge of the enteroids induces a small number of immune-related genes after 4 h which reduce in number with time post challenge.

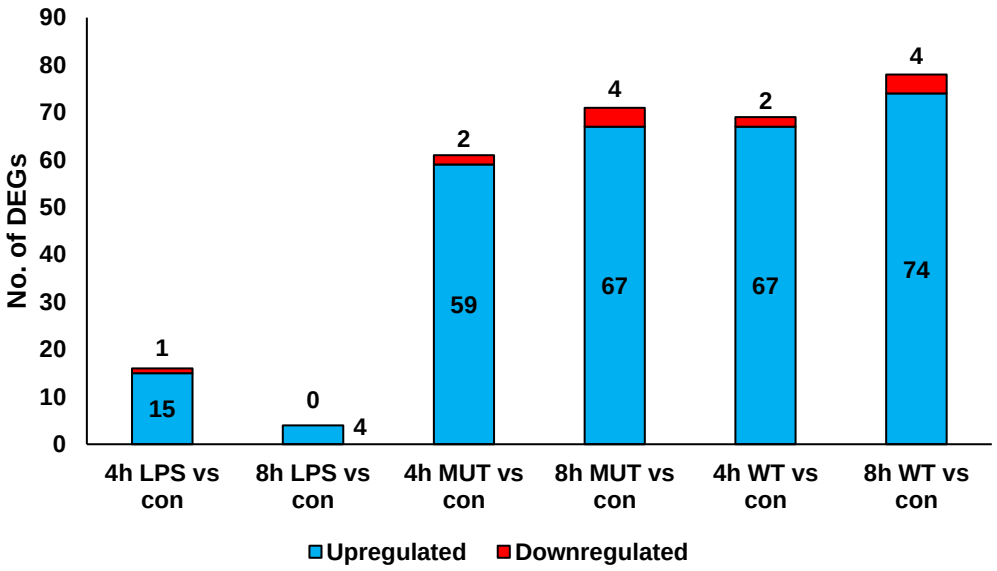

Figure 6.4: Total genes significantly differentially regulated in *S.* Typhimurium LPS challenged and bacteria infected enteroids. Biological replicates were grouped and the number of significant DEGs ($P \leq 0.05$) in an unpaired 2-tail Student's t-test (challenged/infected enteroid sample versus control sample) were compared. Red indicates downregulated and blue indicates upregulated enteroid DEGs in LPS challenged or infected 2 day old enteroid samples as compared to controls at 4 and 8 hpi. Results are from RNA samples run in the qPCR array. Each bar represents an average of 5 biological replicates**.** Con = control, MUT = T3SS1 mutant, WT = wildtype.

a

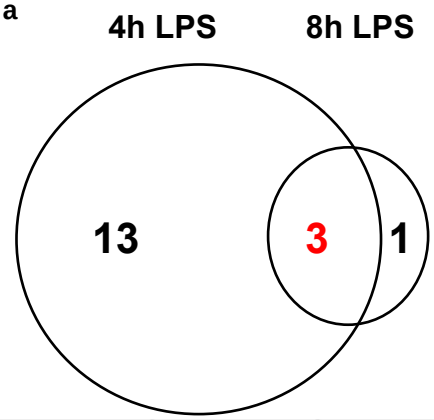

(4h LPS) vs (4h control)	Difference (LPS-control) ΔΔCt	P-Value	(8h LPS) vs (8h control)	Difference (LPS-control) ΔΔCt	P-Value
C3ORF52	1.74508	0.003428	IFIT5	0.48313	0.043077
CD80	1.41226	0.004016			
EAF2	1.91114	0.00464			
SOCS3	2.473	0.005485			
TOLLIP	0.51868	0.008716			
IL1R2	0.56787	0.014992			
HPS5a	0.97177	0.020816			
TLR15	0.99651	0.023534			
IL13RA2	0.52266	0.02531			
CD200L	0.85925	0.025879			
SOCS1	0.40154	0.036862			
TBP	-0.11266	0.041344			
LYG2	0.96431	0.049569			

b

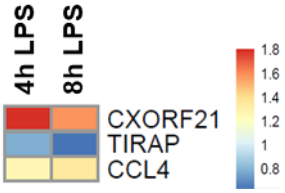

Figure 6.5: Genes significantly differentially regulated in *S.* Typhimurium LPS challenged enteroids. a Venn diagrams comparing DEGs (challenged vs control) between 4 and 8 h LPS challenged 2 day old enteroids. Table describes DEGs not found in common, with positive ΔΔCt values representing upregulated genes and negative values representing downregulated genes. **b** Heatmap shows the ΔΔCt values of DEGs in common at both 4 and 8 h post challenge. Results are from LPS challenged and control samples run in the qPCR array, representing an average of 5 biological replicates.

6.2.5 For WT and T3SS1 mutant infections, number and expression of DEGs increases with time

To investigate enteroid gene expression after *S.* Typhimurium infection over time, Student's t-tests were performed on the 4 and 8 hpi qPCR array data for WT or T3SS1 mutant infected enteroids and their respective controls. A large number of significantly differentially transcribed genes were evident in the bacterial infected enteroids compared to controls and this number increased with time post infection (Fig. 6.4). Even when considering only the most inducible significant DEGs (ΔΔCt of >1) there were 65 DEGs upregulated in 8 hpi WT infected enteroids compared to 50 DEGs at 4 hpi, and 57 DEGs in 8 hpi T3SS1 mutant infected enteroids compared to 41 DEGs at 4 hpi. There was a clear direction of gene regulation at both time points with the majority of DEGs upregulated in infection groups as compared to controls (Fig. 6.4).

To consider the DEGs induced by infection over time in more detail, the significant DEG lists for each bacterial strain were compared at 4 and 8 hpi (Fig. 6.6). Few DEGs were found exclusively at 4 hpi for both strains, with most either found in common or found exclusively at 8 hpi. For WT infections the most significant DEGs upregulated at 8 but not 4 hpi included intracellular signalling receptor *SDC4,* interleukins *IL6 and IL4I1,* cation channel *PKD2L1,* host defence peptide *LYZ*, and co-stimulatory molecule *CD83* which plays a critical role in controlling and resolving immune responses (Fig. 6.6a). In T3SS1 mutant infected enteroids, *SDC4, LYZ and IL4I1* were also exclusively found at 8 hpi as were interleukin receptor *IL13RA2,* myeloid and lymphoid cell transcription factor *NR4A3,* membrane transport mediator *SLCO4C1* and *TIRAP* (Fig. 6.6b).

a

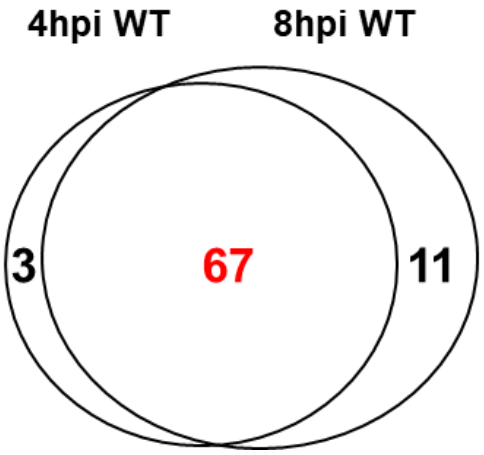

(4hpi mutant) vs (4hpi control)	Difference (WT-control) ΔΔCt	P-Value	(8hpi mutant) vs (8hpi control)	Difference (WT-control) ΔΔCt	P-Value
CCL5	0.66459	0.008892	**TIRAP**	1.79326	4.58E-07
NDNF	0.9866	0.01232	**IL13RA2**	1.08624	0.000101
ACOD1	1.00163	0.015709	**LYZ**	1.36	0.000162
TNIP2	0.36603	0.023136	**SDC4**	1.50438	0.000244
R28S	0.24849	0.025724	MADPRT1	0.90928	0.000282
			ENSGAL53860	1.04244	0.000519
			SELE	-1.24119	0.001071
			ABCG2	-0.65144	0.001157
			CCL19	0.78641	0.001309
			SOCS1	0.40436	0.003702
			SLCO4C1	1.00992	0.004405
			IL4I1	0.76656	0.007235
			NR4A3	2.10303	0.011218
			GUSB	-0.3078	0.029269

c

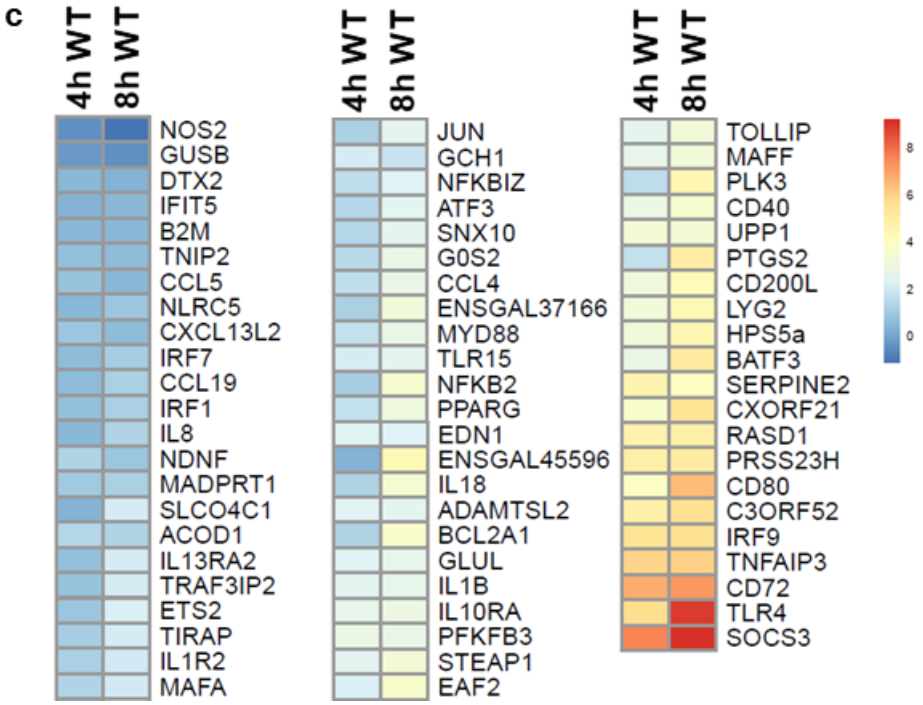

b

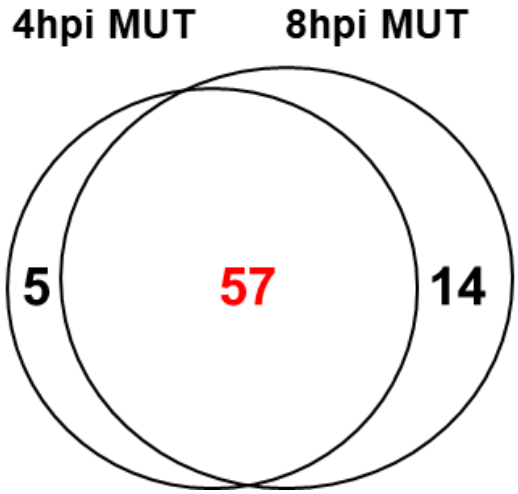

(4hpi mutant) vs (4hpi control)	Difference (WT-control) ΔΔCt	P-Value	(8hpi mutant) vs (8hpi control)	Difference (WT-control) ΔΔCt	P-Value
CCL5	0.66459	0.008892	**TIRAP**	1.79326	4.58E-07
NDNF	0.9866	0.01232	**IL13RA2**	1.08624	0.000101
ACOD1	1.00163	0.015709	**LYZ**	1.36	0.000162
TNIP2	0.36603	0.023136	**SDC4**	1.50438	0.000244
R28S	0.24849	0.025724	MADPRT1	0.90928	0.000282
			ENSGAL53860	1.04244	0.000519
			SELE	-1.24119	0.001071
			ABCG2	-0.65144	0.001157
			CCL19	0.78641	0.001309
			SOCS1	0.40436	0.003702
			SLCO4C1	1.00992	0.004405
			IL4I1	0.76656	0.007235
			NR4A3	2.10303	0.011218
			GUSB	-0.3078	0.029269

d

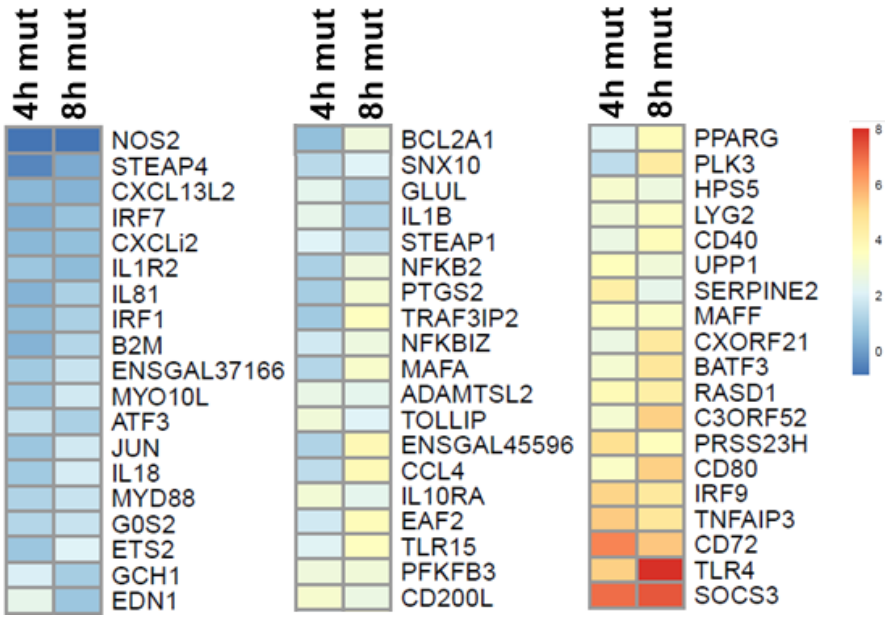

Figure 6.6: Comparison of genes significantly differentially regulated in *S. Typhimurium* infected enteroids over time. Venn diagrams comparing DEG lists (infected vs control, P ≤ 0.05) between (**a**) 4 and 8 hpi WT, and (**b**) 4 and 8 hpi T3SS1 mutant 2 day infected enteroids. Tables describe genes not found in common with positive ΔΔCt values representing upregulated genes and negative values downregulated genes. Genes highlighted in green are most significant DEGs with ΔΔCt values of >1. Heatmaps show the ΔΔCt values of DEGs in common at both 4 and 8 hpi in (**c**) WT and (**d**) T3SS1 mutant (mut) *S.* Typhimurium infected enteroids. Results are from infected and control samples run in the qPCR array, representing average of 5 biological replicates.

For WT infected enteroids most DEGs were found in common between the time points with many of these showing an increase in expression over time. These upregulated genes included pattern recognition receptors (*TLR4, TLR15*), interleukins and interleukin receptors (*IL18, IL8, IL13RA2, IL1R2*), antibacterial enzyme *LYG2*, and *SOCS3* (Fig. 6.6c). In T3SS mutant infected enteroids, most DEGs were also found in common at 4 and 8 hpi, and the trend of increasing expression of the gene set over time was also evident (Fig. 6.6d).

This analysis shows there are more DEGs induced in WT or T3SS1 mutant infected enteroids at 8 hpi compared to 4 hpi, and although most DEGs are shared between the time points, the expression of many of these shared genes increases with time post infection.

6.2.6 WT and T3SS1 mutant strains induce similar DEGs with highest expression in WT infections at 8 hpi

To explore differences in the enteroid immune response between WT or T3SS1 mutant infections, the Student's t-test gene expression data from 6.2.5 was compared between the bacterial strains at each time point. Slightly more DEGs were identified in WT infected enteroids compared to T3SS1 mutant infected enteroids at each time point, with the majority of genes in both strains found to be upregulated (Fig. 6.4). Although most DEGs were found in common between strains, more genes were found exclusively in WT

infected enteroids at both time points. These included *MADPRT1, TIRAP* and *NR4A3* at 4 hpi (Fig. 6.7a), and *IL6, PKD2LI, CD83* and *ACOD1* (a regulator of immunometabolism which is upregulated by activated immune cells in response to pathogen infection[347]) at 8 hpi (Fig. 6.7b). Of the most significant DEGs in the T3SS1 mutant infected enteroids, only *IL18* and *NR4A3* were exclusive, both at 8 hpi.

Of the significant DEGs found in common between bacterial strains at 4 hpi, a small number had markedly higher expression in the WT infected enteroids (Fig. 6.7c). These included *TLR4,* the critical innate immunity signal transduction adaptor *MYD88,* interferon regulator *IRF9,* anti-inflammatory signalling molecules *TNFAIP3* and *SOCS3,* and *PTGS2* which plays a protective role in the intestine through the production of PGE_2[348]. By 8 hpi most DEGs had higher expression in the WT compared to T3SS1 mutant infected enteroids (Fig. 6.7d).

a

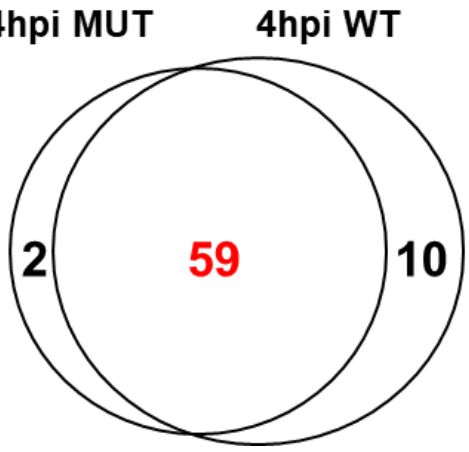

(4hpi mutant) vs (4hpi control)	Difference (WT-control) ΔΔCt	P-Value	(8hpi mutant) vs (8hpi control)	Difference (WT-control) ΔΔCt	P-Value
CCL5	0.66459	0.008892	**TIRAP**	1.79326	4.58E-07
NDNF	0.9866	0.01232	**IL13RA2**	1.08624	0.000101
ACOD1	1.00163	0.015709	**LYZ**	1.36	0.000162
TNIP2	0.36603	0.023136	**SDC4**	1.50438	0.000244
R28S	0.24849	0.025724	MADPRT1	0.90928	0.000282
			ENSGAL53860	1.04244	0.000519
			SELE	-1.24119	0.001071
			ABCG2	-0.65144	0.001157
			CCL19	0.78641	0.001309
			SOCS1	0.40436	0.003702
			SLCO4C1	1.00992	0.004405
			IL4I1	0.76656	0.007235
			NR4A3	2.10303	0.011218
			GUSB	-0.3078	0.029269

c

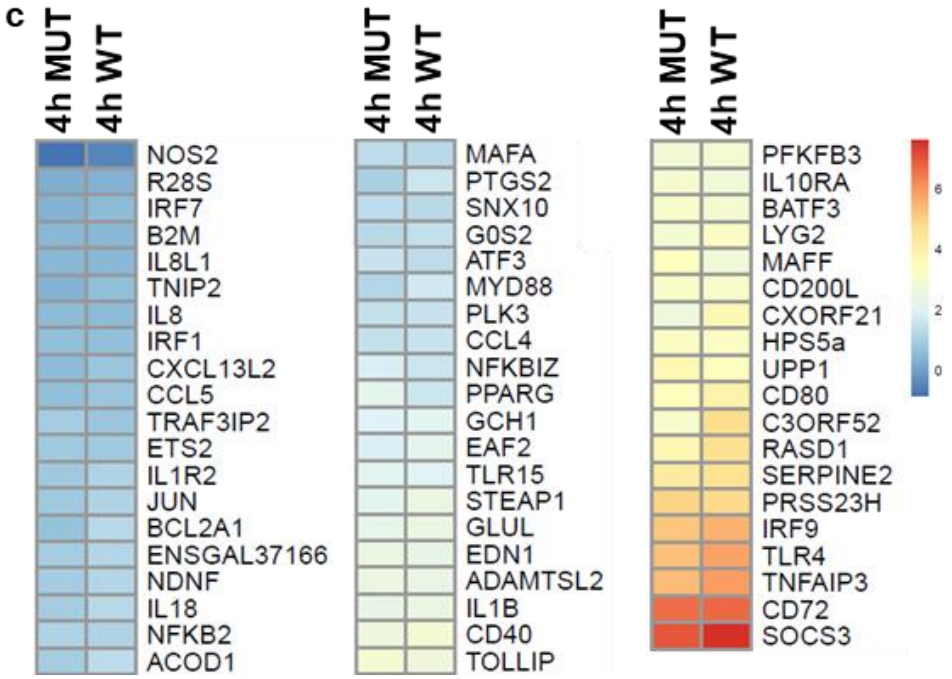

b

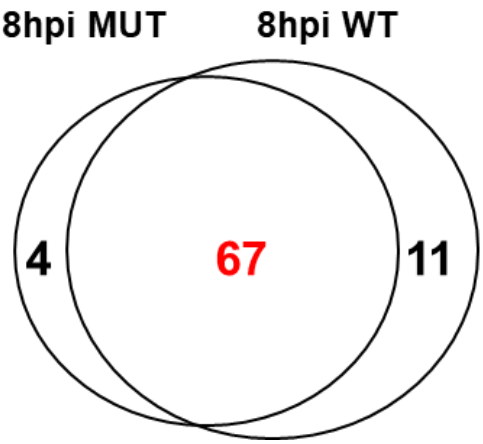

(8hpi mutant) vs (8hpi control)	Difference (mutant-control) ΔΔCt	P-Value	(8hpi wildtype) vs (8hpi control)	Difference (mutant-control) ΔΔCt	P-Value
IL18	1.10748	3.69E-06	**ACOD1**	1.28519	4.67E-05
ABCG2	-0.65144	0.001157	**IL6**	1.31301	0.000255
NR4A3	2.10303	0.011218	NDNF	0.89733	0.001474
STEAP4	0.26079	0.038735	NLRC5	0.87422	0.002462
			DTX2	0.31146	0.004474
			TNIP2	0.57474	0.005121
			PKD2L1	1.35546	0.006846
			IFIT5	0.49069	0.019268
			CD83	1.11035	0.019841
			WDR24	-0.28865	0.02891
			CCL5	0.51264	0.03103

d

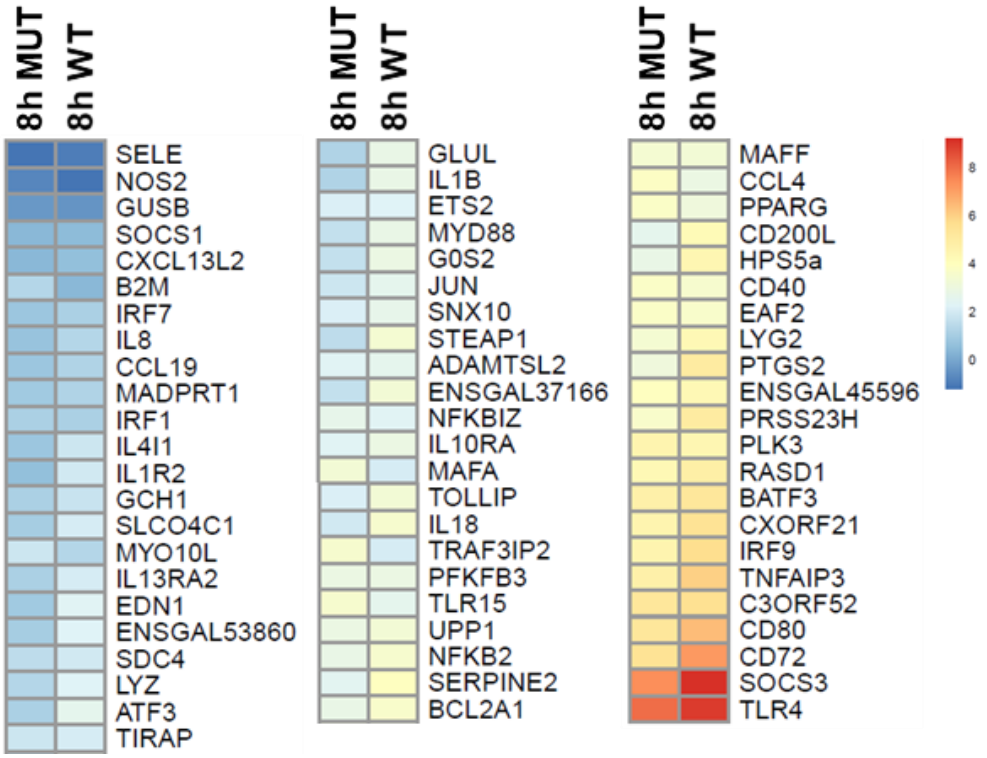

Figure 6.7: Comparison of genes significantly differentially regulated in *S. Typhimurium* infected enteroids between bacterial strains. Venn diagrams comparing DEG lists (infected vs control, P ≤ 0.05) between (**a**) WT and T3SS1 mutant DEGs at 4 hpi, and (**b**) WT and T3SS1 mutant DEGs at 8 hpi in infected 2 day old enteroids. Tables describe genes not found in common with positive ΔΔCt values representing upregulated genes and negative values representing downregulated genes. Genes highlighted in green are the most significant DEGs with ΔΔCt values of >1. Heatmaps show the ΔΔCt values of DEGs in common for both WT and T3SS1 mutant infections at (**c**) 4 hpi and (**d**) 8 hpi. Results are from infected and control samples run in the qPCR array, representing average of 5 biological replicates.

To gain further insight into the immune biology behind the WT and T3SS1 mutant infected enteroids, gene set enrichment analysis was performed on the upregulated genes from the DEG analysis. Since most genes in the 4 hpi DEG analysis were also present at 8 hpi, only the 8 hpi DEGs were analysed. The top 10 significant gene sets in the GO term analysis were very similar for both WT and T3SS1 mutant infections and included cytokine mediated signalling pathways, response to molecules of bacterial origin and defence response gene sets (Table 6.2). KEGG pathway analysis was also similar between strains and showed annotation of cytokine, TLR, NLR and Janus kinase/signal transducers and activators of transcription (JAK-STAT) signalling pathways (Table 6.3).

These comparisons demonstrate there were more genes identified exclusive to WT infections compared to T3SS1 mutant infections, at both time points. However most DEGs in WT and T3SS1 mutant infected enteroids are found in common. In addition, DEG levels are similar at 4 hpi between strains but by 8 hpi most DEGS are more highly expressed in WT infected enteroids.

Table 6.2: Significantly enriched GO terms from DEGs upregulated in *S. Typhimurium* infected enteroids. Top 10 enriched GO term gene sets (biological process) obtained from mapping the significantly upregulated DEGs ($P \leq 0.05$) in WT and T3SS1 mutant infected 2 day old enteroids, as compared to controls, at 8 hpi. GO term numbers are in brackets after name.

8 h mutant				8 h wildtype			
Gene Set Name	**Genes in Gene Set**	**Genes in Overlap**	**P-value**	**Gene Set Name**	**Genes in Gene Set**	**Genes in Overlap**	**P-value**
GOBP RESPONSE TO CYTOKINE **(34097)**	1188	27	3.21E-27	GOBP RESPONSE TO CYTOKINE **(34097)**	1188	32	1.35E-32
GOBP RESPONSE TO BIOTIC STIMULUS **(9607)**	1606	27	9.00E-24	GOBP RESPONSE TO BIOTIC STIMULUS **(9607)**	1606	33	6.28E-30
GOBP CYTOKINE MEDIATED SIGNALING PATHWAY **(19221)**	803	22	1.24E-23	GOBP DEFENSE RESPONSE **(6952)**	1790	33	2.04E-28
GOBP DEFENSE RESPONSE **(6952)**	1790	26	3.21E-21	GOBP CYTOKINE MEDIATED SIGNALING PATHWAY **(19221)**	803	26	4.32E-28
GOBP CELL ACTIVATION **(1775)**	1461	24	1.08E-20	GOBP REGULATION OF IMMUNE SYSTEM PROCESS **(2682)**	1593	29	1.84E-24
GOBP REGULATION OF IMMUNE SYSTEM PROCESS **(2682)**	1593	24	7.96E-20	GOBP RESPONSE TO INTERFERON GAMMA **(34341)**	196	16	1.17E-23
GOBP POSITIVE REGULATION OF MULTICELLULAR ORGANISMAL PROCESS **(51240)**	1397	23	8.45E-20	GOBP DEFENSE RESPONSE TO OTHER ORGANISM **(98542)**	1208	26	1.42E-23
GOBP RESPONSE TO INTERFERON GAMMA **(34341)**	196	13	5.28E-19	GOBP RESPONSE TO MOLECULE OF BACTERIAL ORIGIN **(2237)**	346	18	5.38E-23
GOBP DEFENSE RESPONSE TO OTHER ORGANISM **(98542)**	1208	21	1.75E-18	GOBP CELL ACTIVATION **(1775)**	1461	27	8.20E-23
GOBP REGULATION OF CELL ACTIVATION **(50865)**	626	17	3.96E-18	GOBP INFLAMMATORY RESPONSE **(6954)**	773	22	2.06E-22

Table 6.3: Significantly enriched KEGG pathway terms from DEGs upregulated in *S.* Typhimurium infected enteroids. Top 10 enriched KEGG pathway gene sets obtained from mapping the significantly upregulated DEGs (P ≤0.05) in WT and T3SS1 mutant infected 2 day old enteroids, as compared to controls, at 8 hpi.

8h mutant				8h wildtype			
Gene Set Name	**Genes in Gene Set**	**Genes in Overlap**	**P-value**	**Gene Set Name**	**Genes in Gene Set**	**Genes in Overlap**	**P-value**
KEGG TOLL LIKE RECEPTOR SIGNALING PATHWAY	102	10	1.49E-16	KEGG TOLL LIKE RECEPTOR SIGNALING PATHWAY	102	12	6.86E-20
KEGG LEISHMANIA INFECTION	72	5	4.66E-08	KEGG CYTOSOLIC DNA SENSING PATHWAY	55	6	2.82E-10
KEGG CYTOKINE CYTOKINE RECEPTOR INTERACTION	265	7	6.67E-08	KEGG CYTOKINE CYTOKINE RECEPTOR INTERACTION	265	9	3.00E-10
KEGG CYTOSOLIC DNA SENSING PATHWAY	55	4	9.32E-07	KEGG NOD LIKE RECEPTOR SIGNALING PATHWAY	62	5	4.41E-08
KEGG JAK STAT SIGNALING PATHWAY	155	5	2.14E-06	KEGG LEISHMANIA INFECTION	72	5	9.43E-08
KEGG TYPE II DIABETES MELLITUS	47	3	3.53E-05	KEGG JAK STAT SIGNALING PATHWAY	155	6	1.51E-07
KEGG NOD LIKE RECEPTOR SIGNALING PATHWAY	62	3	8.13E-05	KEGG PRION DISEASES	35	3	2.19E-05
KEGG MAPK SIGNALING PATHWAY	267	4	4.59E-04	KEGG GRAFT VERSUS HOST DISEASE	41	3	3.54E-05
KEGG CELL ADHESION MOLECULES CAMS	133	3	7.70E-04	KEGG TYPE II DIABETES MELLITUS	47	3	5.35E-05
KEGG ALANINE ASPARTATE AND GLUTAMATE METABOLISM	32	2	8.51E-04	KEGG INTESTINAL IMMUNE NETWORK FOR IGA PRODUCTION	48	3	5.70E-05

6.3 Discussion

The overall aim of this chapter was to investigate whether the apical-out chicken enteroids could be infected with a bacterial pathogen and demonstrate host morphological and innate immunological responses comparable to *in vivo* infections. The enteric *S.* Typhimurium 474 bacterium was selected for its economic importance, causing highly mortality in young chicks and globally relevant zoonotic disease. Adherence of bacteria to the cells and actin remodelling was evident on the enteroid epithelial surface after adding WT *S*. Typhimurium to the floating media. This demonstrates active invasion of Salmonella is occurring via membrane ruffles directly

induced by the T3SS1. Mutations in *prgH*, a protein coding gene required for the SPI1 T3SS1 apparatus, have been shown to abolish the secretion of a panel of *S*. Typhimurium proteins used for *Salmonella* invasion into normally non-phagocytic epithelial cells[349]. Accordingly, infection of the enteroids with a T3SS1 *prgH* mutant *S.* Typhimurium showed no actin remodelling on the epithelial surface. The difference in brush border interactions, as well as stark differences in microbial invasion and replication rates demonstrated between the *Salmonella* strains, show the enteroids mimic *in vivo* intestinal cellular machinery making them promising experimental platforms to investigate *Salmonella* infections.

LPS is a phosphoglycolipid which makes up a large component of the outer membrane of gram-negative bacteria. Chickens have a natural resilience to LPS-induced septic shock[350,351], as opposed to pigs and humans[352,353]. This may explain why isolated *S.* Typhimurium LPS did not disrupt enteroid epithelial barrier integrity, and the enteroid immune response was brief and subdued when compared to bacterial infected enteroids. This acute response at 4 h post challenge did include upregulation of chicken specific *TLR15* which has previously been shown to be upregulated in *S*. Typhimurium infected chicken caeca, and in chicken embryonic fibroblasts *in vitro*[354]. TLRs are expressed on both epithelial and immune cells and are key in the host defence to bacterial infection. They activate the MYD88-dependent signalling route involving adaptor protein toll/IL-1R domain-containing adaptor protein *(TIRAP),* which in turn activates cytokines and chemokines including chemokine (C-C motif) ligand 4 (*CCL4)*, interleukin 1 receptor type 2 *(IL1R2)* and chromosome X open reading frame (*CXORF)21,* all of which were upregulated in the enteroids at 4 and 8 h post LPS challenge. The LPS-induced signalling cascade also triggered a large number of anti-inflammatory genes in the enteroids at 4 h post challenge including toll interaction protein *(TOLLIP),* a negative regulator of TLR4 signalling[355], and negative regulators of cytokine signalling interleukin 13 receptor subunit alpha *(IL13RA)2,* suppressor of cytokine signalling (*SOCS)1* and *SOCS3,* which may explain the reduced immune response by 8 h post challenge.

In the absence of acquired immune functions, which don't start to develop in chickens until the first week post-hatch, the innate immune responses of young chicks are critical for adaptation to the microbiome and pathogen challenge[320,356]. Based on the composition of genes upregulated after infection of the enteroids with WT *S.* Typhimurium infection, it is clear that the enteroid response is a coordinated innate reaction of epithelial cells and innate immune cells including macrophages and DCs which increases with time post infection. For example, two of the most significantly upregulated genes in WT infected enteroids included *LYG2* and *CD72,* both of which have been previously identified as upregulated in *S.* Typhimurium and *S.* Enteritidis infected chickens[339,357,358]. *LYG2* is a lysozyme secreted by Paneth-like epithelial cells in the intestine, where this family of antibacterial proteins play an important role in the innate defence against microbial attack[17]. Whereas *CD72* is a transmembrane co-receptor expressed on B cells and NK cells and mice lacking *CD72* have shown an impaired ability to control Salmonella infection[359].

The TLR signalling pathway was the most significant KEGG pathway associated with the WT infected chicken enteroids. The myeloid pattern recognition receptor *TLR4* was one of the most significantly upregulated DEGs at both time points with expression markedly increasing over time. *TLR4* is well known for recognizing LPS and is the main TLR involved in the control of *S.* Typhimurium infection in mice[360]. Other DEGs involved in the TLR-induced MYD88 dependent pathway were also upregulated in WT infected enteroids including *TLR15,* adaptor molecules *MYD88,* TRAF3 interacting protein 2 *(TRAF3IP2)* and *TIRAP,* and transcription factor *NFKB2*. Activation of *NFKB2* induces transcription and induction of pro-inflammatory cytokines, and the annotation of 32 upregulated DEGs in WT infected enteroids to the most significant GO term 'response to cytokine' shows the important role of cytokine and interleukin genes in the enteroid immune response to *S.* Typhimurium. These genes included pro-inflammatory chemokines and cytokines and their receptors e.g. *CCL19, CCL4, IL18, IL1b, IL13RA2* and *IL10RA,* which have all been shown to be upregulated in the

caecum of 1 week old chicks infected with *S.* Typhimurium[339]. STAT3, activated through various cytokines, induces expression of macrophage gene *SOCS3*. This, and other members of the SOCS family, form part of a negative feed-back loop in JAK-STAT signalling, acting to preserve homeostasis and limit damage as a consequence of the inflammatory response (reviewed in[361]). *SOCS3* was one of the most significantly upregulated genes in WT infected enteroids, with expression markedly higher at 8 versus 4 hpi, and has previously been identified as upregulated in non-typhoid *Salmonella* infections[339,362].

The SPI1 T3SS1 is well characterised for its role enabling the invasion of *S.* Typhimurium into non-phagocytic cells. However SPI1 T3SS1 mutants have been shown to invade 3D human models of the intestine, albeit with very limited intracellular growth compared to WT bacteria[363]. This indicates the T3SS1 is dispensable for *Salmonella* invasion but is required for intracellular bacterial growth. This may explain why the SPI1 T3SS1 *S.* Typhimurium mutant used in this study was occasionally identified within the chicken enteroids but without any evidence of actin remodelling, and with extremely low replication levels. The ability of *S.* Typhimurium to invade cells without a functional T3SS1 may also explain why the mutants were able to disrupt the enteroid epithelial barrier at higher CFU and stimulate a comprehensive enteroid immune response which was similar but delayed in comparison to the WT infections. There are disparate findings when looking at the role of *S.* Typhimurium SPI1 in the intestinal colonization of different chicken breeds. A study in 1 day old Light Sussex chicks challenged with SPI1 mutants indicated it is not required for infection[364] whereas a study in 1 day old White Leghorn chicks showed attenuation of mutant strains[365]. It would therefore be interesting the test the T3SS1 mutants in enteroids developed from different chicken breeds to evaluate breeding for resistance.

Although there was a large overlap in the DEGs, GO terms and KEGG pathways in WT and T3SS1 mutant infected enteroids, there were more genes found to be exclusively upregulated in WT infections. These included interferon induced protein with tetratricopepide repeats 5 (*IFIT5),* deltx E3

ubiquitin ligase 2 (*DTX2)* and NLR class 5 (*NLRC5)*. The intracellular NLRs, with the largest in the family being *NLRC5,* are pattern recognition receptors involved in promoting the expression of pro-inflammatory cytokines and the rapid clearance of invasive intracellular pathogens (reviewed in[366]). *DTX2* is a regulator of the Notch signalling pathway which supports IEC homeostasis through stem cell maintenance and secretory and absorptive cell lineage specification roles. Activation of Notch signalling has been demonstrated in IECs in the inflamed mucosa in mice where it appears to play roles in epithelial regeneration as well as limiting bacterial invasion through modulation of antimicrobial proteins[367]. IFITs can bind to the host's own tRNA and in this way interfere with the efficiency of translation, eventually leading to the induction of apoptosis[368]. *IFIT5* been shown to be highly inducible in the caecum of newly hatched chicks and mature chickens infected with *S.* Enteritidis[341,369], where the induction of apoptosis in infected cells may release the intracellular *Salmonella* for phagocytosis by local immune cells. Therefore the genes upregulated in WT but not T3SS1 mutant infected enteroids are often related to intracellular anti-bacterial activity, indicating they may only be triggered by higher levels of bacterial infection and/or are induced by the T3SS1. The qPCR array analysis shows that this T3SS1 mutant *S.* Typhimurium stimulates a rapid and strong innate immune response in the immunologically immature enteroids, similar to that of the WT bacteria but without high levels of bacterial replication or as much disruption of the epithelial barrier. Vaccination of pigs with *S*. Typhimurium *prgH* mutant secreted proteins, produced comparable levels of protection to vaccination with preparations from the parent strain[370]. Therefore although an adaptive response and immune memory formation to infection cannot be demonstrated in this model, this T3SS1 *prgH* mutant could show potential as a vaccine candidate in poultry.

Through a combination of image analysis, replication assays and employing a qPCR array, the chicken enteroid response to LPS challenge, and WT or T3SS1 mutant *S*. Typhimurium infection has been analysed. In line with the chickens known resilience to septic shock, the enteroids demonstrated a

limited acute response to isolated LPS but mimicked many of the morphological and innate immunological infection characteristics of WT *S.* Typhimurium infection seen *in vivo*. The *S.* Typhimurium T3SS1 mutant failed to efficiently replicate in the enteroids however they did induce a comprehensive transcriptional immune response revealing a potential future use of this model in screening the level of attenuation of vaccine candidates. This would contribute to the 3Rs by reduced use of birds for both *Salmonella* vaccine research and batch testing. We conclude that floating chicken enteroids provide a useful platform for interrogating the invasion and replication efficiency, and innate immune interactions of different species and strains of enteric bacteria in the post-hatch chick intestine.

Chapter 7 The mucosal response to *Eimeria tenella* in the chicken enteroid model

Chapter 7 The mucosal response to *Eimeria tenella* in the chicken enteroid model

Eimeria spp. belong to the phylum Apicomplexa, a large group of intracellular parasites containing some of the most widespread zoonotic protozoa including *Toxoplasma gondii* and *Cryptosporidium parvum*. Coccidiosis, a serious intestinal infection caused by *Eimeria* species, is the most frequently reported disease of chickens worldwide and generates a global annual burden of approximately £10 billion on the poultry industry[371]. With legislative pressure to reduce drug use in animal production and ongoing issues with drug-resistant parasite strains, vaccination offers the main long-term solution to the coccidiosis problem. However, with few appropriate *in vitro* models available, most *Eimeria* vaccine research and production is conducted *in vivo*. In this chapter, floating inside-out chicken caecal enteroids demonstrate they can be infected with *Eimeria tenella*, enable the parasite to complete multiple stages of its life cycle, and mount an immune response to infection. This physiologically relevant *in vitro* host-protozoal model could potentially be used for studies into site-specific binding and identifying innate immune molecular markers and lifecycle stage antigens of *Eimeria* spp. infection in chickens.

7.1 Introduction

Chickens in the field are exposed to seven species of WT *Eimeria* parasites, all with individual site specificities for particular segments of the intestine, and to find a commercial poultry flock not infected with *Eimeria* spp. is atypical[372]. These obligate parasites have a complex lifecycle where typical asexual multiplication consists of 3 rounds of merogony, resulting in successive generations of schizonts containing merozoites. During the sexual development phase, microgametocytes produce 100 motile microgametes (male gametocyte) that fertilise a macrogamete (female gametocyte) resulting in formation of a zygote. This becomes encapsulated in a protective wall forming an unsporulated oocyst which is shed into the faeces where it

sporulates in preparation to orally infect other birds (Fig. 7.1a). The asexual stages of the life cycle, where *Eimeria* sporozoites may invade a number of different host cell types, induce the most potent protective immune responses however the sexual stages have also been shown to be the target of immune inhibition (reviewed in[373]).

Currently, assessment of *Eimeria* disease manifestations and vaccine efficacy is predominantly achieved using live chicken challenge experiments with highly variable study designs[374]. Studying host-protozoal interactions *in vitro* is challenging due to the universal difficulties culturing parasites. *E. tenella* is one of the most globally prevalent *Eimeria* species and its sporozoites enter exclusively the chicken caecal epithelial cells causing poor weight gain and occasionally death[375]. Immortalized mammalian cell lines can only support the early part of the *E. tenella* lifecycle, up to the release of first-generation merozoites[376]. So far the full life-cycle of *E. tenella* has only been replicated *in vitro* in primary embryonic chick kidney cells, with very small numbers of unsporulated oocysts produced which sporulated very poorly[377]. Other avian models trialled include the chicken lung cell line (CLEC-213) where the gamete stage was reached after sporozoite infection[378]. Since these chicken models are not intestinal in origin, they cannot fully recapitulate *in vivo* interactions of *E. tenella* with its host. Enteroid cultures have recently been exploited to model *Cryptosporidium* and *Toxoplasma* infections, showing these parasites are able to replicate *in vitro* and induce enteroid innate immune responses[198,210,379,380,381]. However, to replicate the physiological route of entry of these enteric parasites, microinjection[210], transition to 2D enteroid cultures[379] or enteroid fragmentation[198] are required to gain access to the apical epithelial surface. These techniques are costly and time consuming and, for mechanical disruption, both apical and basolateral sides of the enteroid cells are exposed. Protozoal infections have not previously been attempted on apical-out enteroid models or in chicken 3D enteroids.

In this chapter the initial aims were to identify whether chicken caecal enteroids (Chapter 4, 4.2.3) could support infection with *E. tenella,* and to establish how much of the parasites lifecycle could be completed in this model. The next aim was to ascertain whether the enteroids can mount an appropriate immune response to *E. tenella* infection. Development of a chicken-protozoal model could contribute to our understanding of the mechanisms these important parasites use to recognise infection sites and the subsequent species-specific innate host responses, potentially leading to improved targeting and efficacy of pharmaceuticals. In addition, development of an *in vitro* vaccine production and/or batch testing system that does not require the use of live birds would be of tremendous interest to the poultry industry from both an economic and 3Rs perspective.

7.2 Results

7.2.1 Chicken caecal enteroids are susceptible to infection by *Eimeria tenella*

Since each developmental stage of *Eimeria* harbours a distinct number of parasitic divisions, a combination of brightfield and fluorescence microscopy was used to determine whether the enteroid cultures could support parasitic replication. In order to visualise the parasites, *E. tenella* sporozoites were stained with a fluorescent cell-membrane tracking dye, PKH67. At 1 dpi sporozoites were identified in contact with the enteroid apical epithelial surface (Fig. 7.1b) and by 2 dpi they were observed inside epithelial and lamina propria cells (Fig. 7.1c, d). *E. tenella* subsequently divided (Fig. 7.1e - g), as determined by the size and increased number of PKH67+ parasites within a singular cell. The fluorescent membrane shapes and/or divisions in the enteroid cells correlated with what would be expected for distinct parasite life-cycle stages including trophozoites and schizonts (Fig. 7.1a).

To confirm the sexual gametocyte stage was reached, expression of *EtGAM56*, which encodes a macrogamete specific protein incorporated into the oocyst wall, was demonstrated in *E. tenella* infected enteroids at 5, 7, and

9 dpi, but not at 2 dpi (Fig. 7.1h). The PCR bands at 7 and 9 dpi were sequenced to confirm the primers had identified the correct gene (Fig. 7.1i). Combined, this data demonstrates that *E. tenella* can cycle through the sporozoite to gamete stages of its lifecycle in the chicken caecal enteroid model.

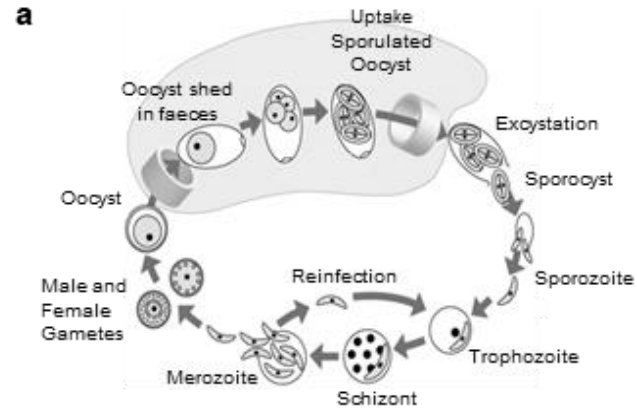

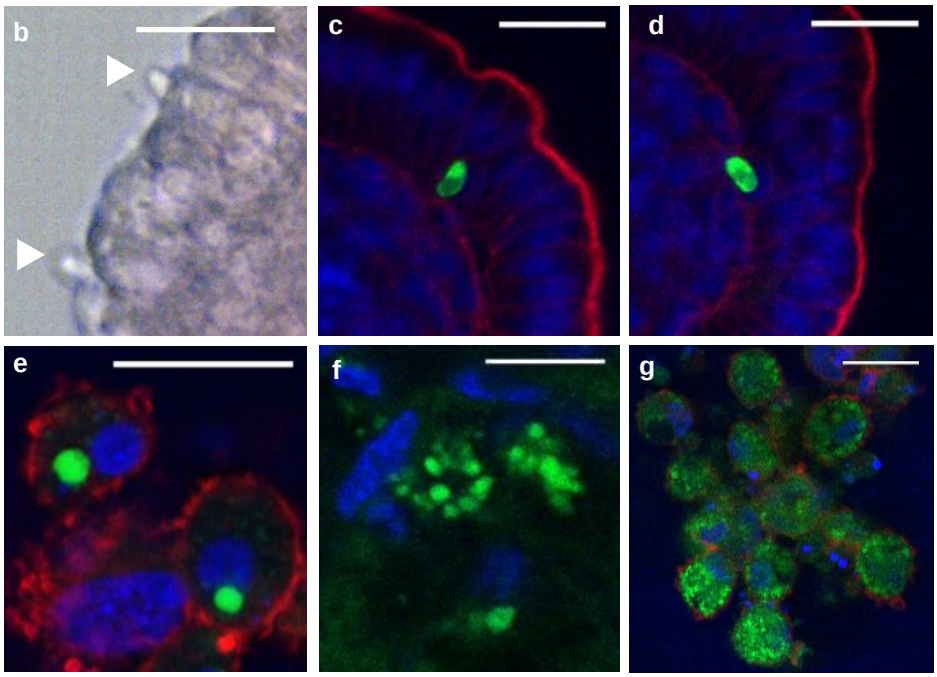

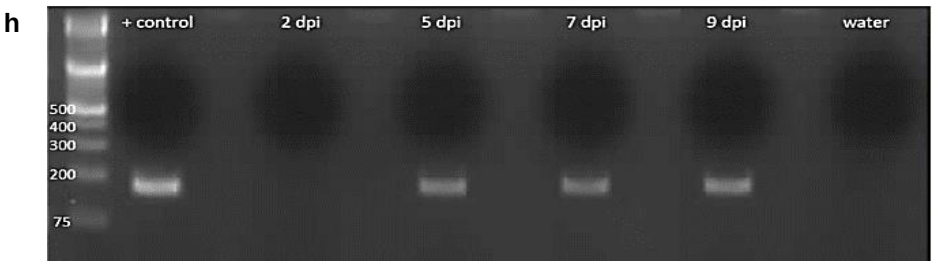

i

```
                131       140       150       160       170       180       190       200       210       220       230       240       250       260
                |---------+---------+---------+---------+---------+---------+---------+---------+---------+---------+---------+---------+---------|
seq1                                                                                                                                  AGTCGATGATGAG
seq2                                                                                                                                  GTCGATGATGAG
seq5                                                                                                                                  GTCGATGATGAG
Etgam56 CGGGGGCCCCCGACGAGAGCAGCACGACCACGACGACTCCCTCGCCGAGCCCCGAGGCCCCTGACCAGTGGCTGGAGAACTTCGTGCGCGCGGTGCAGCGCCAGCTGCAGCTGCAGGAGTCGATGATGAG
seq6                                                                                                                                  GTCGATGATGAG
seq3                                                                                  GTGGCTGGAGAACTTCGTGCGCGCGGTGCAGCGCCAGCTGCAGCTGCAGGAGTCGATGATGAG
seq7                                                                                  GTGGCTGGAGAACTTCGTGCGCGCGGTGCAGCGCCAGCTGCAGCTGCAGGAGTCGATGATGAG
seq8                                                                                  GTGGCTGGAGAACTTCGTGCGCGCGGTGCAGCGCCAGCTGCAGCTGCAGGAGTCGATGATGAG
seq4                                                                                  GTGGCTGGAGAACTTCGTGCGCGCGGTGCAGCGCCAGCTGCAGCTGCAGGAGTCGATGATGAG
Consensus ..........................................................................gtggctggagaacttcgtgcgcgcggtgcagcgccagctgcagctgcaggaGTCGATGATGAG

                261       270       280       290       300       310       320       330       340       350       360       370       380       390
                |---------+---------+---------+---------+---------+---------+---------+---------+---------+---------+---------+---------+---------|
seq1 GCAGCTGGTGAAGGAGATCCAGGAGTACCTGACCCCGCGGTCAACTGGGACGAGAACCAGTCGGCGGCGTACAACCGCGTGAACCAAACCGATGGACATGATCACGAACCGCATATA
seq2 GCAGCTGGTGAAGGAGATCCAGGAGTACCTGAGCCGCGTTCAACTGGGACGAGAACCAGTCGGCGGCGTACAACCGCGTGAACGAAAT-GATGGACATGATCACGAACCGCA
seq5 GCAGCTGGTGAAGGAGATCCAGGAGTACCTGAGCCGCGTTCAACTGGGACGAGAACCAGTCGGCGGCGTACAACCGCGTGAACGAAAT-GATGGACATGATCACGAACCGCA
Etgam56 GCAGCTGGTGAAGGAGATCCAGGAGTACCTGAGCCGCGTTCAACTGGGACGAGAACCAGTCGGCGGCGTACAACCGCGTGAACGAAAT-GATGGACATGATCACGAACCGCATGACCACCGCGCTCGA
seq6 GCAGCTGGTGAAGGAGATCCAGGAGTACCTGAGCCGCGTTCAACTGGGACGAGAACCAGTCGGCGGCGTACAACCGCGTGAACGAAAT-GATGGACATGATCACGAACCGCA
seq3 GCAGCTGGTGAAGGAGATCCAGGAGTACCTGAGCCGCGCG
seq7 GCAGCTGGTGAAGGAGATCCAGGAGTACCTGAGCCGCGCG
seq8 GCAGCTGGTGAAGGAGATCCAGGAGTACCTGAGCCGCGCG
seq4 GCAGCTGGTGAAGGAGATCCAGGAGTACCTGAGCCGCGCG
Consensus GCAGCTGGTGAAGGAGATCCAGGAGTACCTGAgCCgCGCG.tcaactgggacgagaaccagtcggcggcgtacaaccgcgtgaac.aaa..gatggacatgatcacgaaccgca..............
```

Figure 7.1: Infection and replication of *E. tenella* in caecal enteroids. a Schematic diagram of *E. tenella* lifecycle, source: impextraco.com. **b** Brightfield image of sporozoites (closed arrow) entering a caecal enteroid at 1 dpi. **c - g** Representative z-axis projections of chicken caecal enteroids whole-mount stained to detect cell nuclei (DAPI, blue), F-actin-expressing brush border (red) after incubation with PKH-67 labelled *Eimeria tenella* (green). **c** Sporozoite at 2 dpi within enteroid epithelial cell and (**d**) migrating through basement membrane into lamina propria. **e** *E. tenella* trophozoite-like structures. **f - g** Schizogeny within enteroid epithelial cell at 9 dpi. Enteroids were 2 days old at 0 dpi. Scale bar: **b – e, g** 20 µm, **f** 10 µm. Images are representative of data from 5 independent experiments each with 2 - 3 technical replicates containing >3 embryos. **h** PCR of *E. tenella* gamete marker *EtGAM56* in caecal enteroids. Positive (+) control is chicken caecal tissue from 6 dpi and 13 dpi after *in vivo* infection with *E. tenella.* Caecal enteroids were infected with *E. tenella* for 2, 5, 7 and 9 days (enteroids were 2 days old at 0 dpi). Bands at 178 bp are where *EtGAM56* is expected. **i** Sequence analysis of the 7 dpi and 9 dpi PCR gel purified product. (seq1+2/seq3+4 = Forward/Reverse primer EtGAM56 7 dpi gel band, seq5+6/seq7+8 = Forward/Reverse primer EtGAM56 9 dpi gel band)

7.2.2 Infection with *Eimeria* induces an immune response in the enteroids

To determine if *E. tenella* infected enteroids could mount an innate immune response, RNA was extracted from infected and control (PBS) enteroids at 2, 4, 6, and 8 dpi. Gene transcripts were quantified on a highly multiplexed RT-qPCR 96.96 Fluidigm Dynamic Array containing a custom list of 89 chicken innate immunity genes (Chapter 6, Table 6.1)[275]. The processing of the qPCR array results was as described in Chapter 6, 6.2.4. The heatmap of Ct values showed '2dpi con c' (PBS challenged enteroids at 2 dpi, biological replicate c) transcript abundance was more similar to 2 dpi infected samples than other controls for many genes (Fig. 7.2a). Replicate '4 dpi e.t.inf b' (infected enteroids at 4 dpi, biological replicate b) was removed from the analysis as it had abnormally low expression across all genes for both technical replicates, indicating poor cDNA preamplification. Differences in transcript expression between control and infected enteroids, especially in

later time points, were evident on the heatmap for *HPS5, IL4I, TGM4, TLR4, LYZ, TIMD4, IL12B* and *CD72.*

The *E. tenella* infected enteroids generally showed a separation by time point on the PCA in a similar pattern to their respective controls (Fig. 7.2b). There was a distinguishable separation of infected and control groups at each time point except for one 2 dpi and one 4 dpi infection replicate which clustered close to their respective controls (Fig. 7.2b). In summary, the PCA showed infected samples have differences in gene expression compared to their respective controls which particularly notable at the later time points.

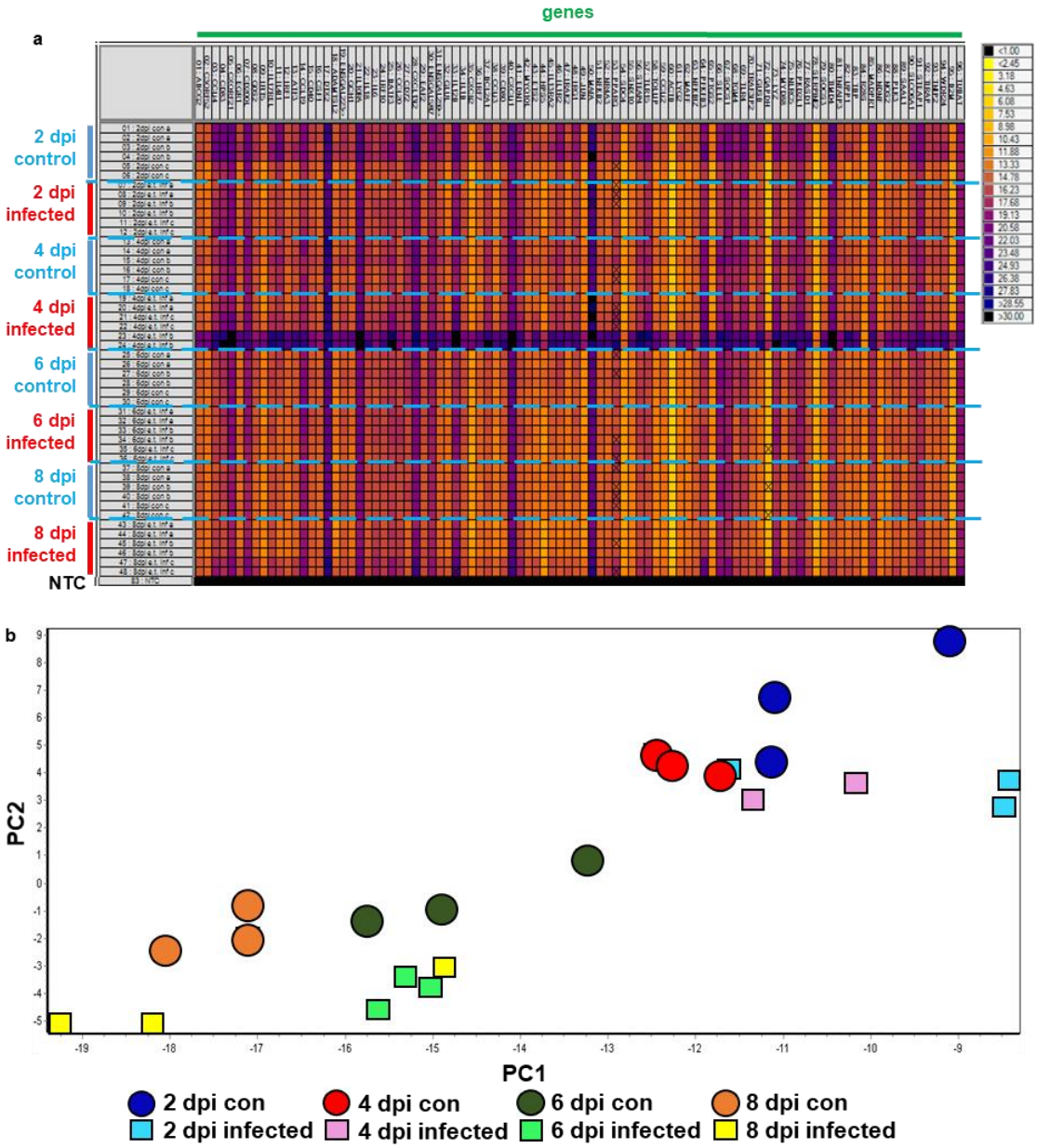

Figure 7.2: Whole dataset immunogenicity patterns in *E. tenella* infected enteroids over time. a Heatmap view of the qPCR array run with individual genes on the x axis and individual samples on y axis. The RNA was extracted from enteroid samples either infected with *E. tenella* or controls at 2, 4, 6 and 8 dpi (enteroids were 2 days old at 0 hpi); 3 biological replicates (a, b, c) were collected per treatment group and were run in duplicate. Black filled squares represent chambers where no gene expression was detected. NTC = non-template control. **b** PCA for qPCR array dataset showing pattern of immune-related gene expression in *E. tenella* infected and control enteroids at 2, 4, 6 and 8 dpi.

7.2.3 Infected enteroid DEGs accumulate with time post infection

In order to explore the differential kinetic immune response elicited by *E tenella* infection in the chicken enteroids, unpaired 2-tail Students t-tests were performed on the gene expression data between infected and control enteroids for each time point. The number of significant DEGs (P ≤0.05) increased as the dpi increased (2 dpi = 10 DEGs, 4 dpi = 15 DEGs, 6 dpi = 21 DEGs and 8 dpi = 24 DEGs; Fig. 7.3). There was no clear direction of gene regulation with slightly more downregulated genes at 2 dpi and 6 dpi and slightly more upregulated genes at 4 dpi and 8 dpi (Fig. 7.3).

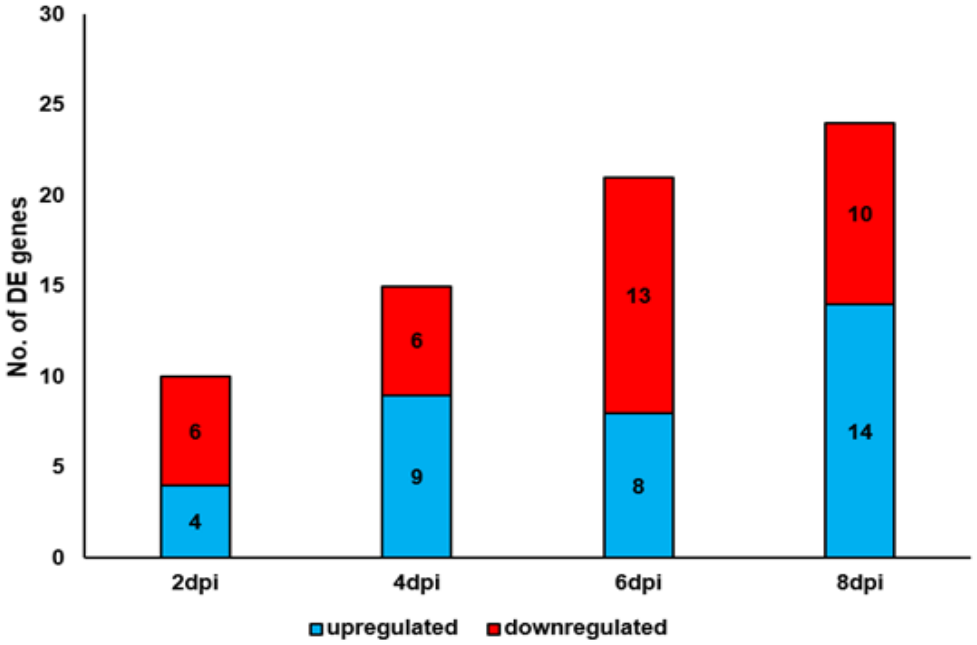

Figure 7.3: Total DEGs in *E. tenella* challenged enteroids. Biological replicates were grouped and number of significant DEGs (P ≤ 0.05) in an unpaired 2-tail Student's t-test (*E. tenella* challenged enteroid sample versus control sample) were compared. Red indicates downregulated and blue indicates upregulated enteroid DEGs in infected samples as compared to controls at 2, 4, 6 and 8 dpi (enteroids were 2 days old at 0 dpi). Results are from RNA samples run in the qPCR array. Each bar represents an average of 3 biological replicates**.**

DEGs significantly upregulated (P ≤0.05) in *E. tenella* infected enteroids as compared to controls included cytokines *IL1Rl2, IL4I1, IL18,* lysosome regulator *HPS5,* C-type lectin *CD72*, transglutaminase*TGM4,* macrophage marker *TIMD4*, cell death regulator *BCL2A1,* immunoadhesion cell surface glycoprotein *SELE* and pattern recognition receptor *TLR4* (Fig. 7.4a - d). Significantly downregulated DEGs in infected enteroids as compared to controls included cytokines *IL6, IL12B,* chemokines *CCL20, CCLi4*, pattern recognition receptor *TLR15*, NFkB inhibitor/anti-inflammatory *TNFAIP3* and host defence peptide *LYZ* (Fig. 7.4a - d). The most significant DEGs were defined as having a cut-off P-value of ≤0.05 and ΔΔCt of >1 (Fig. 7.4a - d). Across the time points there was a cumulative upregulation or downregulation of many of the significant DEGs as the dpi progressed (Fig. 7.5). For example *IL4I1, SLCO6A1, HPS5* and *IL1R2* are upregulated at 2 dpi and remain highly expressed for most of the remaining time points. *TGM4* and *CD72* join the most upregulated DEGs at 6 dpi and remain upregulated at 8 dpi (Fig. 7.5). The downregulated genes are less consistent in their cumulative time points but *IL6* is downregulated in almost all time points and *IL12B, CCL20* and *LYZ* follow suit from 4 dpi (Fig. 7.5).

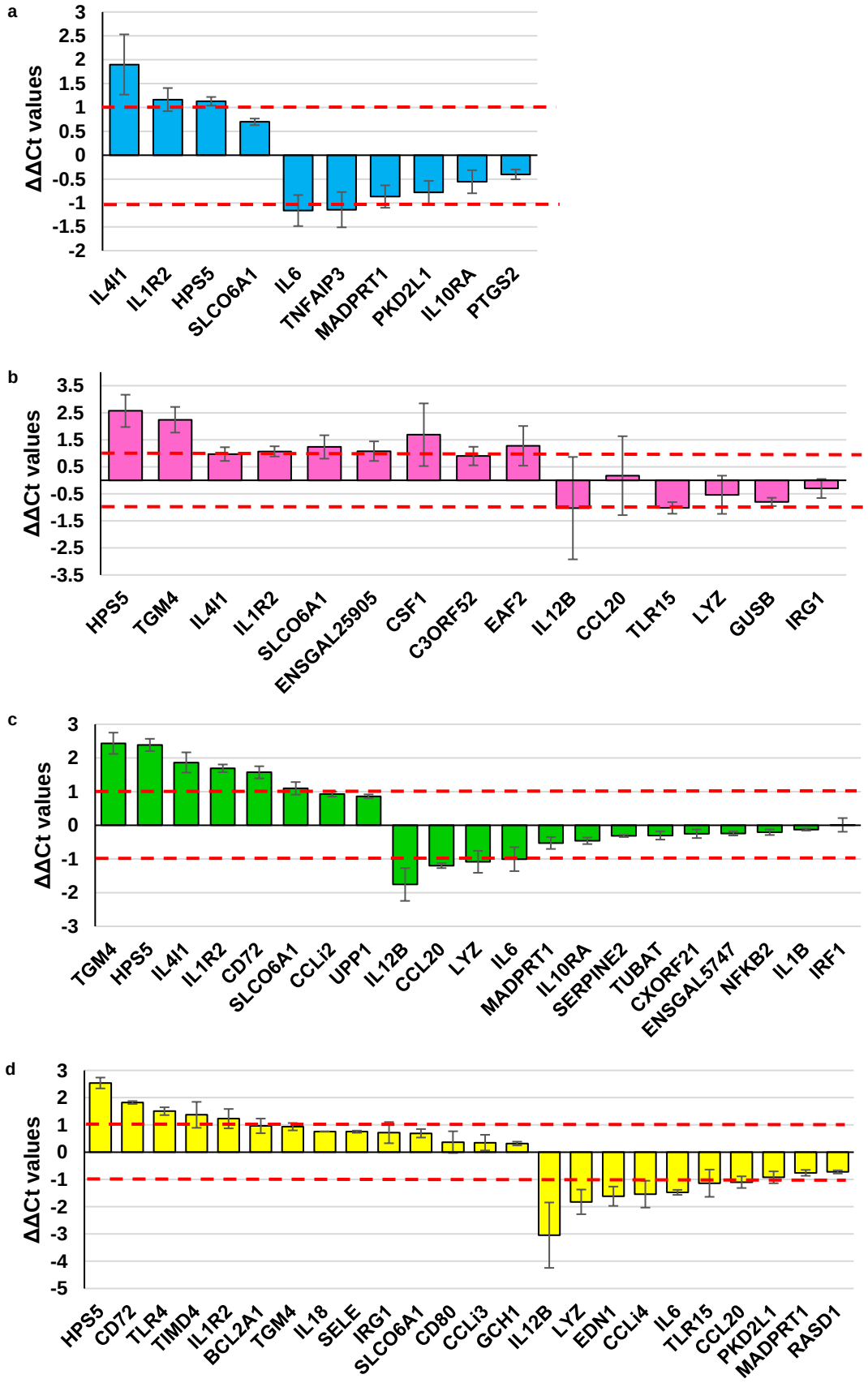
a
ΔΔCt values
3
2.5
2
1.5
1
0.5
0
-0.5
-1
-1.5
-2
IL4I1
IL1R2
HPS5
SLCO6A1
IL6
TNFAIP3
MADPRT1
PKD2L1
IL10RA
PTGS2
b
ΔΔCt values
3.5
2.5
1.5
0.5
-0.5
-1.5
-2.5
-3.5
HPS5
TGM4
IL4I1
IL1R2
SLCO6A1
ENSGAL25905
CSF1
C3ORF52
EAF2
IL12B
CCL20
TLR15
LYZ
GUSB
IRG1
c
ΔΔCt values
3
2
1
0
-1
-2
-3
TGM4
HPS5
IL4I1
IL1R2
CD72
SLCO6A1
CCLi2
UPP1
IL12B
CCL20
LYZ
IL6
MADPRT1
IL10RA
SERPINE2
TUBAT
CXORF21
ENSGAL5747
NFKB2
IL1B
IRF1
d
ΔΔCt values
3
2
1
0
-1
-2
-3
-4
-5
HPS5
CD72
TLR4
TIMD4
IL1R2
BCL2A1
TGM4
IL18
SELE
IRG1
SLCO6A1
CD80
CCLi3
GCH1
IL12B
LYZ
EDN1
CCLi4
IL6
TLR15
CCL20
PKD2L1
MADPRT1
RASD1

Figure 7.4: Individual DEGs in *E. tenella* infected enteroids. a - d The DEG ΔΔCt values (P ≤ 0.05) from t-test comparisons at (**a**) 2 dpi, (**b**) 4 dpi, (**c**) 6 dpi and (**d**) 8 dpi (enteroids were 2 days old at 0 dpi). Dashed red lines denote ΔΔCt values with a >1 cut-off indicating the most significant DEGs. Positive and negative ΔΔCt values represent DEGs upregulated or downregulated respectively. Results are from *E. tenella* infected and control samples run in a qPCR array. Each bar represents average of 3 biological replicates except for 4 dpi E. tenella infected enteroids which only had 2 biological replicates, error bars = SEM.

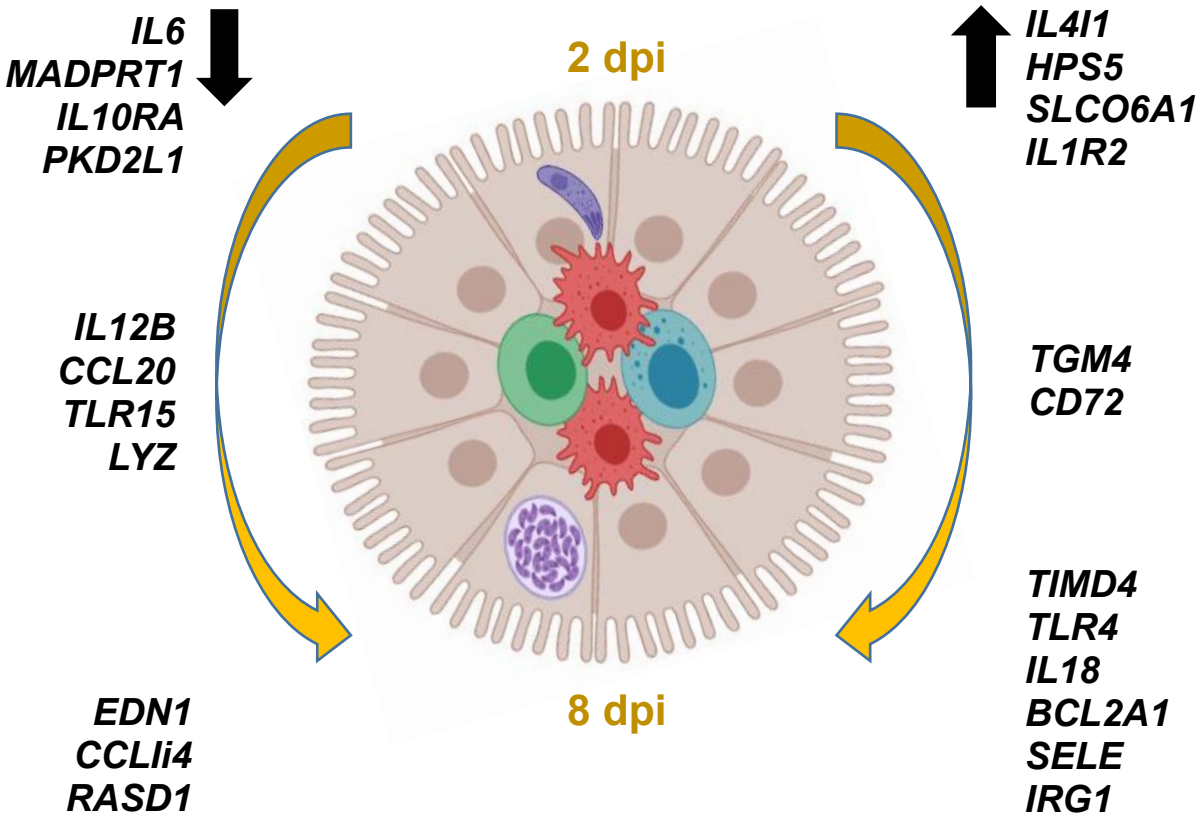

Figure 7.5: Overview of the *E. tenella* infected enteroid cumulative immune response. Global overview of the significant DEGs (P ≤0.05) in *E. tenella* infected chicken caecal enteroids which become cumulatively expressed over dpi (enteroids were 2 days old at 0 dpi). Black upward facing arrow indicates upregulated genes and downward facing arrow indicates downregulated genes. Created in Biorender.com by L Vervelde and E. Nash.

Gene ontology analysis of the enteroid DEGs upregulated in response to *E. tenella* infection confirmed they were involved in cytokine signalling and inflammatory response (Table 7.1). There were also a number of GO terms related to bacterial response demonstrating some overlap in the induction of innate immune response genes to bacterial and protozoal infections e.g. *TLR4, IL18, CD80, ACOD1, SELE* and *GCH1*.

Table 7.1: Significantly enriched GO terms from DEGs upregulated in *E. tenella* infected enteroids. Top 10 enriched GO term gene sets (biological process) obtained from mapping the significantly upregulated DEGs (P ≤0.05) in *E. tenella* infected enteroids, as compared to controls, at 8 dpi (enteroids were 2 days old at 0 dpi).

GO terms	GO term number	Genes in Gene Set	Genes in Overlap	P-value
GOBP RESPONSE TO MOLECULE OF BACTERIAL ORIGIN	2237	1188	6	4.38E-09
GOBP RESPONSE TO CYTOKINE	34097	346	8	1.07E-08
GOBP RESPONSE TO BACTERIUM	9617	717	6	3.25E-07
GOBP POSITIVE REGULATION OF LEUKOCYTE PROLIFERATION	50671	1606	4	4.00E-07
GOBP INFLAMMATORY RESPONSE	6954	773	6	5.04E-07
GOBP T HELPER 1 TYPE IMMUNE RESPONSE	42088	803	3	6.57E-07
GOBP RESPONSE TO LIPID	33993	865	6	9.70E-07
GOBP CELLULAR RESPONSE TO MOLECULE OF BACTERIAL ORIGIN	71219	1790	4	1.58E-06
GOBP REGULATION OF CELLULAR RESPONSE TO MACROPHAGE COLONY STIMULATING FACTOR STIMULUS	1903972	241	2	1.67E-06
GOBP LIPOPOLYSACCHARIDE MEDIATED SIGNALING PATHWAY	31663	1036	3	1.89E-06

7.3 Discussion

Microorganisms that cannot be cultivated *in vitro* for their entire lifecycle are largely inaccessible for experimental studies and this has previously been the case for chicken *Eimeria* spp. infection of the host starts after ingestion of *E.*

tenella oocysts, when sporozoites penetrate the epithelium of the caecal villi, pass through the lamina propria and enter crypt epithelial cells where they undergo several rounds of asexual and sexual proliferation. This chapter demonstrates that the floating chicken caecal enteroids, described in Chapter 4, can be infected by *E. tenella* sporozoites and subsequently undergo both schizogeny and gametogeny, as verified by visualising characteristic parasite staining and measuring macrogamete gene expression.

The innate immune response to Eimeria infection is particularly important in young chickens since the acquired adaptive response do not start to develop until one week of age[123,320]. At 2 dpi in *E. tenella* infected enteroids interleukin 4 induced 1 (*IL4I1), IL1R2* and Hermansky-Pudlak syndrome 5 (*HPS5)* are the most significantly upregulated qPCR array genes and they remain highly expressed throughout most of the remaining infection time points. Key immunoregulatory enzyme IL4I1 acts during infection to limit T cell mediated immunopathology, as well as containing pathogens through antiseptic H_2O_2 production. It is induced by infection with various types of pathogens including *Toxoplasma gondii* in bone marrow-derived mouse macrophages, *Salmonella* Enteritidis in the chicken caecum, and avian leucosis virus subgroup J infection in chicken monocyte-derived macrophages[382,383,384]. *IL1R2* is also involved in reducing tissue damage during infection, acting as a decoy receptor to block powerful pro-inflammatory IL1A and IL1B signalling[385]. *Staphylococcus aureus* was recently shown to induce IL1R2 shedding by myeloid cells in order to evade immune clearance[386]. Since protozoa have evolved multiple mechanisms for evading specific immunity it would be interesting to investigate if *IL1R2* upregulation is a host- or parasite-induced response in *E. tenella* infected enteroids.

Of these immune evasion mechanisms is the secretion of macrophage inhibitory factor (EtMIF) by *E. tenella*. This immunomodulatory protein inhibits chicken macrophage migration and reduces the intestinal inflammatory response[387]. However, at 4 and 6 dpi numerous macrophage-associated genes become some of the most significantly upregulated including

transglutaminase 4 (*TGM4,* an effector protein expressed by macrophages and B cells), *CSF1 (*which controls the proliferation, differentiation and survival of macrophage lineage cells) and *CD72 (*typically a B-cell regulatory molecule but is upregulated in murine macrophages during protozoa *Leishmania amazonensis* infection)[388]. Avian CD72 homologue, chB1 is expressed predominantly in B cells Embryos from different chicken breeds have demonstrated varying levels of resistance to *E. tenella,* so the upregulation of these genes, in addition to 2 dpi induced *IL4I1* (a secreted macrophage/dendritic cell enzyme) and *HPS5 (*involved in the synthesis and function of lysosomes)*,* could be indicative of genetic resistance of the Hy-Line breed to this *Eimeria* species [389,390].

At 8 dpi alongside continued high expression of many of the genes upregulated in previous days, *TLR4* and T cell immunoglobulin and mucin domain containing 4 (*TIMD4*) are significantly induced. *TLR4* is most commonly known for its role in the innate response to bacterial pathogens but it has also been associated with host resistance to protozoal parasites *Toxoplasma gondii* and *Leishmania major*[391,392]. This host defence gene has previously been shown to be highly expressed in the chicken caecum following *E. tenella* infection[393] and in chicken heterophils and monocyte-derived macrophages after stimulation with *E. tenella* sporozoites *in vitro*[394]. *TIMD4* (also known as *TIM4*) is a marker of resident macrophages in the intestine and has multiple biological functions[395,396]. It has been shown to protect mice from LPS-induced septic shock by inhibiting pro-inflammatory cytokines *IL6* and TNF-α[397]. Of the most significantly downregulated genes in the *E. tenella* infected enteroids *IL6* is present at most time points and *TNFAIP3* was present at 2 dpi, indicating *TIMD4* may also play an inhibitory role in Eimeria infections. It may also be the case that by only measuring enteroid immune responses from 2 dpi, the differential expression of acute response genes has been missed. For example, *IL6* was only upregulated in the first 24 hpi in *E. tenella* infected 1 day old chicks and more mature birds also show increased *IL6* expression in the first 6 hpi with *E. tenella*[393,398]. In addition, *TLR15,* which was significantly downregulated in the enteroids at 4

and 8 dpi, was only found to be highly expressed in *E. tenella* infected 1 day old chicks at 3 hpi[393]. *TLR15* induces NF-kB activation and cytokine upregulation in cell lines, therefore the reduced expression of this TLR from 4 dpi may be linked with the concurrent and sustained reduction in *CCL20* and *IL12B*[399].

The development of anti-coccidial recombinant vaccines is currently hampered by a poor molecular understanding of the *Eimeria*-host interface. This chapter demonstrates *E. tenella* invasion, replication and immune response induction in the floating chicken caecal enteroid model. Therefore, although further investigations are required to determine to whether completion of the parasite lifecycle occurs and whether parasite site-specificity is observed in the enteroids, this introduces a new *in vitro* tool to study the mechanisms associated with host immunity and parasite survival in the local microenvironment of the chicken gut.

Chapter 8 The mucosal response to influenza A virus in the chicken enteroid model

Chapter 8 The mucosal response to influenza A Virus in the chicken enteroid model

Avian influenza viruses (AIV) are endemic in certain wild bird populations, and from there spill over into domestic birds and human populations causing recurrent outbreaks of severe disease. AIVs can replicate in epithelial cells of the intestine, are excreted in high concentrations in faeces and, in aquatic birds, the main mode of transmission is via the faecal-oral route. The development of species-specific enteroids would introduce a more physiologically relevant model for the study of AIV than current *in vitro* systems. These could be used in conjunction with *in vitro* respiratory models to reproduce AIV species cross-over events in the laboratory setting. The inside-out chicken enteroids, described in earlier chapters, were investigated for their ability to support viral infection by incubating them with an influenza A virus (IAV) strain, PR8, and checking for viral presence and degree of replication 48 h post incubation. Since the enteroids have an immune cell component, a multiplexed RT-qPCR Fluidigm Dynamic Array was also used to analyse the expression of 84 chicken immune-related genes in the infected enteroids. The findings demonstrate that influenza virus can successfully replicate in the 3D chicken intestinal model and induce innate immune genes similar to the described *in vivo* response. This indicates floating avian enteroids are a suitable and robust host-viral model which could help advance our understanding of mechanisms behind viral host-cell receptor binding, viral-infected intestinal intracellular signalling, and testing of antiviral compounds.

8.1 Introduction

IAVs infect a wide range of host species with a large and antigenically diverse reservoir (haemagglutinin subtypes 1-16) circulating in wild birds. Some of these AIV subtypes occasionally cross into new species including chickens, humans and other mammals (reviewed in[400]). Based on their virulence in chickens, AIVs are classified into two pathotypes; low pathogenic (LPAIV) and highly pathogenic (HPAIV) both of which are generally

maintained in the intestines of waterfowl who develop minimal symptoms and allow, through faecal-oral transmission, viral spread along annual migration routes giving AIV global epidemic potential[401,402]. LPAIVs have a tropism for the respiratory and gastrointestinal tract of chickens, depending on the port of entry and virus strain, and cause mild but not insignificant clinical signs including drop in weight and egg production, gastrointestinal manifestations, respiratory signs and/or neuronal disorders[403,404]. In contrast HPAIV strains, which are generally derived from LPAIV strains by selective adaptation, commonly spread systemically causing peracute death in domestic birds and significant losses to the poultry industry[404,405].

Early mechanisms of virus-host interactions at the mucosal interface can be difficult to elucidate and manipulations of experimental conditions difficult to orchestrate in live animal studies. Therefore, with additional pressure from the increasing implementation of the 3Rs, development of *in vitro* tools to study AIV is essential. Intestinal cell line studies have established that AIV can invade human colon cell lines causing severe epithelial apoptosis, and a recently developed chicken enterocyte cell line allowed influenza virus replication[406,407,408]. Other avian-specific intestinal models used for AIV studies include chicken embryonic primary duodenal cell cultures[85], precision-cut intestinal slices[409], and chicken and duck colon organ cultures[410]. However, these culture systems are either very short lived (2 to 4 days) and/or do not contain the array of differentiated intestinal cells or 3D architecture necessary to represent the *in vivo* intestine. Organoid 3D cultures are now emerging as more robust *in vitro* models for assessing host-influenza interactions. AIVs have been shown to successfully infect and replicate in mouse intestinal organoids[411], and human airway organoids have shown replication competence, tissue tropism and epithelial cytokine production in response to AIV[412,413]. No viral infection studies have yet been performed in the limited chicken enteroid models currently published[215,216,217].

The intestine is a site of particular importance in AIV studies since LPAIV and HPAIV can replicate in the gut of both chicken and ducks, are shed in high concentrations in faeces and can survive in the environment for

weeks[403,414,415]. Due to the limitations of available *in vitro* avian intestinal models, most AIV intestinal experiments are conducted *in vivo*[325,416,417]. The inside-out leukocyte-containing chicken enteroids described in earlier chapters recapitulate *in vitro* the composition and 3D architecture of the intestinal epithelium and lamina propria. The aim of this study was to assess whether the floating chicken enteroids could be infected with, allow replication of and raise an appropriate immune response to influenza virus infection, demonstrating their potential as a host-viral model.

8.2 Results

8.2.1 Chicken enteroids are susceptible to infection by influenza A virus

To observe whether the floating chicken enteroids could demonstrate infection by and replication of a virus, they were incubated with IAV strain PR8 (A/Puerto Rica/8/34) for 1 h, washed (0 hpi) and then cultured for a further 48 hpi. IAV PR8 is a lab adapted H1N1 strain which was used in place of a fully avian strain as accessible biosecurity facilities could be used. Immunofluorescence detected viral nucleoprotein (NP) within the epithelium of the enteroids at 48 hpi (Fig. 8.1). The antibody used for staining is directed against the IAV NP indicating translation of viral mRNA in host cells, which accumulates in the cell nucleus as part of the ribonucleoprotein complex and is subsequently exported into the cell cytoplasm[418]. At 48 hpi PR8 NP was mainly detected in the cell cytoplasm and to a lesser extent in the nucleus of infected IECs (Fig. 8.1a - b1).

To further confirm the presence of virus protein, a western blot was performed to identify influenza virus NP in PR8 infected enteroids as compared to paired mock (construct engineered in parallel with PR8 virus but missing segment 1, encoding polymerase (basic) protein 2) infected controls at 0 and 48 hpi. This showed weak bands at the level of viral NP in 0 h enteroids (likely detecting input virus) and strong bands in 48 h PR8 infected enteroids (Fig. 8.1d). A faint band at the level of viral NP was also present in

controls. NP is encoded on segment 5 of IAV so this band likely represents residual plasmid from mock sample transfections which is producing a small amount of NP in the control enteroids.

Viral replication in the enteroids was verified by measuring infectious virus titers in the supernatant of enteroids, by plaque titration on MDCK cells. No virus was detected in the controls. Titers significantly increased in infected enteroids from 0 to 48 hpi (Fig. 8.1e). These experiments demonstrate the enteroids are susceptible to PR8 infection and support viral replication.

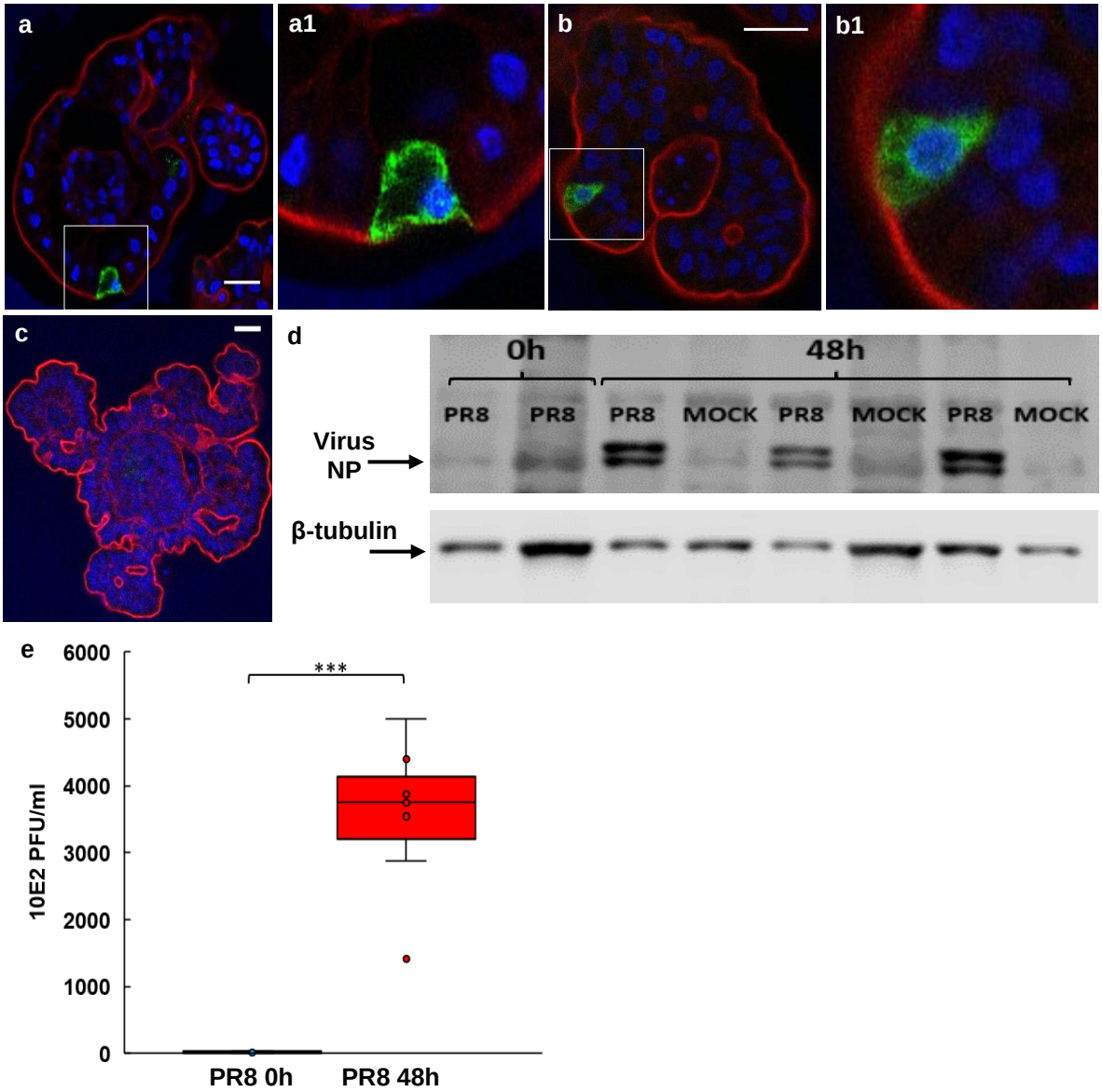

Figure 8.1: Infection and replication of influenza A virus in enteroids. a - b Representative z-axis projections of chicken enteroids, whole-mount stained to detect cell nuclei (DAPI, blue), F-actin-expressing brush border (red) and virus nucleoprotein (NP, green) 48 hpi with IAV (PR8). **a1** Magnified image of **a**. **b2** Magnified image of **b**. **c** Isotype control. **d** Western blot showing virus NP levels (bottom band) in infected enteroids compared to control (mock, virus construct missing segment 1) at 0 hpi and 48 hpi (enteroids were 2 days old at 0 hpi). β-tubulin was detected in every sample. Immunofluorescence and western blot are representative of data from at least 3 independent cultures each, containing 2 - 3 embryos. Scale bar: 20 µm. **e** Box and whisker plot represents viral titers (PFU), determined by plaque assay in supernatant at 0 hpi and 48 hpi (enteroids were 2 days old at 0 hpi). Data is derived from 7 independent experiments each containing 2 - 3 embryos and ~200 seeded enteroids/well. ***P ≤0.0001, T = -8.07, 95% CI for mean difference (-460509, -246168), df = 6 using a paired Students *t*-test (two-sided).

8.2.2 Influenza A virus infected enteroids have a difference in gene transcription compared to controls

The floating chicken enteroids have both intraepithelial and lamina propria leukocytes (Chapter 4) and Chapter 6 showed a comprehensive enteroid immune response to bacterial infection could be elicited. That data was predominantly obtained from a qPCR Array containing chicken innate immunity genes selected from an RNA-seq analysis of the transcriptional response of chicken macrophages, dendritic cells and heterophils to agonists of innate immunity and from published transcriptome data predominantly focusing on responses to bacterial challenge[275]. A second custom qPCR array was subsequently developed to analyse chicken innate immune response to viral infection and contained 6 reference genes and 84 viral innate immunity genes (Table 8.1). Of these 53 genes were selected from the original qPCR array and 37 genes were selected from published transcriptome data related to viral challenge in chickens and unpublished data (pers. comm. L. Vervelde). Screening of the viral qPCR array genes in the raw RNA-seq enteroid transcriptome data (Chapter 5) showed that

almost all qPCR array genes were found in common albeit occasionally under different gene names (Additional file 4). Two genes were not identified in the enteroid transcriptome data; *R28S* which is in the enteroid genome but is unannotated, and type II cytokine receptor *IL22RA2* for which the same is likely true for in the genome assembly used (Table 8.1).

Table 8.1: Genes on the 'viral' qPCR array. 90 genes on the Dynamic Array. Genes highlighted in yellow are unannotated in the RNA-dataset from 0 h (ED18 villi), 1, 3, 4, and 7 day non-challenged enteroid cultures. Genes in blue are reference genes.

ACOD1	FKBP5	IL22RA2	RASD1
ACTB	GAPDH	IL4I1	RPL37
ATF3	GBP	IL6	SDC4
AvBD10	GCH1	IL8	SNX10
AvBD2	GUSB	IL8L1	SOCS1
B2M	IFI6	IRF1	SOCS3
BATF3	IFIT5	IRF7	STAT3
BCL2A1	IFITM1	IRF9/10	STEAP1
CATHL2	IFITM3	JUN	STEAP4
CCL19	IFITM5	LIPI	TBP
CCL20	IFNa	LYG2	TGM4
CCL4	IFNG	LYZ	TLR15
CCL5	IFNL3A	MMP1	TLR21
CCR8L	IFNW1	MX1	TLR3
CD74	IL10	MYD88	TLR4
CD83	IL10RA	NFKB2	TLR7
CD8b	IL10RB	NFKBIZ	TNFAIP3
CD93	IL12B	NOS2	TRAF3IP2
CXCL13L2	IL13RA2	OASL	TRIM25
CXCR1	IL15	PFKFB3	TRIM29
CXCR4	IL17REL	PPARG	TUBA8B
EGR1	IL18	PTX3	
EIF2AK2	IL1B	R28S	

The viral qPCR array was used to investigate if the enteroids could raise an immune response to viral challenge, by analysis of PR8 infected enteroids and controls at 48 hpi. The results were processed as previously described in Chapter 6, section 6.2.4. The heatmap showed the biological replicates within each treatment group generally appeared consistent and there was an obvious difference in transcript abundance between the infected and control samples for *CCL19, CCL4* and *NOS2* (Fig. 8.2a). The PCA of the log2 fold change values showed lose but separate clustering of treatment groups except for one of the controls (Mock 1) which seemed to be clustering with the infected samples (Fig. 8.2b). Since Mock 1 showed no evidence of viral contamination in the plaque assays it was kept in the analysis. In general this data indicates PR8 infection induces a difference in enteroid immune gene expression.

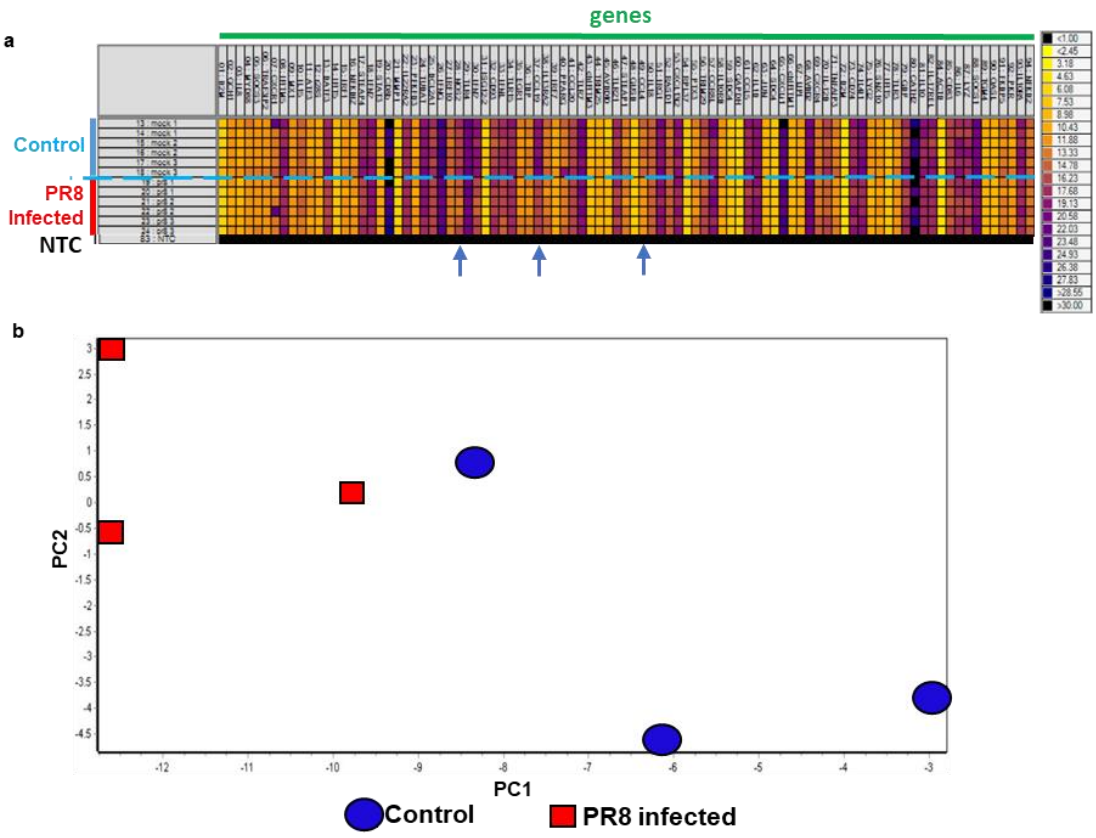

Figure 8.2: Whole dataset immunogenicity patterns in *influenza A virus* infected enteroids over time. a Heatmap view of the qPCR array run with individual genes on the x axis and individual samples on y axis. The RNA was extracted from enteroid samples either infected with PR8 or controls at 48 hpi (enteroids were 2 days old at 0 hpi); 3 biological replicates (1, 2, 3) were collected per treatment group and were run in duplicate. Black filled squares represent chambers where no gene expression was detected. Blue arrows highlight genes with obvious transcript differences between control and infected groups. NTC = non-template control. **b** PCA for qPCR array dataset showing patterns in immune-related genes expressed in PR8 infected and control enteroids at 48 hpi.

8.2.3 IFN pathway genes are upregulated in influenza A virus infected enteroids

To identify the specific genes contributing to the enteroid viral immune response, an unpaired 2-tail Student's t-test was performed on PR8 infected versus control enteroids. As compared to controls, there were 18 significantly differentially expressed genes (DEGs) ($P \leq 0.05$) in the PR8 infected enteroids at 48 hpi (Fig. 8.3). The most significant DEGs, of which there were 7, were defined as having a P-value ≤ 0.05 and difference in ΔΔCt (infected – control) of >1 (Fig. 8.3). All DEGs were upregulated and included two interferons; Type II *IFNG* and Type III *IFNL*, and many IFN stimulated genes (ISGs); *OASL, MX1, chIFITM3*, *IFIT5*, *IRF9/10*, *ISG12-2* and host defence peptide *LYG2* (Fig. 8.3). Pro-inflammatory genes including *NOS2* and chemokines *IL8, CCL4, CCL5* and *CCL19* were also upregulated alongside anti-inflammatory S*OCS1* and *TLR15* (Fig. 8.3). The most significantly differentially expressed genes were *CCL19, CCL4, NOS2, IFNG, SOCS1, LYG2* and *IFNL*. These upregulated genes are representative of a classical antiviral response driven by intestinal epithelial and lamina propria innate immune cells (Fig. 8.4)[419,420].

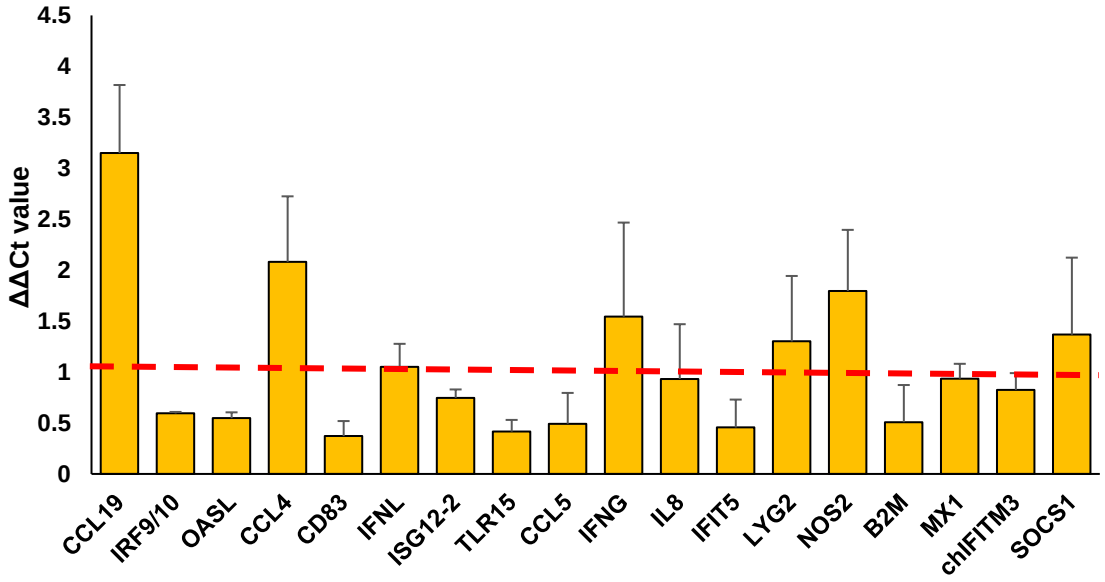

Figure 8.3: Individual genes significantly differentially regulated in influenza challenged 3D enteroids. The DEG ΔΔCt values (P ≤0.05) from t-test comparisons, ranked by significance (lowest P-value on left). Dashed red lines denote ΔΔCt values with a >1 cut-off indicating the most significant DEGs. Positive ΔΔCt values represent genes upregulated in infected samples as compared to controls. Results are from PR8 infected and control samples 48 hpi (enteroids were 2 days old at 0 hpi) run in the qPCR Array. Each bar represents average of 3 biological replicates, error bars = SD.

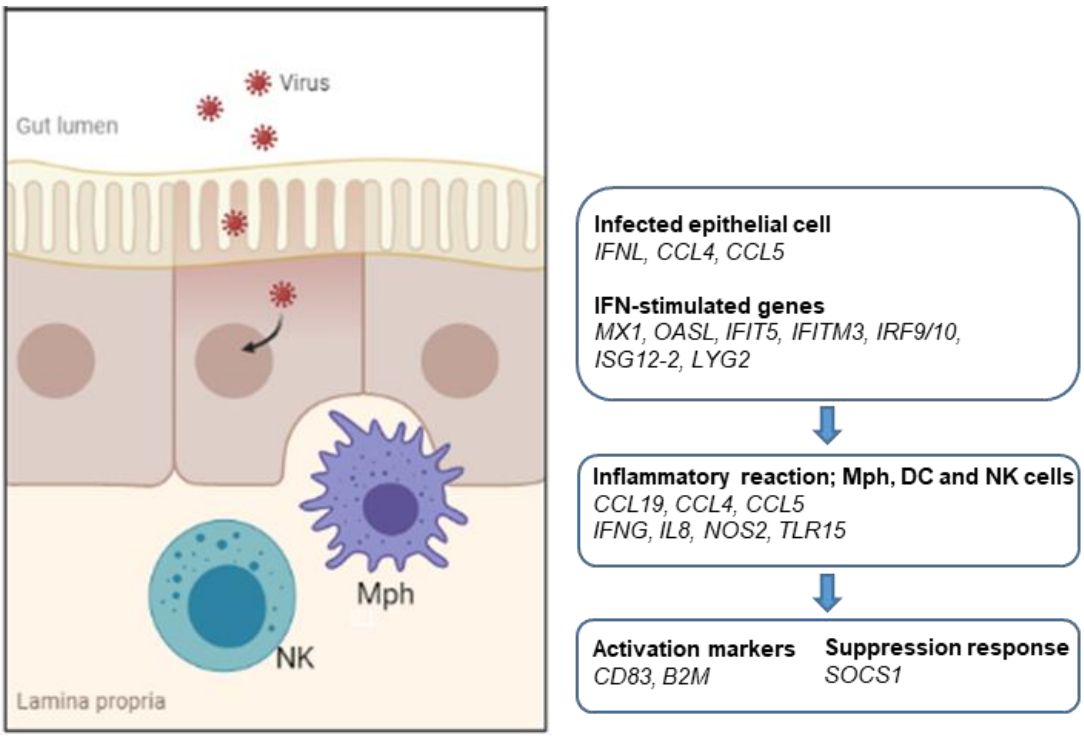

Figure 8.4: Overview of the signaling pathways and immune genes differentially regulated in chicken intestinal epithelial and innate immune lamina propria cells. Global overview of the significant DEGs (P ≤0.05) in PR8 infected enteroids, as compared to controls, at 48 hpi (enteroids were 2 days old at 0 hpi). Mph = macrophage, DC = dendritic cell, NK = natural killer cell.

Gene ontology analysis of the enteroid genes upregulated in response to PR8 infection confirmed they were involved in response to virus, response to interferon gamma, cytokine mediated signalling pathway and innate immunity (Table 8.2).

Table 8.2: Significantly enriched GO terms from DEGs upregulated in PR8 infected enteroids. Top 10 enriched GO term gene sets (biological process) obtained from mapping the significantly upregulated DEGs (P ≤0.05) in PR8 infected enteroids, as compared to controls, at 48 hpi (enteroids were 2 days old at 0 hpi).

GO terms	GO term number	Genes in Gene Set	Genes in Overlap	P-value
GOBP DEFENSE RESPONSE	0006952	1790	13	2.50E-18
GOBP_RESPONSE_TO_BIOTIC_STIMULUS	0009607	1606	12	1.92E-16
GOBP_RESPONSE_TO_INTERFERON_GAMMA	0034341	196	8	3.41E-16
GOBP_DEFENSE_RESPONSE_TO_OTHER_ORGANISM	0009814	1208	11	1.24E-15
GOBP_CYTOKINE_MEDIATED_SIGNALING_PATHWAY	0019221	803	10	2.52E-15
GOBP_INNATE_IMMUNE_RESPONSE	0045087	997	10	2.19E-14
GOBP_RESPONSE_TO_CYTOKINE	0034097	1188	10	1.26E-13
GOBP_POSITIVE_REGULATION_OF_IMMUNE_SYSTEM_PROCESS	0002684	1050	9	3.47E-12
GOBP_RESPONSE_TO_VIRUS	0009615	358	7	6.73E-12
GOBP_REGULATION_OF_VIRAL_GENOME_REPLICATION	0045069	83	5	4.16E-11

8.3 Discussion

In this chapter the potential of the floating chicken enteroid cultures as a host-virus model was explored. Influenza virus was selected for its One Health importance, with the aim of developing an *in vitro* avian intestinal tool that can be used alongside respiratory models to study infection dynamics, immune kinetics and the interspecies transmission potential of emerging AIVs[413,421,422]. By simply adding virus to the floating chicken enteroid media, PR8 successfully infected and replicated in the inside-out enteroids. Using a custom multiplexed qPCR array, PR8 was also shown to trigger an immune response in the enteroids with upregulation of genes related to virus-induced inflammation and innate immunity.

In intestinal epithelial cells, AIV is initially recognized by host pattern recognition receptors such as toll-like receptors (TLR)s. These cells are then

activated to secrete IFNs and pro-inflammatory chemokines such as Chemokine (C-C motif) ligands (*CCL)4* and *CCL5* [423](reviewed in[424]) (Fig. 8.4). These genes were all significantly upregulated in the PR8 infected enteroids alongside Type III interferon lambda (*IFNL)*. Studies, primarily in mice, have shown functional receptors for IFNL are mainly found on epithelial cells where it provides mucosal barrier protection against a wide range of viral pathogens including influenza[425,426,427]. *In ovo* and *in vivo* studies have since shown that *IFNL* plays the same mucosal antiviral defence role during AIV infection in chickens[428]. Chicken embryonic fibroblasts infected with HPAIV[429] and primary duodenal chicken intestinal epithelial cell cultures infected with LPAIV[85] have also demonstrated *IFNL* upregulation, confirming *in vitro* models can induce similar responses to *in vivo* AIV infection.

IFNL will create a receptor complex which activates Janus kinase-signal transducers and activators of transcription (JAK-STAT) signalling and results in induction of a range of ISGs in the epithelial cells (Fig. 8.4)[430]. Steps in the virus life cycle are targeted by ISGs to limit viral replication and enhance IFN production. Such genes include the interferon regulatory factor (IRF) family of which all members have been shown to be involved in the response to influenza infection to varying degrees[431,432,433]. *IRF9/10* was upregulated in the enteroids and was also upregulated in a microarray analysis of lung tissue from chickens infected with HPAIV H5N1[434]. Other ISGs which were highly expressed in the PR8 infected enteroids included myxovirus (influenza virus) resistance 1 (*MX1),* interferon-induced protein with tetratricopeptide repeats (*IFIT5*)*,* chicken interferon-inducible transmembrane protein 3 (*chIFITM3*), interferon stimulated gene (*ISG)12-2* and 2'-5'-oligoadenylate synthetase like (*OASL)*. These genes have all demonstrated antiviral activities and have previously been shown to be upregulated in chicken AIV studies[85,434,435,436,437,438,439]. Of the significantly upregulated genes not all cross the ΔΔCt threshold in the infected enteroids at the 48 h time point. This is likely due to the relatively late sample timing and kinetic immune response studies including earlier time points may demonstrate periods of higher expression.

Antimicrobial peptides are soluble mediators of the innate immune system which are also stimulated by the positive feedback loop of IFNs in influenza infection. These secreted proteins are constitutively expressed by epithelial cells of the skin and mucosal surfaces and during infection will contribute to the development and coordination of innate immune responses. Lysozyme G like protein 2 (*LYG2)* is one such antimicrobial protein produced in the chicken intestine and was found to be significantly upregulated in PR8 infected enteroids. Lysozymes are predominantly known for their antibacterial properties however this chicken specific lysozyme has previously been shown to be upregulated after viral challenge[17,440].

The next step in the intestinal AIV response is activation of key lamina propria innate immune cells such as macrophages, dendritic cells and natural killer cells which produce their own range of pro-inflammatory mediators and cytokines (Fig. 8.4). Nitric oxide synthase (*NOS)2,* an inducible enzyme of the NOS family, was significantly upregulated in PR8-infected enteroids. *NOS2* generates nitric oxide, a free radical secreted by activated macrophages which mediates their cytotoxicity and serves as a potent anti-viral molecule to combat infection[441,442](reviewed in[443]). There is growing evidence for the antiviral activity of inducible *NOS* in the chicken, particularly following influenza infection[444,445]. Cytokine related GO terms were significantly enriched in the PR8 infected enteroids and pro-inflammatory chemokine (C-C motif) ligands *CCL4* and *CCL19* were the most significantly upregulated genes. *CCL19* specifically induces M1 (pro-inflammatory) macrophage chemotaxis in mice and has previously been shown to be important for clearance of virus in chickens[446,447]. Both chemokines were highly upregulated in the lung tissue of HPAIV infected chickens[434]. Interferon gamma (*IFNG)* is critical for immunity against viral infection, in part from its ability to directly inhibit viral replication, and is an important activator of macrophages. This immunoregulatory cytokine was significantly upregulated in infected enteroids and GO terms ‘response to interferon gamma’ and ‘regulation of viral genome replication’ were significantly enriched. *IFNG* has been found to be upregulated in HPAIV and LPAIV chicken lung[448], at protein

level in chicken lymphocytes from lung, spleen and blood[449], and immunocompromised chickens with decreased *IFNG* mRNA expression show relatively higher mortality than normal chickens after AIV infection[450].

Despite the induction of ISGs and pro-inflammatory cytokines and chemokines, AIVs evade the host's immune response to efficiently replicate in the intestine. They achieve this in part by inducing suppressor of cytokine signalling (*SOCS)* molecules which negatively regulate the antiviral TLR and IFN signalling pathways. *SOCS1* was significantly upregulated in the infected enteroids. During influenza infection this ISG has been shown to specifically inhibit *IFNL*, potentiating virus replication but also inducing an adaptive increase in *IFNL* expression by host cells[451,452]. *SOCS* molecules have previously been shown to be upregulated in the respiratory tract and intestine of AIV infected chickens, indicating the response is independent of the infected tissue[453,454].

In this study the floating chicken enteroids allowed efficient replication of PR8 and reflected classical epithelial cell, macrophage and NK cell antiviral responses. The enteroids differentiated epithelial layer and lamina propria component means they are an improved model to study variations in viral strain pathogenicity and immunogenicity, and the effect of antiviral therapies compared to current avian 2D cultures. In addition, floating enteroids developed from various bird species, as demonstrated with quail in Chapter 4, could be used alongside mammalian respiratory and enteroid models to model AIV species crossover events *in vitro*. The floating enteroids could also contribute to the study of other important chicken enteric viruses such as astroviruses, rotaviruses and adenoviruses which have previously been difficult to grow *in vitro*, and whose effective control would have significant economic implications to the global poultry industry[455,456](reviewed in[457]).

Chapter 9 General Discussion

Chapter 9 General Discussion

9.1 Development of the floating chicken enteroid model

Prior to the development of organoids, the fundamental analysis of certain species-specific biological processes such as host-pathogen interactions and metabolism were severely hampered by the lack of appropriate *in vitro* models. Indeed, extrapolating results from unsuitable cell culture systems is a major bottleneck in the drug discovery process. A paucity of species-specific models is a particular issue in livestock species, therefore much of the research on food-production animals is conducted *in vivo*. The introduction of enteroids has provided species- and organ-specific models which create more reliable intestinal responses than current *in vitro* options whilst also contributing to the 3Rs (reviewed in[185,458]). This is especially true now the production of organoids from tissue biopsies has become possible[193,459]. In chickens, employing the classical mammalian enteroid culture systems produces poorly differentiated spherical structures which lack the 3D architecture of the *in vivo* gut and therefore have limited functional applications[195,215,216].

9.1.1 Overview of chicken enteroid development and characterisation results

The global purpose of this study was to develop an improved chicken enteroid culture system which more accurately represents the poultry intestinal mucosa than current *in vitro* models. The initial hypothesis was that protocols could be determined to produce a chicken enteroid model with the differentiated cell types, 3D architecture and functions of the *in vivo* organ. To address this hypothesis I conducted trials with various ISC isolation techniques, culture scaffolds, media supplements and growth factors (Chapter 3). Ultimately removal of the ECM and most exogenous growth factors resulted in a rapidly maturing enteroid model with multiple villus-like

budding structures that lasted in culture for 1 – 2 weeks, as confirmed by various viability analyses. The isolated embryonic villi and enteroids were successfully cryopreserved, and regained normal budding architecture after resuscitation (Chapter 3). Site-specific enteroids from embryonic duodenum, jejunum and caecum were developed as were enteroids from mature chicken jejunal crypts and the small intestine of 2 day old quail (Chapters 3 & 4).

Characterisation of the model was performed using TEM, immunohistochemistry, RNA-seq and functional assays and showed the differentiated epithelial content and epithelial barrier function of the *in vivo* organ were present (Chapter 4). Of particular interest was the discovery of an apical-out orientation of the enteroids with an externally facing brush border and a dense inner core. This core was demonstrated to contain lamina propria cell populations including a diverse population of functional lamina propria and intraepithelial leukocytes (Chapter 4).

RNA-seq of avian enteroid and ED18 intestinal villi samples from multiple biological replicates over multiple time points enabled the construction of a detailed picture of gene expression patterns in developing chicken enteroids and the late-embryonic chicken intestine (Chapter 5). The ED18 model was shown to mature to post-hatch functions in culture, showing transcriptional changes related to development of digestive function and organ development. The transcriptional analysis also confirmed the reproducibility and stability of this model for the first week in culture.

9.1.2 Establishing chicken enteroids in floating culture

Floating culture

Intestinal villi isolated from late embryonic chickens successfully differentiate into budding enteroids when the ECM is not added and they are seeded only in a basic media containing a B27 supplement. The addition of common murine and human growth and inhibitory factors does not appear to positively affect their development or survival in the first 7 days of culture. Epithelial and mesenchymal niches are known to cooperatively and redundantly shape

ISC microenvironments *in vivo*. Murine fibroblasts for example produce a variety of factors which support the proliferative phenotype of ISCs including WNT, RSPO, Noggin, $PGE_{2,}$ IGF1 and EGF[35,245]. Isolated mouse intestinal crypts are unable to develop into enteroids without the presence of contaminating sub-epithelial fibroblasts or exogenous growth factors[43,181]. Although little is known about the growth factors specifically required for ISC homeostasis in birds, steady expression of most common mammalian candidates in the chicken enteroid transcriptome indicates the epithelium and inner stromal cell core are supplying the required ligands for enteroid development and ISC homeostasis. However the floating chicken enteroid model developed by Acharya et al. (2020) do not produce buds without growth factor supplementation indicating the isolation technique and/or basic culture supplements may also influence ISC behaviour[217].

Rapid maturation of chicken enteroid cultures

An interesting observation from monitoring floating chicken enteroid morphology is the speed at which they start budding and subsequently mature. Newly established gel-embedded enteroids from mature mice take 3 days before buds become evident and 7 - 10 days to become fully mature structures[43]. Floating chicken enteroids already have multiple small buds present by 24 hours and are mature structures by 2 - 3 days. In addition, the transcriptional signature of the enteroids also rapidly matures to display a wide variety of post-hatch physiological functions including nutrient absorption, lipid metabolism and barrier function. As a precocial species the post-hatch period in chickens coincides with a rapid increase in general intestinal mass, villus length and crypt depth as well as an increase in brush border enzymes and transporters, enabling chickens to have an almost fully mature intestine shortly after hatch[8,28,72]. The difference in maturation rates is therefore could be due to the age and species of the animal from which the ISCs have been isolated with embryonic chicken enteroids containing an active population of ISCs programmed to undergo profound proliferation. However the difference of the floating versus gel-matrix environment may also play a role..

9.1.3 Long-term culture of chicken enteroids

Extracellular Matrices

The absence of Matrigel in the chicken enteroid cultures is generally welcomed since it requires the sacrifice of mice to manufacture, is difficult to handle, expensive, and varies batch to batch affecting the reproducibility of cultures. In addition, the lack of a scaffold is responsible for the apical-out enteroid orientation allowing easy access to the brush border for experiments[211,299]. However the ability to achieve long-term cultures in apical-out enteroids, with and without the presence of exogenous growth factors, has not been published in any species[211,212,309]. This is in contrast to the ability to repeatedly passage enteroids grown in Matrigel, indicating the floating growth conditions likely prohibits propagation[42,193,195]. A defined synthetic ECM alternative to Matrigel may contribute to the ability to maintain differentiated chicken enteroids longer term in culture (reviewed in[189]). Birds have evolved to be lightweight to minimize the energy required for flight and this selective constraint is reflected in the reduced volume and surface area of their gastrointestinal tracts compared to mammals[460]. These species differences could also have an impact on the density of their intestine ECM. Therefore tuning a synthetic scaffold to replicate the stiffness of the chickens natural tissue environment may positively influence ISC differentiation and encourage crypt-villus enteroid architecture, as has been previously demonstrated in mammals[461,462].

Growth Factors

On a molecular level there is a complex interplay of growth factors and signalling pathways that positively regulate self-renewal in LGR5+ ISCs[38,40,245]. If these could be identified for the chicken it may contribute to successful differentiation of chicken enteroids within an ECM or post-passage in floating culture. Transcriptomic analysis revealed that *RSPO2* and *EGF* were expressed at lower levels in the enteroid transcriptome compared to the isolated villi. The RSPO family are LGR4 and LGR5 ligands locally secreted by subepithelial fibroblasts near the crypts and are critical to

potentiate WNT signalling in ISCs[38,39,463]. Media supplementation of exogenous RSPO is essential for mammalian enteroids since they only contain epithelial cells. In the chicken enteroid transcriptome there is an increase in *RSPO1, RSPO3* and *RSPO4* expression (Fig. 5.4b) but a reduction in *RSPO2* compared to the freshly isolated ED18 intestinal villi. RSPO2 mutants with no binding affinity for LGR4 or LGR5, still potentiate WNT/β-catenin signalling *in vitro* and support the growth of intestinal organoids *in vivo*[464]. Therefore, exogenous RSPO2 supplementation may be capable of increasing WNT receptor levels and supporting chicken enteroid longevity despite the reduced transcript expression of *LGR5*. EGF has indicated roles in intestinal development, including increasing villous height and crypt depth, enhancing enterocyte proliferation, and stimulating secretion of digestive enzymes[465]. Although Paneth cells have been shown to produce EGF, it is supplemented in most mammalian enteroid cultures[40,183,198]. Interestingly, when WNT signalling is untouched but EGF signalling is suppressed, as generally appears to be the case in the chicken enteroids, actively dividing Lgr5+ ISCs convert into quiescent Lgr5+ ISCs[466]. The restoration of EGF signalling has been shown to convert quiescent cells back into their normal active stem cell state indicating it is worth persevering with EGF trials to explore long-term propagation of the enteroids.

Apical-out Orientation

In 2019, Co et al. published an apical-out model for both human and murine enteroids and following from this work, porcine apical-out enteroids have also been established[211,212]. These mammalian cultures are initially established as traditional gel-embedded enteroids for 1 – 3 weeks, before being moved to suspension where their polarity reverses over 3 days. Approximately 20% of these enteroids do not reverse polarise and they are only viable for 3 - 5 days which restricts their use. The reduced viability of these cultures could be due to the apical-out polarisation which may limit contact of media-supplemented growth factors with epithelial basolateral receptors. This may also explain why growth factors and inhibitors useful in other species do not appear to benefit the longevity of the floating chicken enteroid cultures. However,

Acharya et al. (2020) have demonstrated enterotrophic effects of EGF and IGF supplementation in their floating chicken enteroids and Co et al. (2020) showed a higher percentage of proliferating cells in their apical-out enteroids when cultured in a growth media (containing gastrin, EGF, Nicotinamide, p38 MAPK inhibitor, TGF-β inhibitor, 50% L-WRN, CHIR99021 and ROCKi) versus a differentiation media (containing gastrin, EGF, TGF-β inhibitor, ROCKi, FBS, Notch pathway inhibitor DAPT, and Noggin)[211,217]. This indicates that luminal growth factors have some biological relevance and therefore exogenous growth factor trials in the chicken enteroid cultures are still worth pursuing.

9.1.4 Reproducibility and stability of enteroid cultures

Biological variability

To support reproducibility of cell based experiments, a desirable trait for any tissue culture model is culture consistency. This is of particular importance in the chicken enteroids with the multiple cell-types present. The enteroid RNA-seq analysis demonstrated that the main cause for differences between sample transcriptomes was time of culture, with a high degree of similarity in global transcriptional activity between technical and biological replicates. As would be expected of biologically distinct samples with natural variation, there were slight differences in biological replicate transcriptomes identified within the PCA[467]. Individual variability in donor genotype, microbiome and disease status has been shown to affect the epithelial phenotype of enteroid cultures[186,468,469]. Compared to wild chicken breeds, commercial layer chicken lines have a fairly low genotypic diversity therefore the effect of variability of genotype on the Hy-Line chicken enteroid cultures should be low[470]. The use of embryos for the enteroid cultures also reduces the chance that infection in the donor tissue or variability in microbiomes, mostly colonizing the host post-hatch, will influence the culture phenotype. Although some avian viruses can be vertically transmitted[471]. However, ensuring adequate numbers of biological replicates are planned for enteroid experiments, as well as pooling isolated intestinal villi from large numbers of

embryos will improve the efficiency of statistical testing and help to better represent the population under study.

Enteroid intestinal stem cell populations

By 3 days post-hatch in the duodenum, the proportion of proliferating cells lining the villi reduces markedly and the number of villi per intestinal cross-section reaches a plateau[7]. Morphologically the enteroid cultures emulate this *in vivo* growth deceleration, appearing to mature by 3 days of culture and ceasing the rapid budding behaviour of earlier time points. Reduction in the number of cell cycle related GO terms in 3 – 4 day enteroid samples and lack of DEGs between these time points also correlates with the slowing of this intense growth period. However, demonstration of proliferating epithelial and lamina propria cells at 7 days of culture, and steady expression of cell-stress associated and apoptotic genes in the enteroids over the first week indicate the cultures continue to be viable after 3 days.

To explore the enteroid viability in more detail, the ISC transcripts were considered. Despite an initial marked down-regulation of many ISC markers between the ED18 intestinal villi and 1 day enteroids, there is a partial recovery in expression of (marker of proliferation Ki67) *MKI67H, OLFM4 and (*cell division cycle associated 7*) CDCA7.* The recovery in *OLFM4* expression, a gene demonstrated to be a more robust ISC marker than *LGR5* in both mammals and birds, may also be a hallmark of intestinal maturation. This is evidenced in human intestinal crypts and in chicken intestinal studies, where an increase in *OLFM4* staining intensity was noted from 0 to 7 days post-hatch[12,317,472]. The functionally redundant *LGR5* homolog *LGR4*, has high and stable expression throughout the chicken enteroid cultures and has been shown to compensate after genetic deletion of *Lgr5* in mice ISCs[38]. This redundancy could explain the continued steady expression or recovery in WNT receptor complex genes (frizzled class receptor 7) *FZD7*, (lipoprotein receptor-related protein) *LRP5* and *LRP6* and WNT transcription factor *TCF4H* across the enteroid cultures. Also to be considered are studies in which ablated Lgr5+ ISCs were seen to be replaced by an alternative ISC

pool leading to an appreciation that there is a remarkable amount of cellular plasticity within the crypt[473]. This reserve population of enteroendocrine-progenitor cells express *LRIG1, BMI1*, (prospero homeobox 1) *PROX1, SOX9* and *HOPX* in mammals[13]. Although there is a reduction in *HOPX* expression in the chicken enteroids, the other markers are either stable or increase in expression over the cultures which could indicate that this population of ISCs are being recruited.

The bulk RNA seq analysis has allowed a comprehensive characterization of the chicken enteroid expression profiles at different stages of development, helping to answer biological questions regarding e.g. culture supplementation. Alongside histological analysis it was also used for cell-type identification as has previously been published[183]. However single cell sequencing would have been superior for its ability to identify cell-specific properties only activated in small subpopulations of cells which prove difficult to accurately assess using the conventional bulk data e.g. ISCs[279]. Single cell sequencing of the chicken enteroids would be a desirable next step in order to describe the unique variabilities between avian intestinal cell populations.

9.2 Application of the chicken enteroid model for host-pathogen modelling and innate immunity studies

Recent advances in stem cell research have helped to establish organoid models as viable alternatives for many established infection models. Features demonstrated in the floating avian enteroids which make them highly applicable for host-pathogen studies are their apical-out conformation with an easily accessible brush border, epithelial barrier integrity, species- and digestive site-specific models, and the innate presence of lamina propria and intraepithelial leukocyte populations.

9.2.1 Overview of chicken enteroid host-pathogen modelling results

The second major hypothesis was that these reverse polarised chicken enteroid cultures could be used to effectively model host-pathogen infections. To address this hypothesis, microorganisms were simply added to media for a determined timeframe before the enteroids were collected for immunohistochemical analysis, replication assays and functional assays. RNA was also collected for use on a multiplexed RT-qPCR 96.96 Fluidigm Dynamic Array containing a panel of chicken innate immunity genes. Of the pathogens chosen for the host-pathogen studies; *S.* Typhimurium was used as a bacterial model (Chapter 6), *E. tenella* was used as a species-specific protozoal model (Chapter 7), and IAV was chosen for the viral infections (Chapter 8). As discussed in more detail below, these all displayed infection and replication within the enteroids and induced appropriate innate immune responses.

9.2.2 Modelling *Salmonella* infections in chicken enteroids

Salmonella was chosen for the analysis as it is an important zoonotic pathogen which causes serious illness in humans and young chickens. Human salmonellosis is frequently associated with consumption of contaminated poultry and eggs, with *S.* Enteritidis and *S.* Typhimurium accounting for most non-typhoidal infections in both developed and developing counties[474]. Cellular immunity is believed to play a crucial role in the clearance of intracellular *S. Enterica* spp. but our knowledge of the exact roles of individual cell types and mechanisms underlying this protective immunity is incomplete (reviewed in[475]). In most countries *Salmonella* spp. infections in poultry are controlled through various means including vaccination, natural antimicrobial products, genetic selection for resistance and egg washing or irradiation[476]. Using the floating chicken enteroid model I demonstrated active invasion, including membrane ruffling, and replication of WT *S.* Typhimurium in the enteroid cultures with induction of appropriate innate immune responses. In addition, the assessment of enteroid infections

with WT and T3SS1 mutant strains showed both were highly immunogenic but the mutant bacteria showed limited invasion and replication. This indicates the model would be useful to explore the questions relating to intestinal colonisation, host genetics and innate immunity in laying hen breeds, as well as measuring the level of attenuation of live vaccine candidates.

Epithelial Barrier Assessments

The innermost layer of the intestinal luminal surface consists of a single cell thick epithelial lining which acts as a barrier, preventing the entry of microbiota and harmful pathogens while still allowing the selective passage of dietary nutrients, ions, and water[296]. Tight junction proteins together with adherens junctions and desmosomes are essential gut epithelia barrier components which maintain physiological homeostasis and these were demonstrated in the chicken enteroid cultures[297]. Assessing the epithelial barrier *in vitro* can be useful in the study of intestinal inflammation following pathogen infection as well as the effect of feed additives or probiotics. TEER measurements are typically used to measure epithelial integrity in monolayers, however due to the 3D structure of the enteroids they are not suitable for automated TEER. Analytic dye analysis has previously been applied to gel-embedded mammalian enteroids but this is either technically challenging e.g. micro-injection of dye in the enteroid lumen, or only allows analysis of stimulants applied to the basal epithelial surface[477,478,479].

S. Typhimurium has been shown to disrupt tight junction structure and function thereby compromising the protective intestinal barrier[480,481]. Due to the apical-out nature of the chicken enteroids, immersing them in FITC-dextran allowed the quantitative measurement of epithelial permeability after various external challenges including *S.* Typhimurium LPS and bacterial strains. This method is the first demonstration of a dynamic epithelial barrier analysis of multiple apical-out enteroids and could be used to investigate the effects of e.g. natural antimicrobial products on mucosal integrity and elucidate their anti-inflammatory mechanisms.

9.2.3 Modelling *Eimeria* infections in chicken enteroids

An *Eimeria* spp. was selected for protozoal modelling as intestinal coccidiosis is an economically important disease affecting poultry welfare throughout the world. The significant production costs associated with this parasite are predominantly associated with in-feed anticoccidial medications and live vaccines, in addition to reduced feed intake and conversion rates by the stock[371,482]. However public and legislative demands in many countries are placing pressure to reduce the use of antimicrobial feed additives, geographical variations in *Eimeria* spp. challenge the effectiveness of vaccines, and live vaccines are expensive and carry risks of inducing coccidiosis outbreaks (reviewed in[483]). Multivalent vaccines that do not require the use of chickens in their production and will induce cross protection against a combination of *Eimeria* spp. is required. In addition, although natural *Eimeria* infections induce strong cell mediated immune responses, there are no assays which predict how protective a coccidiosis vaccine might be. The ability to study interactions of different *Eimeria* spp. with the host intestinal mucosa *in vitro* could help to identify solutions to these problems and improve the safety and success of vaccines[484,485]. However, protozoal parasites are notoriously difficult to grow through their entire lifecycles in culture.

Digestive-site specific models

Evidence in adult mice has demonstrated that ISCs are intrinsically programmed with their location specific functions and gene expression patterns[486]. Indeed, enteroids in pigs have been shown to retain the phenotype of their digestive segment of origin[186,203]. This explains why late embryonic villi from the duodenum, jejunum, and caecum retained their region-specific morphology without changes in culture conditions. Although regional identity is believed to be specified by gradients of growth factor signalling, transcriptional analyses of the gut mucosa from different intestinal regions are needed to reveal exactly how these are determined in the chicken[487].

The site-specific enteroid models are especially important for host-pathogen studies with *Eimeria,* whose different species only replicate in particular segments of the intestine *in vivo*. Using a species (chicken) and site (caecal) specific enteroid model, I demonstrated active infection and replication of *E. tenella* sporozoites through their asexual and sexual stages up to the production of gametes. In addition, I showed innate immune transcriptional changes in the *E. tenella* infected enteroids which correlated with *in vivo* protozoal infections. Further investigations however are needed to confirm full lifecycle replication (up to oocyst stage) and site-specificity of *Eimeria* spp. in the enteroid model. Initial experiments (data not shown) indicate that *E. tenella* sporozoites also invade duodenal and jejunal chicken enteroids however they do not appear to replicate past the asexual stages. This observation would fit with many cell line studies where *E. tenella* sporozoites will invade the cells but typically only develop up to the first merozoite stage[376,488]. Although further replications of the chicken enteroid experiments are needed to confirm these findings, if *Eimeria* spp. do demonstrate site-specificity in terms of lifecycle replication the enteroids could be useful in the identification of novel candidate antigens and correlates of protection, exploration of chicken breed specific differences to infection, and for live vaccine attenuation screening.

9.2.4 Modelling influenza A virus infections in chicken enteroids

IAV was chosen as the viral pathogen to model as it is recognised as disease of great importance for animal and human health. IAVs cause natural infections of the gastrointestinal and respiratory tract in birds. Both LPAI and HPAI circulate in wild birds and cause outbreaks of AIV in domestic poultry[402,403,405]. The economic consequences for the poultry industry can be severe resulting from flock losses with HPAI or reduction in egg production and quality with LPAI[404]. In addition, due to genetic reassortment, outbreaks of AIV in ducks and chickens have also been associated with human transmission with pandemic potential[401]. Developing species-specific

gastrointestinal *in vitro* models for chickens would be beneficial for the study of newly emerging viral subtypes including their potential for mutation to virulence. I demonstrated the chicken enteroids are susceptible to infection by IAV and exhibit a classical antiviral innate immune response, confirming their use as a model to study the effect of invasion and replication competence of different virus strains, as well as host innate immunity.

Species-specific models

Certain pathogens can infect multiple bird species causing significant economic losses across the poultry industry. This includes AIV which has been detected in various avian species including chicken, duck, quail, pigeon and pheasant[489,490]. I demonstrated that villi/crypts from hatched quail could be isolated and cultured in a manner similar to embryonic chicken villi indicating the floating enteroid culture technique could be used to investigate AIV crossover events between bird species, as well as species jumps into mammals. Further optimisation of post-hatch crypt isolations is required in order to obtain clean cultures from intestines filled with ingesta and coated in thick mucus. In other species this is achieved in part by opening the intestine and scraping off the mucus layer with a glass slide followed by a large number of washing steps prior to the use of dithiothreitol during digestion[43,183]. In addition, culture supplement trials may show additional growth factor and/or scaffold requirements are required in different species and ages of birds to optimally support their ISC populations.

9.2.5 Researching innate immunity using the chicken enteroid model

Typical enteroids are limited in their cellular complexity, only representing the epithelial layer of the intestine with no vasculature, mesenchymal, neuronal or immune cell populations. Human and mouse enteroids have been co-cultured with other select cell populations however this involves complex protocols and ultimately the models don't reflect the natural diversity of cells or their *in vivo* locations[241,244,247](reviewed in[240]). Due to the isolation of villus

tips rather than epithelial crypts from the late embryonic intestine, the resultant enteroids contain an intact lamina propria beneath the epithelial layer. I demonstrated that this core reflects the variety of cell populations expected in the embryonic intestinal mucosa *in vivo.* In addition, the leukocytes have been demonstrated to be viable and functional allowing the exploration of enteroid innate immune responses to pathogen challenge. However the complexity of the model does not allow for the characterisation of immune responses originating from the epithelium only, or the full array of adaptive immune responses.

9.3 General considerations and limitations

Long-term self-renewing propagation

The creation of this *in vitro* chicken intestinal model will address the 3Rs in various areas. For example, gastrointestinal-based experiments which compromise the welfare of birds, or screening of nutritional and pharmaceutical compounds can be performed in chicken enteroids first, thereby reducing the number of animals needed for *in vivo* trials. In addition, *in vitro* models allow the study of early infection events e.g. pathogen adhesion and entry, in far more detail and synchrony than the oral inoculation of birds. The floating cultures also do not use Matrigel or supplemental growth factors which significantly reduces the 3Rs, environmental and financial impact of this model. However, a major drawback of the floating chicken enteroids is that they do not allow for long-term self-renewing propagation. This has been partly addressed with the development of methods to cryopreserve enteroids or villi at the point of isolation. Biobanking of frozen culture material means the enteroids can be reproducibly used across many studies and material can be shared between labs, opening up research into indigenous breeds from other countries. This also removes the need to use fresh tissue, predominantly that of embryos rather than post-hatch birds, for each experiment.

Analytical tools for 3D enteroids

One of the challenges for the high-throughput use of organoids involves the use of ill-defined raw culture components which are expensive and can introduce variation in the physical and biochemical culture conditions. This particular issue has been addressed in the chicken enteroids by omission of an ECM however the apical-out orientation introduces other challenges for analysis. For example, large-scale analytic techniques for apical-out enteroids have not been established, with most technologies aimed at 2D cultures e.g. TEER measurements for epithelial barrier integrity studies[258]. Therefore, alongside the development of novel *in vitro* models, the creation or adaption of analytical tools addressing the model's particular idiosyncrasies also needs to be considered. For the floating chicken enteroids I started to address this issue by adapting the FITC-dextran permeability assay as previously described. Although this method is currently relatively labour intensive, with further refinement it could also be utilised for high throughput screening

Lifecycle stage specific tools for *Eimeria* spp.

Visualisation of the lifecycle stages of *Eimeria* spp. using the size and number of nuclei within a cell, and/or non-specific labelling such as haematoxylin and eosin staining is standard practice in 2D cultures. However these methods proved difficult to employ in the 3D enteroids since intestinal cells undergoing the natural process of anoikis also have fragmented nuclei, and sectioning enteroids for staining is difficult and time-consuming given their size (~300 – 500 µm; data not shown). Staining the *E. tenella* sporozoites with the PKH-67 cell membrane dye and using a gamete specific gene marker partially addressed these problems and allowed us to demonstrate certain lifecycle stages of the parasites. However, in order to reliably monitor the lifecycle development of different *Eimeria* spp. in 3D cultures, a comprehensive selection of lifecycle stage-specific genes and stage specific antibodies, and/or recombinant parasite strains expressing fluorescence genes need to be established.

Limitations of qPCR arrays

Customised qPCR arrays were used for assessment of chicken enteroid immune gene expression in response to pathogen infection. The genes on the qPCR array were selected from in-house RNA-seq analysis and published transcriptome data to represent chicken immune responses to either bacterial or viral infection in various cells and tissues[275]. The qPCR array analysis is therefore limited by the requirement for prior knowledge of the genomic features of infection. In addition, since the genes were not customised for the intestinal immune responses to protozoal infections, some relevant immune genes noted *in vivo* were missing from the array e.g. *IFNG, IL10*, *K203, MIP-1b* and *MGF*[491,492]. To address these concerns conventional qPCRs can be used in combination with the array to investigate missing genes of interest or an infection-specific gene expression array could be developed.

Interpretations of the transcriptomic analysis

Certain conclusions drawn from transcriptomic analysis will be open to interpretation due to the multifunctional nature of most genes. Many of the enteroid RNA-seq findings were substantiated using histology and/or functional assays however there were some areas which would have benefited from additional confirmatory experiments. For example, the development of digestive function in the model could be assessed using functional tests for polarity specific processes such as fatty acid uptake[211], and assessment of EMT could be performed by quantitatively assessing enteroid epithelial morphology in addition to mesenchymal and epithelial marker staining[319]. Although most epithelial and lamina propria cells were identified using immunohistochemistry ±TEM, double staining of certain cell types which do not have cell-specific markers e.g. myofibroblasts, or use of *in situ* hybridization to specifically localise cells e.g. ISCs, would be beneficial to more definitively confirm their identity and location[12,106]. In addition, the immunohistochemistry performed on intestinal sections with the epithelial cell

markers should be repeated with the lamina propria cell markers in order to compare their frequency and location with the enteroid core cell populations.

Quality and validity of enteroid culture systems

Organoids are a relatively new technology and they belong to a rapidly developing field. Therefore the correct concentration and combination of growth factors for each species, digestive site and age are still being optimised. Individual reports describe a variety of methods to generate and maintain enteroid cultures, potentially resulting in variability in the enteroid phenotypes. This is particularly evident in the chicken enteroid field, where no two ISC isolation techniques are the same and an array of growth factors are in use[195,215,217]. Collective efforts should be made to develop standardized organoid culture protocols for each organ and species to help with the consistency of published results. In addition, a clear set of guidelines are required to assess the quality and validity of each system. For example, adult and pluripotent stem cell based organoids face different challenges. The genetic variability and disease status of tissue donors is a particular issue in adult stem cell derived enteroids, and the presence of partially differentiated cells is a problem in pluripotent derived cultures. As previously discussed, the use of embryos will reduce direct disease status issues however indirectly these still need to be considered for innate immunity studies since laying hens infected with e.g. *Eimeria* or *Salmonella* can pass specific maternal antibodies to the embryos[146,147]. Quality controls would also need to vary depending on the question to be studied e.g. developmental biology versus production of therapeutics.

9.4 Future work

Modifying the models for high throughput screening and organ-on-a chip

Enteroids in livestock species are already showing great potential in biomedical, veterinary and agricultural applications including human disease modelling[251], host–pathogen[192,198,232] and host-microbiota interaction

studies[222]. The application of microfluidic organ-on-a chip technology, where mechanical complexity such as oxygen gradients and peristalsis motions are introduced, could further improve the physiological relevance of organoid models and even introduce inter-organ communication[493,494,495]. High throughput screening would be indicated for many commercial applications in poultry enteroids therefore ongoing work is required to decrease variability in the cultures and characterise reproducible responses to challenge. Bioprinting techniques have started to be explored in bovine colon organoids which, alongside microfluidic delivery systems, could overcome many of the scalability limitations of standard enteroid cultures[189,196].

Studying phenotypic diversity between breeds

Organoids derived from individual humans or animals can be used for personalised medicine applications including patient-specific drug testing and autologous-grafting to repair damaged tissues[496,497]. Although these applications are not relevant for livestock species, developing chicken-breed specific enteroids will allow the study of genetic diversity between breeds *in vitro*. Traits of interest that could be analysed include how phenotypes influence disease resistance, microbiota compositions and differences in nutrient absorption[498,499]. Genome editing has been used in human and mouse intestinal organoids to introduce specific genetic mutations to study intestinal disease phenotypes (reviewed in[500]). CRISPR Cas9 technology has not yet been utilised in livestock species enteroids however enteroid cultures were developed from pigs genetically edited to express a mutated myosin 5B gene[251]. This gene is involved in microvillus inclusion disease in humans and the porcine enteroids displayed an appropriately poorly developed brush border and atypical localization of several transporters. Creating enteroids from individuals already harbouring or prone to disease can allow modelling of disease processes without prior knowledge of the causative genes or conditions[501,502].

Host-microbiota studies

In order that enteroids mimic the differentiated form and function of parental tissues, the introduction of monocultures or more complex microbiota cultures is being investigated. So far, cell lines in anaerobic transwells can only sustain microbiota co-cultures for under 24 h[503]. However more complex anaerobic microfluidic-based systems such as Gut-Chips allow 5 day co-cultures, and microbial communities have persisted in 3D human colon organoids for over 4 days after a high-throughput microinjection technique[504,505]. Murine enteroid-microbiota studies have demonstrated a positive correlation between microbial stimulation of the gut and epithelial regeneration, and identified how host lipid metabolism genes are modulated by commensal gut bacteria[506,507,508]. In ED18 chicken enterosphere cultures, the probiotic bacteria *Lactobacillus acidophilus,* a TLR4 ligand*,* and Pam3CSK4, a TLR2 ligand, promoted enterosphere growth and increased PGE_2 production[222]. Developing a host-microbiota system for the apical-out chicken enteroid cultures with an aerobe-anaerobe interface would allow for the controlled exploration of the microbiotas role in e.g. epithelial barrier integrity, nutrient absorption and ISC function, as well as how IECs regulate the composition of the microbiota and distinguish between tolerance of and defense.

Dissecting the epithelial response using 2D enteroids

The fluidigm array analysis highlighted changes in the enteroid innate immune transcriptional landscape that were induced after pathogen sensing by the epithelial and lamina propria cells. In order to dissect the epithelial cell response from that of the immune cells, the 3D enteroid results could be compared with those of 2D enteroid cultures challenged under the same conditions. A 2D enteroid model developed in our lab uses the same Hy-Line embryos at the same embryonic stage and applies the same villus isolation procedure as for the 3D enteroids[509]. In addition, the 2D model has been demonstrated to contain the same differentiated IEC populations and intercellular junctions as the 3D enteroids however they do not contain the

lamina propria leukocytes. This reduction in experimental variables will make it an ideal comparative model to determine which aspects of the 3D immune response are epithelial in origin.

Study of pathogens previously difficult to culture *in vitro*

Cultivation of previously unculturable viruses e.g. human norovirus, is now possible in enteroid models[230]. This indicates that the differentiated cellular environment present in organoids can provide essential factors for the infection and expansion of microorganisms. This attribute could make the floating chicken enteroid system particularly useful for the culture of certain chicken enteric viruses which are currently difficult to study as they do not grow in available cell lines[455,456,457].

9.5 Conclusion

Currently available *in vitro* chicken intestinal models have limited functional potential. For example, primary IEC cultures do not possess 3D architecture or immune cells, and previously published avian enteroids do not display the multiple-budding enteroid phenotype or the array of differentiated epithelial or immune cells seen *in vivo*[164,195,215]. This paucity of physiologically relevant models has limited research in the essential field of poultry gut health and led to an over reliance on the use of live birds for experiments.

The comprehensive 3D chicken intestinal culture developed in these studies, allow isolated late embryonic villi to rapidly and consistently form enteroids within 1 - 2 days. The floating enteroids contain multiple differentiated IEC types and recreate the physiology of the gut and buds with villus-like architecture. Unusual attributes of this model which distinguish it from classical enteroids include an apical-out phenotype and the natural presence of leukocytes. The externally accessible epithelial surface of the chicken enteroids has allowed for the uncomplicated replication of the natural infection process by simply adding viral, bacterial and protozoal pathogens to the media. The enteroids immune-epithelial component has been be characterised using a highly multiplexed qPCR array developed for

evaluation of chicken immune responses. To expand the potential applications of this model, enteroids from different species and ages of poultry, and from different regions of the intestine have also been developed.

This study has demonstrated that the floating chicken enteroids mimic many of the *in vivo* intestinal mucosal functions of the post-hatch chick. These models therefore provide a much more accurate representation of gut architecture and epithelial composition than available *in vitro* options. This makes them promising experimental platforms to screen bioactive compounds and microbiomes; phenotype breeds to understand genetic diversity and its influence on disease resistance, investigate food digestion and nutrient absorption; perform basic biological research to explore responses of the gut to infectious and non-infectious insults; and conduct disease modelling to understand the mechanisms of infectious diseases, especially zoonotic pathogens and those with narrow host or tissue tropisms.

The development of these novel apical-out leukocyte-containing 3D chicken enteroids has advanced the field of avian *in vitro* tools substantially. It overcomes many previous cell culture limitations and as such should reduce the costs and numbers of chickens used in basic and commercial research and development.

REFERENCES

1. Vervelde L, Jeurissen SH. Postnatal development of intra-epithelial leukocytes in the chicken digestive tract: phenotypical characterization in situ. *Cell and Tissue Research* **274**, 295-301 (1993).

2. Glendinning L, Watson KA, Watson M. Development of the duodenal, ileal, jejunal and caecal microbiota in chickens. *Animal Microbiome* **1**, 17 (2019).

3. Ferrer R, Planas JM, Moretó M. Cell apical surface area in enterocytes from chicken small and large intestine during development. *Poultry Science* **74**, (1995).

4. López-Osorio S, Chaparro-Gutiérrez JJ, Gómez-Osorio LM. Overview of poultry Eimeria life cycle and host-parasite interactions. *Frontiers in Veterinary Science* **7**, (2020).

5. Zhang H*, et al.* Cellular composition and differentiation signaling in chicken small intestinal epithelium. *Animals* **9**, 870 (2019).

6. Peterson LW, Artis D. Intestinal epithelial cells: regulators of barrier function and immune homeostasis. *Nature Reviews Immunology* **14**, 141-153 (2014).

7. Geyra A, Uni Z, Sklan D. Enterocyte dynamics and mucosal development in the posthatch chick. *Poultry Science* **80**, 776-782 (2001).

8. Uni Z, Noy Y, Sklan D. Posthatch development of small intestinal function in the poult. *Poultry Science* **78**, 215-222 (1999).

9. Uni Z, Smirnov A, Sklan D. Pre- and posthatch development of goblet cells in the broiler small intestine: effect of delayed access to feed. *Poultry Science* **82**, 320-327 (2003).

10. Rawdon BB, Andrew A. Gut endocrine cells in birds: an overview, with particular reference to the chemistry of gut peptides and the distribution, ontogeny, embryonic origin and differentiation of the endocrine cells. *Progress in Histochemistry and Cytochemistry* **34**, 3-82 (1999).

11. Noah TK, Donahue B, Shroyer NF. Intestinal development and differentiation. *Experimental Cell Research* **317**, 2702-2710 (2011).

12. Zhang H, Wong EA. Identification of cells expressing OLFM4 and LGR5 mRNA by in situ hybridization in the yolk sac and small intestine of embryonic and early post-hatch chicks. *Poultry Science* **97**, 628-633 (2018).

13. Yan KS*, et al.* The intestinal stem cell markers Bmi1 and Lgr5 identify two functionally distinct populations. *Proceedings of the National Academy of Sciences* **109**, 466-471 (2012).

14. Paneth J. Ueber die secernirenden Zellen des Dünndarm-Epithels. *Archiv für Mikroskopische Anatomie* **31**, 113 (1887).

15. Porter EM, Bevins CL, Ghosh D, Ganz T. The multifaceted Paneth cell. *Cellular and Molecular Life Sciences : CMLS* **59**, 156-170 (2002).

16. Wang L*, et al.* Identification of the Paneth cells in chicken small intestine. *Poultry Science* **95**, 1631-1635 (2016).

17. Nile CJ, Townes CL, Michailidis G, Hirst BH, Hall J. Identification of chicken lysozyme g2 and its expression in the intestine. *Cellular and Molecular Life Sciences : CMLS* **61**, 2760-2766 (2004).

18. Bar Shira E, Friedman A. Innate immune functions of avian intestinal epithelial cells: Response to bacterial stimuli and localization of responding cells in the developing avian digestive tract. *PLoS One* **13**, e0200393 (2018).

19. Uni Z, Platin R, Sklan D. Cell proliferation in chicken intestinal epithelium occurs both in the crypt and along the villus. *Journal of Comparative Physiology B* **168**, 241-247 (1998).

20. Mabbott NA, Donaldson DS, Ohno H, Williams IR, Mahajan A. Microfold (M) cells: important immunosurveillance posts in the intestinal epithelium. *Mucosal Immunology* **6**, 666-677 (2013).

21. Balic A*, et al.* Antigen Sampling CSF1R-Expressing Epithelial Cells Are the Functional Equivalents of Mammalian M Cells in the Avian Follicle-Associated Epithelium. *Frontiers in Immunology* **10**, (2019).

22. Casteleyn C, Doom M, Lambrechts E, Van den Broeck W, Simoens P, Cornillie P. Locations of gut-associated lymphoid tissue in the 3-month-old chicken: a review. *Avian Pathology : Journal of the WVPA* **39**, 143-150 (2010).

23. Kajiwara E, Shigeta A, Horiuchi H, Matsuda H, Furusawa S. Development of Peyer's patch and cecal tonsil in gut-associated lymphoid tissues in the chicken embryo. *Journal of Veterinary Medical Science* **65**, 607-614 (2003).

24. Lillehoj HS. Analysis of *Eimeria acervulina*-induced changes in the intestinal T lymphocyte subpopulations in two chicken strains showing different levels of susceptibility to coccidiosis. *Research in Veterinary Science* **56**, 1-7 (1994).

25. Gobel TW, Kaspers B, Stangassinger M. NK and T cells constitute two major, functionally distinct intestinal epithelial lymphocyte subsets in the chicken. *International Immunology* **13**, 757-762 (2001).

26. Chen CH, Göbel TW, Kubota T, Cooper MD. T cell development in the chicken. *Poultry Science* **73**, 1012-1018 (1994).

27. Lillehoj HS, Chung KS. Postnatal development of T-lymphocyte subpopulations in the intestinal intraepithelium and lamina propria in chickens. *Veterinary Immunology and Immunopathology* **31**, 347-360 (1992).

28. Uni Z, Tako E, Gal-Garber O, Sklan D. Morphological, molecular, and functional changes in the chicken small intestine of the late-term embryo. *Poultry Science* **82**, 1747-1754 (2003).

29. Quaroni A. Pre- and postnatal development of differentiated functions in rat intestinal epithelial cells. *Developmental Biology* **111**, 280-292 (1985).

30. Uni Z, Noy Y, Sklan D. Posthatch changes in morphology and function of the small intestines in heavy- and light-strain chicks. *Poultry Science* **74**, 1622-1629 (1995).

31. Bry L, *et al.* Paneth cell differentiation in the developing intestine of normal and transgenic mice. *Procedings of the National Academy Sciences U S A* **91**, 10335-10339 (1994).

32. Dehmer JJ*, et al.* Expansion of intestinal epithelial stem cells during murine development. *PLoS One* **6**, e27070 (2011).

33. Uni Z, Geyra A, Ben-Hur H, Sklan D. Small intestinal development in the young chick: crypt formation and enterocyte proliferation and migration. *British Poultry Science* **41**, 544-551 (2000).

34. Barker N. The canonical Wnt/beta-catenin signalling pathway. *Methods in Molecular Biology* **468**, 5-15 (2008).

35. Sato T, Clevers H. Growing self-organizing mini-guts from a single intestinal stem cell: mechanism and applications. *Science* **340**, 1190-1194 (2013).

36. van Es JH*, et al.* Wnt signalling induces maturation of Paneth cells in intestinal crypts. *Nature Cell Biology* **7**, 381-386 (2005).

37. Batlle E*, et al.* β-Catenin and TCF mediate cell positioning in the intestinal epithelium by controlling the expression of EphB/EphrinB. *Cell* **111**, 251-263 (2002).

38. de Lau W*, et al.* Lgr5 homologues associate with Wnt receptors and mediate R-spondin signalling. *Nature* **476**, 293-297 (2011).

39. Hao HX*, et al.* ZNRF3 promotes Wnt receptor turnover in an R-spondin-sensitive manner. *Nature* **485**, 195-200 (2012).

40. Sato T*, et al.* Paneth cells constitute the niche for Lgr5 stem cells in intestinal crypts. *Nature* **469**, 415-418 (2011).

41. Han YQ*, et al.* Molecular cloning and tissue distribution profiles of the chicken R-spondin1 gene. *Genetics and Molecular Research : GMR* **14**, 3090-3097 (2015).

42. Sato T*, et al.* Long-term expansion of epithelial organoids from human colon, adenoma, adenocarcinoma, and Barrett's epithelium. *Gastroenterology* **141**, 1762-1772 (2011).

43. Sato T*, et al.* Single Lgr5 stem cells build crypt–villus structures in vitro without a mesenchymal niche. *Nature* **459**, 262 (2009).

44. Ueo T*, et al.* The role of Hes genes in intestinal development, homeostasis and tumor formation. *Development* **139**, 1071-1082 (2012).

45. Hansson GC. Role of mucus layers in gut infection and inflammation. *Current Opinions in Microbiology* **15**, 57-62 (2012).

46. Mestecky J, Russell M, Elson C. Intestinal IgA: novel views on its function in the defence of the largest mucosal surface. *Gut* **44**, 2-5 (1999).

47. Bar-Shira E, Cohen I, Elad O, Friedman A. Role of goblet cells and mucin layer in protecting maternal IgA in precocious birds. *Developmental & Comparative Immunology* **44**, 186-194 (2014).

48. Friedman A, Bar-shira E, Sklan D. Ontogeny of gut associated immune competence in the chick. *World's Poultry Science Journal* **59**, 209-219 (2003).

49. Ohashi W, Hara T, Takagishi T, Hase K, Fukada T. Maintenance of intestinal epithelial homeostasis by zinc transporters. *Digestive Diseases and Sciences* **64**, (2019).

50. Nile CJ, Townes CL, Michailidis G, Hirst BH, Hall J. Identification of chicken lysozyme g2 and its expression in the intestine. *Cellular and Molecular Life Sciences CMLS* **61**, 2760-2766 (2004).

51. Sugiarto H, Yu PL. Avian antimicrobial peptides: the defense role of beta-defensins. *Biochemical and Biophysical Research Communications* **323**, 721-727 (2004).

52. Lehrer RI, Barton A, Daher KA, Harwig SS, Ganz T, Selsted ME. Interaction of human defensins with Escherichia coli. Mechanism of bactericidal activity. *Journal of Clinical Investigation* **84**, 553-561 (1989).

53. Wimley WC, Selsted ME, White SH. Interactions between human defensins and lipid bilayers: evidence for formation of multimeric pores. *Protein Science* **3**, 1362-1373 (1994).

54. Lynn DJ*, et al.* Avian beta-defensin nomenclature: a community proposed update. *Immunology Letters* **110**, 86-89 (2007).

55. Cuperus T, van Dijk A, Dwars RM, Haagsman HP. Localization and developmental expression of two chicken host defense peptides: cathelicidin-2 and avian β-defensin 9. *Developmental & Comparative Immunology* **61**, 48-59 (2016).

56. Evans EW, Beach GG, Wunderlich J, Harmon BG. Isolation of antimicrobial peptides from avian heterophils. *Journal of Leukocyte Biology* **56**, 661-665 (1994).

57. Zhao C, Nguyen T, Liu L, Sacco RE, Brogden KA, Lehrer RI. Gallinacin-3, an inducible epithelial beta-defensin in the chicken. *Infection and Immunity* **69**, 2684-2691 (2001).

58. Evans EW, Beach FG, Moore KM, Jackwood MW, Glisson JR, Harmon BG. Antimicrobial activity of chicken and turkey heterophil peptides CHP1, CHP2, THP1, and THP3. *Veterinary Microbiology* **47**, 295-303 (1995).

59. Higgs R*, et al.* The synthetic form of a novel chicken beta-defensin identified in silico is predominantly active against intestinal pathogens. *Immunogenetics* **57**, 90-98 (2005).

60. van Dijk A, *et al*. The beta-defensin gallinacin-6 is expressed in the chicken digestive tract and has antimicrobial activity against food-borne pathogens. *Antimicrobial Agents and Chemotherapy* **51**, 912-922 (2007).

61. Ragland SA, Criss AK. From bacterial killing to immune modulation: Recent insights into the functions of lysozyme. *PLoS Pathogens* **13**, e1006512 (2017).

62. Zerega B, *et al*. Avidin expression during chick chondrocyte and myoblast development in vitro and in vivo: regulation of cell proliferation. *Journal of Cell Science* **114**, 1473-1482 (2001).

63. Odenwald MA, Turner JR. The intestinal epithelial barrier: a therapeutic target? *Nature Reviews Gastroenterology & Hepatology* **14**, 9-21 (2017).

64. Farquhar MG, Palade GE. Junctional complexes in various epithelia. *Journal of Cell Biology* **17**, 375-412 (1963).

65. Nagalingam NA, Lynch SV. Role of the microbiota in inflammatory bowel diseases. *Inflammatory Bowel Diseases* **18**, 968-984 (2012).

66. De Santis S, Cavalcanti E, Mastronardi M, Jirillo E, Chieppa M. Nutritional keys for intestinal barrier modulation. *Frontiers in Immunology* **6**, 612 (2015).

67. Awad WA, Hess C, Hess M. Enteric pathogens and their toxin-induced disruption of the intestinal barrier through alteration of tight junctions in chickens. *Toxins* **9**, (2017).

68. Chelakkot C, Ghim J, Ryu SH. Mechanisms regulating intestinal barrier integrity and its pathological implications. *Experimental & Molecular Medicine* **50**, 1-9 (2018).

69. McWhorter TJ, Caviedes-Vidal E, Karasov WH. The integration of digestion and osmoregulation in the avian gut. *Biological Reviews* **84**, 533-565 (2009).

70. Noy Y, Uni Z, Sklan D. Routes of yolk utilisation in the newly-hatched chick. *British Poultry Science* **37**, 987-996 (1996).

71. Noble R, Moore J. Studies on the lipid metabolism of the chick embryo. *Canadian Journal of Biochemistry* **42**, 1729-1741 (1964).

72. Sklan D. Fat and carbohydrate use in posthatch chicks. *Poultry Science* **82**, 117-122 (2003).

73. Maldonado-Contreras AL, McCormick BA. Intestinal epithelial cells and their role in innate mucosal immunity. *Cell and Tissue Research* **343**, 5-12 (2011).

74. Oakley BB*, et al.* The chicken gastrointestinal microbiome. *FEMS Microbiology Letters* **360**, 100-112 (2014).

75. Roto SM, Rubinelli PM, Ricke SC. An introduction to the avian gut microbiota and the effects of yeast-based prebiotic-type compounds as potential feed additives. *Front Vet Sci* **2**, 28 (2015).

76. Abreu MT. Toll-like receptor signalling in the intestinal epithelium: how bacterial recognition shapes intestinal function. *Nature Reviews Immunology* **10**, 131-144 (2010).

77. Sommer F, Bäckhed F. The gut microbiota—masters of host development and physiology. *Nature Reviews Microbiology* **11**, 227-238 (2013).

78. Kaspers B, Lettmann S, Roell S. Development of the gut associated immune system. In: *20th European Symposium on Poultry Nutrition*) (2015).

79. Zenner C*, et al.* Early-Life Immune System Maturation in Chickens Using a Synthetic Community of Cultured Gut Bacteria. *mSystems* **6**, e01300-01320 (2021).

80. Belkaid Y, Harrison OJ. Homeostatic Immunity and the Microbiota. *Immunity* **46**, 562-576 (2017).

81. Broom LJ, Kogut MH. The role of the gut microbiome in shaping the immune system of chickens. *Veterinary Immunology and Immunopathology* **204**, 44-51 (2018).

82. Gourbeyre P, Denery S, Bodinier M. Probiotics, prebiotics, and synbiotics: impact on the gut immune system and allergic reactions. *Journal of Leukocyte Biology* **89**, 685-695 (2011).

83. Eren U*, et al.* The several elements of intestinal innate immune system at the beginning of the life of broiler chicks. *Microscopy Research and Technique* **79**, 604-614 (2016).

84. Akira S, Hoshino K. Myeloid differentiation factor 88—dependent and —independent pathways in toll-like receptor signaling. *Journal of Infectious Diseases* **187**, S356-363 (2003).

85. Kaiser A*, et al.* Susceptibility of primary chicken intestinal epithelial cells for low pathogenic avian influenza virus and velogenic viscerotropic Newcastle disease virus. *Virus Research* **225**, 50-63 (2016).

86. Li Y-P, Ingmer H, Madsen M, Bang DD. Cytokine responses in primary chicken embryo intestinal cells infected with Campylobacter jejuni strains of human and chicken origin and the expression of bacterial virulence-associated genes. *BMC Microbiology* **8**, 1-10 (2008).

87. Lee Y, Kim WH, Lee S-j, Lillehoj HS. Detection of chicken interleukin-10 production in intestinal epithelial cells and necrotic enteritis induced by Clostridium perfringens using capture ELISA. *Veterinary Immunology and Immunopathology* **204**, 52-58 (2018).

88. Boismenu R, Havran WL. Modulation of epithelial cell growth by intraepithelial gamma delta T cells. *Science* **266**, 1253-1255 (1994).

89. Roberts SJ*, et al.* T-cell alpha beta + and gamma delta + deficient mice display abnormal but distinct phenotypes toward a natural, widespread infection of the intestinal epithelium. *Procedures of the National Academy of Sciences U S A* **93**, 11774-11779 (1996).

90. Ramsburg E, Tigelaar R, Craft J, Hayday A. Age-dependent requirement for gammadelta T cells in the primary but not secondary protective immune response against an intestinal parasite. *Journal of Experimental Medicine* **198**, 1403-1414 (2003).

91. Onai N, Kitabatake M, Zhang YY, Ishikawa H, Ishikawa S, Matsushima K. Pivotal role of CCL25 (TECK)-CCR9 in the formation of gut cryptopatches and consequent appearance of intestinal intraepithelial T lymphocytes. *International Immunology* **14**, 687-694 (2002).

92. Hosoe N*, et al.* Demonstration of functional role of TECK/CCL25 in T lymphocyte-endothelium interaction in inflamed and uninflamed intestinal mucosa. *American Journal of Physiology Gastrointestinal Liver Physiology* **286**, G458-466 (2004).

93. Bar-Shira E, Friedman A. Ontogeny of gut associated immune competence in the chick. *Israel Journal of Veterinary Medicine* **60**, 42-50 (2005).

94. Kogut MH. Dynamics of a protective avian inflammatory response: the role of an IL-8-like cytokine in the recruitment of heterophils to the site of organ invasion by *Salmonella enteritidis*. *Comparative Immunology, Microbiology and Infectious Diseases* **25**, 159-172 (2002).

95. Kogut MH, Iqbal M, He H, Philbin V, Kaiser P, Smith A. Expression and function of Toll-like receptors in chicken heterophils. *Developmental & Comparative Immunology* **29**, 791-807 (2005).

96. Wells LL, Lowry VK, Deloach JR, Kogut MH. Age-dependent phagocytosis and bactericidal activities of the chicken heterophil. *Developmental & Comparative Immunology* **22**, 103-109 (1998).

97. Bockman DE, Cooper MD. Pinocytosis by epithelium associated with lymphoid follicles in the bursa of Fabricius, appendix, and Peyer's patches. An electron microscopic study. *American Journal of Anatomy* **136**, 455-477 (1973).

98. Knoop KA, Miller MJ, Newberry RD. Trans-epithelial antigen delivery in the small intestine: different paths, different outcomes. *Current Opinion in Gastroenterology* **29**, 112 (2013).

99. Birchenough GM, Johansson ME, Gustafsson JK, Bergström JH, Hansson GC. New developments in goblet cell mucus secretion and function. *Mucosal Immunology* **8**, 712-719 (2015).

100. Johansen F-E, Kaetzel C. Regulation of the polymeric immunoglobulin receptor and IgA transport: new advances in environmental factors that stimulate pIgR expression and its role in mucosal immunity. *Mucosal Immunology* **4**, 598-602 (2011).

101. Bani D, Nistri S. New insights into the morphogenic role of stromal cells and their relevance for regenerative medicine. lessons from the heart. *Journal of Cellular and Molecular Medicine* **18**, 363-370 (2014).

102. Nowarski R, Jackson R, Flavell RA. The Stromal Intervention: Regulation of immunity and inflammation at the epithelial-mesenchymal barrier. *Cell* **168**, 362-375 (2017).

103. Daniel E, Cleaver O. Vascularizing organogenesis: Lessons from developmental biology and implications for regenerative medicine. *Current Topics in Developmental Biology* **132**, 177-220 (2019).

104. Powell DW, Pinchuk IV, Saada JI, Chen X, Mifflin RC. Mesenchymal cells of the intestinal lamina propria. *Annual Review of Physiology* **73**, 213-237 (2011).

105. Yason CV, Summers BA, Schat KA. Pathogenesis of rotavirus infection in various age groups of chickens and turkeys: pathology. *American Journal of Veterinary Research* **48**, 927-938 (1987).

106. Powell DW, Mifflin R, Valentich J, Crowe S, Saada J, West A. Myofibroblasts. II. Intestinal subepithelial myofibroblasts. *American Journal of Physiology-Cell Physiology* **277**, C183-C201 (1999).

107. Rosenblum JD, Boyle CM, Schwartz LB. The mesenteric circulation. Anatomy and physiology. *The Surgical Clinics of North America* **77**, 289-306 (1997).

108. Frasher Jr WG, Wayland H. A repeating modular organization of the microcirculation of cat mesentery. *Microvascular Research* **4**, 62-76 (1972).

109. Sugito M, Araki K, Ogata T. Three-dimensional organization of lymphatics in the dog stomach: A scanning electron microscopic study of corrosion casts. *Archives of Histology and Cytology* **59**, 61-70 (1996).

110. Le Douarin NM, Teillet M-Ae. The migration of neural crest cells to the wall of the digestive tract in avian embryo. *Development* **30**, 31-48 (1973).

111. Furness JB. The enteric nervous system and neurogastroenterology. *Nature Reviews Gastroenterology & Hepatology* **9**, 286-294 (2012).

112. Chevalier NR, Dacher N, Jacques C, Langlois L, Guedj C, Faklaris O. Embryogenesis of the peristaltic reflex. *Journal of Physiology* **597**, 2785-2801 (2019).

113. Gulbransen BD, Sharkey KA. Novel functional roles for enteric glia in the gastrointestinal tract. *Nature Reviews Gastroenterology & Hepatology* **9**, 625-632 (2012).

114. Balaskas C, Gabella G. Glial fibrillary acidic protein (GFAP) immunoreactivity in enteric ganglia of the chick embryo. *Brain Research* **804**, 275-283 (1998).

115. Burns RB, Maxwell MH. Ultrastructure of Peyer's patches in the domestic fowl and turkey. *Journal of Anatomy* **147**, 235-243 (1986).

116. Gallego M, del Cacho E, Bascuas JA. Antigen-binding cells in the cecal tonsil and Peyer's patches of the chicken after bovine serum albumin administration. *Poultry Science* **74**, 472-479 (1995).

117. Jeurissen SH, Wagenaar F, Janse EM. Further characterization of M cells in gut-associated lymphoid tissues of the chicken. *Poultry Science* **78**, 965-972 (1999).

118. Kitagawa H, Shiraishi S, Imagawa T, Uehara M. Ultrastructural characteristics and lectin-binding properties of M cells in the follicle-associated epithelium of chicken caecal tonsils. *Journal of Anatomy* **197 Pt 4**, 607-616 (2000).

119. Vaughn LE, Holt PS, Moore RW, Gast RK. Enhanced gross visualization of chicken Peyer's patch: novel staining technique applied to fresh tissue specimens. *Avian Diseases* **50**, 298-302 (2006).

120. Balic A*, et al.* Visualisation of chicken macrophages using transgenic reporter genes: insights into the development of the avian macrophage lineage. *Development* **141**, 3255-3265 (2014).

121. Befus AD, Johnston N, Leslie G, Bienenstock J. Gut-associated lymphoid tissue in the chicken. I. Morphology, ontogeny, and some functional characteristics of Peyer's patches. *Journal of Immunology* **125**, 2626-2632 (1980).

122. Del Moral MG, Fonfria J, Varas A, Jimenez E, Moreno J, Zapata A. Appearance and development of lymphoid cells in the chicken (Gallus gallus) caecal tonsil. *The Anatomical Record: An Official Publication of the American Association of Anatomists* **250**, 182-189 (1998).

123. Bar-Shira E, Sklan D, Friedman A. Establishment of immune competence in the avian GALT during the immediate post-hatch period. *Developmental & Comparative Immunology* **27**, 147-157 (2003).

124. Honjo K, Hagiwara T, Itoh K, Takahashi E, Hirota Y. Immunohistochemical analysis of tissue distribution of B and T cells in germfree and conventional chickens. *Journal of Veterinary Medical Science* **55**, 1031-1034 (1993).

125. Dunon D*, et al.* Ontogeny of the immune system: γ/δ and α/β T cells migrate from thymus to the periphery in alternating waves. *Journal of Experimental Medicine* **186**, 977-988 (1997).

126. Hemmingsson EJ, Linna TJ. Ontogenetic studies on lymphoid cell traffic in the chicken. I. Cell migration from the bursa of Fabricius. *International Archives of Allergy and Applied Immunology* **42**, 693-710 (1972).

127. Burton R, Harrison J. The relative differential leucocyte count of the newly hatched chick. *Poultry Science* **48**, 451-453 (1969).

128. Qureshi MA, Heggen CL, Hussain I. Avian macrophage: effector functions in health and disease. *Developmental & Comparative Immunology* **24**, 103-119 (2000).

129. Neulen M-L, Göbel TW. Chicken CD56 defines NK cell subsets in embryonic spleen and lung. *Developmental & Comparative Immunology* **38**, 410-415 (2012).

130. Rogers SL, Viertlboeck BC, Göbel TW, Kaufman J. Avian NK activities, cells and receptors. In: *Seminars in Immunology* (2008).

131. Göbel TW, Kaspers B, Stangassinger M. NK and T cells constitute two major, functionally distinct intestinal epithelial lymphocyte subsets in the chicken. *International Immunology* **13**, 757-762 (2001).

132. Crosnier C, Stamataki D, Lewis J. Organizing cell renewal in the intestine: stem cells, signals and combinatorial control. *Nature Reviews Genetics* **7**, 349-359 (2006).

133. Thomson CA, Nibbs RJ, McCoy KD, Mowat AM. Immunological roles of intestinal mesenchymal cells. *Immunology* **160**, 313-324 (2020).

134. Savidge TC*, et al.* Enteric glia regulate intestinal barrier function and inflammation via release of S-nitrosoglutathione. *Gastroenterology* **132**, 1344-1358 (2007).

135. Barajon I*, et al.* Toll-like receptors 3, 4, and 7 are expressed in the enteric nervous system and dorsal root ganglia. *Journal of Histochemistry and Cytochemistry : Official Journal of the Histochemistry Society* **57**, 1013-1023 (2009).

136. Hume DA, Ross IL, Himes SR, Sasmono RT, Wells CA, Ravasi T. The mononuclear phagocyte system revisited. *Journal of Leukocyte Biology* **72**, 621-627 (2002).

137. Withanage GSK*, et al.* Rapid expression of chemokines and proinflammatory cytokines in newly hatched chickens infected with Salmonella enterica serovar typhimurium. *Infection and Immunity* **72**, 2152-2159 (2004).

138. Rohde F*, et al.* Characterization of chicken tumor necrosis factor-α, a long missed cytokine in birds. *Frontiers in Immunology* **9**, 605 (2018).

139. Agace WW, McCoy KD. Regionalized Development and Maintenance of the Intestinal Adaptive Immune Landscape. *Immunity* **46**, 532-548 (2017).

140. Romagnani S. Lymphokine production by human T cells in disease states. *Annual Review of Immunology* **12**, 227-257 (1994).

141. Luckheeram RV, Zhou R, Verma AD, Xia B. $CD4^+$T cells: differentiation and functions. *Clinical & Developmental Immunology* **2012**, 925135 (2012).

142. Shanmugasundaram R, Selvaraj RK. Regulatory T cell properties of chicken CD4+ CD25+ cells. *Journal of Immunology* **186**, 1997-2002 (2011).

143. Guo P, *et al*. The chicken TH1 response: Potential therapeutic applications of ChIFN-γ. *Developmental & Comparative Immunology* **41**, 389-396 (2013).

144. Gast RK, Beard CW. Age-related changes in the persistence and pathogenicity of Salmonella typhimurium in chicks. *Poultry Science* **68**, 1454-1460 (1989).

145. Barrow PA, Lovell MA, Szmolleny G, Murphy CK. Effect of enrofloxacin administration on excretion of Salmonella enteritidis by experimentally infected chickens and on quinolone resistance of their Escherichia coli flora. *Avian Pathology : Journal of the WVPA* **27**, 586-590 (1998).

146. Rose ME. Immunity to coccidiosis: maternal transfer in Eimeria maxima infections. *Parasitology* **65**, 273-282 (1972).

147. Hassan JO, Curtiss R, 3rd. Effect of vaccination of hens with an avirulent strain of Salmonella typhimurium on immunity of progeny challenged with wild-Type Salmonella strains. *Infection and Immunity* **64**, 938-944 (1996).

148. Sahin O, Luo N, Huang S, Zhang Q. Effect of Campylobacter-specific maternal antibodies on Campylobacter jejuni colonization in young chickens. *Applied Environmental Microbiology* **69**, 5372-5379 (2003).

149. Food and Agriculture Organisation of the United Nations. FAOSTAT. (2019).

150. Alexandratos N BJ. World agriculture towards 2030/2050: the 2012 revision (ESA working paper no. 12-03). (ed Agricultural Development Economics Division GPST) (2012).

151. Hafez HM, Hauck R. Zoonoses with public health relevance in poultry. In: *Zoonoses-Infections Affecting Humans and Animals*. Springer (2015).

152. Zhou J*, et al.* Infection of bat and human intestinal organoids by SARS-CoV-2. *Nature Medicine* **26**, 1077-1083 (2020).

153. Intarapat S, Stern CD. Chick stem cells: Current progress and future prospects. *Stem Cell Research* **11**, 1378-1392 (2013).

154. Kain KH*, et al.* The chick embryo as an expanding experimental model for cancer and cardiovascular research. *Developmental dynamics : an official publication of the American Association of Anatomists* **243**, 216-228 (2014).

155. Ulmer JB, Valley U, Rappuoli R. Vaccine manufacturing: challenges and solutions. *Nature Biotechnology* **24**, 1377-1383 (2006).

156. Ben-David U*, et al.* Genetic and transcriptional evolution alters cancer cell line drug response. *Nature* **560**, 325-330 (2018).

157. Berschneider H. Development of normal cultured small intestinal epithelial cell lines which transport Na and Cl. *Gastroenterology* **96**, A41 (1989).

158. Schierack P*, et al.* Characterization of a porcine intestinal epithelial cell line for in vitro studies of microbial pathogenesis in swine. *Histochemistry and Cell Biology* **125**, 293-305 (2006).

159. Zakrzewski SS*, et al.* Improved Cell Line IPEC-J2, Characterized as a model for porcine jejunal epithelium. *PLoS One* **8**, e79643 (2013).

160. Miyazawa K*, et al.* Characterization of newly established bovine intestinal epithelial cell line. *Histochemistry and Cell Biology* **133**, 125-134 (2010).

161. Chiba E*, et al.* A newly established bovine intestinal epithelial cell line is effective for in vitro screening of potential antiviral immunobiotic microorganisms for cattle. *Research in Veterinary Science* **93**, 688-694 (2012).

162. Esnault E*, et al.* A novel chicken lung epithelial cell line: characterization and response to low pathogenicity avian influenza virus. *Virus Research* **159**, 32-42 (2011).

163. Dimier-Poisson I, Bout D, Quéré P. Chicken primary enterocytes: inhibition of Eimeria tenella replication after activation with crude interferon-γ supernatants. *Avian Diseases* **48**, 617-624 (2004).

164. Kaiser A, Willer T, Steinberg P, Rautenschlein S. Establishment of an in vitro intestinal epithelial cell culture model of avian origin. *Avian Diseases* **61**, 229-236 (2017).

165. Bai S*, et al.* Uptake of manganese from the manganese-lysine complex in primary chicken intestinal epithelial cells. *Animals* **9**, 559 (2019).

166. Rath NC, Liyanage R, Gupta A, Packialakshmi B, Lay Jr JO. A method to culture chicken enterocytes and their characterization. *Poultry Science* **97**, 4040-4047 (2018).

167. Ghiselli F*, et al.* Isolation, culture, and characterization of chicken intestinal epithelial cells. *BMC Molecular and Cell Biology* **22**, 12 (2021).

168. Rusu D, Loret S, Peulen O, Mainil J, Dandrifosse G. Immunochemical, biomolecular and biochemical characterization of bovine epithelial intestinal primocultures. *BMC Cell Biology* **6**, 1-12 (2005).

169. Girard F, Batisson I, Frankel GM, Harel J, Fairbrother JM. Interaction of enteropathogenic and Shiga toxin-producing Escherichia coli and porcine intestinal mucosa: role of intimin and Tir in adherence. *Infection and Immunity* **73**, 6005-6016 (2005).

170. Kolf-Clauw M*, et al.* Development of a pig jejunal explant culture for studying the gastrointestinal toxicity of the mycotoxin deoxynivalenol: Histopathological analysis. *Toxicology In Vitro* **23**, 1580-1584 (2009).

171. Girard F, Dziva F, van Diemen P, Phillips AD, Stevens MP, Frankel G. Adherence of enterohemorrhagic Escherichia coli O157, O26, and O111 strains to bovine intestinal explants ex vivo. *Applied and Environmental Microbiology* **73**, 3084-3090 (2007).

172. Kallapura G*, et al.* Development of an ex vivo ileal explant culture method for amplified production and differential measurement of nitrite. *International Journal of Poultry Science* **14**, 245 (2015).

173. Zhang Q, Eicher SD, Ajuwon KM, Applegate TJ. Development of a chicken ileal explant culture model for measurement of gut inflammation induced by lipopolysaccharide. *Poultry Science* **96**, 3096-3103 (2017).

174. Parent E, Burns P, Desrochers A, Boulianne M. A ligated intestinal loop model in anesthetized specific pathogen free chickens to study Clostridium perfringens virulence. *Journal of Visualized Experiments : JoVE*, (2018).

175. Valgaeren B*, et al.* The use of an intestinal loop model in semi-ruminating and ruminating calves under complete anaesthesia: an in vivo model with intact neural and vascular systems. In: *BCLAS Symposium 2011* (2011).

176. Hofer M, Lutolf MP. Engineering organoids. *Nature Reviews Materials* **6**, 402-420 (2021).

177. Middendorp S*, et al.* Adult stem cells in the small intestine are intrinsically programmed with their location-specific function. *Stem Cells* **32**, 1083-1091 (2014).

178. Lancaster MA, Knoblich JA. Organogenesis in a dish: Modeling development and disease using organoid technologies. *Science* **345**, 1247125 (2014).

179. Fatehullah A, Tan SH, Barker N. Organoids as an in vitro model of human development and disease. *Nature Cell Biology* **18**, 246-254 (2016).

180. Takahashi K, Yamanaka S. Induction of pluripotent stem cells from mouse embryonic and adult fibroblast cultures by defined factors. *Cell* **126**, 663-676 (2006).

181. Evans GS, Flint N, Somers AS, Eyden B, Potten CS. The development of a method for the preparation of rat intestinal epithelial cell primary cultures. *Journal of Cell Science* **101**, 219-231 (1992).

182. Spence JR*, et al.* Directed differentiation of human pluripotent stem cells into intestinal tissue in vitro. *Nature* **470**, 105-109 (2011).

183. Hamilton CA*, et al.* Development of in vitro enteroids derived from bovine small intestinal crypts. *Veterinary Research* **49**, 54-54 (2018).

184. Gonzalez LM, Williamson I, Piedrahita JA, Blikslager AT, Magness ST. Cell lineage identification and stem cell culture in a porcine model for the study of intestinal epithelial regeneration. *PloS One* **8**, e66465-e66465 (2013).

185. Beaumont M*, et al.* Intestinal organoids in farm animals. *Veterinary Research* **52**, 33 (2021).

186. van der Hee B, Madsen O, Vervoort J, Smidt H, Wells JM. Congruence of transcription programs in adult stem cell-derived jejunum organoids and original tissue during long-term culture. *Frontiers in Cell and Developmental Biology* **8**, 375 (2020).

187. Kleinman HK, Martin GR. Matrigel: basement membrane matrix with biological activity. In: *Seminars in Cancer Biology*). Elsevier (2005).

188. Gjorevski N*, et al.* Designer matrices for intestinal stem cell and organoid culture. *Nature* **539**, 560-564 (2016).

189. Velasco V, Shariati SA, Esfandyarpour R. Microtechnology-based methods for organoid models. *Microsystems & Nanoengineering* **6**, 1-13 (2020).

190. Chusilp S, Li B, Lee D, Lee C, Vejchapipat P, Pierro A. Intestinal organoids in infants and children. *Pediatric Surgery International* **36**, (2020).

191. Lamouille S, Xu J, Derynck R. Molecular mechanisms of epithelial-mesenchymal transition. *Nature Reviews Molecular Cell Biology* **15**, 178-196 (2014).

192. Li L*, et al.* Porcine intestinal enteroids: a new model for studying enteric coronavirus Porcine Epidemic Diarrhea Virus infection and the host innate response. *Journal of Virology* **93**, (2019).

193. Khalil HA*, et al.* A novel culture system for adult porcine intestinal crypts. *Cell and Tissue Research* **365**, 123-134 (2016).

194. Zhou JY*, et al.* Wnt/β-catenin-mediated heat exposure inhibits intestinal epithelial cell proliferation and stem cell expansion through endoplasmic reticulum stress. *Journal of Cellular Physiology* **235**, 5613-5627 (2020).

195. Powell RH, Behnke MS. WRN conditioned media is sufficient for in vitro propagation of intestinal organoids from large farm and small companion animals. *Biology Open* **6**, 698-705 (2017).

196. Töpfer E*, et al.* Bovine colon organoids: From 3D bioprinting to cryopreserved multi-well screening platforms. *Toxicology In Vitro : An International Journal Published in Association with BIBRA* **61**, 104606 (2019).

197. Alfajaro MM*, et al.* Dual recognition of sialic acid and αGal epitopes by the VP8* domains of the Bovine Rotavirus G6P[5] WC3 and of its mono-reassortant G4P[5] RotaTeq vaccine strains. *Journal of Virology* **93**, (2019).

198. Derricott H*, et al.* Developing a 3D intestinal epithelium model for livestock species. *Cell and Tissue Research* **375**, 409-424 (2019).

199. Miyoshi H, Ajima R, Luo CT, Yamaguchi TP, Stappenbeck TS. Wnt5a potentiates TGF-β signaling to promote colonic crypt regeneration after tissue injury. *Science* **338**, 108-113 (2012).

200. van der Hee B, Loonen LMP, Taverne N, Taverne-Thiele JJ, Smidt H, Wells JM. Optimized procedures for generating an enhanced, near physiological 2D culture system from porcine intestinal organoids. *Stem Cell Research* **28**, 165-171 (2018).

201. Duque-Correa MA*, et al.* Development of caecaloids to study host–pathogen interactions: new insights into immunoregulatory functions of Trichuris muris extracellular vesicles in the caecum. *International Journal for Parasitology* **50**, 707-718 (2020).

202. Jung P*, et al.* Isolation and in vitro expansion of human colonic stem cells. *Nature Medicine* **17**, 1225-1227 (2011).

203. Yin L*, et al.* Aminopeptidase N expression, not interferon responses, determines the intestinal segmental tropism of Porcine Deltacoronavirus. *Journal of Virology* **94**, (2020).

204. Mustata RC*, et al.* Identification of Lgr5-independent spheroid-generating progenitors of the mouse fetal intestinal epithelium. *Cell Reports* **5**, 421-432 (2013).

205. Fordham RP*, et al.* Transplantation of expanded fetal intestinal progenitors contributes to colon regeneration after injury. *Cell stem cell* **13**, 734-744 (2013).

206. Senger S*, et al.* Human fetal-derived enterospheres provide insights on intestinal development and a novel model to study Necrotizing Enterocolitis (NEC). *Cell Molecular Gastroenterolgy Hepatology* **5**, 549-568 (2018).

207. Navis M*, et al.* Mouse fetal intestinal organoids: new model to study epithelial maturation from suckling to weaning. *EMBO Reports* **20**, e46221 (2019).

208. Mohammad MA, Didelija IC, Stoll B, Burrin DG, Marini JC. Modeling age-dependent developmental changes in the expression of genes involved in citrulline synthesis using pig enteroids. *Physiological Reports* **8**, e14565 (2020).

209. Sato T*, et al.* Single Lgr5 stem cells build crypt-villus structures in vitro without a mesenchymal niche. *Nature* **459**, 262-265 (2009).

210. Heo I*, et al.* Modelling Cryptosporidium infection in human small intestinal and lung organoids. *Nature Microbiology* **3**, 814-823 (2018).

211. Co JY*, et al.* Controlling epithelial polarity: A human enteroid model for host-pathogen interactions. *Cell Reports* **26**, 2509-2520.e2504 (2019).

212. Li Y*, et al.* Next-generation porcine intestinal organoids : an apical-out organoid model for Swine Enteric Virus infection and immune response investigations. *Journal of Virology* **94**, (2020).

213. d'Aldebert E*, et al.* Characterization of human colon organoids from inflammatory bowel disease patients. *Frontiers in Cell and Developmental Biology* **8**, 363 (2020).

214. Braverman J, Yilmaz Ö H. From 3D organoids back to 2D enteroids. *Developmental Cell* **44**, 533-534 (2018).

215. Pierzchalska M, Grabacka M, Michalik M, Zyla K, Pierzchalski P. Prostaglandin E2 supports growth of chicken embryo intestinal organoids in Matrigel matrix. *BioTechniques* **52**, 307-315 (2012).

216. Li J*, et al.* Culture and characterization of chicken small intestinal crypts. *Poultry Science* **97**, 1536-1543 (2018).

217. Acharya M, Arsi K, Donoghue AM, Liyanage R, Rath NC. Production and characterization of avian crypt-villus enteroids and the effect of chemicals. *BMC Veterinary Research* **16**, 179 (2020).

218. Pierzchalska M, Panek M, Czyrnek M, Grabacka M. The three-dimensional culture of epithelial organoids derived from embryonic chicken intestine. *Methods in Molecular Biology* **1576**, 135-144 (2019).

219. Stelzner M*, et al.* A nomenclature for intestinal in vitro cultures. *American Journal of Physiology Gastrointestinal and Liver Physiology* **302**, G1359-1363 (2012).

220. Panek M, Grabacka M, Pierzchalska M. The formation of intestinal organoids in a hanging drop culture. *Cytotechnology* **70**, 1085-1095 (2018).

221. Pierzchalska M, Panek M, Grabacka M. The migration and fusion events related to ROCK activity strongly influence the morphology of chicken embryo intestinal organoids. *Protoplasma* **256**, 575-581 (2019).

222. Pierzchalska M, Panek M, Czyrnek M, Gielicz A, Mickowska B, Grabacka M. Probiotic Lactobacillus acidophilus bacteria or synthetic TLR2 agonist boost the growth of chicken embryo intestinal organoids in cultures comprising epithelial cells and myofibroblasts. *Comparative Immunology, Microbiology and Infectious Diseases* **53**, 7-18 (2017).

223. Krndija D*, et al.* Active cell migration is critical for steady-state epithelial turnover in the gut. *Science* **365**, 705-710 (2019).

224. Lallès JP. Intestinal alkaline phosphatase: multiple biological roles in maintenance of intestinal homeostasis and modulation by diet. *Nutrition Reviews* **68**, 323-332 (2010).

225. McDougald L, Reid W, Taylor E, Mabon J. Effects of anticoccidial and growth promoting agents on intestinal motility in broilers. *Poultry Science* **51**, 416-418 (1972).

226. Finkbeiner SR, Zeng X-L, Utama B, Atmar RL, Shroyer NF, Estes MK. Stem cell-derived human intestinal organoids as an infection model for Rotaviruses. *mBio* **3**, e00159-00112 (2012).

227. Saxena K*, et al.* Human intestinal enteroids: a new model to study human Rotavirus infection, host restriction, and pathophysiology. *Journal of Virology* **90**, 43-56 (2016).

228. Bartfeld S*, et al.* In vitro expansion of human gastric epithelial stem cells and their responses to bacterial infection. *Gastroenterology* **148**, 126-136.e126 (2015).

229. Hill DR*, et al.* Bacterial colonization stimulates a complex physiological response in the immature human intestinal epithelium. *eLife* **6**, e29132 (2017).

230. Ettayebi K*, et al.* Replication of human noroviruses in stem cell–derived human enteroids. *Science* **353**, 1387-1393 (2016).

231. Noel G*, et al.* A primary human macrophage-enteroid co-culture model to investigate mucosal gut physiology and host-pathogen interactions. *Scientific Reports* **7**, 45270 (2017).

232. Resende TP, Medida RL, Vannucci FA, Saqui-Salces M, Gebhart C. Evaluation of swine enteroids as in vitro models for Lawsonia intracellularis infection1,2. *Journal of Animal Science* **98**, (2020).

233. Luo H*, et al.* Utility evaluation of porcine enteroids as PDCoV infection model in vitro. *Frontiers in Microbiology* **11**, 821 (2020).

234. Fitzgerald SF*, et al.* Shiga toxin sub-type 2a increases the efficiency of Escherichia coli O157 transmission between animals and restricts epithelial regeneration in bovine enteroids. *PLoS Pathogens* **15**, e1008003 (2019).

235. Vermeire B, Gonzalez LM, Jansens RJJ, Cox E, Devriendt B. Porcine small intestinal organoids as a model to explore ETEC-host interactions in the gut. *Veterinary Research* **52,** 107 (2021)

236. Forbester JL*, et al.* Interaction of Salmonella enterica serovar Typhimurium with intestinal organoids derived from human induced pluripotent stem cells. *Infection and Immunity* **83**, 2926-2934 (2015).

237. Karve SS, Pradhan S, Ward DV, Weiss AA. Intestinal organoids model human responses to infection by commensal and Shiga toxin producing Escherichia coli. *PLoS One* **12**, e0178966 (2017).

238. Koltes D, Gabler N. Characterization of porcine intestinal enteroid cultures under a lipopolysaccharide challenge. *Journal of Animal Science* **94**, 335-339 (2016).

239. Ferrandis Vila M*, et al.* Dietary fiber sources and non-starch polysaccharide-degrading enzymes modify mucin expression and the immune profile of the swine ileum. *PLoS One* **13**, e0207196 (2018).

240. Min S, Kim S, Cho S-W. Gastrointestinal tract modeling using organoids engineered with cellular and microbiota niches. *Experimental & Molecular Medicine* **52**, 227-237 (2020).

241. Rogoz A, Reis BS, Karssemeijer RA, Mucida D. A 3-D enteroid-based model to study T-cell and epithelial cell interaction. *Journal of Immunological Methods* **421**, 89-95 (2015).

242. Lindemans CA*, et al.* Interleukin-22 promotes intestinal-stem-cell-mediated epithelial regeneration. *Nature* **528**, 560-564 (2015).

243. Jung KB*, et al.* Interleukin-2 induces the in vitro maturation of human pluripotent stem cell-derived intestinal organoids. *Nature Communications* **9**, 3039 (2018).

244. Nozaki K*, et al.* Co-culture with intestinal epithelial organoids allows efficient expansion and motility analysis of intraepithelial lymphocytes. *Journal of Gastroenterology* **51**, 206-213 (2016).

245. Lahar N*, et al.* Intestinal subepithelial myofibroblasts support in vitro and in vivo growth of human small intestinal epithelium. *PLoS One* **6**, e26898 (2011).

246. Lei NY*, et al.* Intestinal subepithelial myofibroblasts support the growth of intestinal epithelial stem cells. *PLoS One* **9**, e84651 (2014).

247. Workman MJ*, et al.* Engineered human pluripotent-stem-cell-derived intestinal tissues with a functional enteric nervous system. *Nature Medicine* **23**, 49-59 (2017).

248. Knoop KA*, et al.* RANKL is necessary and sufficient to initiate development of antigen-sampling M cells in the intestinal epithelium. *Journal of Immunology* **183**, 5738-5747 (2009).

249. de Lau W*, et al.* Peyer's patch M cells derived from Lgr5(+) stem cells require SpiB and are induced by RankL in cultured "miniguts". *Molecular and Cellular Biology* **32**, 3639-3647 (2012).

250. Sutton KM, Hu T, Wu Z, Siklodi B, Vervelde L, Kaiser P. The functions of the avian receptor activator of NF-κB ligand (RANKL) and its receptors, RANK and osteoprotegerin, are evolutionarily conserved. *Developmental and Comparative Immunology* **51**, 170-184 (2015).

251. Engevik AC*, et al.* Editing myosin VB gene to create porcine model of microvillus inclusion disease, with microvillus-lined inclusions and alterations in sodium transporters. *Gastroenterology* **158**, 2236-2249. e2239 (2020).

252. Zhu M, Qin YC, Gao CQ, Yan HC, Wang XQ. l-Glutamate drives porcine intestinal epithelial renewal by increasing stem cell activity via upregulation of the EGFR-ERK-mTORC1 pathway. *Food & Function* **11**, 2714-2724 (2020).

253. Wang Z*, et al.* Dietary vitamin A affects growth performance, intestinal development, and functions in weaned piglets by affecting intestinal stem cells. *Journal of Animal Science* **98**, (2020).

254. Galipeau HJ, Verdu EF. The complex task of measuring intestinal permeability in basic and clinical science. *Neurogastroenterology & Motility* **28**, 957-965 (2016).

255. Rallabandi HR, Yang H, Oh KB, Lee HC, Byun SJ, Lee BR. Evaluation of intestinal epithelial barrier function in inflammatory bowel diseases using murine intestinal organoids. *Tissue Engineering and Regenerative Medicine* **17**, 641-650 (2020).

256. Bardenbacher M*, et al.* Permeability analyses and three dimensional imaging of interferon gamma-induced barrier disintegration in intestinal organoids. *Stem Cell Research* **35**, 101383 (2019).

257. Leslie JL*, et al.* Persistence and toxin production by Clostridium difficile within human intestinal organoids result in disruption of epithelial paracellular barrier function. *Infection and Immunity* **83**, 138-145 (2015).

258. Roodsant T*, et al.* A human 2D primary organoid-derived epithelial monolayer model to study host-pathogen interaction in the small intestine. *Frontiers in Cellular and Infection Microbiology* **10**, (2020).

259. Good C, Wells AI, Coyne CB. Type III interferon signaling restricts enterovirus 71 infection of goblet cells. *Science Advances* **5**, eaau4255 (2019).

260. Maidji E, Somsouk M, Rivera JM, Hunt PW, Stoddart CA. Replication of CMV in the gut of HIV-infected individuals and epithelial barrier dysfunction. *PLoS Pathogy* **13**, e1006202 (2017).

261. Grabinger T*, et al.* Ex vivo culture of intestinal crypt organoids as a model system for assessing cell death induction in intestinal epithelial cells and enteropathy. *Cell Death & Disease* **5**, e1228-e1228 (2014).

262. Pantzar N, Weström BR, Luts A, Lundin S. Regional small-intestinal permeability in vitro to different-sized dextrans and proteins in the rat. *Scandinavian Journal of Gastroenterology* **28**, 205-211 (1993).

263. Martin M. Cutadapt removes adapter sequences from high-throughput sequencing reads. *Biology* **17**, 3 (2011).

264. Dobin A*, et al.* STAR: ultrafast universal RNA-seq aligner. *Bioinformatics* **29**, 15-21 (2013).

265. Liao Y, Smyth GK, Shi W. featureCounts: an efficient general purpose program for assigning sequence reads to genomic features. *Bioinformatics* **30**, 923-930 (2014).

266. Robinson MD, McCarthy DJ, Smyth GK. edgeR: a Bioconductor package for differential expression analysis of digital gene expression data. *Bioinformatics* **26**, 139-140 (2010).

267. Freeman TC*, et al.* Construction, visualisation, and clustering of transcription networks from microarray expression data (network analysis of transcriptomics data). *PLoS Computational Biology* **3**, e206 (2007).

268. Athanasios T, Stjin Van D, Anton JE, Tom CF. Network visualization and analysis of gene expression data using BioLayout Express3D. *Nature Protocols* **4**, 1535 (2009).

269. Mabbott NA, Baillie JK, Brown H, Freeman TC, Hume DA. An expression atlas of human primary cells: inference of gene function from coexpression networks. *BMC Genomics* **14**, (2013).

270. Aravind S*, et al.* Gene set enrichment analysis: A knowledge-based approach for interpreting genome-wide expression profiles. *Proceedings of the National Academy of Sciences of the United States of America* **102**, 15545 (2005).

271. Kolde R. pheatmap: Pretty Heatmaps (2019).

272. Vohra P, Vrettou C, Hope JC, Hopkins J, Stevens MP. Nature and consequences of interactions between Salmonella enterica serovar Dublin and host cells in cattle. *Veterinary Research* **50**, 99 (2019).

273. Matrosovich M, Matrosovich T, Garten W, Klenk HD. New low-viscosity overlay medium for viral plaque assays. *Virology Journal* **3**, 63 (2006).

274. Walker RA*, et al.* RNA Seq analysis of the Eimeria tenella gametocyte transcriptome reveals clues about the molecular basis for sexual reproduction and oocyst biogenesis. *BMC Genomics* **16**, 94-94 (2015).

275. Borowska D*, et al.* Highly multiplexed quantitative PCR-based platform for evaluation of chicken immune responses. *PloS One* **14**, e0225658-e0225658 (2019).

276. Huang J*, et al.* Identification of the fatty acid synthase interaction network via iTRAQ-based proteomics indicates the potential molecular mechanisms of liver cancer metastasis. *Cancer Cell International* **20**, 332 (2020).

277. Borowska D, Rothwell L, Bailey RA, Watson K, Kaiser P. Identification of stable reference genes for quantitative PCR in cells derived from chicken lymphoid organs. *Veterinary Immunology and Immunopathology* **170**, 20-24 (2016).

278. Zachos NC*, et al.* Human enteroids/colonoids and intestinal organoids functionally recapitulate normal intestinal physiology and pathophysiology. *Journal of Biological Chemistry* **291**, 3759-3766 (2016).

279. Haber AL*, et al.* A single-cell survey of the small intestinal epithelium. *Nature* **551**, 333-339 (2017).

280. Gregorieff A, Liu Y, Inanlou MR, Khomchuk Y, Wrana JL. Yap-dependent reprogramming of Lgr5(+) stem cells drives intestinal regeneration and cancer. *Nature* **526**, 715-718 (2015).

281. Imajo M, Ebisuya M, Nishida E. Dual role of YAP and TAZ in renewal of the intestinal epithelium. *Nature Cell Biology* **17**, 7-19 (2015).

282. Aragona M*, et al.* A mechanical checkpoint controls multicellular growth through YAP/TAZ regulation by actin-processing factors. *Cell* **154**, 1047-1059 (2013).

283. Vogel V, Sheetz M. Local force and geometry sensing regulate cell functions. *Nature Reviews Molecular Cell Biology* **7**, 265-275 (2006).

284. Matano M*, et al.* Modeling colorectal cancer using CRISPR-Cas9–mediated engineering of human intestinal organoids. *Nature Medicine* **21**, 256-262 (2015).

285. Godugu C, Patel AR, Desai U, Andey T, Sams A, Singh M. AlgiMatrix™ based 3D cell culture system as an in-vitro tumor model for anticancer studies. *PLoS One* **8**, e53708 (2013).

286. Friedrich J, Seidel C, Ebner R, Kunz-Schughart LA. Spheroid-based drug screen: considerations and practical approach. *Nature Protocols* **4**, 309-324 (2009).

287. Grün D*, et al.* Single-cell messenger RNA sequencing reveals rare intestinal cell types. *Nature* **525**, 251-255 (2015).

288. Pat Bucy R, Chen C-IH, Cooper MD. Development of cytoplasmic CD3+/T cell receptor-negative cells in the peripheral lymphoid tissues of chickens. *European Journal of Immunology* **20**, 1345-1350 (1990).

289. Ratié L, Ware M, Jagline H, David V, Dupé V. Dynamic expression of Notch-dependent neurogenic markers in the chick embryonic nervous system. *Frontiers in Neuroanatomy* **8**, (2014).

290. Boesmans W*, et al.* Structurally defined signaling in neuro-glia units in the enteric nervous system. *Glia* **67**, 1167-1178 (2019).

291. Kim KK, Adelstein RS, Kawamoto S. Identification of neuronal nuclei (NeuN) as Fox-3, a new member of the Fox-1 gene family of splicing factors. *Journal of Biological Chemistry* **284**, 31052-31061 (2009).

292. García-Moreno F, Molnár Z. Subset of early radial glial progenitors that contribute to the development of callosal neurons is absent from avian brain. *Proceedings of the National Academy of Sciences* **112**, E5058-E5067 (2015).

293. Pece S, Confalonieri S, P RR, Di Fiore PP. NUMB-ing down cancer by more than just a NOTCH. *Biochimica et Biophysica Acta* **1815**, 26-43 (2011).

294. Lee MK, Tuttle JB, Rebhun LI, Cleveland DW, Frankfurter A. The expression and posttranslational modification of a neuron-specific beta-tubulin isotype during chick embryogenesis. *Cell Motility and the Cytoskeleton* **17**, 118-132 (1990).

295. Foudah D*, et al.* Expression of neural markers by undifferentiated mesenchymal-like stem cells from different sources. *Journal of Immunology Research* **2014**, 987678-987678 (2014).

296. Russell MW, Mestecky J, Strober W, Lambrecht BN, Kelsall BL, Cheroutre H. Chapter 1 - Overview: The mucosal immune system. In: *Mucosal Immunology (Fourth Edition)* Academic Press (2015).

297. Garcia MA, Nelson WJ, Chavez N. Cell-cell junctions organize structural and signaling networks. *Cold Spring Harbour Perspectives Biology* **10**, (2018).

298. Wang AZ, Ojakian GK, Nelson WJ. Steps in the morphogenesis of a polarized epithelium. II. Disassembly and assembly of plasma membrane domains during reversal of epithelial cell polarity in multicellular epithelial (MDCK) cysts. *Journal of Cell Science* **95**, 153-165 (1990).

299. Ojakian GK, Schwimmer R. Regulation of epithelial cell surface polarity reversal by beta 1 integrins. *Journal of Cell Science* **107 (Pt 3)**, 561-576 (1994).

300. Yu W*, et al.* Beta1-integrin orients epithelial polarity via Rac1 and laminin. *Molecular Biology of the Cell* **16**, 433-445 (2005).

301. Bissell MJ, Hall HG, Parry G. How does the extracellular matrix direct gene expression? *Journal of Theoretical Biology* **99**, 31-68 (1982).

302. Bonnans C, Chou J, Werb Z. Remodelling the extracellular matrix in development and disease. *Nature Reviews Molecular Cell Biology* **15**, 786-801 (2014).

303. Frisch SM, Francis H. Disruption of epithelial cell-matrix interactions induces apoptosis. *Journal of Cellular Biology* **124**, 619-626 (1994).

304. Kantak SS, Kramer RH. E-cadherin regulates anchorage-independent growth and survival in oral squamous cell carcinoma cells. *Journal of Biological Chemistry* **273**, 16953-16961 (1998).

305. Jacobson A, Yang D, Vella M, Chiu IM. The intestinal neuro-immune axis: crosstalk between neurons, immune cells, and microbes. *Mucosal Immunology*, (2021).

306. Noel G*, et al.* A primary human macrophage-enteroid co-culture model to investigate mucosal gut physiology and host-pathogen interactions. *Scientific Reports* **7**, 45270 (2017).

307. Rogoz A, Reis BS, Karssemeijer RA, Mucida D. A 3-D enteroid-based model to study T-cell and epithelial cell interaction. *Journal of Immunology Methods* **421**, 89-95 (2015).

308. Meran L, Baulies A, Li VSW. Intestinal stem cell niche: The extracellular matrix and cellular components. *Stem Cells International* **2017**, 7970385 (2017).

309. Nash TJ, Morris KM, Mabbott NA, Vervelde L. Inside-out chicken enteroids with leukocyte component as a model to study host–pathogen interactions. *Communications Biology* **4**, 377 (2021).

310. Liu R*, et al.* Relevance of the intestinal health-related pathways to broiler residual feed intake revealed by duodenal transcriptome profiling. *Poultry Science* **98**, 1102-1110 (2019).

311. Sabino M*, et al.* Dietary supplementation with olive mill wastewaters induces modifications on chicken jejunum epithelial cell transcriptome and modulates jejunum morphology. *BMC Genomics* **19**, 576 (2018).

312. Xiao C, Deng J, Zeng L, Sun T, Yang Z, Yang X. Transcriptome Analysis Identifies Candidate Genes and Signaling Pathways Associated With Feed Efficiency in Xiayan Chicken. *Frontiers in Genetics* **12**, (2021).

313. Wang H*, et al.* Application of RNA-Seq technology for screening differentially expressed genes in chicken small intestine cells affected by avian pathogenic Escherichia coli. *Chinese Journal of Preventive Veterinary Medicine* **38**, 111-115 (2016).

314. Truong AD, Hong YH, Lillehoj HS. High-throughput sequencing reveals differing immune responses in the intestinal mucosa of two inbred lines afflicted with necrotic enteritis. *Veterinary Immunology and Immunopathology* **166**, 116-124 (2015).

315. Flanagan DJ, Austin CR, Vincan E, Phesse TJ. Wnt signalling in gastrointestinal epithelial stem cells. *Genes* **9**, 178 (2018).

316. Lickert H, Kispert A, Kutsch S, Kemler R. Expression patterns of Wnt genes in mouse gut development. *Mechanisms of Development* **105**, 181-184 (2001).

317. Finkbeiner SR*, et al.* Transcriptome-wide analysis reveals hallmarks of human intestine development and maturation in vitro and in vivo. *Stem Cell Reports* **4**, 1140-1155 (2015).

318. Workman MJ*, et al.* Engineered human pluripotent-stem-cell-derived intestinal tissues with a functional enteric nervous system. *Nature Medicine* **23**, 49-59 (2017).

319. Kalluri R, Weinberg RA. The basics of epithelial-mesenchymal transition. *Journal of Clinical Investigations* **119**, 1420-1428 (2009).

320. Bar-Shira E, Friedman A. Development and adaptations of innate immunity in the gastrointestinal tract of the newly hatched chick. *Developmental and Comparative Immunology* **30**, 930-941 (2006).

321. Bar Shira E, Friedman A. Innate immune functions of avian intestinal epithelial cells: Response to bacterial stimuli and localization of responding cells in the developing avian digestive tract. *PloS One* **13**, e0200393-e0200393 (2018).

322. Jordan AR, Racine RR, Hennig MJ, Lokeshwar VB. The Role of CD44 in Disease Pathophysiology and Targeted Treatment. *Frontiers in Immunology* **6**, 182 (2015).

323. Sklan D. Development of the digestive tract of poultry. *World's Poultry Science Journal* **57**, 415-428 (2001).

324. Xie BY, Wu AW. Organoid culture of isolated cells from patient-derived tissues with colorectal cancer. *Chinese Medical Journal* **129**, 2469-2475 (2016).

325. Li H*, et al.* Avian Influenza Virus subtype H9N2 affects intestinal microbiota, barrier structure injury, and inflammatory intestinal disease in the chicken ileum. *Viruses* **10**, 270 (2018).

326. Moustakas A, Heldin CH. Signaling networks guiding epithelial-mesenchymal transitions during embryogenesis and cancer progression. *Cancer Science* **98**, 1512-1520 (2007).

327. Hahn S*, et al.* Organoid-based epithelial to mesenchymal transition (OEMT) model: from an intestinal fibrosis perspective. *Scientific Reports* **7**, 2435 (2017).

328. Kabiri Z*, et al.* Stroma provides an intestinal stem cell niche in the absence of epithelial Wnts. *Development* **141**, 2206-2215 (2014).

329. Aoki R*, et al.* Foxl1-expressing mesenchymal cells constitute the intestinal stem cell niche. *Cellular and Molecular Gastroenterology and Hepatology* **2**, 175-188 (2016).

330. Raslan AA, Yoon JK. R-spondins: Multi-mode WNT signaling regulators in adult stem cells. *The International Journal of Biochemistry & Cell Biology* **106**, 26-34 (2019).

331. Playford RJ, Hanby AM, Gschmeissner S, Peiffer LP, Wright NA, McGarrity T. The epidermal growth factor receptor (EGF-R) is present on the basolateral, but not the apical, surface of enterocytes in the human gastrointestinal tract. *Gut* **39**, 262-266 (1996).

332. Eng S-K, Pusparajah P, Ab Mutalib N-S, Ser H-L, Chan K-G, Lee L-H. Salmonella: a review on pathogenesis, epidemiology and antibiotic resistance. *Frontiers in Life Science* **8**, 284-293 (2015).

333. Clark MA, Reed KA, Lodge J, Stephen J, Hirst BH, Jepson MA. Invasion of murine intestinal M cells by Salmonella typhimurium inv mutants severely deficient for invasion of cultured cells. *Infection and Immunity* **64**, 4363-4368 (1996).

334. Galan JE, Curtiss R. Cloning and molecular characterization of genes whose products allow Salmonella typhimurium to penetrate tissue culture cells. *Proceedings of the National Academy of Sciences* **86**, 6383-6387 (1989).

335. Ramos-Morales F. Impact of Salmonella enterica type III secretion system effectors on the eukaryotic host cell. *International Scholarly Research Notices*, (2012).

336. Ly KT, Casanova JE. Mechanisms of Salmonella entry into host cells. *Cellular Microbiology* **9**, 2103-2111 (2007).

337. EFSA and ECDC (European Food Safety Authority and European Centre for Disease Prevention and Control), 2019. The European Union One Health 2018 Zoonoses Report. *EFSA Journal* **17**, e05926 (2019).

338. Barrow P, Huggins M, Lovell M, Simpson J. Observations on the pathogenesis of experimental Salmonella typhimurium infection in chickens. *Research in Veterinary Science* **42**, 194-199 (1987).

339. Khan S, Chousalkar KK. Transcriptome profiling analysis of caeca in chicks challenged with Salmonella Typhimurium reveals differential expression of genes involved in host mucosal immune response. *Applied Microbiology and Biotechnology* **104**, 9327-9342 (2020).

340. Fasina Y, Holt P, Moran E, Moore R, Conner D, McKee S. Intestinal cytokine responses to Salmonella enterica serovar typhimurium infection in young chicks. *Developmental and Comparative Immunology* **87**, 1335-1346 (2008).

341. Rychlik I, Elsheimer-Matulova M, Kyrova K. Gene expression in the chicken caecum in response to infections with non-typhoid Salmonella. *Veterinary Research* **45**, 119 (2014).

342. Withanage G*, et al.* Cytokine and chemokine responses associated with clearance of a primary Salmonella enterica serovar Typhimurium infection in the chicken and in protective immunity to rechallenge. *Infection and immunity* **73**, 5173-5182 (2005).

343. Zhang YG, Wu S, Xia Y, Sun J. Salmonella-infected crypt-derived intestinal organoid culture system for host-bacterial interactions. *Physiological Reports* **2**, (2014).

344. Forbester JL*, et al.* Interaction of Salmonella enterica serovar Typhimurium with intestinal organoids derived from human induced pluripotent stem cells. *Infection and Immunity* **83**, 2926-2934 (2015).

345. Finlay BB, Falkow S. Salmonella interactions with polarized human intestinal Caco-2 epithelial cells. *Journal of Infectious Diseases* **162**, 1096-1106 (1990).

346. Hecht G. Bugs and barriers: enteric pathogens exploit yet another epithelial function. *Physiology* **10**, 160-166 (1995).

347. Wu R, Chen F, Wang N, Tang D, Kang R. ACOD1 in immunometabolism and disease. *Cellular & Molecular Immunology*, 1-12 (2020).

348. Tessner TG, Muhale F, Riehl TE, Anant S, Stenson WF. Prostaglandin E2 reduces radiation-induced epithelial apoptosis through a mechanism involving AKT activation and bax translocation. *Journal of Clinical Investigations* **114**, 1676-1685 (2004).

349. Behlau I, Miller SI. A PhoP-repressed gene promotes Salmonella typhimurium invasion of epithelial cells. *Journal of Bacteriology* **175**, 4475-4484 (1993).

350. Keestra AM, de Zoete MR, Bouwman LI, Vaezirad MM, van Putten JP. Unique features of chicken Toll-like receptors. *Developmental & Comparative Immunology* **41**, 316-323 (2013).

351. Roeder DJ, Lei M-G, Morrison DC. Endotoxic-lipopolysaccharide-specific binding proteins on lymphoid cells of various animal species: association with endotoxin susceptibility. *Infection and Immunity* **57**, 1054-1058 (1989).

352. Aschenbach J*, et al.* Luminal salmonella endotoxin affects epithelial and mast cell function in the proximal colon of pigs. *Scandinavian Journal of Gastroenterology* **38**, 719-726 (2003).

353. Angus DC, Linde-Zwirble WT, Lidicker J, Clermont G, Carcillo J, Pinsky MR. Epidemiology of severe sepsis in the United States: analysis of incidence, outcome, and associated costs of care. *Critical Care Medicine* **29**, 1303-1310 (2001).

354. Higgs R*, et al.* Induction of a novel chicken Toll-like receptor following Salmonella enterica serovar Typhimurium infection. *Infection and Immunity* **74**, 1692-1698 (2006).

355. Zhang G, Ghosh S. Negative regulation of toll-like receptor-mediated signaling by Tollip. *Journal of Biological Chemistry* **277**, 7059-7065 (2002).

356. Alkie TN, Yitbarek A, Hodgins DC, Kulkarni RR, Taha-Abdelaziz K, Sharif S. Development of innate immunity in chicken embryos and newly hatched chicks: a disease control perspective. *Avian Pathology : Journal of the WVPA* **48**, 288-310 (2019).

357. Schokker D, Peters T, Hoekman A, Rebel J, Smits M. Differences in the early response of hatchlings of different chicken breeding lines to Salmonella enterica serovar Enteritidis infection. *Poultry Science* **91**, 346-353 (2012).

358. Matulova M*, et al.* Chicken innate immune response to oral infection with Salmonella enterica serovar Enteritidis. *Veterinary Research* **44**, 1-11 (2013).

359. Lino AC*, et al.* LAG-3 Inhibitory receptor expression identifies immunosuppressive natural regulatory plasma cells. *Immunity* **49**, 120-133.e129 (2018).

360. O'Brien GC, Wang JH, Redmond HP. Bacterial lipoprotein induces resistance to Gram-negative sepsis in TLR4-deficient mice via enhanced bacterial clearance. *Journal of Immunology* **174**, 1020-1026 (2005).

361. Rottenberg ME, Carow B. SOCS3, a major regulator of infection and inflammation. *Frontiers in Immunology* **5**, 58 (2014).

362. Song J*, et al.* Effects of inulin supplementation on intestinal barrier function and immunity in specific pathogen-free chickens with Salmonella infection. *Journal of Animal Science* **98**, (2020).

363. Radtke AL, Wilson JW, Sarker S, Nickerson CA. Analysis of interactions of Salmonella type three secretion mutants with 3-D intestinal epithelial cells. *PLoS One* **5**, e15750 (2010).

364. Morgan E*, et al.* Identification of host-specific colonization factors of Salmonella enterica serovar Typhimurium. *Molecular Microbiology* **54**, 994-1010 (2004).

365. Porter SB, Curtiss R, 3rd. Effect of inv mutations on Salmonella virulence and colonization in 1-day-old White Leghorn chicks. *Avian Diseases* **41**, 45-57 (1997).

366. Wu Y, Shi T, Li J. NLRC5: a paradigm for NLRs in immunological and inflammatory reaction. *Cancer letters* **451**, 92-99 (2019).

367. Okamoto R*, et al.* Requirement of Notch activation during regeneration of the intestinal epithelia. *American Journal of Physiology-Gastrointestinal and Liver Physiology* **296**, G23-G35 (2009).

368. Fensterl V, Sen GC. The ISG56/IFIT1 gene family. *Journal of Interferon & Cytokine Research* **31**, 71-78 (2011).

369. Elsheimer-Matulova M*, et al.* phoP, SPI1, SPI2 and aroA mutants of Salmonella Enteritidis induce a different immune response in chickens. *Veterinary Research* **46**, 1-12 (2015).

370. Carnell SC, Bowen A, Morgan E, Maskell DJ, Wallis TS, Stevens MP. Role in virulence and protective efficacy in pigs of Salmonella enterica serovar Typhimurium secreted components identified by signature-tagged mutagenesis. *Microbiology* **153**, 1940-1952 (2007).

371. Blake DP*, et al.* Re-calculating the cost of coccidiosis in chickens. *Veterinary Research* **51**, 115 (2020).

372. Clark EL*, et al.* Cryptic Eimeria genotypes are common across the southern but not northern hemisphere. *International Journal of Parasitology* **46**, 537-544 (2016).

373. Shirley MW, Smith AL, Tomley FM. The biology of avian Eimeria with an emphasis on their control by vaccination. In: *Advances in Parasitology*. Academic Press (2005).

374. Soutter F, Werling D, Tomley FM, Blake DP. Poultry coccidiosis: Design and interpretation of vaccine studies. *Frontiers in Veterinary Science* **7**, 101 (2020).

375. Jordan A*, et al.* Eimeria tenella oocyst shedding and output in cecal or fecal contents following experimental challenge in broilers. *Poultry Science* **90**, 990-995 (2011).

376. Tierney J, Mulcahy G. Comparative development of Eimeria tenella (Apicomplexa) in host cells in vitro. *Parasitology Research* **90**, 301-304 (2003).

377. Hofmann J, Raether W. Improved techniques for the in vitro cultivation of Eimeria tenella in primary chick kidney cells. *Parasitology Research* **76**, 479-486 (1990).

378. Bussière FI*, et al.* Establishment of an in vitro chicken epithelial cell line model to investigate Eimeria tenella gamete development. *Parasites & Vectors* **11**, 44 (2018).

379. Luu L*, et al.* An open-format enteroid culture system for interrogation of interactions between Toxoplasma gondii and the intestinal epithelium. *Frontiers in Cellular and Infection Microbiology* **9**, (2019).

380. Zhang XT*, et al.* Cryptosporidium parvum infection attenuates the ex vivo propagation of murine intestinal enteroids. *Physiological Reports* **4**, (2016).

381. Cardenas D*, et al.* Two-and three-dimensional bioengineered human intestinal tissue models for Cryptosporidium. *Cryptosporidium*. Springer (2020).

382. Elsheimer-Matulova M*, et al.* Interleukin 4 inducible 1 gene (IL4I1) is induced in chicken phagocytes by Salmonella Enteritidis infection. *Veterinary Research* **51**, 1-8 (2020).

383. Feng M*, et al.* A balanced game: chicken macrophage response to ALV-J infection. *Veterinary Research* **50**, 20 (2019)

384. Beiting DP*, et al.* Differential induction of TLR3-dependent innate immune signaling by closely related parasite species. *PLoS One* **9**, e88398 (2014).

385. Colotta F*, et al.* Type II interleukin-1 receptor is not expressed in cultured endothelial cells and is not involved in endothelial cell activation. *Blood* **81**, 1347-51 (1993).

386. Giai C*, et al.* Staphylococcus aureus induces shedding of IL-1RII in monocytes and neutrophils. *Journal of Innate Immunity* **8**, 284-298 (2016).

387. Miska KB, Kim S, Fetterer RH, Dalloul RA, Jenkins MC. Macrophage migration inhibitory factor (MIF) of the protozoan parasite Eimeria influences the components of the immune system of its host, the chicken. *Parasitology Research* **112**, 1935-1944 (2013).

388. Probst CM*, et al.* A comparison of two distinct murine macrophage gene expression profiles in response to Leishmania amazonensis infection. *BMC Microbiology* **12**, 22-22 (2012).

389. Long PL. Observations on the growth of Eimeria tenella in cultured cells from the parasitized chorioallantoic membranes of the developing chick embryo. *Parasitology* **59**, 757-765 (1969).

390. Wu Z*, et al.* Regulation and function of macrophage colony-stimulating factor (CSF1) in the chicken immune system. *Developmental and Comparative Immunology* **105**, 103586 (2020).

391. Mun HS*, et al.* TLR2 as an essential molecule for protective immunity against Toxoplasma gondii infection. *International Immunology* **15**, 1081-1087 (2003).

392. Kropf P*, et al.* Toll-like receptor 4 contributes to efficient control of infection with the protozoan parasite Leishmania major. *Infection and Immunity* **72**, 1920-1928 (2004).

393. Zhang L*, et al.* Eimeria tenella: expression profiling of toll-like receptors and associated cytokines in the cecum of infected day-old and three-week old SPF chickens. *Experimental Parasitology* **130**, 442-448 (2012).

394. Zhou Z*, et al.* Upregulation of chicken TLR4, TLR15 and MyD88 in heterophils and monocyte-derived macrophages stimulated with Eimeria tenella in vitro. *Experimental Parasitology* **133**, 427-433 (2013).

395. Shaw TN*, et al.* Tissue-resident macrophages in the intestine are long lived and defined by Tim-4 and CD4 expression. *Journal of Experimental Medicine* **215**, 1507-1518 (2018).

396. Hu T*, et al.* Characterization of Subpopulations of Chicken Mononuclear Phagocytes That Express TIM4 and CSF1R. *Journal of Immunology* **202**, 1186-1199 (2019).

397. Xu L*, et al.* Tim-4 protects mice against lipopolysaccharide-induced endotoxic shock by suppressing the NF-κ B signaling pathway. *Laboratory Investigation* **96**, 1189-1197 (2016).

398. Lynagh GR, Bailey M, Kaiser P. Interleukin-6 is produced during both murine and avian Eimeria infections. *Veterinary Immunology and Immunopathology* **76**, 89-102 (2000).

399. Boyd AC, Peroval MY, Hammond JA, Prickett MD, Young JR, Smith AL. TLR15 Is Unique to Avian and Reptilian Lineages and Recognizes a Yeast-Derived Agonist. *Journal of Immunology* **189**, 4930-4938 (2012).

400. Long JS, Mistry B, Haslam SM, Barclay WS. Host and viral determinants of influenza A virus species specificity. *Nature Reviews Microbiology* **17**, 67-81 (2019).

401. Runstadler J, Hill N, Hussein IT, Puryear W, Keogh M. Connecting the study of wild influenza with the potential for pandemic disease. *Infection, Genetics and Evolution : Journal of Molecular Epidemiology and Evolutionary Genetics in Infectious Diseases* **17**, 162-187 (2013).

402. Stallknecht DE. Ecology and epidemiology of avian influenza viruses in wild bird populations: waterfowl, shorebirds, pelicans, cormorants, etc. *Avian Diseases* **47**, 61-69 (2003).

403. Post J, de Geus ED, Vervelde L, Cornelissen JBWJ, Rebel JMJ. Systemic distribution of different low pathogenic avian influenza (LPAI) viruses in chicken. *Virology Journal* **10**, 23 (2013).

404. Swayne DE, Pantin-Jackwood M. Pathogenicity of avian influenza viruses in poultry. *Developmental Biology* **124**, 61-67 (2006).

405. Swayne DE. Understanding the complex pathobiology of high pathogenicity avian influenza viruses in birds. *Avian Diseases* **51**, 242-249 (2007).

406. Han X, Bertzbach LD, Veit M. Mimicking the passage of avian influenza viruses through the gastrointestinal tract of chickens. *Veterinary Microbiology* **239**, 108462 (2019).

407. Jahangir A*, et al.* Evaluation of human intestinal epithelial differentiated cells (Caco-2) for replication, plaque formation and isolation of avian influenza viruses. *Journal of Virological Methods* **169**, 232-238 (2010).

408. Qu B*, et al.* Human intestinal epithelial cells are susceptible to influenza virus subtype H9N2. *Virus Research* **163**, 151-159 (2012).

409. Punyadarsaniya D*, et al.* Precision-cut intestinal slices as a culture system to analyze the infection of differentiated intestinal epithelial cells by avian influenza viruses. *Journal of Virological Methods* **212**, 71-75 (2015).

410. Ohta C, Yanagawa R, Kida H. Growth of avian and human influenza viruses in organ cultures of duck and chicken colons. *Archives of Virology* **70**, 137-145 (1981).

411. Huang L, Hou Q, Ye L, Yang Q, Yu Q. Crosstalk between H9N2 avian influenza virus and crypt-derived intestinal organoids. *Veterinary Research* **48**, 71-71 (2017).

412. Zhou J*, et al.* Differentiated human airway organoids to assess infectivity of emerging influenza virus. *Proceedings of the National Academy of Sciences U S A* **115**, 6822-6827 (2018).

413. Hui KPY*, et al.* Tropism, replication competence, and innate immune responses of influenza virus: an analysis of human airway organoids and ex-vivo bronchus cultures. *The Lancet Respiratory Medicine* **6**, 846-854 (2018).

414. Webster RG, Yakhno M, Hinshaw VS, Bean WJ, Murti KC. Intestinal influenza: replication and characterization of influenza viruses in ducks. *Virology* **84**, 268-278 (1978).

415. Hinshaw VS, Webster RG, Turner B. Water-borne transmission of influenza A viruses? *Intervirology* **11**, 66-68 (1979).

416. Post J*, et al.* Systemic virus distribution and host responses in brain and intestine of chickens infected with low pathogenic or high pathogenic avian influenza virus. *Virology Journal* **9**, 61 (2012).

417. Kuchipudi SV, Nelli R, White GA, Bain M, Chang KC, Dunham S. Differences in influenza virus receptors in chickens and ducks: Implications for interspecies transmission. *Journal of Molecular and Genetic Medicine* **3**, 143-151 (2009).

418. Boulo S, Akarsu H, Ruigrok RW, Baudin F. Nuclear traffic of influenza virus proteins and ribonucleoprotein complexes. *Virus Research* **124**, 12-21 (2007).

419. Albarracin L*, et al.* Transcriptomic Analysis of the Innate Antiviral Immune Response in Porcine Intestinal Epithelial Cells: Influence of Immunobiotic Lactobacilli. *Frontiers in Immunology* **8**, 57 (2017).

420. Chen X, Liu S, Goraya MU, Maarouf M, Huang S, Chen JL. Host Immune Response to Influenza A Virus Infection. *Frontiers in Immunology* **9**, 320 (2018).

421. Hennion RM. The preparation of chicken tracheal organ cultures for virus isolation, propagation, and titration. *Methods in Molecular Biology* **1282**, 51-56 (2015).

422. Bryson KJ*, et al.* Precision cut lung slices: a novel versatile tool to examine host-pathogen interaction in the chicken lung. *Veterinary Research* **51**, 2 (2020).

423. Gao S*, et al.* Immune Responses of Chickens Infected with Wild Bird-Origin H5N6 Avian Influenza Virus. *Frontiers in Microbiology* **8**, (2017).

424. Iwasaki A, Medzhitov R. Toll-like receptor control of the adaptive immune responses. *Nature Immunology* **5**, 987-995 (2004).

425. Crotta S, Davidson S, Mahlakoiv T, Desmet C, Buckwalter M. Type I and Type III Interferons Drive Redundant Amplification Loops to induce a transcriptional signature in influenza-infected airway epithalia. *PLoS Pathogens* **9**, e1003773 (2013).

426. Klinkhammer J*, et al.* IFN-λ prevents influenza virus spread from the upper airways to the lungs and limits virus transmission. *Elife* **7**, e33354 (2018).

427. Galani IE*, et al.* Interferon-λ mediates non-redundant front-line antiviral protection against influenza virus infection without compromising host fitness. *Immunity* **46**, 875-890 (2017).

428. Reuter A*, et al.* Antiviral activity of lambda interferon in chickens. *Journal of Virology* **88**, 2835-2843 (2014).

429. Liang Q-l, Luo J, Zhou K, Dong J-x, He H-x. Immune-related gene expression in response to H5N1 avian influenza virus infection in chicken and duck embryonic fibroblasts. *Molecular Immunology* **48**, 924-930 (2011).

430. O'Shea JJ, Gadina M, Schreiber RD. Cytokine Signaling in 2002: New Surprises in the Jak/Stat Pathway. *Cell* **109**, S121-S131 (2002).

431. Tuerxun W*, et al.* Expression pattern of the interferon regulatory factor family members in influenza virus induced local and systemic inflammatory responses. *Clinical Immunology* **217**, 108469 (2020).

432. Sasai M, Linehan MM, Iwasaki A. Bifurcation of Toll-Like Receptor 9 Signaling by Adaptor Protein 3. *Science* **329**, 1530-1534 (2010).

433. Honda K*, et al.* IRF-7 is the master regulator of type-I interferon-dependent immune responses. *Nature* **434**, 772-777 (2005).

434. Ranaware PB*, et al.* Genome Wide Host Gene Expression Analysis in Chicken Lungs Infected with Avian Influenza Viruses. *PLoS One* **11**, e0153671 (2016).

435. Uchida Y*, et al.* Identification of host genes linked with the survivability of chickens infected with recombinant viruses possessing H5N1 surface antigens from a highly pathogenic avian influenza virus. *Journal of Virology* **86**, 2686-2695 (2012).

436. Cheriyath V, Leaman DW, Borden EC. Emerging Roles of FAM14 Family Members (G1P3/ISG 6–16 and ISG12/IFI27) in Innate Immunity and Cancer. *Journal of Interferon & Cytokine Research* **31**, 173-181 (2010).

437. Smith SE*, et al.* Chicken interferon-inducible transmembrane protein 3 restricts influenza viruses and lyssaviruses in vitro. *Journal of Virology* **87**, 12957-12966 (2013).

438. Wang Y*, et al.* Integrated analysis of microRNA expression and mRNA transcriptome in lungs of avian influenza virus infected broilers. *BMC Genomics* **13**, 1-15 (2012).

439. Ko J-H*, et al.* Polymorphisms and the differential antiviral activity of the chicken Mx gene. *Genome Research* **12**, 595-601 (2002).

440. Smith J, Sadeyen J-R, Cavanagh D, Kaiser P, Burt DW. The early immune response to infection of chickens with Infectious Bronchitis Virus (IBV) in susceptible and resistant birds. *BMC Veterinary Research* **11**, 256-256 (2015).

441. Mayer B, Hemmens B. Biosynthesis and action of nitric oxide in mammalian cells. *Trends in Biochemical Sciences* **22**, 477-481 (1997).

442. Nathan C. Nitric oxide as a secretory product of mammalian cells. *FASEB Journal* **6**, 3051-3064 (1992).

443. Karupiah G, Xie Q, Buller R, Nathan C, Duarte C, MacMicking J. Inhibition of viral replication by interferon-gamma-induced nitric oxide synthase. *Science* **261**, 1445-1448 (1993).

444. Burggraaf S, Bingham J, Payne J, Kimpton WG, Lowenthal JW, Bean AGD. Increased inducible nitric oxide synthase expression in organs is associated with a higher severity of H5N1 Influenza Virus infection. *PLoS One* **6**, e14561 (2011).

445. Wasilenko JL, Sarmento L, Pantin-Jackwood MJ. A single substitution in amino acid 184 of the NP protein alters the replication and pathogenicity of H5N1 avian influenza viruses in chickens. *Archives of Virology* **154**, 969-979 (2009).

446. Wang Q*, et al.* CC chemokine ligand 19 might act as the main bursal T cell chemoattractant factor during IBDV infection. *Poultry Sciences* **98**, 688-694 (2019).

447. Xuan W, Qu Q, Zheng B, Xiong S, Fan GH. The chemotaxis of M1 and M2 macrophages is regulated by different chemokines. *Journal of Leukocyte Biology* **97**, 61-69 (2015).

448. Rebel JMJ, Peeters B, Fijten H, Post J, Cornelissen J, Vervelde L. Highly pathogenic or low pathogenic avian influenza virus subtype H7N1 infection in chicken lungs: small differences in general acute responses. *Veterinary Research* **42**, 10 (2011).

449. Reemers SSN, van Haarlem DA, Sijts AJAM, Vervelde L, Jansen CA. Identification of novel Avian Influenza Virus derived CD8+ T-Cell epitopes. *PLoS One* **7**, e31953 (2012).

450. Kwon JS*, et al.* Immune responses and pathogenesis in immunocompromised chickens in response to infection with the H9N2 low pathogenic avian influenza virus. *Virus Research* **133**, 187-194 (2008).

451. Wei H*, et al.* Suppression of interferon lambda signaling by SOCS-1 results in their excessive production during influenza virus infection. *PLoS Pathogens* **10**, e1003845 (2014).

452. Giotis ES, Ross CS, Robey RC, Nohturfft A, Goodbourn S, Skinner MA. Constitutively elevated levels of SOCS1 suppress innate responses in DF-1 immortalised chicken fibroblast cells. *Scientific Reports* **7**, 17485 (2017).

453. Cao Y*, et al.* Differential responses of innate immunity triggered by different subtypes of influenza a viruses in human and avian hosts. *BMC Medical Genomics* **10**, 70 (2017).

454. Reemers SS*, et al.* Early host responses to avian influenza A virus are prolonged and enhanced at transcriptional level depending on maturation of the immune system. *Molecular Immunology* **47**, 1675-1685 (2010).

455. Mettifogo E*, et al.* Emergence of enteric viruses in production chickens is a concern for avian health. *The Scientific World Journal* **2014**, 450423 (2014).

456. Adebiyi AI, Tregaskis PL, Oluwayelu DO, Smyth VJ. Investigation of enteric viruses associated with runting and stunting in day-old chicks and older broilers in Southwest Nigeria. *Frontiers in Veterinary Science* **6**, 239 (2019)

457. Day JM, Zsak L. Recent progress in the characterization of Avian Enteric Viruses. *Avian Diseases* **57**, 573-580 (2013).

458. Kar SK*, et al.* Organoids: a promising new in vitro platform in livestock and veterinary research. *Veterinary Research* **52**, 43 (2021).

459. Tsai YH*, et al.* A Method for Cryogenic Preservation of Human Biopsy Specimens and Subsequent Organoid Culture. *Cellular and Molecular Gastroenterolgy and Hepatology* **6**, 218-222.e217 (2018).

460. Lavin S, Karasov W, Ives A, Middleton K, Garland T. Morphometrics of the avian small intestine, compared with nonflying mammals: a phylogenetic approach. *Physiological and Biochemical Zoology* **81**, 526-550 (2008).

461. Vining KH, Mooney DJ. Mechanical forces direct stem cell behaviour in development and regeneration. *Nature Reviews Molecular Cell Biology* **18**, 728-742 (2017).

462. Engler AJ, Sen S, Sweeney HL, Discher DE. Matrix elasticity directs stem cell lineage specification. *Cell* **126**, 677-689 (2006).

463. Carmon KS, Gong X, Lin Q, Thomas A, Liu Q. R-spondins function as ligands of the orphan receptors LGR4 and LGR5 to regulate Wnt/beta-catenin signaling. *Proceeding of the National Academy of Sciences U S A* **108**, 11452-11457 (2011).

464. Park S, Cui J, Yu W, Wu L, Carmon KS, Liu QJ. Differential activities and mechanisms of the four R-spondins in potentiating Wnt/β-catenin signaling. *Journal of Biological Chemistry* **293**, 9759-9769 (2018).

465. Tang X, Liu H, Yang S, Li Z, Zhong J, Fang R. Epidermal growth factor and intestinal barrier function. *Mediators of Inflammation* **2016**, (2016).

466. Basak O, Beumer J, Wiebrands K, Seno H, van Oudenaarden A, Clevers H. Induced quiescence of Lgr5+ stem cells in intestinal organoids enables differentiation of hormone-producing enteroendocrine cells. *Cell Stem Cell* **20**, 177-190.e174 (2017).

467. Blainey P, Krzywinski M, Altman N. Points of significance: replication. *Nature Methods* **11**, 879-880 (2014).

468. Noben M*, et al.* Epithelial organoid cultures from patients with ulcerative colitis and Crohn's disease: a truly long-term model to study the molecular basis for inflammatory bowel disease? *Gut* **66**, 2193-2195 (2017).

469. Abo H*, et al.* Erythroid differentiation regulator-1 induced by microbiota in early life drives intestinal stem cell proliferation and regeneration. *Nature Communications* **11**, 513 (2020).

470. Malomane DK, Simianer H, Weigend A, Reimer C, Schmitt AO, Weigend S. The SYNBREED chicken diversity panel: a global resource to assess chicken diversity at high genomic resolution. *BMC Genomics* **20**, 345 (2019).

471. Guy JS. Virus infections of the gastrointestinal tract of poultry. *Poultry Science* **77**, 1166-1175 (1998).

472. Schuijers J, van der Flier LG, van Es J, Clevers H. Robust cre-mediated recombination in small intestinal stem cells utilizing the olfm4 locus. *Stem Cell Reports* **3**, 234-241 (2014).

473. Tian H*, et al.* A reserve stem cell population in small intestine renders Lgr5-positive cells dispensable. *Nature* **478**, 255-259 (2011).

474. Authority EFS, Prevention ECfD, Control. The European Union summary report on trends and sources of zoonoses, zoonotic agents and food-borne outbreaks in 2017. *EFSA Journal* **16**, e05500 (2018).

475. Wigley P. Salmonella enterica in the Chicken: How it has Helped Our Understanding of Immunology in a Non-Biomedical Model Species. *Frontiers in Immunology* **5**, 482-482 (2014).

476. Hazards EPanel oB*, et al.* Salmonella control in poultry flocks and its public health impact. *EFSA Journal* **17**, e05596 (2019).

477. Bardenbacher M*, et al.* Permeability analyses and three dimensional imaging of interferon gamma-induced barrier disintegration in intestinal organoids. *Stem Cell Research* **35**, 101383 (2019).

478. Hill DR*, et al.* Bacterial colonization stimulates a complex physiological response in the immature human intestinal epithelium. *Elife* **6**, e29132 (2017).

479. Pearce SC*, et al.* An organoid model to study the effect of bacterial metabolites on the intestinal epithelium. *FASEB Journal* **32**, lb358-lb358 (2018).

480. Jepson MA, Collares-Buzato CB, Clark MA, Hirst BH, Simmons NL. Rapid disruption of epithelial barrier function by Salmonella typhimurium is associated with structural modification of intercellular junctions. *Infection and Immunity* **63**, 356-359 (1995).

481. Jepson MA, Schlecht HB, Collares-Buzato CB. Localization of dysfunctional tight junctions in Salmonella enterica serovar typhimurium-infected epithelial layers. *Infection and Immunity* **68**, 7202-7208 (2000).

482. Williams RB. A compartmentalised model for the estimation of the cost of coccidiosis to the world's chicken production industry. *International Journal of Parasitology* **29**, 1209-1229 (1999).

483. Khater HF*, et al.* Avian coccidiosis: Recent advances in alternative control strategies and vaccine development. *Agrobiological Records* **1**, 11-25 (2020).

484. Blake DP*, et al.* Genetic mapping identifies novel highly protective antigens for an apicomplexan parasite. *PLoS Pathogens* **7**, e1001279 (2011).

485. Liu T*, et al.* Protective immunity against Eimeria maxima induced by vaccines of Em14-3-3 antigen. *Veterinary Parasitology* **253**, 79-86 (2018).

486. Middendorp S*, et al.* Adult stem cells in the small intestine are intrinsically programmed with their location-specific function. *Stem Cells* **32**, 1083-1091 (2014).

487. Tsai Y-H*, et al.* In vitro patterning of pluripotent stem cell-derived intestine recapitulates in vivo human development. *Development* **144**, 1045-1055 (2017).

488. Kogut MH, Lange C. Interferon-gamma-mediated inhibition of the development of Eimeria tenella in cultured cells. *Journal of Parasitology* **75**, 313-317 (1989).

489. Alexander DJ. A review of avian influenza in different bird species. *Veterinary Microbiology* **74**, 3-13 (2000).

490. Guan Y, Shortridge KF, Krauss S, Webster RG. Molecular characterization of H9N2 influenza viruses: were they the donors of the "internal" genes of H5N1 viruses in Hong Kong? *Proceedings of the National Academy of Sciences U S A* **96**, 9363-9367 (1999).

491. Laurent F, Mancassola R, Lacroix S, Menezes R, Naciri M. Analysis of chicken mucosal immune response to Eimeria tenella and Eimeria maxima infection by quantitative reverse transcription-PCR. *Infection and Immunity* **69**, 2527-2534 (2001).

492. Bremner A*, et al.* Kinetics of the cellular and transcriptomic Response to Eimeria maxima in relatively resistant and susceptible chicken lines. *Frontiers in Immunology* **12**, 653085 (2021).

493. Sidar B, Jenkins BR, Huang S, Spence JR, Walk ST, Wilking JN. Long-term flow through human intestinal organoids with the gut organoid flow chip (GOFlowChip). *Lab on a chip* **19**, 3552-3562 (2019).

494. Nikolaev M*, et al.* Homeostatic mini-intestines through scaffold-guided organoid morphogenesis. *Nature* **585**, 574-578 (2020).

495. Skardal A*, et al.* Drug compound screening in single and integrated multi-organoid body-on-a-chip systems. *Biofabrication* **12**, 025017 (2020).

496. Kondo J, Inoue M. Application of cancer organoid model for drug screening and personalized therapy. *Cells* **8**, (2019).

497. Sugimoto S*, et al.* An organoid-based organ-repurposing approach to treat short bowel syndrome. *Nature* **592**, 99-104 (2021).

498. Giuffra E, Tuggle CK, Consortium F. Functional annotation of animal genomes (FAANG): current achievements and roadmap. *Annual Review of Animal Biosciences* **7**, 65-88 (2019).

499. Clark EL*, et al.* From FAANG to fork: application of highly annotated genomes to improve farmed animal production. *Genome Biology* **21**, 285 (2020).

500. Roper J, Yilmaz ÖH. Breakthrough Moments: Genome Editing and Organoids. *Cell Stem Cell* **24**, 841-842 (2019).

501. Dekkers JF*, et al.* A functional CFTR assay using primary cystic fibrosis intestinal organoids. *Nature Medicine* **19**, 939-945 (2013).

502. Chandra L*, et al.* Derivation of adult canine intestinal organoids for translational research in gastroenterology. *BMC Biology* **17**, 33 (2019).

503. Ulluwishewa D*, et al.* Live Faecalibacterium prausnitzii in an apical anaerobic model of the intestinal epithelial barrier. *Cellular Microbiology* **17**, 226-240 (2015).

504. Tottey W*, et al.* The human gut chip "HuGChip", an explorative phylogenetic microarray for determining gut microbiome diversity at family level. *PLoS One* **8**, e62544 (2013).

505. Williamson IA*, et al.* A High-Throughput Organoid Microinjection Platform to Study Gastrointestinal Microbiota and Luminal Physiology. *Cellular and Molecular Gastroenterology and Hepatology* **6**, 301-319 (2018).

506. Nigro G, Rossi R, Commere P-H, Jay P, Sansonetti Philippe J. The cytosolic bacterial peptidoglycan sensor Nod2 affords stem cell protection and links microbes to gut epithelial regeneration. *Cell Host & Microbe* **15**, 792-798 (2014).

507. Park J-H*, et al.* Promotion of intestinal epithelial cell turnover by commensal bacteria: Role of short-chain fatty acids. *PloS One* **11**, e0156334-e0156334 (2016).

508. Lukovac S*, et al.* Differential modulation by Akkermansia muciniphila and Faecalibacterium prausnitzii of host peripheral lipid metabolism and histone acetylation in mouse gut organoids. *mBio* **5**, e01438-01414 (2014).

509. Orr B*, et al.* Novel chicken two-dimensional intestinal model comprising all key epithelial cell types and a mesenchymal sub-layer. *Vet Res* **52**, 142 (2021).